Investigation of differentially expressed genes that contribute to therapeutic effects of bevacizumab in BRAF mutant melanoma

Submission for the degree of Doctor of Philosophy (DPhil) in Oncology

Dr Nicholas A Coupe

Christchurch

University of Oxford

Department of Oncology

ACKNOWLEDGEMENTS

I would like to thank my supervisors, A/Prof Val Macaulay and Prof Mark Middleton for their guidance during this project. I am particularly grateful to Dr Macaulay for her time, support and skills she has given me throughout this period. I would also like to thank all members of the Macaulay lab group for their friendship and encouragement.

I would also like to separately acknowledge Leticia Campo from the Good Clinical Laboratory within the University's Oncology Department for her immunohistochemistry work used for chapter 3. I am also grateful for the time and histopathological expertise provided by Dr Olivia Espinosa and Dr Richard Colling, both NHS pathologists, which was necessary to quantify VEGF and CD31 in chapter 3. I would like to thank DPhil student, Lina Guo for generating the isogenic melanoma cell model used in a number of experiments in this thesis. Special thanks to Dr Naveed Akbar for his help with exosome quantification and Andrea Marshall for assistance with statistics pertaining to the AVAST-M clinical trial data.

Lastly, I will be eternally grateful to my wife, Claire and children, William and Charlotte for their support and patience during the countless weekends and evenings dedicated to his project. You now have me back.

ABSTRACT

Malignant melanoma is a highly aggressive and often lethal disease. In 2012, patient outcomes were poor after resection of high-risk stage II and III melanoma, and vascular endothelial growth factor (VEGF) has been implicated in melanoma progression. The phase III AVAST-M clinical trial (recruiting between 2007-2012) randomized patients with high risk melanoma to 1 year of adjuvant bevacizumab (anti-VEGF antibody) or observation. Patients treated with bevacizumab experienced superior disease-free survival (DFS), and $BRAF^{V600E}$ mutation was unexpectedly predictive of benefit. The aim in this project was to investigate this novel association between $BRAF^{V600E}$ and VEGF, based on the hypothesis that $BRAF^{V600E}$ melanomas are dependent on VEGF and more sensitive to its inhibition.

VEGF and CD31 expression were quantified in tissue microarrays (TMAs) and whole mount sections of AVAST-M melanomas. Although no differences were identified between $BRAF^{V600E}$ and wildtype (WT) tumours from TMAs, there was a trend towards higher VEGF and CD31 expression in $BRAF^{V600E}$ whole mounts. In three independent transcriptomic datasets including NanoString analysis of melanomas from the AVAST-M clinical trial, VEGF itself was not differentially expressed, but all identified receptor kinase ROR2 as overexpressed in $BRAF^{V600E}$ melanomas. Differential ROR2 expression was confirmed in a $BRAF^{V600E}$/WT isogenic melanoma model. ROR2 expression decreased with pharmacological MEK inhibition, supporting regulation by MAPK signalling. *In vitro,* ROR2 expression associated with invasive and proliferative phenotypes, with novel evidence that ROR2 regulates VEGF secretion in $BRAF^{V600E}$ mutant melanoma cells. The putative ROR2 ligand Wnt5a was also identified as regulated by MAPK signalling, and MEK inhibition of

$BRAF^{V600E}$ mutant ROR2-overexpressing cells was shown to suppress Wnt5a expression and VEGF secretion. An exploratory transcriptomic analysis of bevacizumab treated $BRAF^{V600E}$/WT isogenic melanoma xenografts identified gene expression changes in the tumour and stroma, that were mutually exclusive between $BRAF^{V600E}$ and WT tumours, both basally and after bevacizumab treatment, and included upregulation of ROR2 in the tumours and Wnt5a in the stroma of $BRAF^{V600E}$ xenografts. Finally, as a predictive biomarker in AVAST-M patient samples, patients with melanomas containing high ROR2 expression trended towards a prolonged DFS after treatment with bevacizumab. In summary, this work identifies Wnt5a-ROR2 signalling as upregulated in BRAF mutant melanomas, contributing to increased VEGF secretion and potentially also to bevacizumab response.

ACKNOWLEDGEMENTS **2**

ABSTRACT **3**

1. Chapter I: Introduction **9**
1.1. Melanoma 9
1.1.1. Incidence, risk factors, staging and treatment 9
1.1.2. Staging for melanoma 12
1.1.3. Treatment of Melanoma 15
1.1.4. Adjuvant treatment of high-risk melanoma 19
1.2. Molecular biology of Melanoma 20
1.2.1. MAPK pathway in melanoma 20
1.2.2. Mutational landscape in melanoma 23
1.2.2.1. NRAS mutations 23
1.2.2.2. NF-1 mutations 24
1.2.2.3. BRAF mutations 25
1.2.2.4. "Triple wild type" 27
1.2.3. Adaptive phenotype switching 28
1.2.3.1. Wnt signalling pathway and its role in phenotype switching 31
1.3. Vascular endothelial growth factor (VEGF) and angiogenesis 32
1.3.1. VEGF and VEGF receptors 32
1.3.2. Regulation of VEGF expression and function 35
1.3.2.1. HIF-1α 35
1.3.2.2. Growth factors and oncogenic mutations 37
1.3.2.3. VEGF bioavailability 37
1.4. Targeting VEGF in melanoma 38
1.4.1. Angiogenesis 38
1.4.2. Angiogenesis and VEGF in melanoma 39
1.4.3. Bevacizumab in melanoma 40
1.4.4. The AVAST-M clinical trial 44
1.5. Hypothesis 46

2. Chapter II: Materials and Methods **48**
2.1. Cell lines and culture 48
2.2. Cell treatments 49
2.2.1. siRNA knockdown of ROR2 49
2.2.2. siRNA knockdown of Osteopontin 50
2.2.3. Small molecule inhibitors 50
2.3. Western blotting 51
2.4. RNA analysis 52
2.4.1. RNA extraction 52
2.4.2. Reverse transcription 53
2.4.3. Real time quantitative Polymerase Chain Reaction (qRT-PCR) 54
2.4.3.1. Primer design 54
2.4.3.2. qRT-PCR 56
2.4.3.3. Relative quantification of mRNA of genes of interest 57
2.5. Cell based assays 58
2.5.1. Cell proliferation assay 58
2.5.2. Cell invasion assay 58
2.5.3. Endothelial proliferation assay 60
2.6. VEGF enzyme-linked immunosorbent assay (ELISA) 60
2.6.1. Sample preparation 60
2.6.2. VEGF ELISA procedure 61
2.7. Recombinant MMP2 treatment 62
2.8. ROR2 overexpression 63
2.8.1. Plasmid transformation into competent E.coli bacteria 63

2.8.2. Transient transfection of ROR2/control plasmids into A375M cells 64
2.8.3. Stable transfection of ROR2/control plasmids in A375M and CHL1 65
2.9. Gel electrophoresis 66
2.10. Exosome quantification 67
2.11. VEGF and CD31 immunohistochemistry (IHC) on AVAST-M samples 67
2.12. Gene expression microarray analysis 68
2.13. HUVEC spheroid sprouting assay 69
2.14. Statistical analysis 69

3. Chapter III: Testing associations within the AVAST-M clinical trial between angiogenesis markers and the BRAF^{V600} mutation 70
3.1. Introduction 70
3.2. A comparison of VEGF serum concentrations between BRAF^{V600} mutant a nd BRAF wildtype melanomas from patients recruited to the AVAST-M trial 71
3.3. Comparison of melanoma VEGF expression between BRAF^{V600} and wildtype from patient samples from the AVAST-M trial 74
3.4. Comparison of stromal VEGF expression between BRAF^{V600} mutant and wildtype AVAST-M patient samples 77
3.5. Comparison of peri-tumoural blood vessel VEGF between BRAF mutant and wildtype AVAST-M samples 78
3.6. A comparison of VEGF expression between BRAF^{V600} and wildtype melanomas -whole slide analysis 79
3.7. A comparison of CD31 positivity between BRAF^{V600} and wildtype melanomas resected in the AVAST- trial 85
3.8. Comparison of CD31 expression in whole mount sections of BRAF^{V600E} and wildtype melanomas from the AVAST-M clinical trial 87
3.9. Discussion 91

4. Chapter IV: Identification of Genes differentially expressed between BRAFV600E mutant and wildtype melanoma 97
4.1. Data sets identifying genes differentially expressed between BRAFV600E and wildtype melanoma 97
4.1.1. Data set 1: AVAST-M patient samples: Analysis performed by Associate Professor Francesca Buffa and Dr Ruud van Stiphout 97
4.1.2. Data set 2: Gene expression data from The Cancer Genome Atlas 99
4.1.3. Data set 3: BRAFV600E/wildtype melanoma isogenic cell model 103
4.2. Integrative analysis of the datasets 106
4.3. Testing for differential expression of VEGF between BRAF^{V600} mutant and wildtype melanoma in the datasets 110
4.3.1. VEGF expression compared between BRAF^{V600} and wildtype samples in the AVAST-M and TCGA data sets (datasets 1 and 2) 110
4.3.2. Expression of VEGF in the BRAF^{V600E}/wildtype isogenic cell model 111
4.3.2.1. VEGF mRNA expression 111
4.3.2.2. VEGF protein expression 112
4.3.2.3. Relationship between BRAF^{V600E} and HIF-1α and VEGFR2 115
4.4. Identification and validation of genes differentially expressed in BRAF^{V600} mutant melanomas that impact upon VEGF expression 117
4.5. Initial interrogation of Osteopontin as a candidate gene of interest 120
4.6. Selection of ROR2 as a gene expressed in association with the BRAFV600E mutation 123
4.6.1. Selection of ROR2 for further investigation 123
4.6.2. Validation of differential expression of ROR2 at the protein level 124
4.6.3. ROR2 expression in a panel of non-isogenic BRAFV600E and wildtype melanoma cell lines 127
4.7. The effect of pharmacological inhibition of BRAF signalling on ROR2 expression 128
4.7.1. ROR2 mRNA expression in BRAF^{V600E} mutant isogenic clone 128
4.7.2. ROR2 protein expression in BRAF^{V600E} mutant isogenic clone and in A375P cells 129
4.8. Discussion 133

5. Chapter V: Phenotypes associated with ROR2 141
5.1. The effect of ROR2 depletion on proliferation of melanoma cell lines 141
5.2. The effect of ROR2 on invasion in melanoma 143
5.3. Relationship of ROR2 expression to VEGF expression 144
5.4. The effect of ROR2 on VEGF mRNA expression 145
5.5. Effect of ROR2 silencing on VEGFA intracellular protein expression 147
5.6. The effect of ROR2 depletion on secretion of VEGF 148
5.7. Testing the effect of siRNA transfection procedure on VEGF secretion 151
5.8. Effect of ROR2 siRNA on downstream targets 152
5.9. Creation of ROR2 expressing stable cell lines 154
5.9.1. ROR2 overexpression in CHL1 154
5.9.2. The effect of ROR2 overexpression on migration in the CHL1 cell line 156
5.9.3. The effect of ROR2 overexpression on VEGF secretion on the CHL1 cell line 159
5.9.4. Testing ROR2 ligand expression in CHL1 and A375M cells 160
5.10. Phenotypes associated with transient ROR2 overexpression in A375M 161
5.11. Stable ROR2 expression in A375M 162
5.12. VEGF expression in stable ROR2 overexpressing A375M cell lines 164
5.12.1. The effect of ROR2 on VEGF secretion 164
5.12.2. The effect of ROR2 overexpression on intracellular VEGF protein and VEGF mRNA 165
5.13. The effect of pharmacological $BRAF^{V600E}$ inhibition on VEGF secretion in the context of ROR2 overexpression 167
5.14. Wnt5a is associated with constitutive BRAF activity and its interaction with ROR2 potentially influences VEGF secretion. 168
5.15. VEGF secreted in response to ROR2 overexpression is pro-angiogenic 172
5.16. Discussion 175

6. Chapter VI: Mechanisms linking ROR2 with increased VEGF secretion in $BRAF^{V600E}$ mutant melanoma 183
6.1. Investigating HIF-1α as a candidate mediating the effect of the $BRAF^{V600E}$ mutation and ROR2 upregulation 183
6.2. Investigating MMP2 as an intermediary between ROR2 and VEGF secretion 185
6.2.1. The effect of ROR2 depletion on MMP2 expression in A375M cells 186
6.2.2. Testing the effect of MMP2 inhibition on VEGF secretion in the A375M cell line 187
6.2.3. Testing effect of recombinant MMP2 on VEGF secretion 189
6.2.4. Expression of MMP2 mRNA in ROR2 overexpressing A375M clones 190
6.3. The effect of ROR2 expression on exosome secretion 191
6.4. Discussion 195
6.4.1. HIF-1α 195
6.4.2. MMP2 199
6.4.3. Exosome secretion 201

7. Chapter VII: The effect of the BRAFV600E mutation on tumour and stromal gene expression, identification of genes responsive to treatment with bevacizumab and exploration of ROR2 as a biomarker for bevacizumab sensitivity in the AVAST-M clinical trial 205
7.1. In vivo model of $BRAF^{V600E}$ and wildtype isogenic melanomas treated with bevacizumab 205
7.2. Gene expression differences, in vivo, between $BRAF^{V600E}$ vs wildtype isogenic clones and surrounding stroma 207
7.2.1. Differentially expressed genes between $BRAF^{V600E}$ vs wildtype melanomas 208
7.2.2. Comparison of stromal gene expression between $BRAF^{V600E}$ and wildtype xenografts 213
7.2.3. A comparison of bevacizumab regulated genes between $BRAF^{V600E}$ mutant and wildtype human melanoma xenografts 215
7.2.4. A comparison of stromal derived genes influenced by treatment with bevacizumab between BRAFV600E mutant and wildtype melanoma xenografts 217

7.3. Assessment of ROR2 as a predictive biomarker for bevacizumab sensitivity in patients recruited into the AVAST-M clinical trial 219
7.4. Discussion 222

8. Conclusions, summary and future directions 232

LIST OF FIGURES 239

LIST OF TABLES 242

LIST OF COMMON ABBREVIATIONS 243

Bibliography 245

1. Chapter I: Introduction

1.1. Melanoma

1.1.1. Incidence, risk factors, staging and treatment

Cutaneous melanoma is the deadliest of all skin cancers. In the UK alone, 15,970 cases were diagnosed between 2014 and 2016, and in 2016 alone the disease was responsible for 2200 deaths (www.cancerresearchuk.org). In the UK, melanoma ranks as the 5th most common cancer in both men and woman and accounts for 5% of all new cancer diagnoses (www.cancerresearchuk.org). The risk of melanoma increases with age, with a peak incidence between 55 and 74. The disease however disproportionally impacts upon younger populations and is the most common malignancy diagnosed in women between the ages of 20 and 29 (www.seer.cancer.gov).

In contrast to the majority of solid tumours, the incidence of melanoma is increasing and has more than doubled in the UK since 1990. Over this time, the incidence has increased by 180% in males and doubled in women (www.cancerresearchuk.org). This trend has also been evident across Europe with average annual percent change increases in incidence in the period between 1995 and 2012 for males and females of 4% and 3%, respectively (Sacchetto *et al.*, 2018). This increase is projected to continue for at least the next 20 years (www.cancerresearchuk.org). The cause for this is unclear. Despite common belief, increased screening and early detection are unlikely to explain the growing incidence as in the USA between 1992 to 2004, melanoma diagnosis rates increased across all histological subtypes and Breslow thickness, arguing against more diagnoses simply due to increased resection of early stage disease (Linos *et al.*, 2009). Although direct causality has never been shown experimentally, ultraviolet (UV) light exposure via increased use of tanning beds,

estimated to be used by one third of Caucasian women in the USA in 2010 (Guy *et al.*, 2013), has also been considered at least partially responsible for the trend (Boniol *et al.*, 2012; Wehner *et al.*, 2014; Marie-Louise Robertson *et al.*, 2017).

There is general consensus that UV exposure is the dominant melanoma risk factor. Geographically, the incidence of melanoma decreases with distance from the equator which corresponds to a reduction in UV exposure (Bulliard *et al.*, 1994) . Melanoma predominately occurs in areas vulnerable to sunburn and is more common in Caucasian populations, presumably due to lack of pigment allowing greater UV penetration (Gilchrest *et al.*, 1999). Intermittent, intense sun exposure resulting in sunburn, particularly in younger individuals, increases the risk of melanoma with 5 or more sunburns during childhood doubling the lifetime of risk of developing melanoma (Wu *et al.*, 2014). In contrast, chronic occupational sun exposure is not associated with an increased risk (Elwood *et al.*, 1997) underscoring the association between high intensity UV exposure and the risk of developing the disease.

UV radiation consists of two separate waveforms that induce melanoma through separate biological mechanisms. In mammalian models, UVA, with a wavelength 320-400nm promotes oxidative DNA damage in melanocytes only in the presence of pigment (Noonan *et al.*, 2012). Exposure to UVA generates reactive oxygen and nitrogen species within melanin (pigment) which induces a cytosine to thymine transition mutation and results in impaired DNA replication (Premi *et al.*, 2015). In contrast UVB (wavelength 280-320 nm), which has less epidermal penetration compared to UVA, directly damages DNA independent of radicals present in pigment (Noonan *et al.*, 2012). The mechanism of UVB induced damage is better understood compared to UVA. UVB induces cyclopyrimidine dimers (CPDs) and pyrimidine photoproducts, referred to as (6-4)PPPs (Craig *et al.*, 2018). Both lesions

occur at regions of DNA where pyrimidine bases lie adjacent to one another. (6-4)PPS induced DNA lesions are efficiently removed are therefore less mutagenic than CPDs (You *et al.*, 2001). CPDs induce single or double covalent bonds between adjacent pyrimidine bases. This event is repaired by nucleotide excision repair (NER) which results in base substitutions from C>T and CC>TT (Budden *et al.*, 2013). Such genomic errors alter the shape of DNA are an essential component of melanogenesis. This pattern of DNA damage is unique and tumours with a greater than 60% C>T substitutions contain what is now referred to as "UV signature" (Brash, 2015; Craig *et al.*, 2018).

UV induced DNA damage is uniquely mutagenic and responsible for cutaneous melanoma containing the highest mutational burden of all cancers (Lawrence *et al.*, 2013). The mutational burden drives the production of neo-antigens and is predictive in the clinical setting of benefit to immunotherapy (Snyder *et al.*, 2014).

Other notable risk factors include a personal history of melanoma (Chen *et al.*, 2015), a poor tanning ability associated with pale skin, freckles and red or blond hair (Gandini *et al.*, 2005) or immunosuppression (Ascha *et al.*, 2017). Genetic background is also relevant. The familial atypical multiple mole and melanoma syndrome (FAMMM) refers to families with high rates of melanoma associated with large moles containing red pigment. Individual family members carry a cumulative of developing melanoma that approaches 100% (Lynch *et al.*, 1978). Germline mutations in the tumour suppressor gene CDKN2A are associated with early onset melanoma, multiple primary melanomas and other non-melanoma tumours (Goldstein *et al.*, 2007). Mutations in BAP1, inherited in an autosomal dominant manor are associated with both cutaneous and uveal cancer. Cutaneous BAP1 deficient melanomas are atypically pale and distinct in appearance from commonly acquired

naevi (Wiesner *et al.*, 2011) .

1.1.2. Staging for melanoma

At the time of diagnosis, patients with melanoma are staged to provide prognostic information required to guide further interventions and surveillance patterns. Staging refers to an assessment of the primary melanoma (tumour depth and ulceration), the degree of involved regional lymph nodes and the presence or absent of distant metastatic spread. The American Joint Committee on Cancer (AJCC) is the premier body that defines melanoma staging and regularly updates its classification systems. Since 2017, melanoma has been staged with the 8th AJCC staging system (Gershenwald *et al.*, 2017) whereas the 7th version was in use at the commencement of this project and is presented below (tables 1-1 and 1-2)**.** The survival statistics reflect patient outcomes based upon treatments available in 2009, when the AJCC 7th edition was compiled.

Melanoma thickness (mm)	**T stage** a =non-ulcerated b= ulcerated	**Number of metastatic lymph nodes**	**N stage** a =micrometastases* b=macrometastases** c=in transit metastases without metastatic lymph nodes	**Metastatic burden**	**M stage**
≤ 1.00	**T1**	0	**N0**	No distant metastases	**M0**
1.01-2.00	**T2**	1	**N1**	Distant skin, subcutaneous or nodal metastases	**M1a**
2.01-4.00	**T3**	2-3	**N2**	Lung metastasis	**M1b**
> 4.00	**T4**	>4 (or intransit metastases/satellites with metastatic nodes)	**N3**	All other visceral metastases OR Any distant metastases with elevated serum lactate dehydrogenase (LDH)	**M1c**

* metastases not detectable clinically or radiologically but pathologically only

** metastases detectable clinically or radiologically and confirmed pathologically

Table 1-1: Tumour, Node and Metastases (TNM) descriptions based upon the AJCC 7th staging edition for melanoma (Balch *et al.*, 2009)

Stage group	T stage	N stage	M stage	10 year survival rate (%)
IA	T1a	N0	M0	95
1B	T1b	N0	M0	86
	T2a	N0	M0	
IIA	T2b	N0	M0	67
	T3b	N0	M0	
IIB	T3b	N0	M0	57
	T4a	N0	M0	
IIC	T4b	N0	M0	40
IIIA	T1-4a	N1a	M0	68
	T1-4a	N2a	M0	
IIIB	T1-4b	N1a	M0	43
	T1-4b	N2a	M0	
	T1-4a	N1b	M0	
	T1-4a	N2b	M0	
	T1-4a	N2c	M0	
IIIC	T1-4b	N1b	M0	24
	T1-4b	N2b	M0	
	T1-4b	N2c	M0	
	Any T	N3	M0	
IV	Any T	Any N	M1 (a-c)	10

Table 1-2: Pathological stage groupings and prognosis according to the AJCC 7th staging edition for melanoma (Balch *et al.*, 2009).

Melanoma is diagnosed by a surgical excision biopsy of a suspicious lesion and then assessed for thickness, ulceration, histological subtype and mitotic count (Marsden *et al.*, 2010). Further surgery, termed wide local excision, to the deep fascia is the definitive surgical treatment for all primary melanomas to reduce the risk of local recurrence. The extent of additional surgery is determined by thickness of the primary

tumour: Melanomas <1mm require a 1cm margin, lesions 1-4 mm require a 2cm margin and lesions >4mm necessitate a 3cm margin (Marsden *et al.*, 2010). Pathological assessment of regional lymph nodes via a sentinel node biopsy is also necessary to accurately stage a melanoma as clinical assessment alone has both poor sensitivity and specificity (Rodrigues *et al.*, 2000). Sentinel node assessment allows for accurate staging, clinical trial participation and in recent times, selection of patients suitable for adjuvant systemic treatments. The procedure does not, however, improve overall survival. For patients with positive sentinel node(s), complete regional nodal dissection is an option although this approach is not associated with a melanoma specific survival benefit and carries a significant risk of morbidity, particularly lymphoedema (Faries *et al.*, 2017). A potential benefit of the procedure however is to reduce the morbidity associated with regional recurrence in high risk patients (Leiter *et al.*, 2016). Cross sectional imaging with Computerised Tomography (CT) or Positron Emission Tomography (PET) allows for detection of distant metastases and is the final component of staging.

1.1.3. Treatment of Melanoma

Surgical resection is the standard of care for stage I to III melanoma and is curative for the majority of stage I and II melanomas (table 1-2). Post-operative surveillance is appropriate to identify locoregional recurrence as well as new primary melanomas (Faries *et al.*, 2017), as the risk of a secondary primary melanoma is increased by between 2 and 5% in melanoma survivors (Goggins *et al.*, 2003). In the UK guidelines advise 5 years of surveillance at deescalating intervals of 3 to 6 months for patients with stage IB to IIIC melanomas (based on AJCC 7th edition criteria).

Surveillance consists of clinical examination and the consideration of cross-sectional imaging for stage IIC and III disease (https://pathways.nice.org.uk/).

The management of high-risk stage II and stage III disease will be described separately.

Stage IV melanoma is incurable and treatment is primarily medical with the goals of improving symptom control and overall survival. Prior to the discovery of immunotherapy and BRAF/MEK inhibitors, discussed later, chemotherapy was considered the only effective systemic therapy. Dacarbazine (DTIC) was the standard of care for approximately 40 years (Yang *et al.*, 2009) and was generally unsatisfactory. Patients treated with DTIC experienced objective response rates of approximately 10-15% and median survival intervals of approximately 6-8 months (Cocconi *et al.*, 1992). Combination chemotherapy is associated with higher response rates but only minimally improves overall survival compared to DTIC, at the cost of significant toxicity (Yang *et al.*, 2009). Due to the failure of any chemotherapy agent, either alone or in combination, to demonstrate superiority to DTIC, the standard of care remained static for approximately 40 years. The efficacy of chemotherapy agents as single agents and as combinations, tested in stage IV melanoma is summarised in table 1-3.

Author and year	Drug(s)	Response rate (%)	Median Overall Survival (months)
Cocconi *et al.*, 1992	DTIC	10	6.3
Middleton *et al.*, 2000	Temozolomide	13.5	7.7
Goodnight *et al.*, 1979	Cisplatin	10	Not reported
Avril *et al.*, 2004	Fotomustine	15.2	7.3
Bedikian *et al.*, 1995	Docetaxel	15.6	7
Walker *et al.*, 2005	Paclitaxel	0	7.6
Chapman *et al.*, 1999	DTIC+Carmustine+Cisplatin+Tamoxifen	18.5	7
Legha *et al.*, 1989	Cisplatin+Vinblastine+DTIC	40	9
Hodi *et al.*, 2002	Carboplatin+Paclitaxel	20	9

Table 1-3: Chemotherapy drugs, either alone or in combination in the treatment of stage IV cutaneous melanoma

Outcomes for patients with advanced melanoma were revolutionised after 2011 following the almost simultaneous, separate discoveries of effective immunotherapy and the importance of the oncogenic BRAF mutation in the disease.

Immunotherapy has long been considered relevant for the treatment of metastatic melanoma. This was initially shown in studies involving interleukin-2 (IL-2), which although associated with response rates of only 18% and a median overall survival of 9.6 months, was shown to promote durable responses for up to 5 years in responding

patients (Davar *et al.*, 2017). The discovery of inhibitory "immune checkpoints" programmed death-ligand 1 (PD-1) and cytotoxic T-lymphocyte-associated protein 4 (CTLA4) and their exploitation by malignant melanomas has resulted in the development of inhibitors that were approved for clinical use for metastatic melanoma in 2011 and 2016, respectively (Emens *et al.*, 2017). Ipilimumab, an anti-CTLA4 monoclonal antibody is associated with response rates of 20-30% and importantly, durable responses in 20% of patients (Hodi *et al.*, 2010), an extension of the benefit seen previously with IL-2. Nivolumab and Pembrolizumab, both PD-1 inhibitors and discovered more recently have a 40% response rate in metastatic melanoma and median overall survival of 33-38 months (Long *et al.*, 2016; Robert *et al.*, 2019), far exceeding the data previously demonstrated for chemotherapy.

The other major breakthrough in the treatment of metastatic melanoma occurred in 2002, when oncogenic $BRAF^{V600E}$ mutations were identified in approximately 60% of cutaneous melanomas (Davies *et al.*, 2002). Pharmacological inhibition of mutant BRAF with Vemurafenib, an oral inhibitor selective for the mutant BRAF kinase resulted in response rate of 48% and prolonged survival compared to DTIC (Chapman *et al.*, 2011). Dabrafenib, an alternative BRAF kinase inhibitor has similar clinical activity (Hauschild *et al.*, 2012). Combined BRAF and MEK inhibition, justified to decrease resistance and treatment related toxicity has improved outcomes relative to BRAF inhibition alone, with overall response rates of 70%, median survival of 24 months and prolonged survival in a subset of patients (Long, Flaherty, *et al.*, 2017). Taken together, the improvements in systemic treatment within the last decade for metastatic melanoma with the use of immunotherapy and oncogenic mutant BRAF inhibition have vastly improved patient outcomes and have essentially rendered chemotherapy obsolete.

1.1.4. Adjuvant treatment of high-risk melanoma

In contrast to improvements in the treatment of advanced melanoma, adjuvant therapy in high-risk melanoma has been a slowly evolving field. Appreciating that 10-year survival is less than 50% for patients with stage IIC and the majority of stage III melanomas (table 1-2), adjuvant therapies to reduce recurrence risk have been identified as an area of need. Despite much effort, effective adjuvant treatment after resection of high risk melanoma was almost non-existent prior to 2017 (Napolitano *et al.*, 2018), the time period when this project was undertaken. Consistent with the limited activity in the metastatic setting, adjuvant chemotherapy has not been shown to reduce recurrence rates compared to observation alone. Randomised clinical trials in patients with high risk stage II and III melanoma comparing observation to lomustine (Fisher *et al.*, 1981), DTIC (Veronesi *et al.*, 1982) or even myeloablative chemotherapy with autologous bone marrow transplant support (Meisenberg *et al.*, 1993) did not report significant differences in overall survival. Interferon-α, an immunotherapy known at the time to influence dendritic cell mediated T-cell priming was also explored in the adjuvant setting (Davar, *et al.*, 2012). A meta-analysis of 14 randomised controlled trials reported an overall survival benefit (HR for death = 0.89, 95% CI = 0.83 to 0.96; P = 0.002) favouring Interferon-α over observation (Mocellin *et al.*, 2010). Despite the benefit, treatment with interferon-α was associated with over 60% chance of grade 3 toxicity (Kirkwood *et al.*, 1996) and consequently the marginal survival benefit was considered insufficient by many to justify routine use. The standard of care in the UK for patients with resected high-risk stage II and III melanoma at the time of initiation of this project was therefore observation alone.

Effective adjuvant therapy for melanoma became a reality in 2018 with clear benefit demonstrated for post-operative treatment with either PD-1 inhibitors or, for patients with $BRAF^{V600}$ mutant melanoma, combined BRAF/MEK inhibition. In the KEYNOTE-054 study, patients with completely resected stage III melanoma treated with adjuvant Pembrolizumab had a 43% lower risk of recurrence compared to placebo with an acceptable 14.7% incidence of serious adverse events (Eggermont *et al.*, 2018). Similarly, 12 months of post-operative treatment with Dabrafenib/Trametinib for patients with resected stage III $BRAF^{V600}$ mutant melanoma reduced the risk of recurrence by 51% and risk of death at 3 years by 43% (Hauschild *et al.*, 2018).

Both these recent therapies have been licensed for post-operative treatment of completely resected stage III melanoma in the UK since 2018 although neither is approved for use in high risk stage II disease where high risk surveillance remains the standard of care (www.pathways.nice.org.uk).

1.2. Molecular biology of Melanoma

1.2.1. MAPK pathway in melanoma

Melanocytes exist within the dermis to protect underlying keratinocytes from the harmful effects of UV damage (Abdel-Malek *et al.*, 2010). Melanocyte physiology is regulated by the paracrine secretion of factors that activate intracellular signalling, predominately through the mitogen activated protein kinase (MAPK) signalling pathway (Hirobe, 2011). The MAPK pathways are signalling cascades activated via linear phosphorylation of a series of kinases and responsible for linking extracellular signals with factors that modulate multiple intracellular processes (Amaral *et al.*,

2017). There have been 14 MAP kinases identified which are grouped into three distinct cascades: the extracellular signal related kinases (ERKs), c-Jun N-terminal kinases (JNKs) and stress-activated protein kinases (p38/SAPK) (Savoia *et al.*, 2019). The MAP/ERK cascade is the most relevant to melanoma appreciating that activating mutations of this pathway are the most frequent in melanoma and subsequently constitutive activation of this pathway is almost universally present in the disease (Hayward *et al.*, 2017).

Activation of the MAPK pathway commences with the binding of a growth factor or mitogen to a receptor kinase that results in receptor auto-phosphorylation. The phosphorylated tyrosine residues on the receptor serves as docking sites for the adapter protein Grb2 which binds via its SH2 domain. Docked Grb2 binds to and activates guanine nucleotide exchange factors, predominately Son of Sevenless (SOS) which is bound via its SH3 binding domain (Simanshu *et al.*, 2017). SOS catalyses the dissociation of GDP and activates RAS via conversion from an inactive GDP bound state to an active GTP bound state. Activated Ras phosphorylates the serine/threonine kinase RAF which is present in three isoforms, ARAF, BRAF and CRAF resulting in dimerization (Niault *et al.*, 2010) .The activated RAF dimers then phosphorylate two further serine/threonine/tyrosine kinases, MEK1 and MEK2 which subsequently phosphorylate specific threonine and tyrosine sites on the extracellular regulated kinases (ERK) 1 and 2 (Plotnikov *et al.*, 2011). Phosphorylated ERK targets substrates in both the cytosol and nucleus. Cytoplasmic targets include FOS and JUN which dimerise to form the transcription factor Activator Protein-1 (AP-1) (Monje *et al.*, 2005). Ribosomal S6 kinase, another cytosolic target regulates transcription via cAMP response element-binding protein (CREB) (Song *et al.*, 2003). Phosphorylated ERK1/2 also has direct nuclear substrates, including the transcription factor MYC.

The MAPK pathway is negatively regulated by a number of well characterised mechanisms. Ribosomal S6 kinase negatively regulates SOS and prevents the conversion of RAS kinase to an active state (Saha *et al.*, 2012). Neurofibromin (NF1) similarly inhibits RAS activation and is described in more detail below. Dual specificity phosphatases (DUSPs) 5 and 6 inhibit ERK activity in both the cell nucleus and cytoplasm (Karlsson *et al.*, 2004; Kidger *et al.*, 2017). In summary the MAPK/ERK pathway is a regulated linear signalling cascade allowing extracellular mitogens and growth factors to modulate cellular functions.

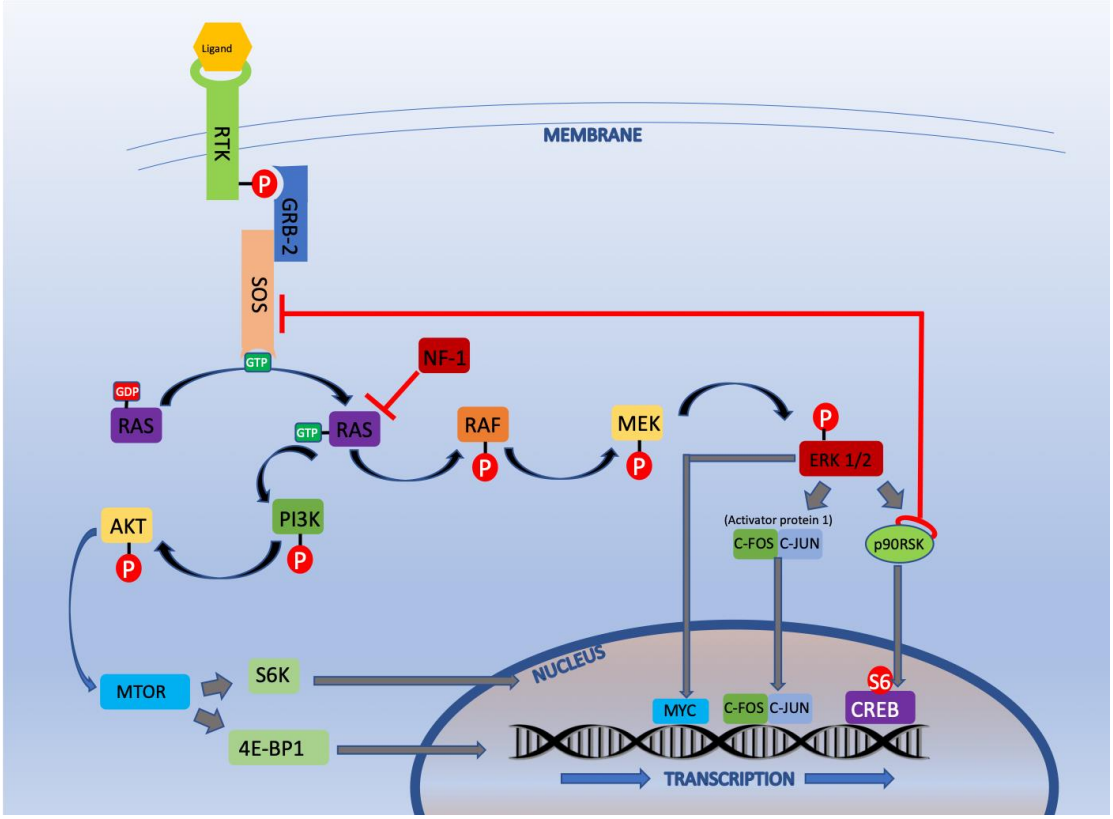

Figure 1-1: MAP-K/ERK signalling pathway. RTK = Receptor tyrosine kinase. P=phosphorylation

1.2.2. Mutational landscape in melanoma

The importance of the MAPK pathway in cutaneous melanoma is reflected in the fact that mutations activating this pathway are present in over 90% of cutaneous melanomas (Hayward *et al.*, 2017). Mutations in 3 genes *NRAS* (30% of cases), *BRAF* (50%) and *NF1* (14%), all generally mutually exclusive are present in over 85% of cutaneous melanomas (Akbani *et al.*, 2015; Hayward *et al.*, 2017). A group not containing any of the above mutations has been termed "wild type" and cutaneous melanomas in this group have a higher proportion of mutations in cyclin-dependent kinase inhibitor 2A *(CDNK2A)*, *TP53*, *GNAQ* and Splicing factor 3B subunit 1 (*SF3BP1)* (Hayward *et al.*, 2017).

1.2.2.1. NRAS mutations

The Rat Sarcoma (RAS) protein is an integral component early in the MAPK signalling pathway, as outlined above. Many RAS proteins exist, however only 3 are commonly mutated in cancer, *HRAS, KRAS* and *NRAS*. Of these, *NRAS* mutations are the most common in cutaneous melanoma, occurring in approximately 30% (Hayward *et al.*, 2017). *HRAS* and *KRAS* mutations are much rarer, occurring in approximately 5% of cases (Hayward *et al.*, 2017) contrasting with the other solid malignancies where mutations in *KRAS* account for over 80% of *RAS* mutations (Cicenas *et al.*, 2017). The most common *NRAS* mutation is a substitution of glutamine with either lysine or arginine at position 61 ($NRAS^{Q61R/K/L}$) (Forbes *et al.*, 2017). The Q61 *NRAS* mutation locks the GTPase into an active conformation state that subsequently activates downstream targets of the MAPK cascade (Burd *et al.*, 2014). Less common mutations, $NRAS^{G12}$ and $NRAS^{G13}$ decrease NRAS GTPase sensitivity to GTPase

activating proteins (GAPs) which also maintains the GTPase in its active state (Cicenas *et al.*, 2017). Unlike activating *BRAF* mutations which only signals down the MAPK pathway, *NRAS* mutations can also enhance downstream signalling through PI3K pathway (Savoia *et al.*, 2019). *NRAS* mutated melanomas are associated with increased tumour depth although a clear link with adverse clinical outcomes has not been clearly defined (Bucheit *et al.*, 2013).

1.2.2.2. NF-1 mutations

Somatic mutations in the neurofibromin 1 gene, (*NF1*) are present in approximately 15% of primary cutaneous melanomas and are typically mutually exclusive from mutations in *BRAF* and *NRAS* (Hayward *et al.*, 2017). Neurofibromin 1, the protein encoded by the gene, is a RAS-GAP that negatively regulates RAS by converting active RAS-GTP to inactive RAS-GDP (Kiuru *et al.*, 2017). Somatic driver *NF1* mutations in melanoma are typically loss of function mutations that prevent NF1 from acting as a tumour suppressor and consequently promote constitutive RAS activity and signalling down both MAPK and PI3K pathways (Viskochil *et al.*, 1990; Philpott *et al.*, 2017). *NF1* mutations are more common in melanomas that arise from chronically sun damaged skin and in older patients. *NF1* mutations are also more common in desmoplastic melanoma, a specific clinicopathological subtype characterised histologically by an abundance of collagen and molecularly by a high mutational burden (Krauthammer *et al.*, 2015; Wiesner *et al.*, 2015). Exploiting the therapeutic relevance of *NF1* mutations therapeutically remains an area of research.

1.2.2.3. BRAF mutations

The most common mutation of the MAPK pathway in melanoma is in the *BRAF* gene, occurring in over 50% of cases (Akbani *et al.*, 2015; Hayward *et al.*, 2017). Only hairy cell leukaemia has a higher rate (approaching 100%), whereas the mutation has been reported in lower frequencies in colorectal cancer, non-small cell lung cancer and papillary thyroid cancer (Badalian-Very *et al.*, 2010). Over 20 different *BRAF* mutations have been reported and the most common of these is $BRAF^{V600E}$, which is responsible for over 80% of all mutations of the gene (Menzies *et al.*, 2012). The $BRAF^{V600E}$ mutation results from a c1799T>A transversion which causes a valine to glutamic acid amino acid substitution at position 600 on the BRAF protein. Other less common, but clinically relevant mutations are the $BRAF^{V600K}$, $BRAF^{V600R}$ and $BRAF^{V600D}$ (Lovly *et al.*, 2012; Menzies *et al.*, 2012).

The BRAF protein is a serine/threonine kinase consisting of 2 lobes, a smaller N-terminal lobe, and larger C-terminal lobe. The two lobes are separated by a catalytic cleft. In the inactive state, hydrophobic bonds between segments G596-V600 in the activation segment, the segment phosphorylated during BRAF activation, and the P-loop on the N-terminal lobe render the catalytic cleft inaccessible to ATP. Phosphorylation of the activation segments disrupts the hydrophobic bonds and allows ATP to bind to the catalytic cleft, thereby activating the kinase. $BRAF^{V600}$ mutations destabilise the hydrophobic bonds thereby allowing unrestricted ATP access into the catalytic cleft and permanently activating the kinase. Once constitutively activated the BRAF kinase has activity over 700-fold greater than wild-type BRAF (Wan *et al.*, 2004).

Distinct clinicopathological subtypes are defined by the specific BRAF mutation. $BRAF^{V600E}$ mutant melanomas are more common in younger patients and associated with intermittent sun exposure whereas the $BRAF^{V600K}$ is relatively more common in elderly patients with high cumulative sun exposure (Menzies *et al.*, 2012). Compared to wildtype, *BRAF* mutant melanomas occur more frequently on the trunk and have a significantly higher mutational burden (Candido *et al.*, 2014).

As a single event, a *BRAF* mutation paradoxically induces apoptosis as opposed to proliferation and tumour growth, via oncogene induced senescence (Cisowski *et al.*, 2016). High levels of MAPK induced oncogenic stress upregulate tumour suppressors such as $p16^{INK4A}$ (Agger *et al.*, 2009), insulin Like Growth Factor Binding Protein 7 (IGFBP7) (Wajapeyee *et al.*, 2008) and cell cycle arrest through induction of cyclin dependent kinase inhibitor $P21^{Cip1}$ (Woods *et al.*, 1997). These mechanisms presumably protect cells against uncontrolled growth in the context of a potential tumorigenic aberration such as a *BRAF* mutation. Indeed, *BRAF* mutations are relatively common in benign naevi, which frequently exist in a growth arrested state (Niault *et al.*, 2010). Survival, and indeed malignant transformation of a melanocyte in a state of mutant BRAF induced senescence requires a number of secondary events including loss of the p53 pathway and deletion of retinoblastoma (*Rb)* (Yu *et al.*, 2009).

BRAF kinase inhibitors are small molecule inhibitors that occupy the ATP binding site on the activation segment and stabilise the kinase, preventing further activity (Savoia *et al.*, 2019). The first BRAF mutant kinase inhibitor, N-(3-(5-chloro-1H-pyrrolo[2,3-b]pyridine-3-carbonyl)- 2,4-difluorophenyl)propane-1-sulfonamide, known as PLX4720 is highly specific for the $BRAF^{V600E}$ kinase and selectively

inhibits ERK phosphorylation in $BRAF^{V600E}$ mutant melanoma cell lines but not cells with wild type BRAF. Consistent with this specific effect, it also effectively induces apoptosis and cell cycle arrest in $BRAF^{V600E}$ mutant melanoma cell lines with an IC_{50} of 13nM (Tsai *et al.*, 2008). PLX4032, a related compound with superior pharmacokinetics compared to PLX4720, was renamed Vemurafenib, and was evaluated clinically in the landmark BRIM-3 study, where patients with $BRAF^{V600E}$ mutant metastatic melanoma were randomised to treatment with vemurafenib or DTIC. Objective response rates were 48% vs 5% ($p<0.001$) and overall survival (hazard ratio (HR) for death 0.37 (95% Confidence Interval (CI), 0.26 to 0.55; $p<0.001$) in favour of vemurafenib (Chapman *et al.*, 2011) and thus reaffirmed the preclinical data in a clinical context. More recently, in the metastatic setting, simultaneous treatment with $BRAF^{V600E}$ and MEK inhibitors has been shown to prolong resistance and paradoxically improve toxicity compared to $BRAF^{V600E}$ inhibition alone (Long, Flaherty, *et al.*, 2017).

1.2.2.4. "Triple wild type"

A fourth molecular melanoma subtype not containing mutations in *NRAS*, *BRAF* or *NF1* has been referred to as "triple wild type". This heterogenous subtype has a lower incidence of a UV- damage signature and contains significantly more copy number alterations compared with the other classes (Akbani *et al.*, 2015). Common mutations in this group include *KIT, GNAQ, GNA11* and *CDK4* (Akbani *et al.*, 2015). KIT, a receptor tyrosine kinase promotes melanoma proliferation via signalling down both MAPK and PI3K signalling pathways. While rare in cutaneous melanomas, KIT

mutations occur in up to 20% of acral and mucosal melanomas (Curtin *et al.*, 2006; Hayward *et al.*, 2017). The most common KIT mutations are the L576P and K642P, which both constitutively activate the kinase (Willmore-Payne *et al.*, 2005; Tzen *et al.*, 2014). GNAQ and GNA11 mutations are relatively more common in uveal compared to cutaneous melanomas (Van Raamsdonk *et al.*, 2009). These activating mutations converge and upregulate the MAPK pathway (Shaughnessy *et al.*, 2018). CDK4 regulates cell cycle progression by binding to p16INK4A and inhibiting phosphorylation of the RB tumour suppressor, which inhibits E2F transcription factors necessary for S-phase cell cycle progression (Shapiro, 2006). Mutations in *CDK4* are most commonly located at the P16INK4A binding site. As CDK4 is negatively regulated by P16INK4A, mutations prevent this interaction, constitutively activating CDK4 and inhibiting RB activity, resulting in uncontrolled transcription and cell cycle progression (Sheppard *et al.*, 2013).

1.2.3. Adaptive phenotype switching

A key component required by many solid tumours to develop specific malignant properties is epithelial-mesenchymal transition (EMT). EMT confers on cancer cells the properties of increased invasion, metastatic potential and loss of cell polarity (Thiery, 2002) that is characterised by reduced expression of E-cadherin (Perl *et al.*, 1998). The expression of E-cadherin is tightly regulated by numerous transcription factors that bind to and repress the E-cadherin promoter including, SNAI2, ZEB1, TWIST and transcription factor 4 (TCF4) (Comijn *et al.*, 2001; Bolos *et al.*, 2003; Yang *et al.*, 2004; Moreno-Bueno *et al.*, 2006; Aigner *et al.*, 2007). E-cadherin

repression has also been reported as a consequence of MAPK/ERK signalling, via induction of another transcription factor, SNAI1 (Grotegut *et al.*, 2006).

A similar phenotype switching model has been reported as a requirement for primary melanomas to develop characteristics necessary to metastasise (Bennett, 2008). Unlike EMT transition in solid tumours which is a progressive and one-directional process from primary lesion to metastatic deposit, the process in melanoma is dynamic, can be switched on and off, and its activity varies within individual tumours (Hoek *et al.*, 2008). A concept coined adaptive phenotype switching has been described referring to the ability of melanoma to switch between phenotypic states depending on context. One state includes melanomas that are highly invasive, migratory and have high metastatic potential. The other is characterised by high levels of proliferation but reduced invasion and metastatic potential (Hoek *et al.*, 2006, 2008). An example of this phenotypic switch is during the transition of a melanoma from the radial growth phase (highly proliferative, poorly invasive) to vertical growth phase (less proliferation, increased invasion and high metastatic potential) (O'Connell *et al.*, 2009). The ability to dynamically switch between these two states allow melanomas to adopt stem like properties required to progress (Hoek *et al.*, 2010).

Many traditional drivers of EMT transition in solid tumours including SNAI1, SNAI2, TWIST and ZEB1 also drive the aggressive phenotypes in melanoma where they are associated with poorer prognosis (Caramel *et al.*, 2013; Li *et al.*, 2015). Microphthalmia-associated transcription factor (MITF) has been proposed as a melanoma specific regulator controlling the switching between differing phenotypic states. MITF acts as a "rheostat", alternating phenotypes in response to various environmental triggers including oxygen tension, nutrients and growth factors

(Vandamme *et al.*, 2014). MITF modulates melanocyte differentiation through manipulation of cell cycle arrest (Loercher *et al.*, 2005). Melanomas with MITF up-regulation are proliferative but not invasive, whereas MITF depletion is associated with an invasive phenotype associated with stem cell properties (Hoek *et al.*, 2010). ZEB2 has been reported as a regulator of MITF. Mice lacking ZEB2 in the melanocyte lineage exhibit melanocyte dedifferentiation associated with MITF depletion and upregulation of ZEB1 (Denecker *et al.*, 2014). Consistent with this, reduced *ZEB2* expression in primary melanoma samples correlates with a poor prognosis (Denecker et al., 2014). ZEB1 and TWIST, in contrast, are down-regulated by MITF promoting a proliferating and a poorly metastatic phenotype (Vandamme *et al.*, 2014).

MAPK signalling has also been implicated in phenotype switching between the two states. Melanocytes transfected with a constitutively active $BRAF^{V600E}$ vector upregulated ZEB1 and TWIST and downregulated ZEB2 and SNAI2. Consistent with this result, treatment of BRAF mutant A375P cells with a PLX4720 (BRAF inhibitor) or U0126 (MEK inhibitor) also downregulated ZEB1 and TWIST and upregulated ZEB2 and SNAI2 (Caramel *et al.*, 2013). MAPK signalling may thus be another driver of invasive melanoma phenotypes.

1.2.3.1. Wnt signalling pathway and its role in phenotype switching

Wnt signalling is further pathway implicated in phenotype switching in melanoma. Wnt signalling is characterised as canonical and non-canonical. The Wnt ligands Wnt1, 3 and 7 activate the canonical pathway, whereas Wnt5a, 5b and 11 are involved in non-canonical signalling activation (Debebe *et al.*, 2015). Canonical Wnt signalling involves ligand binding to one of ten Frizzled (FZD) receptors concurrently with a lipoprotein receptor related protein (LRP) co-receptor (Ford *et al.*, 2013). In the absence of active Wnt signalling, a complex formed by β-catenin, APC and AXIN is phosphorylated by casein kinase Ia (CKIα) and glycogen synthase kinase 3β (GSK3β), marking β-catenin for proteosomal degradation (Katoh *et al.*, 2007). Canonical Wnt pathway activation associates GSK3β and CK1α with the plasma membrane followed by dishevelled (DVL), allowing non-phosphorylated β-catenin to accumulate and translocate from the cytoplasm to the nucleus. Nuclear β-catenin then complexes with T-cell factors (TCF) and Lymphoid enhancer factor (LEF), to form transcription factors promoting expression of genes involved in cellular proliferation and differentiation including *WISP1, CCND1* and *MYC* (Katoh *et al.*, 2007).
Non-canonical Wnt signalling is less well characterised compared to the canonical pathway but is described encompassing two pathways. Firstly, the Wnt/Ca^{2+} pathway, involves the effectors CaMKII, NFAT and protein kinase C (PKC), and secondly the planar-cell polarity pathway (PCP) (Katoh *et al.*, 2007; Ford *et al.*, 2013).
Binding of Wnt5a to the FZD receptor concurrently with the co-receptor, ROR2 activates the PCP pathway by recruiting DVL, which activates the GTPases RHO and RAC1 and ROCK culminating in the activation of the c-Jun N-terminal kinase (JNK). The alternative Wnt/Ca^{2+} pathway requires ligand binding to the FZD/ROR2 complex, which activates Phospholipase C, initiating fluxes in intracellular calcium

and subsequently activation of PKC, Calcineurin and CaMKII (Zhan *et al.*, 2016). Non-canonical Wnt signalling is another mediator of invasive melanoma phenotype switching and has been implicated in aggressive melanoma phenotypes in the clinical setting. In a series of 59 primary melanomas with matched metastases, Wnt5a expression significantly increased as melanomas progressed from the radial growth phase to the invasive vertical growth phase and a further again in metastatic deposits. Wnt5a expression was associated with decreased overall survival, independent of other established pathological predictors, such as breslow thickness (Da Forno *et al.*, 2008).

Wnt5a also overlaps functionally with MITF. *In vitro,* overexpression of Wnt5a is associated with MITF downregulation, which in turn also decreases MART1, a marker of melanocyte differentiation (Dissanayake *et al.*, 2008). Taken together, non-canonical Wnt signalling is another mechanism driving invasive, increasingly metastatic and poorly differentiated melanoma phenotypes.

1.3. Vascular endothelial growth factor (VEGF) and angiogenesis

1.3.1. VEGF and VEGF receptors

The concept of angiogenesis as a means to sustain tumour growth was first proposed over a century ago. Although tumours were known to be highly vascular when observed, the mechanism driving the adaptive process was not recognised until 1971. In that year Folkman proposed that tumour cells secrete a factor that stimulated endothelial cell proliferation and indirectly increased tumour growth (Folkman, 1971). In 1989, a secreted protein, VEGF was identified, shown to be related to platelet derived growth factor (PDGF), and at the time was considered specific to

endothelial cells, against which it was shown to induce a mitogenic effect (Connolly *et al.*, 1989).

VEGF is now known to be a family of proteins, consisting of 5 members, VEGFA, VEGFB, VEGFC, VEGFD and VEGFE (Ferrara and Anthony P. Adamis, 2016). Although structurally related, the VEGF family members have differing and broad roles in many organ systems including the central nervous system, renal and gastrointestinal tracts (Simons *et al.*, 2016). VEGFB has a role in fatty acid uptake and angiogenesis in cardiovascular muscle (Olofsson *et al.*, 1996). VEGFC regulates lymphatic vessel generation, specifically via its interaction with the VEGFR3 receptor (Karkkainen *et al.*, 2004). VEGFD induces specific morphological changes in fibroblasts that are reported to contribute towards malignant phenotypes (Orlandini *et al.*, 1996).

VEGFA is considered the most important VEGF member relevant to pathological angiogenesis and is the form most extensively studied to date. VEGFA, referred to simply as VEGF, is encoded by the *VEGF* gene located on the short arm of chromosome 6, which is comprised of 8 exons and 6 introns. The VEGF protein exists in multiple isoforms, all of which arise due to alternative splicing of exons 6 and 7. Splicing of exons 1-5 is identical throughout all isoforms (Ng, 2008; Ferrara and Adamis, 2016). The isoforms are: $VEGF_{121}$, $VEGF_{165}$, $VEGF_{189}$ and $VEGF_{206}$. The nomenclature indicates that the isoforms contain 121, 165, 189 and 206 amino acids, respectively (Ng, 2008). The different isoforms have distinct biological properties determined by their ability to bind heparin, defined by the relative presence of heparin binding domains (Ng, 2008). $VEGF_{189}$ contains 2 heparin binding domains and consequently remains tightly bound to extracellular matrix by heparan sulfate

proteoglycans (HSPGs) (Houck *et al.*, 1992). Conversely, $VEGF_{121}$ does not bind heparin and is therefore diffusible. $VEGF_{165}$ contains only one heparin binding domain, and can therefore exist in either a bound or diffusible state (Ng, 2008). $VEGF_{165}$ itself can form another isoform, $VEGF_{165b}$, via splicing at an additional site at exon 8. Although $VEGF_{165b}$ has an identical molecular mass to $VEGF_{165}$ and binds to the same receptor, it has an opposing biological function (Woolard *et al.*, 2004). $VEGF_{165}$ is considered the isoform with the highest degree of physiological relevance and is chief driver of VEGF associated tumour angiogenesis (Apte *et al.*, 2019).

VEGFs bind three receptors, Vascular endothelial growth factor 1 (VEGFR1; also referred to as fms-like tyrosine kinase (FLT1)), VEGFR2 (alternatively referred to as kinase insert domain receptor (KDR)) and VEGFR3. All three receptors are receptor tyrosine kinases that homo or heterodimerise to autophosphorylate intracellular tyrosine residues to initiate downstream signalling pathways (Simons *et al.*, 2016). VEGFR1 binds VEGFA and VEGFB and can form either homodimers or heterodimers with VEGFR2 depending on the ligand (Gabhann *et al.*, 2007). It also exists in a soluble form, sVEGFR1 (Shibuya, 2013). VEGFR1 binds VEGF with higher affinity than VEGFR2, but subsequent receptor phosphorylation is weak (Ito et al., 1998), and therefore the receptor and its soluble variant have been coined "VEGF traps" that bind VEGF and serve as negative regulators of angiogenesis (Simons *et al.*, 2016). VEGFR3 is expressed on blood and lymphatic endothelial cells and binds to unprocessed VEGFC and VEGFD. Proteolytically cleaved ligands induce heterodimerisation of the receptor with VEGFR2. VEGFR3 is expressed on lymphatic endothelial cells during embryonic development and on blood vessels in specific contexts such as retinal angiogenesis (Alitalo, 2011; Benedito *et al.*, 2012).

VEGFR2 is expressed on all blood vascular endothelial cells and transduces all the known effects of VEGFA (Ferrara *et al.*, 2003). VEGFA is the primary ligand for the receptor, although it can also form heterodimers in response to binding to processed VEGFC and VEGFD, as discussed above. Once bound by VEGF, VEGFR2 forms a homodimer, and one receptor molecule trans-phosphorylates intracellular tyrosine residues on the other (Koch *et al.*, 2011). Once phosphorylated, VEGFR2 internalises into early antigen 1 (EEA) positive endosomes with subsequent Ca^{2+} signalling via phospholipase Cγ (PLCγ) which activates the NFAT signalling pathway and, via PKC, the MAPK/ERK pathway resulting in endothelial migration, proliferation and lumen formation (Ferrara *et al.*, 2003; Simons *et al.*, 2016).

VEGFR2 signalling is augmented by the Neuropilin (NRP) co-receptors. NRP1 binds to VEGF via an exon 7 encoded sequence and consequently binds $VEGF_{165}$. This sequence is absent in the diffusible $VEGF_{121}$ isoform and is one explanation for the greater mitogenic potential of $VEGF_{165}$ compared to $VEGF_{121}$ (Soker *et al.*, 1998). NRPs have an important role in VEGFR2 intra-cellular trafficking. NRP1 simultaneously binding VEGF with VEGFR2 forms a VEGFR/NRP1 complex that is essential for endosomal translocation and downstream signalling (Lanahan *et al.*, 2013). NRPs can also bind VEGF without VEGFR2, although the biological consequences of this remain largely unknown (Ellis, 2006).

1.3.2. Regulation of VEGF expression and function

1.3.2.1. HIF-1α

VEGF expression is highly regulated by oxygen tension where hypoxic conditions result in the transcription of *VEGF* mRNA (Ferrara and Adamis, 2016). HIF-1α is

chiefly implicated in this process. The HIF-1α protein is tightly regulated by oxygen tension. Under normoxic conditions, hydroxylation and acetylation of oxygen sensitive proline and lysine residues mark HIF-1α for ubiquitination by the tumour suppressor, von Hippel-Lindau protein (pVHL) and subsequent proteosomal destruction (Weidemann *et al.*, 2008). An isoform, HIF-2α undergoes similar oxygen dependent proteosomal destruction as HIF-1α, although its expression is more limited and although both forms have many overlapping functions, neither is unlikely to be redundant (Wiesener *et al.*, 2003).

In hypoxic conditions, HIF-1α is not marked for destruction by pVHL and its expression persists. Once stabilised, HIF-1α translocates to the cell nucleus and binds to constitutively active HIF-1β. The resulting complex binds to the hypoxic responsive element (HRE) on promoter or enhancer sequences within a number of well characterised target genes, most notably *VEGF* to initiate transcription (Masoud *et al.*, 2015).

Many other genes are known to be upregulated in hypoxia. The expression of HIF-1α target genes allows cells to shift metabolic processes in order to survive under hypoxic conditions. A central adaption is a shift in the glucose metabolism. In brief, in normoxia, glucose is converted efficiently into pyvuvate which is subsequently catabolized through the citric acid cycle and oxidative phosphorylation in mitochondria, whereas in hypoxic conditions pyruvate is metabolised less efficiently to lactic acid, the process known as Warburg effect and described almost 100 years ago (Warburg *et al.*, 1927). Other HIF-1α target genes, including carbonic anhydrases IX and XII preserve intracellular pH, a necessary adaption resulting to lactic acid accumulation (Weidemann *et al.*, 2008).

1.3.2.2. Growth factors and oncogenic mutations

VEGF expression is also influenced by growth factors and oncogenic mutations. Transforming growth factor β (TGFβ) and insulin like growth factor 1 (IGF1) increase *VEGF* mRNA (Pertovaara *et al.*, 1994; Warren *et al.*, 1996). Thyroid stimulating hormone (TSH) and adrenocorticotropic hormone (ACTH) have been shown to increase VEGF secretion (Soh *et al.*, 1996; Gaillard *et al.*, 2000). Oncogenic mutations are also associated with increased VEGF expression. NIH-3HT cells transformed with an oncogenic *RAS* mutation increase transcription and secretion of VEGF (Grugel *et al.*, 1995). In a separate experiment, KRAS mutant colorectal cell lines DLD-1 and HCT-116 transfected with a $VEGF_{121}$ antisense vector were less tumourigenic *in vivo.* KRAS knockout in the same cells minimised tumour growth, and the phenotype was partially rescued by transfection with a $VEGF_{121}$ expression vector, suggesting that VEGF has a role in KRAS driven malignant phenotypes (Okada *et al.*, 1998). Separate studies in melanoma cell lines have shown that $BRAF^{V600E}$ increases HIF-1α stabilisation and downregulates pVHL to improve survival in hypoxic conditions (Kumar *et al.*, 2007). Regulation of HIF-1α by the MAPK axis involves at least 2 mechanisms: firstly, ERK mediated phosphorylation of 4E-BP1 increases HIF-1α translation and secondly, MAPK/ERK signalling recruits the co-factor p300 to HIF-1α, which enhances transcription of HIF-1α target genes (Sang *et al.*, 2003).

1.3.2.3. VEGF bioavailability

VEGF function is further regulated by its bioavailability. With the exception of $VEGF_{121}$, all isoforms of VEGF contain a heparin binding domain that facilitates

binding to the extracellular matrix (ECM) via HSPGs (K. A. Houck *et al.*, 1992). The binding of VEGF to the ECM establishes an effective storage mechanism for cells to readily release bioactive VEGF when necessary through actions of the matrix metalloproteinase (MMP) family (Hawinkels *et al.*, 2008). MMP2 and MMP9 have been directly associated with VEGF release. Ovarian cancer cell lines SKOV3 and OVCAR3 release biologically active VEGF when treated with recombinant MMP2 and MMP9 (Belotti *et al.*, 2003). Bergers et al reported MMP2, and in particular MMP9 also induce VEGF secretion from normal pancreatic islet cells. Interestingly, in context of an established tumour, they discovered the source of MMP9 to be infiltrating inflammatory cells and not the tumour cells themselves (Bergers *et al.*, 2000).

1.4. Targeting VEGF in melanoma

1.4.1. Angiogenesis

The process of angiogenesis, a dynamic process involving new blood vessel formation is well characterised and has been identified as a hallmark of malignancy (Hanahan *et al.*, 2018). Physiologically, angiogenesis is important in wound healing, embryogenesis and the female reproductive cycle (Dewing *et al.*, 2012). The importance of angiogenesis in malignancy is highlighted by the fact that oxygen has a diffusion limit of 100-200 microns (Schumacker *et al.*, 1989) and therefore growing tumours are vulnerable to ischaemic stress if not for the capability to vascularise as they progress. Central to the process is the "angiogenic switch", where tumours in response to stressors including hypoxia, acidosis and oncogenic mutations, tumours transcribe genes required for survival (Kandel *et al.*, 1991; Dewing *et al.*, 2012).

VEGF is a key component of the switch and driver of angiogenesis and was identified as such over 30 years ago (Senger *et al.*, 1983) as described above. VEGF initiates angiogenesis by increasing endothelial cell permeability, allowing extravasation of plasma proteins to degrade the adjacent ECM, in preparation for endothelial cell migration (Kevil *et al.*, 1998). Angiogenesis is next orchestrated by the designation and co-ordination of endothelial cells into "tip" and "stalk" phenotypes. VEGF binds concurrently to VEGFR2 and NRP1 on endothelial cells to initiate downstream signalling as discussed above. Delta-like ligand 4 (DLL4) is upregulated and binds to Notch in adjacent endothelial cells and these adjacent cells upregulate the "VEGF traps" VEGFR1 and sVEGFR1, reduce VEGFR2 expression and consequently develop a "stalk" phenotype (Blanco *et al.*, 2013). Conversely, the "tip" phenotype form in other endothelial cells as DLL4 is antagonised by Jagged-1 (JAG1) which downregulates Notch signalling and increases VEGFR2 expression (Hellstrom *et al.*, 2007). Angiogenesis proceeds as tip cells migrate towards a VEGF source and are supported by proliferating stalk cells. Vessel maturation later occurs with ECM deposition and pericyte coverage (Blanco *et al.*, 2013). The end product is a new blood vessel capable of nutrient delivery.

1.4.2. Angiogenesis and VEGF in melanoma

Melanoma is a vascular tumour and blood flow has been detected via doppler ultrasound in melanomas as small as 0.9mm (Srivastava *et al.*, 1986). Tumour vascularity has been shown to correlate with recurrence risk in a series of primary melanomas (Srivastava *et al.*, 1988). A separate study in primary melanomas has shown an association between the percentage of vascular coverage and maximal

tumour thickness (Fallowfield *et al.*, 1991).

Consistent with its role in angiogenesis, VEGF has also been associated with melanoma progression. VEGF is expressed in at least 50% of primary melanomas (Simonetti *et al.*, 2002). Serum VEGF positively correlates disease stage (Ugurel *et al.*, 2001). In a large study quantifying VEGF, VEGFR1 and VEGFR2 in 988 immunohistochemistry (IHC) microarray samples consisting of benign naevi, primary and metastatic melanoma samples, VEGFA and VEGFR2 expression was higher in malignant compared to benign melanomas and in metastatic compared to primary tumours (Mehnert *et al.*, 2007).

Based upon its likely role in propagating the progression of melanoma, VEGF has been identified as a valid therapeutic target and strategies to mitigate its function have been explored clinically.

1.4.3. Bevacizumab in melanoma

Anti-VEGF therapies can be classified into two broad groups: monoclonal antibodies and small molecule tyrosine kinase inhibitors targeting the VEGFR2 receptor (Corrie *et al.*, 2010).

The tyrosine kinase inhibitors block intracellular VEGF signalling and typically block more than one enzymatic target. Multiple agents have been tested in clinical trials recruiting patients with metastatic melanoma, either as single agents or in combination with other treatments: Sorafenib (targeting VEGFR2, VEGFR3 and BRAF), Sunitinib (VEGFR1, VEGFR2, PDGFα, PDGFβ, KIT, FLT3, RET and CSF1R), Axitinib (VEGFR1, VEGFR2, PDGFR and KIT), Valatanib (VEGFR1, VEGFR2, PDGFR, KIT and c-FMS) and Cediranib (VEGFR1, VEGFR2 and

VEGFR3) (Corrie *et al.*, 2010; McWhirter *et al.*, 2016).

Activity has generally been disappointing, with response rates in all trials consistently below 20% (summarised in Corrie, Basu and Zaki, 2010), and none of these therapies are liscensed for routine clinical use in melanoma (www.pathways.nice.org.uk) .

Bevacizumab is a humanised monoclonal antibody that bind to and neutralises VEGF, preventing it from binding to VEGFR2 (Ferrara *et al.*, 2005). Bevacizumab is the most frequently investigated anti-angiogenic drug in melanoma and most clincial trials to date have been conducted in patients with metastatic disease.

Bevacizumab was first evaulated in metastatic melanoma in 2007 where it was given alone or in combination with interferon-α2b. The two arms did not differ with respect to clinical benefit and overall survival was 10 months although durable responses were reported (Varker *et al.*, 2007). A subsequent trial with high dose interferon-α2b reported better outcomes, with a median overall survival of 17 months in the combination arm (Grignol *et al.*, 2011). In the randomised phase II BEAM clinical trial from 2012, patients with previously untreated metastatic melanoma, received chemotherapy (carboplatin and paclitaxel) with or without bevaciuzumab. Overall survival was not statistically different between the two arms and reached a figure of 12.3 months in the combination arm, comparable to earlier studies. This figure however was probably better than expected appreciating that 73% of patients had stage M1c disease (Kim *et al.*, 2012). A phase II trial published in 2015 treated 50 patients with metastatic melanoma with first line nanoparticle albumin–bound (nab) paclitaxel plus bevacizumab and reported 30% response rate and 17 month median overall survival. Encouragingly, 10 patients (20%) were still alive at 41 months, suggesting this may be a promising combination (Spitler *et al.*, 2015). A summary of

clinical trials testing bevacizumab in patients with metastatic melanoma is presented in Table 1-4.

Author	Setting	Regimen	No. patients	Response Rate (CR +PR) (%)	Median PFS (months)	Median OS (months)
(Varker et al., 2007)	Metastatic	Bev	16	(not reported)	3	8.5
		Bev+ interferon-α2b	16		3	10
(Peyton et al., 2009)	Metastatic	Bev + everolimus	28	4	4	(not reported)
(Slingluff et al., 2013)	Metastatic	Temsirolimus + bev	17	17.7	(not reported)	(not reported)
(Kottschade et al., 2013)	Metastatic	Temozolamide + bev	42	23.8	3.8	12.3
		Carboplatin + nab paclitaxel + bev	51	33.3	6.9	14.7
(Kim et al., 2012)	Metastatic	Carboplatin + paclitaxel +placebo	71	16	4.2	8.6
		Carboplatin + Paclitaxel +bev	143	26	5.6	12.3
(Grignol et al., 2011)	Metastatic	Bev + interferon-α2b	25	24	4.8	17
(McWilliams et al., 2018)	Metastatic	Carboplatin +paclitaxel + bev	75	13	5.6	14.5
		Carboplatin +paclitaxel + bev + everolimus	73	26	5.1	11.2
(Ferrucci et al., 2015)	Metastatic	Dacarbazine + bev	37	19	5.5	11.4
(Spitler et al., 2015)	Metastatic	Bev+ nab paclitaxel	50	36	7.6	16.8

Table 1-4: Outcomes from phase II and III trials evaluating bevacizumab in the treatment of metastatic melanoma. Bev = bevacizumab, CR = complete response, PR = partial response, PFS = progression free survival, OS = overall survival

Despite some promising results, bevacizumab did not generate sufficient evidence to become part of the standard of care for the treatment of patients with metastatic melanoma. Presently, in the era of successful oncogenic BRAF targeting and immune checkpoint inhibitors, the role of bevacizumab in metastatic disease is unclear. Despite this, the immunomodulatory role of VEGF is an active area of research, and clinical trial data evaluating bevacizumab in combination with checkpoint inhibition

are awaited (Yang *et al.*, 2018).

1.4.4. The AVAST-M clinical trial

A therapeutic role for targeting VEGF to reduce post-operative melanoma recurrence was explored in the phase III AVAST-M adjuvant clinical trial (Corrie *et al.*, 2014). The trial was based on a hypothesis that VEGF driven angiogenesis is necessary for the progression of micro-metastatic disease to advanced metastatic disease and therefore the trial targeted VEGF aiming to reduce post-operative recurrence for patients with high-risk melanomas. Between 2007 and 2012, the AVAST-M trial recruited 1343 patients with AJCC 7th defined stage IIB, IIC or III melanoma who were randomised 12 months of adjuvant bevacizumab or observation, the standard of care at the time. The study was powered to detect a difference in overall survival and an interim analysis reported no significant differences between the two arms (HR 0.97, 95% CI 0.78–1.22; p=0.76). However, patients treated with bevacizumab experienced a greater disease free survival compared to those in the observation arm (HR 0.83, 95% CI 0.70–0.98, p=0.03) and in a pre-planned subgroup analysis, performed 1 year after all patients had completed treatment, the disease free survival benefit observed in the bevacizumab arm was almost exclusively in those patients harbouring BRAF^{V600E} mutant melanomas (Corrie *et al.*, 2014) (figure 1-2).

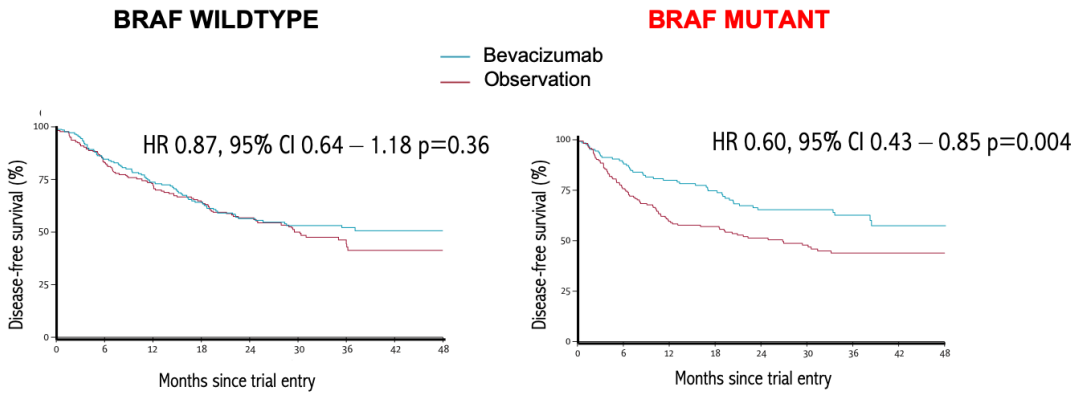

Figure 1-2: Kaplan Meier Curves demonstrating superior benefit in disease free survival in patients treated with bevacizumab whose tumours harboured a $BRAF^{V600E}$ mutation. Adapted from Corrie *et al.*, 2014

The mature trial data presented in 2017 reported a persisting disease free survival benefit in the bevacizumab arm (HR 0.85; 95% CI 0.74-0.99, p=0.04), although this did not translate into an improvement in overall survival (HR 0.99; CI 0.84-1.18, p=0.96). Patients with BRAF mutant melanomas treated with bevacizumab no longer exhibited an improved disease-free survival (HR 0.79 95% CI 0.58-1.08, p=0.14) nor overall survival (HR 0.79; 95% CI 0.55-1.13, p=0.20). In contrast, bevacizumab treated patients with BRAF wildtype melanomas had a significantly inferior disease free survival (HR 1.39; 95% CI 1.03-1.88; p=0.03) and however no worse overall survival (HR 1.18; 95% CI 0.85-1.62, p=0.20) (Corrie *et al.*, 2017).

The improved clinical outcomes seen in the interim analysis (available at the beginning of this project) for patients with BRAF mutant melanomas treated with bevacizumab had not previously been reported and implies differential sensitivity of BRAF mutant melanomas to VEGF inhibition. Although increased HIF-1α expression has been reported in $BRAF^{V600E}$ mutant melanomas previously (Kumar *et al.*, 2007), VEGF expression has not been compared between mutant and wildtype genotypes.

Furthermore, genes differentially expressed between $BRAF^{V600E}$ and wildtype melanomas that upregulate VEGF or promote differentially sensitivity to bevacizumab remain unexplored.

1.5. Hypothesis

The AVAST-M clinical trial described a novel association between the $BRAF^{V600E}$ mutation in melanoma and increased sensitivity to anti-VEGF monoclonal antibody, bevacizumab (Corrie *et al.*, 2014). The $BRAF^{V600E}$ mutation has not previously been reported as a biomarker for bevacizumab sensitivity. Furthermore $BRAF^{V600E}$ driven mechanisms linking to angiogenesis and VEGF expression were poorly understood.

The fundamental hypotheses of this project were that:

1) The $BRAF^{V600E}$ mutation in melanoma increases the expression of VEGF.
2) The $BRAF^{V600E}$ mutation drives transcriptional changes that promote expression of VEGF.
3) $BRAF^{V600E}$ mutant melanomas are more dependent on VEGF, explaining their sensitivity to bevacizumab.

The goals of this project were to gain an insight into the clinical effect observed in the AVAST-M trial. This project aimed to explore the biology arising from the $BRAF^{V600E}$ mutation with the ultimate goal of understanding the response to VEGF inhibition and potentially discovering new therapeutic targets for patients with malignant melanoma.

2. Chapter II: Materials and Methods

2.1. Cell lines and culture

Melanoma cell lines were cultured in Dulbecco's Modified Eagle Medium (DMEM) (Gibco®) or RPMI 1640 that was supplemented with 10% foetal calf serum (FCS, Thermo Fisher) with 100 units/ml of penicillin and 0.1 mg/ml streptomycin. Cells were incubated at 37°C in a humidified atmosphere of 10% CO_2 and 90% air. For hypoxic experiments, cells were incubated at 37°C with humidified atmosphere of 1% O_2.

The CHL1 cell line was obtained from the American Type Culture Collection (ATCC). A375P and A375M cells were obtained from Professor Colin Goding (Ludwig Institute for Cancer Research Oxford), SKMEL28 from Cancer Research UK Cell Services and SKMEL23 from Professor Vincenzo Cerundolo (Weatherall Institute of Molecular Medicine Oxford). Human umbilical vein endothelial cells (HUVEC) cells were purchased from Lonza (#2517A) and cultured in EGM^{TM}-2 supplemented with Growth Medium-2 BulletKit^{TM} (Lonza, #CC-3162) at 10% CO2. LM cell lines were obtained under a Material Transfer Agreement from the Ludwig Institute for Cancer Research in Melbourne, Australia (Behren *et al.*, 2013). Cell lines were authenticated using the Human cell line authentication services provided by Eurofins Genomics. All cell lines were regularly tested for mycoplasma (MycoAlert kit, Lonza Rockland Inc, Rockland US). When cells were approximately 80% confluent, they were trypsinised using a 1 x solution (Trypsin-EDTA, Lonza) and passaged at 1:10 or 1:20 ratio for sub-culturing, before they were discarded after 20 passages. Cells were banked with freezing medium containing 10% dimethyl 40 sulphoxide (DMSO) and 90% FBS and transferred to cryovials followed by snap

freezing the “Mr Frosty” freezing contained, placed in -80°C for slow cooling, then transferred to nitrogen vapour for long term storage. Melanoma cell lines used for this project are listed in table 2-1**.**

Cell line	Medium	BRAF	NRAS	Other notable mutations
A375P	DMEM	V600E	WT	
A375M	DMEM	V600E	WT	
CHL1	DMEM	WT	WT	p53, CDKN2A
SKMEL 5	DMEM	V600E	WT	
SKMEL28	DMEM	V600E	WT	p53
SKMEL23	DMEM	WT	WT	
CHL1 isogenic clones	DMEM	WT/V600E	WT	
A375M ROR2 cDNA clones	DMEM	V600E	WT	
CHL1 ROR2 cDNA clones	DMEM	WT	WT	
LM19	RPMI 1640	WT	Q61K	
LM44	RPMI 1640	WT	WT	

Table 2-1: Melanoma cell lines used in this project. Mutation information obtained from The Cancer Cell Line Encyclopaedia at www.portals.broadinstitute.org

2.2. Cell treatments

2.2.1. siRNA knockdown of ROR2

ROR2 (Life Technologies, #AM51331 and Qiagen, # SI00287518) and AllStars negative control siRNA was prepared at 20μM stocks and stored at -20°C and thawed on ice. Cells were seeded 6-8 x 10^5/10cm dish (to achieve 40% confluency) and the following day were transfected with 20nM of the appropriate siRNA using Lipofectamine 2000 (Life Technologies) as the transfection reagent. For a 10cm dish transfection, 9μl of siRNA was mixed with 1.5mls of OptiMEM® (Life Technologies)

and incubated for 5 minutes at room temperature. In parallel, 9µl of Lipofectamine 2000 was mixed with 1.5mls of OptiMEM and also incubated at room temperature for 5 minutes. The siRNA and Lipofectamine 2000 solutions were then mixed and incubated for 25 minutes. Cells were washed once with OptiMEM. The siRNA/Lipofectamine 2000 mixture was added dropwise to the cells followed by a further 6mls of OptiMEM. Cells were incubated for 6 hours, after which the OptiMEM/siRNA/Lipofectamine solution was removed and replaced with 10mls medium (DMEM with 10% FCS). Cells were harvested 48 hours after transfection for further analysis.

2.2.2. siRNA knockdown of Osteopontin

A total of 1 x 10^6 cells were seeded in a 10cm dish on Day minus 1 (D-1). On D0, 6.8µl of 20nM Osteopontin siRNA (Dharmacon) of All Stars negative control was added to 1.5mls of OptiMEM. In parallel, 12µl of Oligofectamine (Invitrogen) was mixed with 409µl OptiMEM. Both solutions were incubated separately for 5 minutes and then mixed and incubated for a further 25 minutes. Cells were washed twice in OptiMEM and then the siRNA/Oligofectamine mixture was added dropwise with a further 777µl of OptiMEM. Cells were incubated cells for 4 hours and then topped up with DMEM +10%FCS to a total volume of 10mls. Cells were harvested for analysis 48 hours later.

2.2.3. Small molecule inhibitors

All small molecule inhibitors were available as 10mM stock solutions, reconstituted in DMSO. PLX4720 (Selleck, #S1152) is a small molecule selective inhibitor of $BRAF^{V600E}$. It was stored in aliquots at -20°C. Trametinib (Selleck, #S2673) is a MEK inhibitor and aliquots were stored at -80°C. CT1746, a MMP inhibitor, was

kindly provided by Professor Yoshi Itoh (Kennedy Institute of Rheumatology, Oxford University) and was stored at -20°C. All aliquots were used once to avoid repeated freeze/thawing cycles.

2.3. Western blotting

Cells were treated as required and harvested at 80-90% confluence. Cells were washed with ice-cold phosphate buffered saline (PBS) twice and treated with 1ml of 1xTrypin/ Ethylenediaminetetraacetic acid (EDTA) solution and incubated at 37°C for 3 minutes. 4mls of DMEM + 10% FCS was then added to the cells and the entire mixture collected centrifuged at 1200 rpm for 5 minutes at 4 °C. After removing the supernatant, 100 µl of Radioimmunoprecipitation (RIPA) buffer (Thermo Scientific, #89900) containing protease and phosphatase inhibitors (Thermo Scientific, #78444) was added. After incubating on ice for 30 minutes, the cell lysate was centrifuged at 15,000 rpm for 15 minutes at 4 °C to remove cell debris. Soluble protein was then quantified using the Pierce Bicinchoninic Acid (BCA) protein assay (Thermo Fisher Scientific, UK) and equal amounts of protein were denatured in 3 x Laemmli Buffer (70 mM Tris pH 6.8, 5% (v/v) β-mercaptoethanol, 40% (v/v) glycerol, 3% (v/v) SDS, 0.05% (v/v) Bromophenol Blue) at 95 °C for 5 minutes. Proteins were separated by molecular weight by SDS polyacrylamide gel electrophoresis on 4-12% gradient Bis-Tris pre-cast gels (Life Technologies, #NP0335BOX). Proteins were transferred to methanol activated polyvinylidene difluoride (PVDF) membrane in transfer buffer (BioRad TransBlot Turbo transfer buffer) using the Trans-Blot® TurboTM Transfer System (BioRad) 2.5A and 25V for 10 minutes. Membranes were blocked to reduce nonspecific protein binding, with 5% (w/v) non-fat dairy milk (Sigma) in TBST (Tris-

buffered saline with 0.1% Tween 20 [Sigma]) at room temperature for 1 hour. Membranes were incubated overnight at 4°C overnight with primary antibodies (table 2-2). After washing with TBS-T for 3 times with 5 minutes each time, membranes were incubated with goat anti-rabbit or goat anti-mouse secondary antibody conjugated to horse-radish peroxidase for one hour at room temperature. Membranes were then washed again and proteins were detected using Enhanced Chemiluminescence (ECLplus, Amersham Pharmacia Biotech).

Antibody (species)	**Source (catalog number)**	**Dilution (1°)**	**Dilution (2°)**
ROR2 (mouse)	Santa-cruz (sc-374174)	1:1000	1:10000
pERK (rabbit)	Cell Signalling; #4370	1:1000	1:10000
Total ERK (rabbit)	Cell Signalling; #4695	1:1000	1:10000
HIF-1α (mouse)	BD Transduction Laboratory #610959	1:1000	1:10000
β-tubulin (mouse)	Cell Signalling; #2146	1:5000	1:10000

Table 2-2: Antibodies used for western blotting in this project

2.4. RNA analysis

2.4.1. RNA extraction

Cells were harvested and pelleted as described for protein harvesting. RNA was extracted from cell pellets using the PureLink RNA Mini Kit (Life Technologies, #12183018A) according to the manufacturer's protocol. Cells were lysed in 600µl of

lysis buffer from the kit with 1% β- mercaptoethanol added. Lysates were passed through a 19 gauge needle 5-6 times, before they were transferred to a extraction column for the RNA to bind to the membrane. DNase I (Life Technologies, #12185010) reconstituted in RNAse free water, was then added to the membrane to digest the genomic DNA. The column was incubated at room temperature for 15 minutes and washed as per the kit protocol. RNA was eluted in 30µl of RNase-free water, and then quantified using the NanoDrop 2000c Spectrophotometer. RNA purity was determined by the ratio of absorbance at 260nm versus 280nm with ideal values around 2.0. RNA was stored at -80°C.

2.4.2. Reverse transcription

Complementary DNA (cDNA) was reverse transcribed from RNA samples using the SuperScript® III First-Strand Synthesis SuperMix (Invitrogen, #11752-050) according to the manufacturer's protocol. To make the reaction mix, 2µl of the enzyme mix containing reverse transcriptase, 1µg of total RNA and 10µl of 2x reverse transcriptase reaction buffer (containing random primers and dNTPs) were added to a PCR tube, before RNase free water was added to make the final volume of 20µl. The contents were gently mixed and placed in a Thermo Cycler to incubate with the following conditions: 10 minutes at 25 °C, then 30 minutes at 50 °C, then 5 minutes at 85 °C. After the incubation, the PCR tubes were placed on ice to chill and 1µl of E. coli RNase H was added to digest any remaining RNA. Tubes were incubated at 37 °C for 20 minutes. The cDNA samples were either used immediately or stored at -20 °C.

2.4.3. Real time quantitative Polymerase Chain Reaction (qRT-PCR)

2.4.3.1. Primer design

Primers for qRT-PCR were designed and their specificity checked using the online National Centre for Biotechnical Information (NCBI) Primer BLAST programme (https://www.ncbi.nlm.nih.gov/tools/primer-blast/). NCBI mRNA reference sequence accession numbers were used to generate primers for each target gene. Primers were designed to generate products between 100 and 400 base pairs (products less than 200 base pairs were preferentially selected), have a GC content of between 50 and 60% and avoid 3′ complementarity. In select cases, sequences referenced in publications were used following confirmation for target sensitivity using Primer BLAST.
The primers used for this project and their sequences are described in table 2-3:

Gene	Forward primer	Reverse primer
β2-M	TGCTGTCTCCATGTTTGATGTATCT	TCTCTGCTCCCCACCTCTAAGT
FGFR1	AGGTGGCTTGGTGTAGAAGC	GAAGACGGAATCCTCCCCTG
FLT1	CAAATAAGCACACCACGCCC	TTCTTCCCACAGTCCCAACT
HIF-1α	GCCAGACGATCATGCAGCTA	ATCCATTGATTGCCCCAGCA
IGFBP2	ACACTTCTTCCCTGCGTGC	GGGAGTAGAGGTGCTCCAGA
LEF1	CCCGAAGAGGAAGGCGATTTA	GGGAAAACCAGCCAAGAGGT
MMP2	GGCGGTCACAGCTACTTCTT	GCCTAGCCAGTCGGATTTGA
MMP9	TCTATGGTCCTCGCCCTGAA	CATCGTCCACCGGACTCAAA
MART1	CACGGCCACTCTTACACCAC	GGAGCATTGGGAACCACAGG
MITF	CCCATGGCTATGCTTACGCT	CCCATGGCTATGCTTACGCT
NDRG1	GGTGAAGCCTTTGGTGGAGA	GGTGAAGCCTTTGGTGGAGA
PDGRFA	TCACCTATCAAGTTGCCCGAG	TCCACTTCACGGGCAGAAAG
ROR2	GCACAGACTTCCCTGAGCTT	AGGGTACGTCACACAGTTCC
SCUBE2	CATCCTGCTTCATCTGCCTGA	TGGATGAAGTTTTACACTGGGTT
SETDB2	TCAATAAAGGATCCTATGCCTGTG	TCAATAAAGGATCCTATGCCTGTG
SFRP1	GCGAGTACGACTACGTGAGC	AGGTGGCTTGGTGTAGAAGC
SNAI1	CCCCAATCGGAAGCCTAACT	GGACAGAGTCCCAGATGAGC
SPP1	ATCTCCTAGCCCCACAGACC	AACCACACTATCACCTCGGC
TCF4	GCCTTAGGGACGGACAAAGAG	GGGCTTGGATGTCCTCCATT
TRRAP	ATTTCCGAGTGCGGGAGATG	AGAGGTCTGGCGTCTTTGTG
TUBA6	CCCCTTCAAGTTCTAGTCATGC	ATTGCCAATCTGGACACCA
UBC	ATTTGGGTCGCGGTTCTTG	TGCCTTGACATTCTCGATGGT
$VEGF_{165}$	ATCTTCAAGCCATCCTGTGTGC	CAAGGCCCACAGGGATTTTC
VEGFR2	GGCCCAATAATCAGAGTGGCA	CCAGTGTCATTTCCGATCACTTT
WISP1	TGGCTGTGAGTGCTGTAAGA	ACACTTCTTCCCTGCGTGC
Wnt5a	TAAGCCCAGGAGTTGCTTTG	GCAGAGAGGCTGTGCTCCTA
ZEB1	GGATGACCTGCCAACAGACCA	CATCCTGCTTCATCTGCCTGA

Table 2-3: Sequences of all primers uses in this project

2.4.3.2. qRT-PCR

For ROR2 mRNA quantification in A375M, SKMEL28 and the $BRAF^{V600E}$ and wildtype isogenic CRISPR clones, a one-step qRT-PCR process was used. Luna® Universal One-Step qRT-PCR kit (New England Biolabs #E3005S) was used. The reaction master mix contained DNA Polymerase, dNTPs, a fluorescent dsDNA-binding dye, and all required buffer components. The PCR reaction consisted of 10µl reaction master mix, 1µl Luna Warm-Start® reverse transcriptase, 1.26µl each of forward and reverse primers (0.4µM final concentration), template RNA and nuclease free water up to a total volume of 20µl. A mock reverse transcription reaction excluding RNA template served as a "non-template control" to exclude amplification of contaminating genomic DNA and RNA material. The quantity of template RNA was the lowest amount necessary to generate a C_T value below that of the non-template control and was in the range of 800-1500 ng per reaction.
PCR conditions were: 55°C for 10 minutes, 95°C for 1 minute followed by 40 cycles alternating between 95°C for 10 seconds and 60°C for 1 minute. Reactions were carried out in triplicate, unless otherwise stated.

For other qRT-PCR reactions, a 2-step procedure was used. This consisted of SYBR Select master mix (Life Technologies, #4472908) containing SYBR® Green Dye, DNA polymerase, ROXTM dye Passive Reference, dNTPs and optimized buffer components. Reactions were performed according to the manufacturer's protocol. For each reaction, 20ng of cDNA template and 10µl of forward and reverse primers (final concentration 0.5µM) were added to 10µl of the master mix. RNase-free water was added to make the final volume of 20µl. The reaction mix was then placed on the Applied Biosystems® 7500 Real-Time PCR System using the following settings:

50°C for 2 minutes, 95°C for 2 minutes followed by 40 cycles alternating between 95°C for 15 seconds and 60°C for 1 minute. Reactions were carried out in triplicate, unless otherwise stated.

2.4.3.3. Relative quantification of mRNA of genes of interest

Relative quantification was performed using the $2^{-\Delta\Delta Ct}$ method reported by Livak et al (Livak *et al.*, 2001) to express fold differences in the levels of mRNA in a test sample compared to control. mRNA levels of a reference housekeeping gene (HKG) were used to normalise differences encountered in loading between samples. The formula used was therefore:

ΔC_T (test sample) = C_T (target gene, test) - C_T (HKG, test)

ΔC_T (control sample) = C_T (target gene, control) - C_T (HKG, control)

The ΔC_T of the test sample was then normalised to that of the control:

$\Delta\Delta C_T = \Delta C_T$ (test sample) - ΔC_T (control sample)

The fold change was then calculated as:

$2^{-\Delta\Delta CT}$ (the normalised expression ratio).

For experiments where fold change against a single control was not appropriate, C_T values were still normalised however not as expressed as ratio using the formula:

$2^{-\Delta CT \text{ (test sample)}}$

2.5. Cell based assays

2.5.1. Cell proliferation assay

Cells were treated, harvested and maintained in solution. Cell count was determined using the Countess™ automated cell counter (Thermo Fisher). Cells were diluted to a concentration of 4 x 10^4 cells per ml, and 50µl cell suspension (containing 2000 cells) was seeded into each well of a flat bottom 96 well plate. Triplicate wells were plated out for each time point. Cells were stained using solution of Hoechst 33342 Solution (20mM) mixed with an equal volume of Propidium Iodide (1.0 mg/ml), diluted to 1:1000. At each time point, 50µl of the Hoechst and Propidium Iodide solution was added to the relevant well incubated for 30 minutes. Cell count was performed using the Celigo (Nexcelcom) automated imaging cytometer. Focus and exposure were automatically determined. Cell count was reported as the total cell count.

2.5.2. Cell invasion assay

Cell invasion was measured using the xCELLigence® Real-Time Cell Analysis instrument following the manufacturers protocol. Culture medium in cells was replaced with serum free medium, and cells serum starved for 6 hours. Cells were washed once with PBS, trypsinised using trypTLE (Gibco #12605036) and re-suspended in serum free medium. Cells were counted using the Countess™

automated cell counter. Concentrations as described of growth factor reduced Matrigel™ (Corning #356230) in volume of 50µl were plated onto a microporous membrane containing 8µm pores within a 16 well, 2 unit Boyden chamber (Acebio #5665817001) and then incubated at 37°C for 2 hours. From the serum free cell suspension, 40,000 cells in a volume of 100µl were added on top of the hardened matrigel. The chamber was then placed directly on top of a lower chamber with wells containing culture medium with 10% FCS to served as a chemoattractant.

An electrical current passing through microelectrodes beneath the matrigel continually measured impedance. Cells migrating onto the microelectrodes increased impedance and thus provided a readout for invasion, arbitrarily defined as the "cell index". Readings were taken every 15 minutes. A schematic for this experiment is presented in figure 2-1.

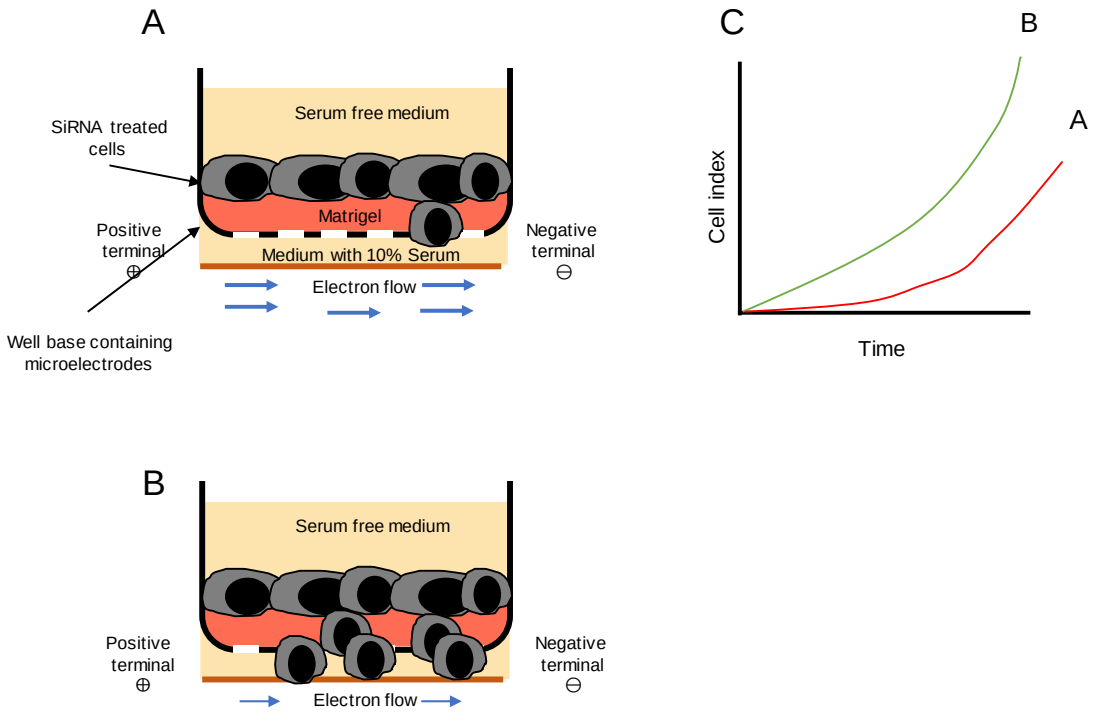

Figure 2-1: Quantification of cell invasion using the xCELLigence® Real-Time Cell Analysis system

2.5.3. Endothelial proliferation assay

Human umbilical vein endothelial cells (HUVECs) in culture for no more than 6 passages were washed twice with PBS, harvested using TryptLE® and suspended in 5-10 mls DMEM + 10% FCS. Cells were counted and a known quantity was removed and centrifuged (1200 rpm for 5 minutes). The supernatant was removed and the cell pellet resuspended in EGM^{TM}-2 Growth Medium-2, containing all BulletKit^{TM} components as provided by the kit with the deliberate omission of VEGF. Then, 50µl of this solution containing 2000 HUVECSs was plated into wells of a 96 well, flat bottomed plate and 50µl of conditioned medium taken from ROR2 or control siRNA transfected A375M cells was added to the endothelial cells. As a positive control, 1µl of recombinant $VEGF_{165}$ (50ng/mL) was added to the relevant wells. The concentration selected was in excess of that shown to promote endothelial cell proliferation in the literature (Keyt et al., 1996) At inervals, HUVECS were stained with 1µl Hoechst and Propidium Iodide solution described above and an automated cell count was performed using the Celligo imaging cytometer using the same settings as in section 2.5.1. Total cell count was selected as the readout.

2.6. VEGF enzyme-linked immunosorbent assay (ELISA)

2.6.1. Sample preparation

Cells were cultured to a maximum of 80% confluence then trypsinised, harvested and suspended in DMEM + 10% FCS. Cell concentration was determined using the Countess^{TM} automated cell counter. Resuspended cells were centrifuged for 5 minutes

at 1200 rpm. The supernatant was removed and immediately stored at -80°C. Cell pellets were snap frozen and also stored at -80°C. At the time of analysis, cell pellets were lysed in 200µl of RIPA buffer containing protease and phosphatase inhibitors. Culture supernatants were thawed at room temperature and centrifuged at 1200 rpm for 5 minutes to remove cell debris.

2.6.2. VEGF ELISA procedure

VEGF in conditioned media samples and in the cell lysates was measured with the R&D system VEGF ELISA kit (R&D system, #DVE00) following the manufacturers instructions. The ELISA kit contained baculovirus expressed recombinant human $VEGF_{165}$ antibodies raised against the recombinant $VEGF_{165}$ protein. Data provided by the manufacturer demonstrated that antibodies in the kit were cross-reactive with both $VEGF_{165}$ and $VEGF_{121}$ and therefore the assay was appropriate for the detection of both isoforms.

Wash buffer and standard dilutions were prepared according to the manufacturer's protocol, and 50µl of assay diluent was added to each well of the 96 well microplate that was pre-coated with VEGF-specific monoclonal antibody. Standard (200µl) or samples (200µl for conditioned medium, 100µl for lysates), each in duplicate, were added to the respective wells, and the plate was covered with a plate sealer, and incubated at room temptation for 2 hours. The plate was washed with kit provided wash buffer for 3 times, before 200µl conjugate solution was added to each well and then incubated at room temperature for a further 2 hours. The plate was then washed with wash buffer for 3 times, before 200µl of activated substrate solution (a mixture of stabilized hydrogen peroxide and tetramethylbenzidine) was added. The plate was sealed again and placed in the dark for 20 minutes. After the incubation, 50µl of stop

solution containing 0.2M sulfuric acid was added to each well. The plate was then read at 450 nm using the POLARstar Omega (BMG labtech) plate reader with a wavelength correction at 540 nm.

From the standard curve, VEGF concentrations (pg/ml) for each sample well were determined.

To reduce variability between samples attributable to cell number, VEGF concentrations for each sample were adjusted using the ratio of cell concentration between the sample and control for an individual experiment using the formula:

$$\textbf{Adjusted VEGF concentration} = \textbf{Raw VEGF concentration} \times \frac{\textbf{cell concentration } \left(\frac{\textbf{cells}}{\textbf{ml}}\right)_{\textit{control sample}}}{\textbf{cell concentration } \left(\frac{\textbf{cells}}{\textbf{ml}}\right)_{\textit{sample}}}$$

Data were expressed in terms of fold change relative to control.

2.7. Recombinant MMP2 treatment

Cells were transfected with siRNA as described earlier. Recombinant MMP2 (R&D #902-MP-010), 10µg, purchased in powder form was reconstituted in PBS containing 0.005% bovine serum albumin (BSA) to a volume of 1000µl (concentration 10µg/ml). 20µl of MMP2 or DMSO were then added to a (1mM) solution of p-aminophenylmercuric acetate (APMA), (Sigma # A-9563) mixed in PBS and incubated at 37°C for 1 hour. APMA was then removed using column filtration equilibrated in PBS performed to achieve an elutate of 3.5mls. Medium was removed from target cells and replaced with 8.83mls fresh medium (DMEM+10% FCS) and 1.16µl of activated MMP2/DMSO to a final concentration of 6.6ng/ml. Cells were incubated at 37°C and harvested for VEGF analysis the following day.

2.8. ROR2 overexpression

A ROR2 expression plasmid was purchased from Origene (www.origene.com # RC215640), of 7.7kb in size that contained the ROR2 cDNA downstream from a CMV promoter. The plasmid also contained genes coding for resistance to the antibiotic Kanamycin (for bacteria) and Neomycin/G418 (for mammalian cells). (figure 2-2 A-B). Empty vector plasmid (pCMV6 #PS100001) also containing a CMV promoter and the same antibiotic resistance genes was kindly provided by Dr James Chettle (post doctoral scientist, Department of Oncology, Oxford).

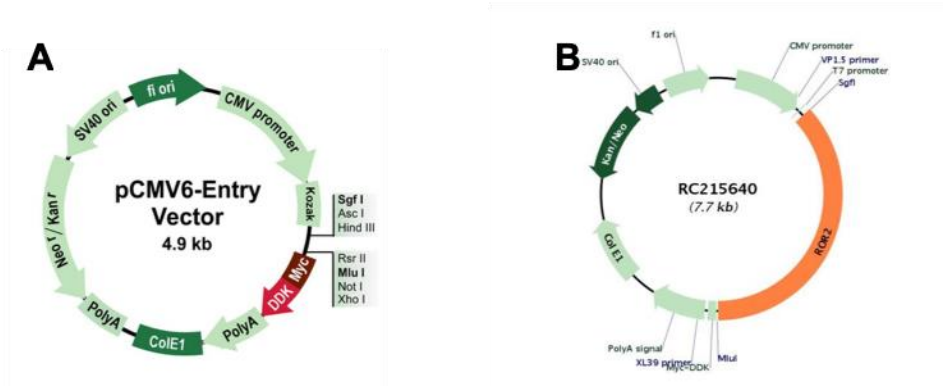

Figure 2-2: Plasmids used for the creation of ROR2 overexpressing cell lines A. Empty Vector B. ROR2 cDNA containing plasmid

2.8.1. Plasmid transformation into competent E.coli bacteria

Plasmids were transformed into One Shot^{TM} TOP10 Chemically Competent E. coli (#C4040-10) as per the manufacturer's instructions. E. coli cells were thawed on ice. For each reaction 10ng of DNA was added and mixed gently. The mixture was incubated on ice for 30 minutes followed by heat shock for 30 seconds at 42°C in a water bath. Kit provided Super Optimal Broth (SOC) medium (250µl) was added and the mixture was incubated for 1 hour at 37°C in a shaking incubator at 225rpm. Using a flame sterilised cell spreader, 30ul of the mixture was evenly spread over pre-mixed LB agar plates containing kanamycin 50µg/ml. Plates were incubated at 37°C

overnight. Colonies were selected and transferred into Falcon tubes containing 10 ml autoclaved LB medium also containing Kanamycin 50µg/ml and incubated in a shaker overnight at 37°C.

Plasmid DNA was extracted using the QIAprep spin miniprep kit (Qiagen #27104). Bacterial cells were collected by centrifugation at 2000 rpm for 5 minutes, before adding 250µl of P1 buffer to resuspend the cells. Cells were lysed with 250µl P2 buffer and incubated for 3 minutes at room temperature. After the incubation, neutralising solution N3 buffer was added and the tube was inverted for 10-12 times until the solution became clear. The tubes were centrifuged for 10 minutes, before the supernatant was transferred to a spin column. The spin column was then washed with 500µl Buffer PB and then buffer PE before the plasmid DNA was eluted in 50µl of RNAse free water. The concentration of DNA samples was determined by measuring absorbance at 260 nm using the NanoDrop 2000c Spectrophotometer.

2.8.2. Transient transfection of ROR2/control plasmids into A375M cells

Cells were cultured in a 6 well plate and once approximately 70% confluent, the medium was replaced with 2ml of fresh medium (DMEM + 10% FCS). Separately, in a 1ml eppendorf tube, 2µg of plasmid DNA was added to 180µL of OptiMEM followed by 6µl of Lipofectamine 2000. The mixture was incubated for 15 minutes at room temperature and then added dropwise to the cells, which were incubated at 37°C. After 48 hours, the conditioned medium and cells were harvested for further analysis.

2.8.3. Stable transfection of ROR2/control plasmids in A375M and CHL1

Initially, kill curves were set up by culturing melanoma cells in a range of escalating concentrations (0, 100, 400, 800, 1000, 1500 μg/ml) of G418. The dose range was informed by similar experiments on the same cell lines in the literature (Li et al., 2014).

The lowest concentration that was effective at killing >95% (with visual estimation) of cells after 7 days was chosen as the dose for selection of stable transfectants. This concentration was 700μg/ml for A375M and 800μg/ml for CHL1. Cells were cultured in a 6-well plate. As per the transient transfection procedure, a mixture of 2μg of plasmid DNA and 6μl Lipofectamine 2000 was added to 180μl OptiMEM and incubated for 20 minutes at room temperature. The mixture was added to cells cultured in 2ml fresh medium (DMEM + 10% FCS). The following day, the culture medium was replaced with fresh medium containing G418, at an appropriate concentration as determined earlier. Untransfected cells were cultured in the same medium, in parallel, as controls. Following a period of initial growth, cells were passaged into a 10cm plate and cultured in DMEM + G418. Medium was changed every 3-4 days. After approximately 7 days, following widespread cell death, small colonies were visible in the transfected cells. Colonies were marked on the bottom side of the culture plate with a marker pen. After removal of medium, identified colonies were disassociated with 5μl of trypsin (1:10) added dropwise, and transferred using a sterile tip to individual wells of a 6 well plate containing DMEM + G418 and cultured. Once confluent, cells were passaged and a proportion of the yield was screened for ROR2 expression using western blot.

2.9. Gel electrophoresis

To analyse the PCR products, 1% agarose gels were made by melting 1g of agarose (Gibco-BRL) in 100 ml Tris-acetate-EDTA (TAE) buffer (Thermo Scientific, #28354). The melted gel cooled to 55°C, before adding 50µg of ethidium bromide (Pierce, #61734). The gel was then poured into a gel tank to set. Tris base, acetic acid and EDTA (TAE) buffer was then added to the tank to submerge the gel and PCR products were mixed with DNA loading dye (6x) and loaded into the wells, alongside a DNA ladder (Thermo Scientific, #R0611). Electrophoresis was performed at 125 volts for 45 minutes, before the gel was visualised using BIO-RAD Gel DocTM XR+.

2.10. Exosome quantification

Cells were transfected with siRNA as described above and after 6 hours incubation, the OptiMEM/siRNA/Lipofectamine 2000 mixture was aspirated and replaced with DMEM containing 10% exosome depleted FCS (Thermo Fischer # A272080) and incubated at 37°C. After 48 hours, conditioned medium was collected and stored at -80°C. Cells were harvested and counted. ROR2 overexpressing A375M cells were cultured in exosome depleted FCS (10%) plus DMEM for 48 hours before conditioned medium was harvested and cells counted. Media were thawed at room temperature and then ultra-centrifuged at 120,000g for 120 minutes at room termpature to pellet any extracellular vesicles.

Nanoparticle analysis (NTA) was performed by Dr Naveed Akbar (Division of Cardiovascular Medicine, Radcliffe Department of Medicine) using a protocol used in his previously published work (Akbar *et al.*, 2017).

2.11. VEGF and CD31 immunohistochemistry (IHC) on AVAST-M samples

Tissue preparation and antibody staining was performed by Leticia Campo from the Good Clinical Practice (GCP) laboratory, Oxford University. Patient samples were

available as formalin fixed tissue embedded in paraffin (FFPE). For tissue micro array (TMA) samples, 1mm cores were taken from donor blocks and embedded into recipient blocks. Whole slides were cut directly from the FFPE blocks. Automated staining was carried out with the Leica BOND-MAX autostainer (Leica, Microsystem) using the following conditions: antigen retrieval at 100ºC for 20 min with Epitope Retrieval Solution 2 (Leica Biosystems #AR9640); primary antibody incubation with either mouse anti-VEGF antibody (DAKO # M727329-8) or anti-mouse CD31 antibodies (Roche #JC70) at 1:400 dilution or IgG control for 1 h then detection using the BOND™ Polymer Refine Detection System (DS9800, Leica Biosystems) as per manufacturer's instructions.

2.12. Gene expression microarray analysis

RNA was extracted from human tumour xenografts by D.Phil student Lina Guo. Microarray analysis was performed at the Central Biotechnology Services (Henry Wellcome Building, Cardiff University School of Medicine) using the GeneChip® Human Genome U133 Plus 2.0 (Thermo Fisher #900466) and Affymetrix® mouse 4302 arrays (Thermo Fisher #900495). RNA integrity was checked by Dr Redfern, Microarray technologist, of Central Biotechnology Services, with a minimal value of 8.0 considered acceptable. Expression data were exported on .CEL files. Data analysis was performed using Transcriptome Analysis Console (TAC) v4.01 available online (https://www.thermofisher.com/uk/en/home/life-science/microarray-analysis/microarray-analysis-instruments-software-services/microarray-analysis-software/affymetrix-transcriptome-analysis-console-software.html). Library files for each array were downloaded and installed. Expression data .CEL files were uploaded. The inbuilt comparison wizard was used to guide the analysis. Differential expression

was defined by the default adjusted p-value of <0.05.

2.13. HUVEC spheroid sprouting assay

HUVEC endothelial cells were harvested and resuspended in 20ml EGM™-Plus Growth Medium to a density of 2.5 x 104 cells/ml and 200µl of 0.25% methylcellulose was added. Then 20ul drops of this suspension were added to 15cm culture dishes, inverted and incubated overnight to form spheroids. The following day, spheroids were collected, centrifuged at 1000g for 1min and resuspended in 2mls fibrinogen (2.5mg/ml in PBSA). 12.5µl of thrombin (50U/ml H2O) was added to wells in a 24 well plate and incubated at 37ºC for 15 minutes. Conditioned medium was mixed with VEGF-free EGM™-Plus Growth Medium in a 1:1 ratio to total volume 1ml. Positive control consisted of EGM™-Plus Growth Medium supplemented with 100pg of VEGF (provided by Post-doctoral researcher, Dr Helen Sheldon, Department of Oncology, Oxford University) and negative controls were cultured inVEGF-free EGM™-Plus Growth Medium alone. Medium was changed every other day.

2.14. Statistical analysis

Data were analysed using Microsoft Excel for Mac and GraphPad Prism 7 (GraphPad Software Inc, USA). Statistical significance was determined using a student t-test to compare 2 groups, one-way ANOVA for three or more groups or two-way ANOVA for comparisons between curves. A p-value < 0.05 was considered statistically significant.

3. Chapter III: Testing associations within the AVAST-M clinical trial between angiogenesis markers and the $BRAF^{V600}$ mutation

3.1. Introduction

Interim data from the AVAST-M clinical trial reported an increase in disease free survival in those patients with $BRAF^{V600}$ mutant tumours treated with the anti-VEGF monoclonal antibody, bevacizumab (HR 0.60, 95% CI 0.43–0.85, p=0·004) (Corrie *et al.*, 2014). No similar benefit was identified in those patients with BRAF wildtype tumours. This observation gave rise to the hypothesis that $BRAF^{V600E}$ mutant melanomas express higher amounts of VEGF relative to wild-type counterparts and as a consequence are more dependent up VEGF for their survival.

VEGF is a key driver of angiogenesis, which has an important role in melanoma. Studies in clinical samples have demonstrated increased expression of VEGF staining in patient melanoma samples tissues (Mehnert *et al.*, 2007). Furthermore, VEGF expression increases with the clinical stage of melanoma, suggesting angiogenesis may play a role in progression of melanoma (Rajabi *et al.*, 2012). VEGF may also contribute to the transition from melanocyte to melanoma as *in vivo* studies have shown VEGF is minimally expressed in the former, but strongly expressed in the latter (Gitay-Goren *et al.*, 1993).

Secretion of VEGF appears to follow in parallel. Patients with advanced melanoma have been shown to have higher concentrations of VEGF in their serum compared to healthy comparators, and VEGF level is positively proportional to tumour burden and stage (Ugurel *et al.*, 2001). Existing data, therefore suggests that VEGF may be an important component related to the progression of melanoma. Within the AVAST-M clinical trial which recruited patients with high risk stage II and stage III melanoma,

patients with BRAF mutant tumours, at the interim analysis had a superior disease free survival from post-operative treatment with bevacizumab (Corrie *et al.*, 2014), suggesting that VEGF may also have a role in the progression of melanoma at the earlier stages of disease.

The relationship between the $BRAF^{V600E}$ mutation and VEGF expression and markers of tumour angiogenesis has not previously been explored within patient samples. The hypothesis that $BRAF^{V600E}$ mutant melanomas express more VEGF compared with wildtype was explored initially by quantifying VEGF expression from AVAST-M clinical trial samples. VEGF concentration was determined in stored patient serum samples and separately in archived tumour tissue and the data compared between patients with BRAF mutant vs wildtype melanomas.

3.2. A comparison of VEGF serum concentrations between $BRAF^{V600}$ mutant and BRAF wildtype melanomas from patients recruited to the AVAST-M trial

The effect of the $BRAF^{V600}$ mutation on serum VEGF concentrations was initially explored. Patients participating in the AVAST-M clinical trial had serum and plasma samples taken and stored immediately post-operatively and then at 3 and 12 months. In total, 205 samples were available for those patients with a documented $BRAF^{V600}$ mutational result. Of these, 79 serum samples were from patients with a $BRAF^{V600}$ mutant melanoma and 126 from those with wildtype tumours. The specific sample numbers for each time point is presented in table 3-1.

Serum VEGF was quantified using a commercially available ELISA kit (R&D) by research assistant Leticia Campo from the Good Clinical Practice (GCP) laboratory within Oxford University, using the recommended protocol. This specific kit has specificity for VEGF isoforms $VEGF_{165}$ and $VEGF_{121,}$ diffusible isoforms considered

to be most relevant to angiogenesis (Ferrara and Adamis, 2016). Serum VEGF concentrations were calculated in the serum at each time point and grouped by BRAF mutational status.

Serum VEGF concentrations did not differ between $BRAF^{V600}$ mutant and wildtype ($p=0.12$) (table 3-1, figure 3-1) at any timepoints. Of note, the number of assessable samples decreased considerably throughout the study, presumably due to patients leaving the study and lost to follow up. Consequently, patient numbers at the 24-month assessment point were small, compromising statistical evaluation at this time point.

A comparison of circulating VEGF in response to treatment with bevacizumab is presented in figure 3-1 B. Treatment with bevacizumab resulted in a decrease in circulating VEGF levels in both patients with $BRAF^{V600E}$ and wildtype melanomas ($p<0.0001$) however the effect of the treatment did not have a differential effect based on genotype ($p=0.55$) (figure 3-1 B).

	$BRAF^{V600E}$	Wildtype
Baseline		
n	79	126
Median (pg/mL)	270.41	328.79
Range (pg/mL)	47.68 - 861.61	35.19 - 929.80
3 months		
n	77	120
Median (pg/mL)	167.29	131.10
Range (pg/mL)	35.00 - 950.37	31.19 - 994.35
12 months		
n	61	101
Median (pg/mL)	188.19	149.63
Range (pg/mL)	42.80 - 770.92	32.30 - 865.12
24 months		
n	18	39
Median (pg/mL)	272.69	283.12
Range (pg/mL)	62.64 - 690.00	32.30 - 740.00

Table 3-1: Serum VEGF concentrations from patients recruited to the AVAST-M study, stratified by BRAF mutational status. Serum samples were collected at baseline, 3, 12 and 24 months and VEGF concentrations compared between genotypes using a students t-test for each time point.

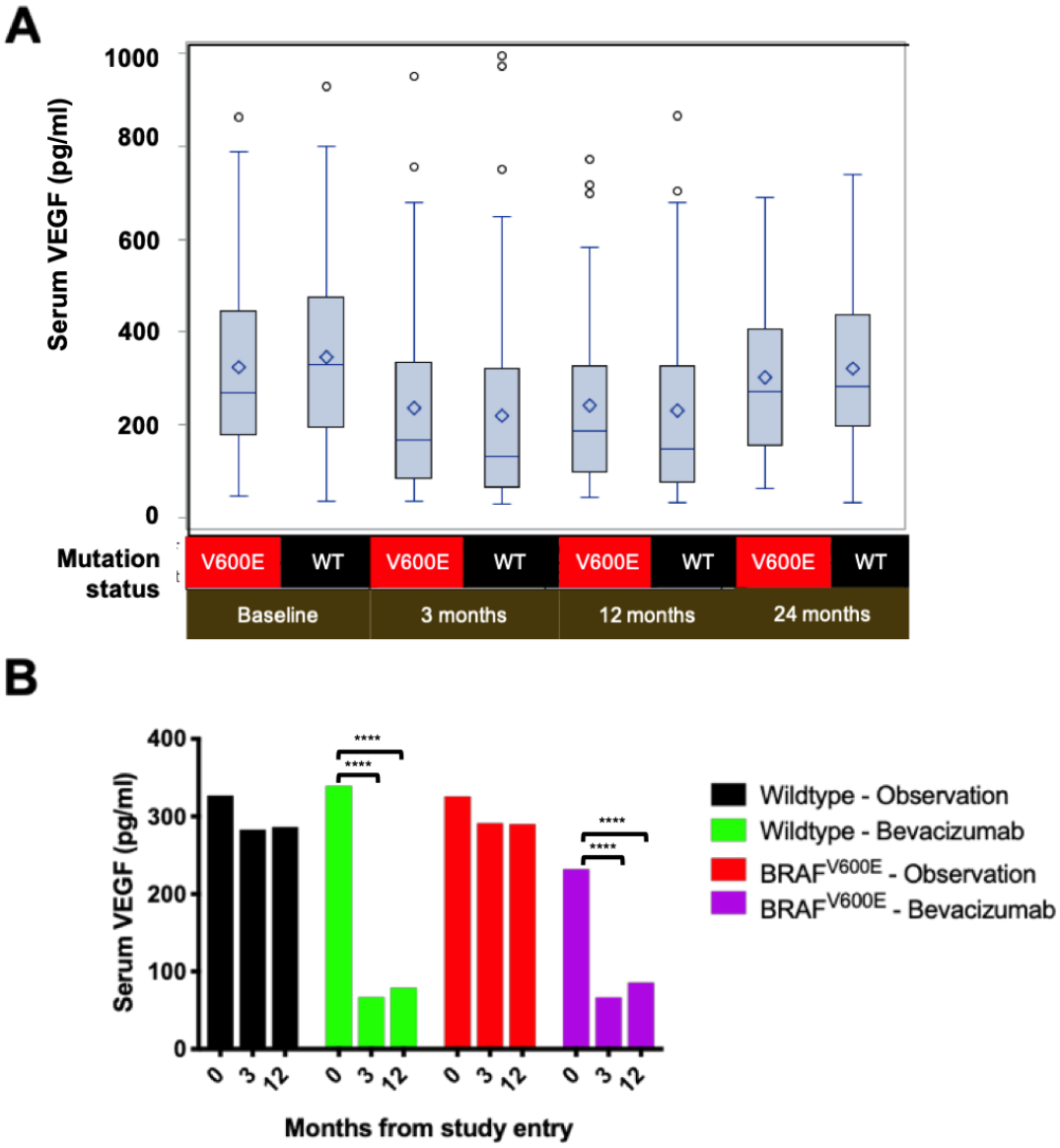

Figure 3-1: A comparison of serum VEGF Concentrations between patients with $BRAF^{V600E}$ vs wildtype tumours from the AVAST-M clinical trial. A. Tukey box plot detailing median serum VEGF concentrations stratified by genotype at specified timepoints. Figure provided by Andrea Marshall, Principal Research Fellow in Medical Statistics, Warwick Clinical Trials Unit, Division of Health Sciences, University of Warwick. Horizontal line refers to median value, diamond, the mean and whiskers the 25th and 75th centile values, respectively. B. Median serum VEGF concentrations stratified by treatment arm, time point and BRAF genotype. Statistics performed using one-way ANOVA ****p<0.0001

3.3. Comparison of melanoma VEGF expression between $BRAF^{V600}$ and wildtype from patient samples from the AVAST-M trial

VEGF expression can be quantified via immunohistochemistry (IHC) on clinical tissue (Rajabi *et al.*, 2012). While expression is typically higher in metastatic

deposits, positive staining has been reported in up to a third of primary melanomas (Salven *et al.*, 1997) and increases during the transition from the horizontal to vertical growth phase (Erhard *et al.*, 1997). VEGF expression is reported to be minimal in normal tissue and therefore quantification of tumour specific VEGF in resected melanomas is feasible (Pufe *et al.*, 2003).

The association of the $BRAF^{V600E}$ mutation with VEGF expression was next assessed in archival patient samples from the AVAST-M trial. Melanomas resected from patients participating in the AVAST-M trial were processed into formalin fixed paraffin embedded tissue as part of the original trial protocol. These fixed tissues were processed as whole slides. Separately 1mm cores from these blocks were compiled into tissue micro array (TMA) format by Leticia Campo.

Primary melanomas made up the majority of tissue samples stained, however as the eligibility criteria for the AVAST-M study included patients with AJCC 7^{th} edition defined stage III melanoma (ie patients with lymph node metastasis), the tissue source varied. Primary melanomas constituted 345 samples and 272 were from lymph node metastases. Additional samples were also procured from patients during the trial, where feasible, in the event of recurrence. From these patients, 50 locally recurrent and 27 distant metastatic melanomas were also included. In 10 cases, the tissue of origin was not available. The total number of samples available was 704. Due to the fact that tumours could be resected from multiple sites (eg primary tumour and lymph node) from the same patient, the total quantity of 704 melanoma samples were resected from 385 patients.

TMA samples were stained for VEGF by staff in the GCP laboratory. Positive and negative controls are presented in figure 3-2 A -B.

VEGF expression was scored using a semi-quantified method that combined both percentage of positive staining ("coverage") with the staining intensity ("intensity"). This method of VEGF IHC quantification using a combination of both variables has used and published by other groups (Schneider *et al.*, 2008; Maae *et al.*, 2011). Intensity and coverage were both scored manually by a qualified skin histopathologist Dr Olivia Espinosa (Oxford University Hospitals NHS Foundation Trust), and data entered and analysed by myself.

Coverage was scored between 0-3 (0 = Nil coverage, 1 = 1-24%, 2 = 25-50% and 3 = >50%), and intensity also between 0-3 (0 = nil staining, 1 = weak, 2 = moderate, 3 = strong). Inadequate tissue cores were excluded from the analysis. Each sample was scored for both coverage and intensity and the total score calculated as the product of both variables to generate a semi-quantitative score ("VEGF IHC score"), ranging from 0-9. Only TMA cores containing melanoma were included in the analysis. VEGF was quantified in three separate regions: within the tumour, within stromal tissue and within blood vessels contained within the tumour. Examples of a high and low scoring sample are presented in figure 3-3.

Of a total 704 TMA cores, 335 (48%) were excluded because of an absence of melanoma (97 samples, 14%) or insufficient tissue quality (238 samples, 34%). The remaining 369 (52%) TMA cores were scored. Of these, 158 (43%) contained $BRAF^{V600}$ mutant melanoma, and 211 (57%) were wild-type tumours. Positive VEGF staining was present in 234 (64%) of cases and absent in 134 (36%). In all cases of positive VEGF staining, staining was located in the cytoplasm. A

representative example is presented in figure 3-2 C. The cytoplasmic distribution of VEGF staining (as opposed to membrane or nuclear) is consistent with reports in the literature (Pisacane *et al.*, 2005).

The mean VEGF IHC staining scores for cores containing $BRAF^{V600}$ mutant melanoma vs wildtype did not differ significantly between the two groups (2.223 vs 2.175 for $BRAF^{V600E}$ vs wildtype tumours, respectively (p=0.832) (figure 3-4 A).

3.4. Comparison of stromal VEGF expression between $BRAF^{V600}$ mutant and wildtype AVAST-M patient samples

Tumour associated stroma has been identified as a source of VEGF (Fukumura *et al.*, 1998; Pinto *et al.*, 2010; Tayama *et al.*, 2011) that may have an influence over prognosis (Tayama *et al.*, 2011). *In vivo*, stroma derived VEGF has also been shown to drive tumour angiogenesis and proliferation (Pinto *et al.*, 2010). Further experiments have demonstrated activation of the VEGF promoter in peri-tumoural fibroblasts, in response to uncharacterised signals presumably derived from the adjacent malignant cells (Fukumura *et al.*, 1998). Appreciating the lack of difference in VEGF expression between BRAF mutant and wildtype tumours thus far, VEGF expression was next quantified in the surrounding stroma in the TMA cores, using the same semi-quantitative method of assessment described previously.

All 704 TMA cores were assessed for stromal VEGF expression. Of these 241 (34%) cores were not assessable due to inadequate tissue quality, leaving 463 samples for the analysis. The presence of tumour was not mandatory for this analysis, explaining the higher number of samples compared to the tumour analysis. Of the analysable cores, 194 (42%) were $BRAF^{V600E}$ mutant and 269 (58%) were wildtype. Stromal VEGF staining was absent in the majority (255 cores, 55%) of evaluated cores and

overall stromal staining was weak. A representative example is presented in figure 3-2 D.

Stromal VEGF did not differ significantly between cores derived from resected $BRAF^{V600E}$ and wildtype melanomas (mean score 1.25 ± 1.88 vs 1.13 ± 1.86, respectively, p=0.42) (figure 3-4 C).

3.5. Comparison of peri-tumoural blood vessel VEGF between BRAF mutant and wildtype AVAST-M samples

Although high levels of VEGF expression are associated with malignant cells, expression has also been reported in blood vessels. Blomgren et al described prominent expression of both VEGF and VEGFR2 within endometrial capillaries, leading to speculation that an autocrine signalling pathway may influence angiogenesis (Blomgren *et al.*, 2002). VEGF expression has also been reported in smooth muscle cells covering intracerebral capillaries (Saito *et al.*, 2011). Therefore, as an exploratory assessment VEGF expression was also quantified in vessels adjacent to the melanomas in the AVAST-M TMAs.

This analysis was performed on 462 TMA cores. Blood vessels present within a TMA core were assessed for VEGF expression. The results did not reveal significant differences between $BRAF^{V600E}$ and wildtype tumours, with mean scores of 1.276 ± 0.1503 vs 1.586 ± 0.1479, (p=0.1525) for the two groups, respectively (figure 3-4 E). Overlapping considerably with the assessment of stroma derived VEGF, most (257 (57%) of TMA cores did not express any VEGF within the visible vessels (figure 3-4 F).

3.6. A comparison of VEGF expression between BRAF^{V600} and wildtype melanomas -whole slide analysis

Tissue microarrays are often representative of the whole mounts from which they derived and the technology has been validated in multiple tumour types (Camp *et al.*, 2000). Others groups however have reported limitations with significant variations on accuracy (Khouja *et al.*, 2010). Three hundred and thirty six (47%) of the TMA cores assessed in the above analysis were excluded as they did not either contain tumour or were of unsuitable quality. Such a high number of un-interpretable cores was in part because the TMA cores had sampled non-malignant tissue. To address the possibility of sampling error influence, VEGF was also quantified in a selection of whole mount slides.

Forty-five whole mount slides (22 BRAF^{V600}, 23 wildtype) were cut from AVAST-M patient tumour blocks known to contain a primary melanoma, as opposed to lymph node metastases, for consistency. All slides were stained for VEGF using the protocol used for the TMA analysis. VEGF was scored and quantified by a qualified skin pathologist Dr Richard Colling (Oxford University Hospitals NHS Foundation Trust), using the semi-quantitative method used on the TMAs.

VEGF staining of tumour tissue was predominately cytoplasmic, present in 44 of 45 samples, however unlike the TMAs, expression was also detected in the plasma membrane of 15 of 45 melanomas and nucleus of 2 of 45. Semi-quantitative VEGF scores did not differ between BRAF^{V600} mutant and wildtype melanomas scored in the cytoplasm (mean score ± SEM1.86 ± 0.20 vs 1.52 ± 0.20, respectively, p=0.24), the membrane (mean score 0.54 ± 0.14 vs 0.26 ± 0.11, respectively, p=0.12) or nucleus (mean score 0 ± 0 vs 0.09 ± 0.06, respectively, p=0.15) (figure 3-5 A, C and E).

VEGF expression with tumour vessels was also quantified in whole mount sections. The 45 whole mounts (22 $BRAF^{V600E}$/23 wildtype) that had been stained for VEGF were assessed for VEGF expression within intra-tumoural blood vessels. Quantification was again performed by Dr Richard Colling, scoring the product of the scores for intensity and coverage. Intensity was determined by calculating the number of quadrants containing positively stained vessels, identified morphologically. The scoring system for staining intensity was: 0 = no staining, 1= positive vessels in one quadrant of the whole slide, 2 = positive vessels in 2 quadrants of the whole slide 3 = positive vessels in 3 or more quadrants. Semi-quantitative scores for VEGF expression within intra-tumoural blood vessels did not differ between $BRAF^{V600E}$ and wildtype melanomas (mean ± SEM, 2.27 ± 2.16 vs 2.26 ± 2.40, respectively, ($p=0.983$) (figure 3-5 G).

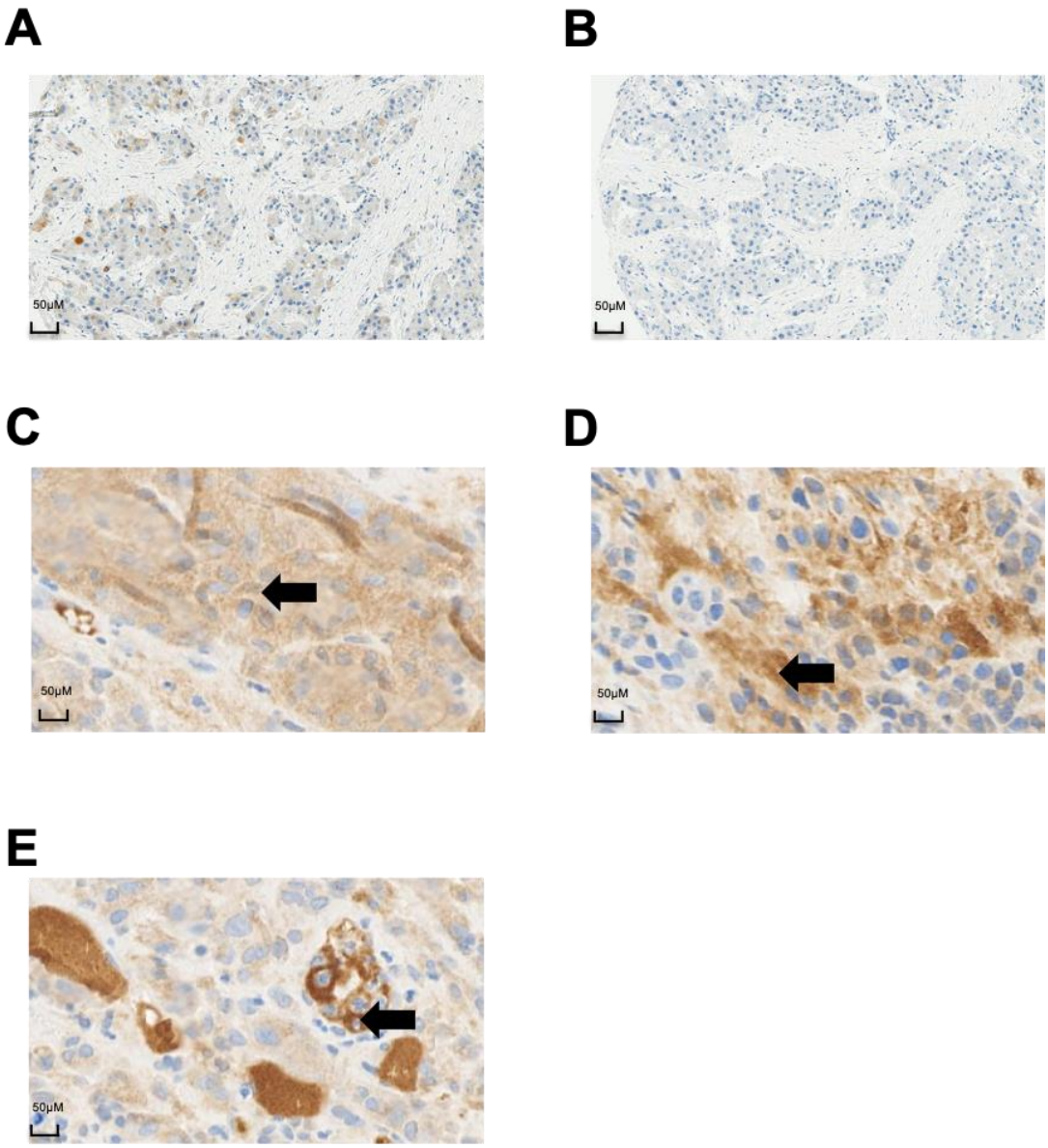

Figure 3-2: A. VEGF antibody positive control (Human Tonsil) showing positive cytoplasmic staining B. IgG alone negative control. (staining performed and images provided by Leticia Campo) C. Representative cytoplasmic VEGF positive staining (arrowhead). D. Representative stromal VEGF positive staining (arrowhead) E. Representative vascular VEGF positive staining (arrowhead). Images provided by Dr Olivia Espinosa.

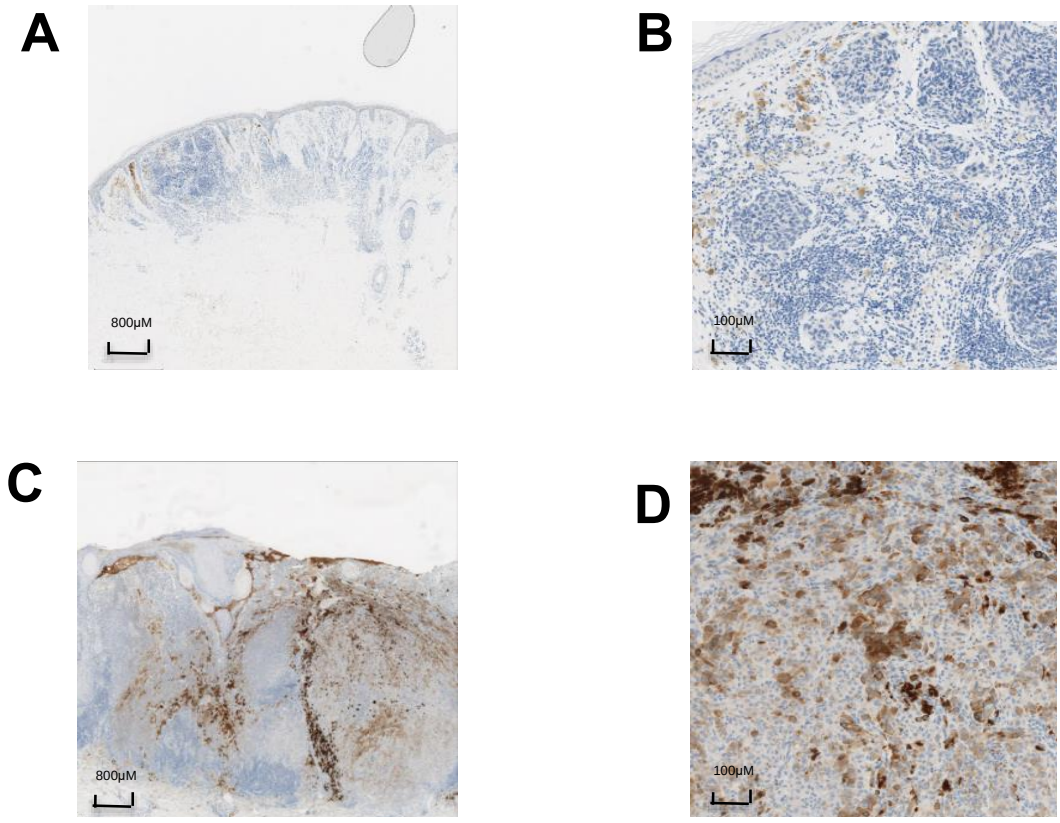

Figure 3-3: Examples of semi-quantitative method used to score VEGF. Whole mount slides used to demonstrate A and B: Examples of low scoring sample (A. Positive VEGF staining in 1-24% of section of the slide containing tumour (coverage score = 1). B VEGF staining intensity graded as "weak" (intensity score = 1). Total score for slide = 1 x 1 = 1) C and D: Examples of high scoring sample (C. Positive VEGF staining in >50% of cells (coverage score =3). D. VEGF staining intensity graded as "strong" (intensity score = 3). Total score for slide = 3 x 3 = 9.

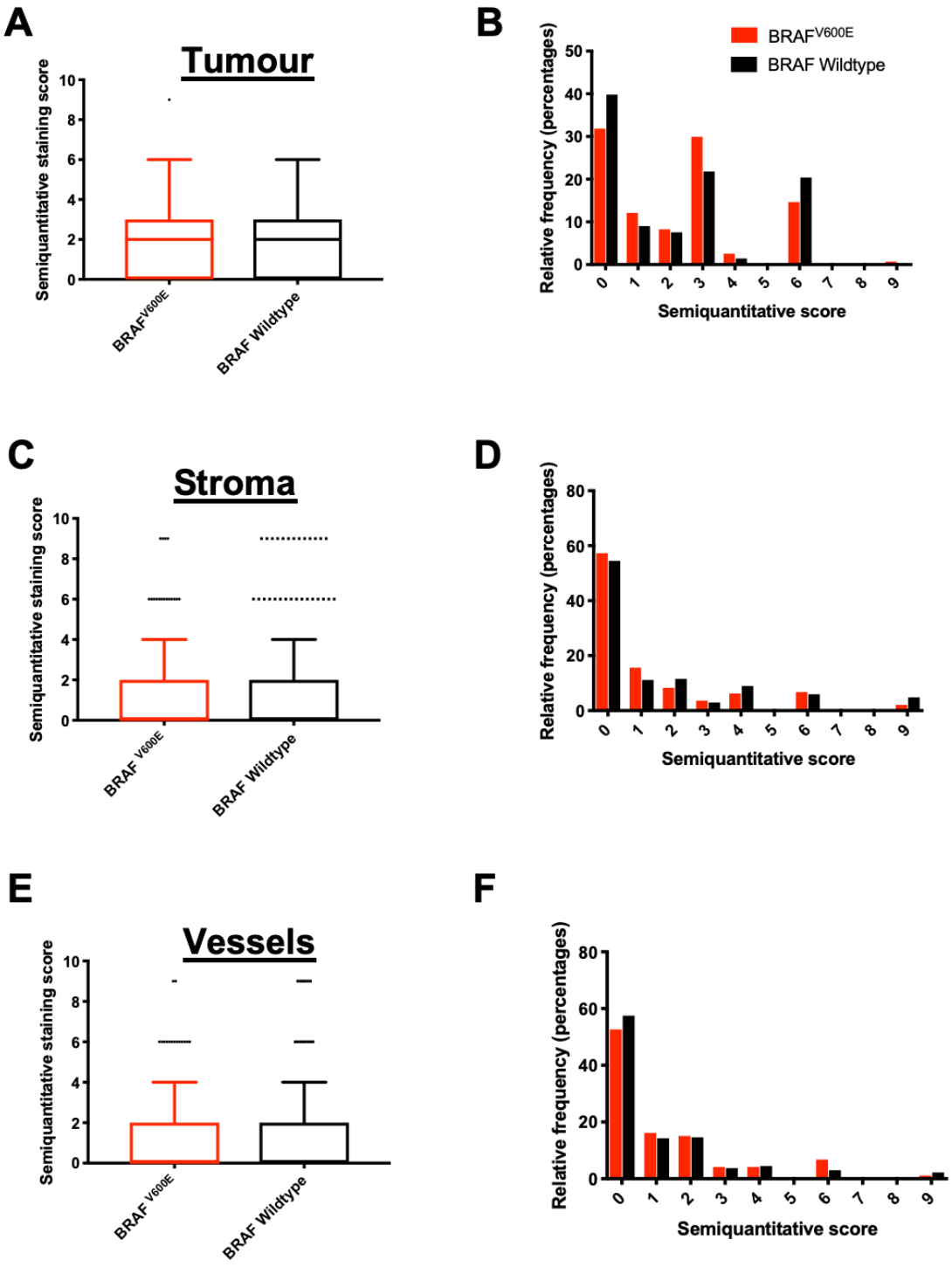

Figure 3-4: Quantification and comparison of VEGF expression between BRAF^{V600E} and wildtype samples procured from the AVAST-M clinical trial and arranged into TMAs. A. Comparison of tumour-VEGF expression between BRAF^{V600} and wildtype melanoma. Tukey box and whiskers plot comparing VEGF staining scores between BRAF^{V600E} and wildtype tumours (n=368), indicating 25th percentile (box) and 75th percentile (whisker). Values outside this range are portrayed as dots. B. Histogram detailing frequency of scores (for tumour VEGF expression) across both BRAF^{V600} and wildtype samples. C. Comparison of stromal VEGF expression between BRAF^{V600E} and wildtype samples (n=462). D. Histogram scores for stromal VEGF expression. E. Tukey box plot comparing VEGF expression within vessels. F. Histogram of scores for vessel VEGF expression.

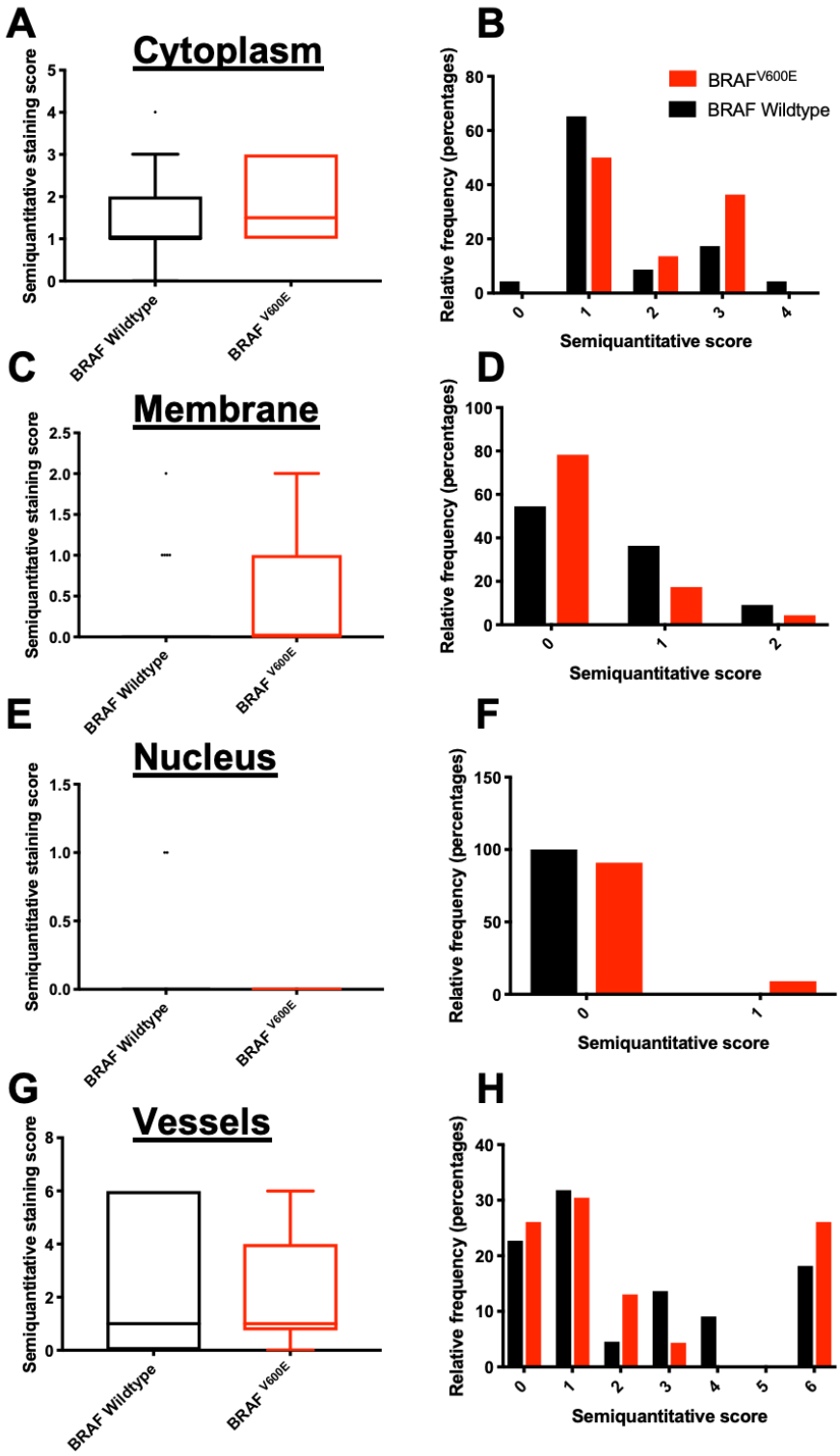

Figure 3-5: Quantification of VEGF staining in whole mount sections of primary melanomas from the AVAST-M clinical trial. VEGF expression was tested in 43 tumours and quantified using a semiquantitative score. A. Tukey box plot depicting cytoplasmic VEGF expression and B. histogram detailing frequency distribution of scores. C and D. Membrane VEGF expression and histogram. E and F. Nuclear VEGF expression and histogram G and H. VEGF expression with intra-tumoural blood vessels identified within the whole mount sections and H. histogram showing frequency distribution. No significant differences between $BRAF^{V600E}$ and wildtype melanomas were identified using a students t-test.

3.7. A comparison of CD31 positivity between BRAF^{V600} and wildtype melanomas resected in the AVAST- trial

CD31 immunohistochemistry was performed in parallel with VEGF staining to quantify differences in angiogenesis. CD31, also referred to as Platelet And Endothelial Cell Adhesion Molecule 1 (PECAM-1), is a molecule expressed on endothelial cells and is also expressed by haematopoietic cells and multiple immune cell types (Woodfin *et al.*, 2007). The biological role of CD31 appears is as a signalling molecule involved in, but not limited to a number of functions including cellular permeability, cytoskeletal filament organisation and β-catenin localisation and transcriptional activities (Ilan *et al.*, 2003; Lertkiatmongkol *et al.*, 2016). It may also play a key role in a number of pathological conditions such as atherosclerosis and thrombosis (Woodfin *et al.*, 2007). CD31 also has a functional role in angiogenesis where *in vitro*, CD31 inhibition impedes endothelial capillary cell tube formation (Matsumura *et al.*, 1997).

CD31 is considered to be a specific marker of endothelial cells using immunohistochemistry. Within skin tissue, CD31 antibody reacts with small arterioles and venules without significant background activity (Pusztaszeri *et al.*, 2006). Given its specific expression on vascular cells, immunohistochemistry for CD31 has emerged as an effective method of identifying endothelial cells histologically and is generally regarded as the best marker for endothelial cell differentiation (Pusztaszeri *et al.*, 2006). CD31 positivity is reported in melanoma (Pisacane *et al.*, 2007). Tissue vascularisation can be quantified by calculating the density of positive staining endothelial cells over a defined area, a measurement referred to as microvascular density (MVD) (Carmeliet, 2005). This method has been published by other groups and has been shown to correlate with other markers of angiogenesis, such as VEGF

expression (Chantrain *et al.*, 2003; Marien *et al.*, 2016). MVD can be calculated electronically using appropriate software, resulting in reproducibility of scoring across multiple observers (Chantrain *et al.*, 2003), depending on an initial accurate designation of the region of interest.

CD31 antibody was optimised for immunohistochemistry by Research Assistant, Letica Campo, employed by the Good Clinical Practice (GCP) laboratory. Positive and negative controls are presented in figure 3-6 A-B.

After staining with CD31 antibody, the AVAST-M TMAs were digitally scanned. Mapping and CD31 staining quantification were performed electronically, overseen by pathologist Dr Richard Colling. TMAs were de-arrayed by the Tissuearray© module (Visopharm), and the original glass slides used for comparison. CD31 quantification was then performed sequentially using two separate software platforms (again, overseen by Dr Colling). Specifically designed for Oxford University, the first program (Visiopharm) automatically identified tissue within each de-arrayed image. The Tumour Neovascularisation app (Visiopharm) calculated the area of tissue followed by the number of CD31 positive blood vessels, providing an output of total vessel number and vessel density of each core (vessel count per mm^2). Detection thresholds were modified by Dr Colling to achieve the optimum balance between CD31 positive vessels and minimal background staining. Representative digital images are provided in figures 3-6 C and D. Each core was viewed manually (Dr Colling) after analysis check correlation between the digital and visual degree of CD31 staining.

Of 297 TMA cores from AVAST-M trial patients that were stained for CD31, 123 cores (41%) contained a $BRAF^{V600}$ mutant melanoma and the remaining 174 (59%)

were wild-type.

CD31 quantification was assessed using two methods: total vessel number per TMA core, and vessel density expressed as number of vessels per mm^2.

Data presented in figure 3-6 demonstrated no significant difference in endothelial blood vessel content between $BRAF^{V600E}$ mutant and wildtype melanomas in terms of total number of vessels (mean (SD), 135 (145) vs 112 (117), p=0.317) (figure 3-7 C) or vessel density (154 (150) vs 132 (132), p = 0.217), respectively (figure 3-7 A).

3.8. Comparison of CD31 expression in whole mount sections of $BRAF^{V600E}$ and wildtype melanomas from the AVAST-M clinical trial

Analysis of CD31 positivity was also performed on the 45 whole mounts sections of resected tumours from the AVAST-M trial, as used for VEGF analysis in figure 3-5. The 45 whole slides were selected and stained for CD31. Tumour area was defined manually by Dr Richard Colling, with a region of interest selected as the most representative section of tumour. Inflammatory cells also stained strongly for CD31 and so areas with inflammatory cell infiltrates were not included. Intratumoural stroma was included and taken to mean connective tissue within the boundaries of discrete tumour foci. Peri-tumoural stroma was excluded from the region of interest. Software employed for the CD31 TMA analysis was used to quantify CD31 positivity in this analysis.

Six slides were excluded from the analysis. In 4 slides, the quality of the scanned slides was unsatisfactory for further assessment and in 2 slides, excess background staining was present. Of the resulting 39 slides 19 were $BRAF^{V600E}$ mutant and 20 wildtype melanomas. The median vessel density of the $BRAF^{V600E}$ mutant melanomas was higher than wildtype melanomas (148.5 vessels per mm^2 (interquartile range

(IQR) 89.7) vs 112.5 (IQR 139.5) vessels per mm^2, respectively), but the difference was not statistically significant (p=0.4487) **(**figure 3-7 E).

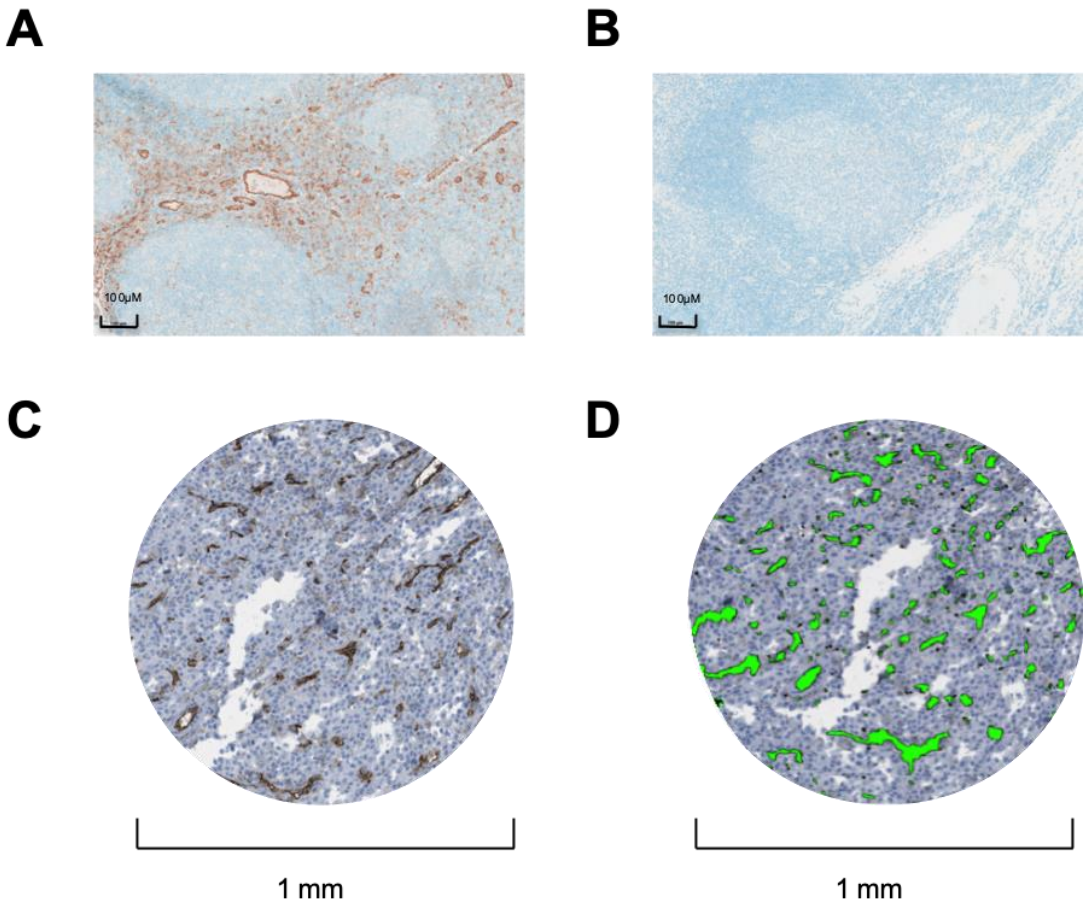

Figure 3-6: A. CD31 positive control. Human tonsil stained with CD31 antibody B. CD31 negative control. Human tonsil treated with IgG alone. Staining performed by and images provided by Leticia Campo C. Representative example of an AVAST-M TMA core stained with CD31 antibody prior to automated analysis. CD31 blood vessels are stained brown D. Automated CD31 positive blood vessel detection (visiopharm) in a TMA core. Green areas indicate blood vessels used for quantification of MVD. Images provided by Dr Richard Colling

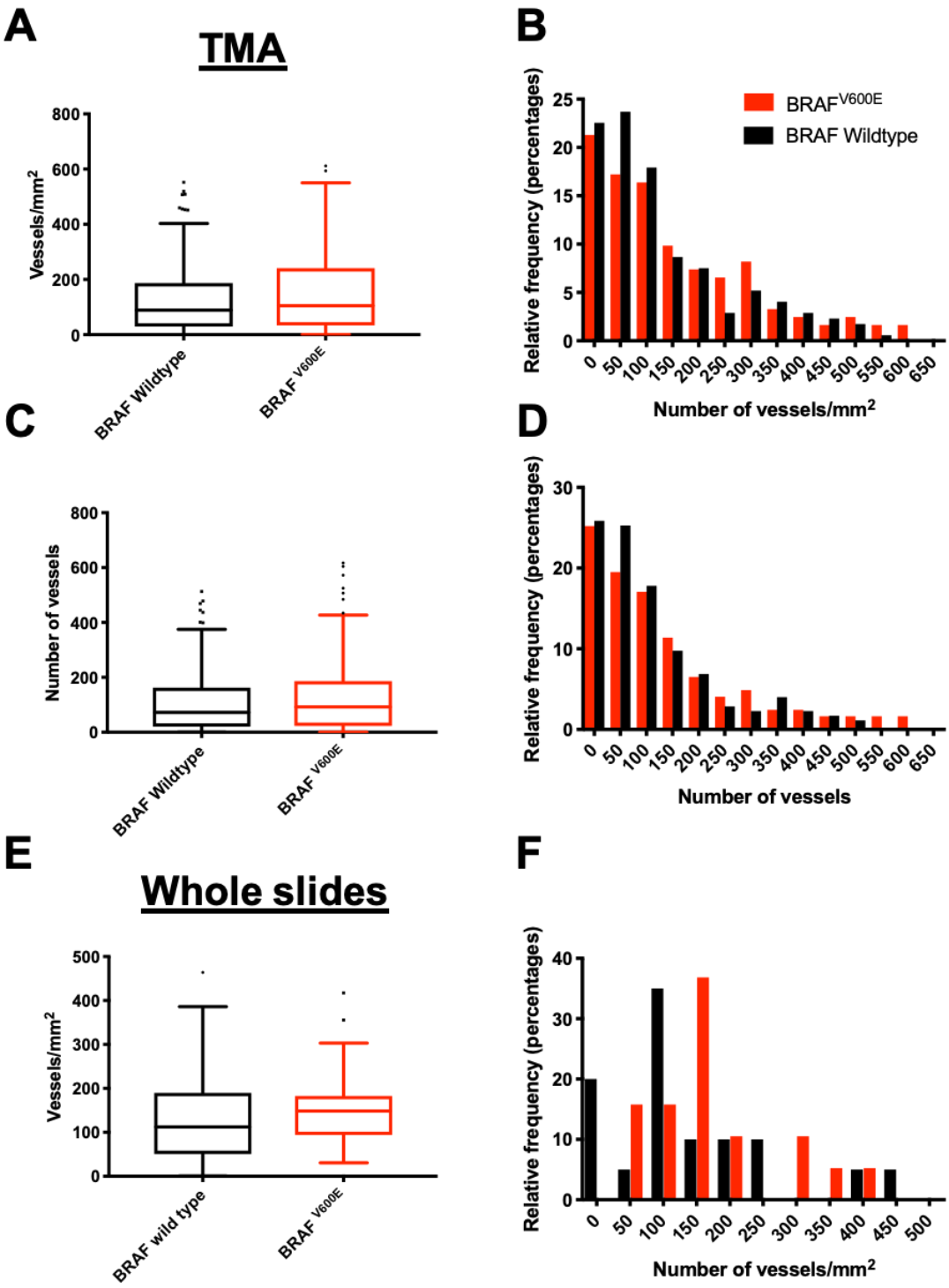

Figure 3-7: Comparison of CD31 expression between BRAF^{V600E} and wildtype samples from the AVAST-M clinical trial. Box and whisker plots comparing A. total vessel number per analysed TMA core (n=297) with frequency histogram, D. E. vessel density over a defined area of 1mm² and frequency histogram F. Statistics performed using Mann-Whitney U test. G. Vessel density quantified on whole mount sections (n=39) with frequency histogram, H.

3.9. Discussion

Serum VEGF concentrations in all patients (table 3-1) were similar to physiological levels (Kusumanto *et al.*, 2007) and were not influenced by $BRAF^{V600E}$ status (figure 3-1 A-B). This result was not unexpected as patients were recruited to the AVAST-M study after surgery performed with curative intent and therefore any residual tumour volumes were occult and unlikely to influence total circulating VEGF levels.

The observed decrease in VEGF in response to bevacizumab (figure 3-1 B) needs to be interpreted with caution, as studies have reported that bevacizumab-VEGF complex formation interfere with the ELISA assay and under-report circulating "biologically active" VEGF (Takahashi *et al.*, 2001).

When assessing tissue VEGF, $BRAF^{V600}$ mutant TMA cores did not have significantly different VEGF semiquantitative score compared to wildtype samples. Relatively low sample numbers may have contributed to this result. Approximately 50% of TMA cores were not assessable due to either quality or an absence of melanoma, and a greater number may be required to determine if there are any real differences.

Because TMA cores sample only a small fraction of each tumour, the analysis was repeated on whole mount sections. Mean melanoma cytoplasmic VEGF score differed by a greater margin ($BRAF^{V600E}$ vs wildtype 1.86 vs 1.52 – figure 3-5 A) however again this result was insignificant. Analysis of only 45 samples may have contributed the non-significant result. There was no difference in stromal VEGF expression in the $BRAF^{V600E}$ mutant TMA cores (figure 3-4 C), most likely due to absent VEGF staining in a large proportion of the samples (figure 3-4 D).

The semi-quantitative method for determining VEGF expression combining both variables of staining intensity and coverage has been reported and utilised by others (Schneider *et al.*, 2008; Osman *et al.*, 2015; Hafez *et al.*, 2016). Schneider et al scored VEGF expression by calculating the percentage of cells with positive staining cytoplasm from an entire whole slide (Schneider *et al.*, 2008). Variations of this method have also been investigated. Maae and colleagues compared two manual methods of VEGF IHC expression in a series of ductal carcinomas of the breast: one method quantified VEGF expression as a function of staining intensity alone, the other method a combination of staining intensity and coverage. The investigators found that both intra and inter observer reproducibility was in fact poorer with the combined score, and this method failed to satisfy their pre-defined measure for acceptability (Maae *et al.*, 2011). The authors theorised that subjectively quantifying two variables may have increased the lack of reproducibility. Better intra -observer concordance using a semi-quantitative method was reported in another study (Rydén *et al.*, 2005), which analysed TMAs. The higher degree of intra-observer concordance may have been because a smaller tissue area was analysed. TMAs however fail to fully account for heterogenous staining. The fact the semi-quantitative VEGF scores were more supportive of the original hypothesis in the whole mount sections as opposed to the TMA analysis may have been because VEGF is heterogeneously distributed and better assessed in a large assessable area.

Stromal VEGF staining has been reported as minimal, and has even been used as a negative control in some studies (Maae *et al.*, 2011). This observation is consistent in the current study, where stromal expression was poor with the majority of tumours scoring zero for both $BRAF^{V600E}$ and wildtype tumours.

Semi quantitative assessment of VEGF by IHC does not take into account VEGF genotype which also influences biological activity. Multiple single nucleotide polymorphisms (SNPs) in the VEGF promoter have been identified (Koutras *et al.*, 2015), some of which have been shown to be prognostic as well as influence toxicity and efficacy to treatment with bevacizumab (Jain, 2005; Schneider *et al.*, 2008). At least two studies have shown that where polymorphisms in the VEGF genotype are predictive of benefit with bevacizumab, VEGF expression using IHC alone does not distinguish between the various VEGF genotypes and therefore may lack the specificity to detect biologically relevant isoforms (Schneider *et al.*, 2008; Sa-Nguanraksa *et al.*, 2014). The importance of recognising the different effect of the numerous VEGF isoforms was not appreciated in this part of the project. Experiments by others have shown that not only do VEGF isoforms differ in their ability to diffuse into the circulation, they also have distant phenotypes, in terms of morphological changes they promote in over-expressing cells, as well as mitogenic signalling capacity (Kanthou *et al.*, 2014). The distinct biological functions may also impact on prognosis and predict sensitivity to anti-angiogenic therapy. Separate studies in patients with metastatic non-small cell lung cancer and colorectal cancer treated with bevacizumab have reported the ratio of the angiogenic $VEGF_{165a}$ isoform to the anti-antiangiogenic $_{165b}$ splice variant is predictive of an improved disease free survival (Bates *et al.*, 2012; Garcia-Foncillas *et al.*, 2013). The antibody for IHC used for quantifying VEGF in this project detected total VEGF ($VEGF_{165}$, $VEGF_{121}$ and $VEGF_{188}$). Tumour RNA assessment with qRT-PCR would be required to determine the specific isoforms (Garcia-Foncillas *et al.*, 2013) and may have identified a slice variant either associated with the $BRAF^{V600}$ mutation or predictive of benefit to

bevacizumab (discussed in chapter 7).

VEGF scores were not normalised to stage. The AVAST-M trial recruited patients with stage IIB - IIIC melanoma. VEGF expression has been shown to increase with tumour stage (Rajabi *et al.*, 2012). In future it may be informative to compare VEGF scores between the $BRAF^{V600E}$ and wildtype tumours across each stage, however given a lack of an overall difference and time constraints, this was not pursued.

Taken together, this study identified no differences in VEGF in the serum or tumour VEGF between $BRAF^{V600E}$ and wildtype melanomas in patient recruited to the AVAST-M study. Ideally, to confidently reject the hypothesis, the analysis should be repeated on high quality whole mount primary melanomas, in significant numbers and scoring performed by 2 independent dermatopathologists with minimal intra and interobserver reliability. Due to time constraints, the samples presented in this work were not scored by a second observer. With reference to the whole slide analysis, based on the mean values of each group ($BRAF^{V600E}$ and wildtype) and standard deviation of the wildtype group and setting a power of 0.8 and α of 0.05, a sample size of 268 slides (134 in each group) would be required to determine a significant difference between the samples, using a 2 sided t test (https://www.stat.ubc.ca/~rollin/stats/ssize/n2.html).

Paralleling the result with respect to VEGF, CD31 expression was not significantly higher in $BRAF^{V600E}$ mutant patient melanoma samples (figure 3-7 E). The difference between $BRAF^{V600E}$ and wildtype vessel density was again higher in the whole mount sections raising the possibility that heterogenous CD31 staining patterns may have made TMAs an insufficiently sensitive tissue source for this analysis.

The quantification of tissue vascularisation, using MVD has numerous challenges.

Tortuous capillaries, for example, may be double counted, and significantly affect the accuracy of vessel counting when performed manually (Simpson *et al.*, 1996). To overcome this and other limitations, automated methods of determining MVD have been developed. Computerised MVD quantification can be performed by a number of different methods. An early method relies on the automated selection of a region(s) of apparent high MVD (referred to as a "hot spot") that is considered representative of an entire sample. MVD determination by this method has been shown to correlate with MVD determined by a pathologist, although others report unacceptable levels of reproducibility (Chantrain *et al.*, 2003). The "hot spot" technique is less effective in cases of heterogeneous MVD. For example conflicting studies report clustered areas of high MVD (West *et al.*, 2005) in sarcoma, whereas others report MVD as evenly distributed throughout the same tumour type (Tomlinson *et al.*, 1999).

Alternative methods involving sampling multiple regions of interest provide more globally representative and reproducible data (Marien *et al.*, 2016) however such methods are time consuming, which has limited their application.

Variations on each method were used in this study. Within the TMA analysis, all detectable tissue within a core was selected as a single region of interest, regardless if the tissue contained melanoma cells or not. In the whole mount analysis the region of interest was manually defined to include tumour alone and excluded stroma, inflammatory cells and other potentially confounding elements. The whole mount analysis method incorporating all visible tumour was more consistent with a global approach rather than the "hot spot" method. The TMA analysis, in contrast calculated MVD from a single core, and was thus vulnerable to sampling error. Taken together the whole mount method may have been both more sensitive and specific than the TMA analysis, although it was limited by small numbers.

In summary, various methods of endothelial vessel quantification exist. Whereas analysing a smaller region is feasible, accuracy is increased by sampling multiple regions that are selected (either automatically or manually) as representative. The literature supports quantification of a large proportion of a tumour and this suggests that the manual selection technique used in the whole mount analysis may be more reflective of true MVD in the AVAST-M patient samples.

In conclusion there was no difference in intra-tumoural expression of VEGF and CD31 in $BRAF^{V600E}$ melanomas from the AVAST-M trial.
Data from the whole mount samples may have more accurately reflected the whole tumour compared with the TMA's, largely on account of tissue quality, sampling error and heterogeneous staining patterns. These trends in support of the hypothesis suggest that there may be merit in extending the whole mount analysis for both VEGF and CD31 in a larger cohort including independent datasets.

4. Chapter IV: Identification of Genes differentially expressed between BRAFV600E mutant and wildtype melanoma

4.1. Data sets identifying genes differentially expressed between BRAFV600E and wildtype melanoma

Having interrogated the AVAST-M clinical trial material for associations between the $BRAF^{V600E}$ mutation and VEGF expression and angiogenesis within patient samples, genes differentially expressed in $BRAF^{V600E}$ mutant melanoma that are associated with the expression of VEGF, and by extension, may link with enhanced sensitivity to bevacizumab were identified. To address this question, three large melanoma gene expression data sets were analysed to determine genes differentially expressed between $BRAF^{V600E}$ and wildtype melanomas that may impact upon this phenotype. These data sets were generated by others as stipulated in the text. They are presented here as they are crucial to the gene selection process required for further work in this project.

4.1.1. Data set 1: AVAST-M patient samples: Analysis performed by Associate Professor Francesca Buffa and Dr Ruud van Stiphout

The first data set analysed comprised of gene expression data derived from melanomas resected from AVAST-M clinical trial patients. Patients who consented to the trial provided written permission allowing translational research on their specimens. Gene expression was measured using RNA-Nanostring technology in which RNA-Nanostring fluorescent barcode primers are hybridised directly to specific nucleic acid sequences allowing for the measurement of over 800 predefined targets in a simultaneous reaction (Veldman-Jones *et al.*, 2015).This is an effective method to quantify many mRNA transcripts in tissue samples. The system has

comparable sensitivity to real time PCR (Geiss *et al.*, 2008). It is also particularly useful in the analysis of clinical samples, where its analysis of mRNA extracted from FFPE is accurate and reproducible (Veldman-Jones *et al.*, 2015).

Samples were selected from the AVAST-M tumour bank (containing over 700 samples). Extracted RNA was analysed using the NanoString ncounter platform performed commercially by Genentech. Data were returned to Oxford University and analysed within the University's Oncology Department, by bioinformaticians A/Prof Francesca Buffa and Dr Ruud van Stiphout. Tumour samples were not micro-dissected to remove non-malignant tissue. The extracted RNA therefore reflected gene expression in both the resected melanoma and its surrounding stroma.

The NanoString platform provided gene expression data on ~800 genes.

Genes significantly differentially expressed between $BRAF^{V600E}$ and wildtype melanomas were identified. Associate Professor Francesca Buffa generated a list of genes that were differentially expressed with an un-adjusted p-value of <0.05 that were also differentially expressed (defined by a q-value of <0.05) in a publicly available dataset of melanoma samples from The Cancer Genome Atlas (TCGA). This list of genes was compared to further datasets as presented next in this chapter. This list comprising of 44 genes, complete with adjusted and unadjusted p-values is presented in table 4-1.

Upregulated in $BRAF^{V600}$ mutant melanomas				Downregulated in $BRAF^{V600}$ mutant melanomas			
Gene symbol	**t-value**	**p-value**	**adjusted p-value**	**Gene symbol**	**t-value**	**p-value**	**adjusted p-value**
SFRP1	4.390084	1.53E-05	0.004559	BTRC	-4.77456	2.78E-06	0.002476
LEF1	4.155733	4.24E-05	0.005649	BRPF1	-4.40898	1.42E-05	0.004559
FGFR1	3.549535	0.000443	0.039462	BCL2	-3.93482	0.000102	0.010097
WISP1	3.499816	0.000531	0.039462	NRAS	-3.51013	0.000521	0.039462
LY6E	3.382768	0.000805	0.045061	GNA13	-3.42984	0.000691	0.045061
FLT1	3.350761	0.000901	0.047259	MYC	-3.38171	0.000808	0.045061
IGFBP2	3.273375	0.00118	0.049427	DUSP3	-3.2143	0.001441	0.049427
TCF4	2.920112	0.003747	0.089448	TP53BP2	-2.89832	0.004011	0.089448
CASP8	2.900148	0.003993	0.089448	SEMA6A	-2.80125	0.005395	0.104616
TRRAP	2.869945	0.004374	0.092235	RAF1	-2.73436	0.006595	0.106953
POSTN	2.833029	0.004902	0.099387	KDM4A	-2.64917	0.008468	0.124325
SPP1	2.785863	0.005651	0.104706	HDAC6	-2.55805	0.011004	0.1456
MMP9	2.748032	0.006332	0.106953	PMEL	-2.51704	0.012315	0.151515
NDRG1	2.734807	0.006589	0.106953	CDK2	-2.51665	0.012329	0.151515
ETV4	2.71261	0.007033	0.110065	CDYL	-2.26956	0.023923	0.227942
SNAI1	2.56254	0.010847	0.1456	ERCC2	-2.2659	0.024649	0.230493
STRA6	2.480539	0.013986	0.166342	MITF	-2.09482	0.036972	0.263831
SCUBE2	2.293696	0.022444	0.222443	SETDB2	-2.01526	0.044745	0.287225
ETV1	2.28326	0.023069	0.22613				
ZEB1	2.240617	0.025732	0.234447				
BRAF	2.240294	0.025758	0.234447				
GUSB	2.185729	0.029549	0.246331				
GCNT1	2.141427	0.032996	0.255724				
FAP	2.117072	0.036235	0.262784				
PDGFRA	2.110015	0.03562	0.262784				
ROR2	2.099049	0.036591	0.263216				

Table 4-1: Genes differentially expressed between $BRAF^{V600E}$ and wildtype melanoma samples from patients recruited to the AVAST-M clinical trial as defined by an un-adjusted p-value of <0.05 that were also differentially expressed in data from the TCGA (defined by a q-value of <0.05). t-value refers to magnitude of change (in terms of standard error) relative to expression in $BRAF^{V600}$ mutant tumours (ie positive t-values refer to genes overexpressed in $BRAF^{V600}$ mutant tumours).

4.1.2. Data set 2: Gene expression data from The Cancer Genome Atlas

In parallel, a similar comparison of gene expression between $BRAF^{V600E}$ mutant and wildtype patient derived melanomas was performed using data publicly available by myself. Using the cBioPortal online application (www.cbioportal.org), a cutaneous melanoma data set of patient samples (from the TGCA) was selected, as this data set contained mRNA as well as genomic data for analysis. mRNA for this dataset was analysed using RNAseq based technology. which were adjusted for differences between platforms. The data source was labelled the TCGA "Firehose Legacy",

which is a depository of NCI generated data available for public analysis. Gene expression was interrogated using software embedded within the cbioportal application. Of the 287 patient melanoma samples, a BRAF mutation was present in 134 (47%), consisting of $BRAF^{V600E}$ in 121 (41%), $BRAF^{V600M}$ in 17 (6%) and $BRAF^{V600G}$ in 2 (0.7%). Gene expression was analysed on the basis of BRAF mutation. Differentially expressed genes were defined as those differentially expressed with adjusted p-value (false discoveries corrected using the Benjamini-Hochberg procedure) of <0.05. In this analysis, 2071 genes were differentially expressed. The top 100 genes upregulated and top 100 genes downregulated in $BRAF^{V600}$ mutant melanomas are presented in table 4-2.

Upregulated in $BRAF^{V600}$ mutant melanomas				Downregulated in $BRAF^{V600}$ mutant melanomas			
Gene symbol	**Log^2 Ratio**	**p-Value**	**Adjusted p-value**	**Gene symbol**	**Log^2 Ratio**	**p-Value**	**Adjusted p-value**
SERPINA3	2.26	1.45E-07	3.19E-05	SUSD5	-1.58	2.70E-07	4.57E-05
ITIH5	1.75	2.31E-06	2.06E-04	PMEL	-1.53	4.18E-03	0.0311
LOXL4	1.75	1.93E-05	8.44E-04	MME	-1.3	8.36E-04	0.0104
LIF	1.68	6.72E-08	2.05E-05	CA14	-1.27	1.82E-03	0.0176
PHKA1	1.6	1.69E-05	7.79E-04	CPNE7	-1.1	1.17E-05	6.10E-04
ITGA10	1.54	5.24E-05	1.60E-03	ZNF540	-1.01	4.25E-07	6.38E-05
TMEM158	1.52	3.47E-10	5.42E-07	TFAP2A	-0.92	2.38E-05	9.54E-04
SEMA3A	1.48	1.09E-05	6.01E-04	RAB33A	-0.91	5.76E-05	1.71E-03
KCNN4	1.47	8.43E-08	2.34E-05	SEMA6A	-0.9	3.63E-05	1.26E-03
TFAP2C	1.45	3.41E-05	1.20E-03	NCKAP5	-0.85	1.63E-04	3.48E-03
MIA	1.44	5.99E-07	8.05E-05	MTURN	-0.84	1.63E-07	3.35E-05
MMP9	1.42	6.73E-07	8.86E-05	SLC6A15	-0.84	2.25E-03	0.0204
CMBL	1.42	2.30E-06	2.06E-04	EGR1	-0.82	3.23E-06	2.49E-04
ITGB3	1.4	5.00E-06	3.31E-04	TUBB4A	-0.82	9.37E-04	0.0111
SPP1	1.39	9.46E-08	2.47E-05	IRS1	-0.78	2.42E-06	2.10E-04
MAOB	1.37	8.30E-05	2.19E-03	DUSP8	-0.78	7.11E-05	1.97E-03
PTPRZ1	1.36	6.55E-05	1.86E-03	CABLES1	-0.78	6.33E-04	8.51E-03
SRPX2	1.35	1.39E-07	3.16E-05	CELSR3	-0.77	2.46E-05	9.67E-04
FMOD	1.33	3.42E-07	5.53E-05	KCNAB2	-0.77	3.74E-04	6.00E-03
CHL1	1.3	2.86E-05	1.06E-03	NINL	-0.75	1.62E-05	7.67E-04
C1QTNF3	1.29	8.93E-04	0.0108	EFHD1	-0.75	4.54E-03	0.0331
PRR4	1.28	9.53E-09	5.10E-06	CAPN3	-0.74	5.92E-03	0.0397
TRPV4	1.27	2.21E-07	4.24E-05	TPCN2	-0.72	4.42E-06	3.05E-04
TMEM163	1.27	4.76E-04	7.04E-03	ATP8A1	-0.72	3.15E-03	0.0256
CEMIP	1.25	3.35E-06	2.50E-04	GCNT2	-0.7	4.63E-04	6.88E-03
GPC6	1.22	1.85E-05	8.19E-04	PAG1	-0.69	1.13E-05	6.05E-04
NNMT	1.2	2.66E-08	1.07E-05	SNAI2	-0.69	5.97E-05	1.76E-03
SLC2A10	1.2	1.30E-07	3.09E-05	NR4A3	-0.69	4.02E-03	0.0302
GJB2	1.19	9.79E-04	0.0114	C16ORF74	-0.68	3.89E-03	0.0295
FGF2	1.18	1.28E-05	6.50E-04	TDRP	-0.67	1.08E-03	0.0123
STRA6	1.18	1.45E-04	3.19E-03	FAM53B	-0.65	6.09E-08	1.95E-05
CHI3L1	1.17	3.04E-04	5.19E-03	ZNF607	-0.65	1.04E-03	0.0119
FGFBP2	1.13	1.14E-04	2.70E-03	PER3	-0.64	2.57E-07	4.57E-05
CA12	1.13	2.35E-04	4.38E-03	LRIG3	-0.64	4.36E-05	1.41E-03
IGFBP3	1.12	1.31E-07	3.09E-05	CEACAM19	-0.64	9.76E-04	0.0114
LRATD2	1.11	3.36E-06	2.50E-04	SBK1	-0.64	2.86E-03	0.0241
CFI	1.11	5.01E-06	3.31E-04	ATP6V1G2	-0.62	7.56E-05	2.06E-03
CSPG5	1.11	2.48E-05	9.70E-04	TFAP2E	-0.61	1.45E-03	0.015
CNIH3	1.1	3.93E-05	1.32E-03	AATBC	-0.61	5.45E-03	0.0375
FAM131B	1.1	1.02E-04	2.48E-03	RTTN	-0.6	2.08E-05	8.83E-04
IGFBP2	1.09	2.82E-05	1.06E-03	SYDE2	-0.6	1.89E-03	0.0181
PRRX1	1.08	9.88E-07	1.15E-04	CPEB2	-0.59	2.03E-05	8.76E-04
ELOVL2	1.08	1.14E-03	0.0128	BCL2	-0.59	4.64E-05	1.47E-03
MRC2	1.07	9.26E-07	1.12E-04	DAPK1	-0.59	4.84E-05	1.51E-03
PPL	1.07	2.02E-04	3.97E-03	GRK3	-0.59	4.24E-04	6.49E-03
PDLIM4	1.07	1.50E-03	0.0154	LIMS2	-0.59	1.18E-03	0.0131
STC1	1.06	3.83E-06	2.71E-04	KLF5	-0.59	2.60E-03	0.0226
SLC26A4	1.06	5.50E-05	1.65E-03	MCC	-0.58	3.79E-04	6.04E-03
DNALI1	1.06	4.45E-04	6.67E-03	ATP11A	-0.58	9.94E-04	0.0116
SCUBE2	1.06	2.39E-03	0.0213	IER2	-0.57	2.56E-09	2.00E-06
ATP1B2	1.05	6.73E-04	8.91E-03	SNHG7	-0.57	1.12E-05	6.05E-04
CSPG4	1.04	3.82E-07	5.89E-05	OBSCN	-0.57	6.37E-03	0.0418
CLU	1.04	7.05E-04	9.22E-03	MEX3A	-0.57	7.12E-03	0.0448
SDC2	1.03	1.22E-06	1.35E-04	TET1	-0.56	2.11E-04	4.07E-03
S100B	1.03	2.78E-05	1.05E-03	FOS	-0.56	3.95E-04	6.21E-03
CDCP1	1.03	1.76E-04	3.63E-03	PHACTR1	-0.56	1.68E-03	0.0166
IL1B	1.02	1.06E-04	2.55E-03	BMF	-0.55	2.24E-05	9.32E-04
THBS2	1.02	1.12E-04	2.68E-03	ZFP30	-0.55	3.29E-03	0.0262
RARRES1	1.01	4.84E-06	3.26E-04	HPDL	-0.55	4.67E-03	0.0337
TIMP1	1	2.74E-11	1.14E-07	P2RX7	-0.55	5.24E-03	0.0366
SMIM3	1	4.79E-08	1.67E-05	ZNF697	-0.54	1.81E-04	3.67E-03

Upregulated in $BRAF^{V600}$ mutant melanomas				Downregulated in $BRAF^{V600}$ mutant melanomas			
Gene symbol	**Log^2 Ratio**	**p-Value**	**Adjusted p-value**	**Gene symbol**	**Log^2 Ratio**	**p-Value**	**Adjusted p-value**
FAM20A	1	2.66E-06	2.20E-04	PTK7	-0.54	1.91E-03	0.0182
P3H2	1	6.24E-04	8.43E-03	ARSG	-0.54	5.77E-03	0.0389
TPD52L1	1	6.84E-04	9.00E-03	ABL2	-0.53	1.31E-06	1.41E-04
DYNLT3	0.99	1.18E-06	1.32E-04	BCL7A	-0.53	2.89E-05	1.06E-03
COL13A1	0.99	1.80E-05	8.05E-04	ZBED3	-0.53	1.18E-04	2.75E-03
CREB5	0.99	8.26E-05	2.18E-03	PPM1H	-0.53	5.03E-03	0.0355
CHST6	0.97	3.76E-07	5.88E-05	KLF11	-0.52	1.50E-09	1.42E-06
POSTN	0.97	2.09E-04	4.05E-03	LZTS3	-0.52	2.89E-05	1.06E-03
OPLAH	0.97	7.19E-04	9.34E-03	FAM86B1	-0.52	1.38E-03	0.0145
HFE	0.96	1.50E-05	7.31E-04	ACVR2B	-0.51	2.95E-05	1.07E-03
EMILIN1	0.96	2.44E-05	9.64E-04	NUTM2A	-0.51	3.90E-05	1.32E-03
SKAP1	0.96	1.74E-03	0.0171	ZNF571	-0.51	8.95E-05	2.27E-03
MT2A	0.95	5.21E-07	7.40E-05	WTIP	-0.51	4.15E-04	6.42E-03
TSPAN13	0.95	3.50E-06	2.53E-04	PLEKHG3	-0.51	4.42E-04	6.64E-03
SNED1	0.95	5.20E-05	1.59E-03	PARD6G	-0.5	5.83E-06	3.74E-04
PRTFDC1	0.95	2.48E-04	4.51E-03	AMOTL2	-0.5	1.92E-05	8.44E-04
SPOCD1	0.95	3.21E-04	5.40E-03	MYC	-0.5	1.33E-04	3.00E-03
KCNJ10	0.95	4.26E-03	0.0315	EPM2A	-0.49	8.48E-06	4.91E-04
MICALL2	0.94	8.18E-08	2.33E-05	NEK3	-0.49	1.79E-04	3.65E-03
PCOLCE	0.94	5.26E-05	1.60E-03	PRKX	-0.49	5.80E-04	8.02E-03
HOXB2	0.94	6.97E-05	1.95E-03	CYP2U1	-0.49	1.37E-03	0.0144
ALDH1A3	0.94	1.90E-03	0.0182	Mar-0	-0.48	1.97E-06	1.87E-04
IL27RA	0.93	7.60E-07	9.69E-05	ATP7A	-0.48	2.27E-05	9.39E-04
CITED4	0.93	1.15E-05	6.09E-04	ZKSCAN8	-0.48	6.00E-05	1.77E-03
SULF1	0.93	2.54E-05	9.78E-04	STK32C	-0.48	4.24E-04	6.49E-03
SORL1	0.93	7.37E-05	2.04E-03	LCOR	-0.48	8.16E-04	0.0102
COL9A2	0.93	1.92E-04	3.83E-03	RAC3	-0.48	5.45E-03	0.0375
PPP1R9A	0.93	8.39E-04	0.0104	LRIG2	-0.47	2.12E-08	8.83E-06
LOXL3	0.93	1.25E-03	0.0136	KLF6	-0.47	6.51E-06	4.05E-04
MISP3	0.92	4.71E-06	3.20E-04	NLN	-0.47	1.12E-05	6.05E-04
CTHRC1	0.92	5.50E-06	3.58E-04	FBXL2	-0.47	1.65E-04	3.50E-03
PDGFRL	0.92	1.26E-05	6.39E-04	FRAT2	-0.46	1.19E-08	5.49E-06
IGFBP6	0.91	6.21E-06	3.90E-04	RPS18	-0.46	2.57E-06	2.17E-04
FAP	0.91	9.20E-06	5.25E-04	RHOBTB1	-0.46	6.22E-05	1.80E-03
OCIAD2	0.91	5.35E-04	7.58E-03	TAF4B	-0.46	2.24E-04	4.22E-03
CAVIN3	0.9	1.22E-07	3.05E-05	R3HCC1L	-0.45	3.99E-06	2.80E-04
COPZ2	0.9	1.00E-06	1.15E-04	TRAK2	-0.45	1.70E-05	7.79E-04
CHST1	0.9	2.63E-06	2.19E-04	SLC7A1	-0.45	1.92E-05	8.44E-04
GFPT2	0.9	1.62E-05	7.67E-04	ZNF251	-0.45	2.47E-05	9.68E-04

Table 4-2: 2071 genes were differentially expressed in $BRAF^{V600E}$/wildtype patient melanomas in data extracted from the TCGA firehouse legacy dataset. Top 100 genes differentially expressed (ranked by Log^2 ratio)

4.1.3. Data set 3: BRAF^{V600E}/wildtype melanoma isogenic cell model

The third data set emerged from gene expression profiling performed on a BRAF^{V600E}/wildtype isogenic cell model, created in house by DPhil candidate Lina Guo, and work pertaining to the creation of this model is credited to her.

This model was critical for my project and therefore I will briefly describe how it was created and characterised.

The isogenic cell model was created from the BRAF wildtype melanoma cell line, CHL1. CHL1 was selected from three BRAF wildtype melanoma cell lines (CHL1, SKMEL2 and LM25) on account of its relatively low aneuploidy, lowest BRAF gene copy number (3-4 copies, on average per cell) and high transfection efficiency. A *BRAF^{V600E}* mutation was inserted into CHL1 using CRISPR. A BRAF wildtype guide RNA associated with Cas9 (designed by Horizon discovery) targeted the BRAF gene at exon 15. Once cut via cas9, a donor plasmid containing the *BRAF^{V600E}* mutation was inserted into the double stranded DNA break via homologous recombination. The mutant sequence also contained three unique silent mutations to prevent re-cutting of the donor sequence and to assist in selection experiments aimed at differentiating experimentally inserted *BRAF^{V600E}* for endogenous WT BRAF expression. The donor sequence also encoded for the selection marker eGFP under control of a CMV promoter. Transfected cells were selected, and successful genomic BRAF^{V600E} integration was confirmed via PCR using primers specific for the introduced sequence.

Clones that appeared to be homozygous for *BRAF^{V600E}* with no detectable BRAF wildtype mRNA on PCR were selected for further experiments. These clones were compared with the parental CHL1 cell line and with individual BRAF wildtype clones

derived from bulk culture.

The introduced *BRAF*^{V600E} mutation was shown to activate downstream targets MEK and ERK. This activation was inhibited by the BRAF^{V600E} inhibitor PLX4720. *BRAF*^{V600E} mutant clones demonstrated increased sensitivity to PLX4720, which was not seen in *BRAF* wildtype clones suggesting a degree of oncogene addiction in the *BRAF*^{V600E} mutant clones.

Gene expression profiling was next performed using RNA extracted from four *BRAF*^{V600E} mutant clones, three *BRAF* wildtype clones, and the parental CHL1 cells. Following quality control and amplification, cRNAs were hybridised to Human HT12v4.0 Illumina arrays. The raw beadchip data were first pre- processed by Wellcome Trust Centre for Human Genetics in Oxford, and the subsequent data for each probe further processed by Dr Ruud Van Stiphout (Associate Professor Francesca Buffa's group, University of Oxford). The LIMMA method was used to identify differentially expressed genes between BRAF^{V600E} mutant and wildtype clones. A heat map demonstrated two distinct expression profiles as determined by BRAF mutation status, confirming adequate clustering of clones into either genomic group. The analysis identified 814 differentially expressed genes (adjusted p-value <0.05) between the two groups. The top 100 differentially expressed genes are presented in table 4-3.

Upregulated in $BRAF^{V600}$ mutant melanomas				Downregulated in $BRAF^{V600}$ mutant melanomas			
Gene symbol	**Log^2 Ratio**	**p-Value**	**Adjusted p-Value**	**Gene symbol**	**Log^2 Ratio**	**p-Value**	**Adjusted p-Value**
STC1	2.70	1.40E-10	6.63E-09	SLN	-3.61	3.72E-17	3.44E-14
VGF	2.65	1.22E-11	9.38E-10	CD96	-2.35	1.89E-13	4.98E-11
BMP7	2.31	2.27E-13	5.24E-11	DUSP23	-2.34	6.55E-11	3.78E-09
LYPD1	2.28	1.14E-17	2.11E-14	CD96	-2.27	2.04E-12	2.51E-10
HIST1H1C	2.26	1.05E-08	1.80E-07	BCAS1	-2.06	3.73E-12	3.83E-10
SLITRK3	2.13	6.45E-07	4.17E-06	BCAS1	-1.91	6.82E-12	6.30E-10
LOC100134073	1.99	3.84E-16	2.37E-13	BEX1	-1.89	2.25E-12	2.60E-10
MGC39900	1.99	3.82E-11	2.43E-09	ENPP2	-1.89	1.02E-08	1.77E-07
TGFBI	1.92	5.11E-10	1.97E-08	ENPP2	-1.86	2.67E-09	6.85E-08
SORBS2	1.90	2.53E-09	6.63E-08	COL9A1	-1.82	6.89E-15	3.18E-12
RFTN1	1.83	2.09E-05	7.10E-05	PEG10	-1.80	2.82E-08	3.52E-07
GPR18	1.76	3.38E-07	2.45E-06	PTGS1	-1.78	2.42E-11	1.60E-09
HIST2H2AA3	1.74	3.55E-06	1.64E-05	MAG	-1.75	7.73E-12	6.80E-10
HIST1H2BK	1.72	1.46E-07	1.26E-06	ABLIM1	-1.62	4.92E-08	5.44E-07
PPARG	1.71	2.81E-07	2.13E-06	IL1RL1	-1.55	6.12E-06	2.54E-05
SORBS2	1.71	6.12E-09	1.27E-07	VCAN	-1.47	4.76E-07	3.25E-06
HIST1H2BK	1.69	1.37E-06	7.67E-06	RHOU	-1.43	1.92E-11	1.32E-09
ODC1	1.65	1.23E-07	1.10E-06	SCRG1	-1.42	6.98E-07	4.40E-06
PHLDA1	1.65	5.47E-11	3.26E-09	TF	-1.40	1.87E-08	2.65E-07
ADORA2B	1.64	2.71E-08	3.48E-07	EGR1	-1.39	1.11E-06	6.54E-06
PPARG	1.57	2.20E-06	1.11E-05	PEG10	-1.38	3.16E-10	1.33E-08
CXCL12	1.57	1.94E-08	2.72E-07	C18orf51	-1.36	1.91E-09	5.25E-08
NT5E	1.54	2.69E-13	5.52E-11	ABLIM1	-1.36	5.13E-08	5.54E-07
HTRA1	1.49	2.82E-08	3.52E-07	OLFML2B	-1.33	2.38E-10	1.04E-08
CXCL12	1.49	2.29E-08	3.10E-07	S100A4	-1.33	3.11E-06	1.49E-05
RAB31	1.46	5.95E-10	2.16E-08	COL15A1	-1.31	9.26E-07	5.64E-06
CXCL12	1.46	1.03E-07	9.67E-07	S100A4	-1.29	0.00011027	0.00029475
PLAUR	1.45	4.28E-13	6.59E-11	CARD10	-1.29	3.90E-13	6.59E-11
PLAUR	1.43	9.33E-15	3.45E-12	KIAA0363	-1.28	2.55E-09	6.63E-08
HIST2H2AA3	1.42	4.45E-06	1.97E-05	CAPS	-1.28	1.60E-07	1.35E-06
UCN2	1.42	6.44E-09	1.31E-07	LPP	-1.26	2.35E-06	1.17E-05
HIST2H2AA4	1.41	4.58E-06	2.01E-05	CD55	-1.25	3.85E-07	2.71E-06
PLAUR	1.40	2.41E-12	2.62E-10	NLGN4X	-1.25	1.89E-09	5.25E-08
KYNU	1.40	1.94E-11	1.32E-09	MGAT4C	-1.24	4.68E-08	5.23E-07
KYNU	1.35	1.58E-10	7.13E-09	GABBR2	-1.24	5.13E-08	5.54E-07
BCL6	1.30	1.34E-11	9.88E-10	PPFIBP2	-1.23	1.07E-11	8.60E-10
TGFA	1.29	9.91E-09	1.74E-07	C18orf51	-1.22	1.27E-09	3.98E-08
TNFRSF12A	1.27	3.41E-08	4.14E-07	CRABP1	-1.21	1.01E-10	4.92E-09
SEPT3	1.27	6.83E-11	3.82E-09	NEUROG2	-1.21	7.87E-09	1.55E-07
FBXL21	1.23	3.03E-10	1.30E-08	TAGLN3	-1.19	8.56E-13	1.22E-10
PLIN2	1.23	3.63E-05	0.00011267	BAMBI	-1.19	7.98E-07	4.94E-06
GLDC	1.23	9.47E-10	3.30E-08	RPS6KC1	-1.18	1.52E-08	2.30E-07
GEM	1.21	5.44E-05	0.00015954	NLGN4X	-1.17	5.24E-08	5.60E-07
ACSL3	1.19	1.74E-08	2.53E-07	SGCE	-1.15	3.80E-07	2.69E-06
NDRG1	1.18	6.88E-07	4.38E-06	COL11A2	-1.11	6.81E-09	1.35E-07
ADRB2	1.18	3.89E-09	9.37E-08	IL1RL1	-1.10	6.81E-06	2.77E-05
TSPAN13	1.16	2.18E-07	1.75E-06	FOXC1	-1.10	5.21E-08	5.59E-07
FAM87A	1.16	4.33E-09	9.95E-08	SCML1	-1.10	1.73E-09	5.00E-08
PERP	1.16	4.27E-06	1.92E-05	PLOD2	-1.10	1.05E-08	1.80E-07
PRKCH	1.15	1.35E-08	2.13E-07	SLC6A12	-1.08	7.72E-08	7.67E-07
OPN3	1.14	2.14E-05	7.26E-05	SCARB1	-1.07	4.66E-11	2.87E-09
MT2A	1.14	4.54E-12	4.42E-10	ACOT9	-1.07	0.00013256	0.00034485
PLIN2	1.14	0.00015536	0.00039524	CXorf26	-1.07	4.95E-05	0.00014883
FKBP11	1.13	1.08E-09	3.47E-08	STOM	-1.07	5.56E-07	3.68E-06
GEM	1.13	0.00014011	0.00036245	RXRG	-1.06	9.16E-12	7.69E-10
HES6	1.12	6.68E-09	1.34E-07	LDB2	-1.06	8.14E-06	3.21E-05
ADAMTS9	1.11	2.41E-09	6.46E-08	SNRPN	-1.05	8.87E-11	4.55E-09
IL7R	1.09	8.74E-08	8.63E-07	PNLIP	-1.04	7.62E-08	7.60E-07
SEC14L4	1.08	1.38E-08	2.16E-07	SH2D7	-1.04	8.96E-08	8.76E-07
WSCD1	1.08	1.47E-14	4.54E-12	INSIG1	-1.03	2.17E-06	1.11E-05
KRT10	1.07	2.15E-07	1.74E-06	TFAP2A	-1.03	4.60E-05	0.00013904

Upregulated in BRAF^{V600} mutant melanomas				Downregulated in BRAF^{V600} mutant melanomas			
Gene symbol	**Log^2 Ratio**	**p-Value**	**Adjusted p-Value**	**Gene symbol**	**Log^2 Ratio**	**p-Value**	**Adjusted p-Value**
WFDC2	1.06	4.02E-13	6.59E-11	PLOD2	-1.02	5.67E-08	5.92E-07
FHL2	1.04	1.47E-09	4.45E-08	EPB41L3	-1.02	1.07E-06	6.34E-06
PCK1	1.03	1.63E-07	1.37E-06	NOSTRIN	-1.02	5.38E-10	2.03E-08
TBX18	1.03	6.00E-09	1.26E-07	RPS6KC1	-1.02	1.11E-07	1.02E-06
NBL1	1.02	9.06E-09	1.66E-07	CDH15	-1.00	1.44E-08	2.23E-07
HBA2	1.01	2.73E-08	3.48E-07	CALD1	-1.00	0.00018147	0.00045112
LMO4	1.00	8.03E-05	0.00022231	PRKCB1	-1.00	6.26E-09	1.28E-07
TSPAN13	1.00	5.70E-07	3.76E-06	MGAT4C	-1.00	1.11E-07	1.02E-06
DKK1	0.99	9.81E-05	0.00026612	BCYRN1	-0.99	2.34E-08	3.14E-07
MKX	0.98	3.42E-07	2.48E-06	NUAK1	-0.99	2.85E-08	3.53E-07
MALT1	0.98	2.63E-06	1.28E-05	XYLT1	-0.99	5.84E-10	2.16E-08
HIST2H2AC	0.98	3.27E-05	0.00010361	IFI16	-0.99	6.01E-05	0.00017352
POR	0.97	3.31E-07	2.42E-06	PAM	-0.98	0.00025772	0.00061499
FAM123A	0.97	1.46E-07	1.26E-06	FST	-0.98	1.24E-08	2.02E-07
CTH	0.97	1.89E-08	2.67E-07	C14orf169	-0.98	4.36E-09	9.95E-08
HIST1H2AC	0.97	2.85E-05	9.17E-05	ACTL8	-0.97	7.22E-11	3.92E-09
CREB5	0.97	1.19E-07	1.08E-06	FEZ1	-0.97	2.09E-06	1.09E-05
GPC4	0.96	8.12E-06	3.21E-05	SNURF	-0.96	9.73E-08	9.36E-07
KIF5C	0.95	1.01E-09	3.43E-08	PLP1	-0.96	4.93E-10	1.94E-08
MT1A	0.95	1.01E-10	4.92E-09	ADAM23	-0.95	8.93E-09	1.66E-07
SHISA2	0.94	2.23E-05	7.52E-05	DPYSL2	-0.95	9.30E-08	9.04E-07
LMO4	0.94	6.63E-05	0.00018904	TBL1X	-0.95	1.19E-07	1.08E-06
AGPAT9	0.94	9.08E-06	3.50E-05	ARPP-21	-0.94	5.08E-08	5.54E-07
MAL2	0.94	1.38E-05	5.06E-05	PCDH18	-0.93	1.15E-06	6.68E-06
KCNMB4	0.93	1.31E-07	1.15E-06	LMCD1	-0.93	9.92E-09	1.74E-07
DCLK1	0.92	5.30E-05	0.00015604	ID2	-0.93	7.31E-06	2.94E-05
LYPD1	0.92	7.62E-11	4.02E-09	FUCA2	-0.92	0.00011761	0.00031166
CXCR7	0.92	4.02E-05	0.00012384	TUBB4	-0.92	1.07E-07	9.96E-07
ROR2	0.92	1.35E-12	1.78E-10	MAGED1	-0.92	6.93E-07	4.39E-06
DPP7	0.91	2.73E-08	3.48E-07	ETFB	-0.92	2.28E-07	1.82E-06
TGFA	0.91	4.20E-07	2.93E-06	PLP1	-0.92	4.90E-08	5.44E-07
CD24	0.91	5.27E-05	0.00015586	NRG1	-0.91	4.61E-09	1.04E-07
CXCR7	0.90	0.00011294	0.00030102	PCDH18	-0.90	4.32E-08	4.93E-07
ACSL3	0.89	1.50E-07	1.29E-06	FAM43A	-0.90	6.54E-08	6.71E-07
UBE2E3	0.88	1.58E-07	1.34E-06	CAPS	-0.90	1.17E-06	6.70E-06
SHANK3	0.87	9.98E-08	9.45E-07	ARPP-21	-0.89	5.25E-09	1.13E-07
LPHN2	0.87	1.52E-07	1.30E-06	LRRN1	-0.89	1.72E-08	2.51E-07
GTF2I	0.86	7.71E-06	3.08E-05	PPP1R14A	-0.89	9.45E-08	9.14E-07
IGSF3	0.86	5.63E-06	2.37E-05	SLN	-3.61	3.72E-17	3.44E-14
IL7R	0.85	1.74E-06	9.35E-06	CD96	-2.35	1.89E-13	4.98E-11

Table 4-3: Top 100 differentially expressed genes between BRAF^{V600E} mutant and wildtype clones, in the isogenic cell line model, ranked by log fold change. Log FC = Log fold change relative to BRAF^{V600E} mutant clone

4.2. Integrative analysis of the datasets

To explore the hypothesis that the BRAF^{V600} mutation influenced angiogenesis, I analysed the three datasets to determine associations between differentially expressed genes and relationships to angiogenesis and specifically, the expression of VEGF. Genes listed in table 4-1 (both those up and downregulated in BRAF^{V600} mutant

tumours) were analysed and characterised into signalling pathways using the web-based Panther Classification system (http://www.pantherdb.org) based on pre-defined signaling pathways. (figure 4-1 A).

From the TCGA firehose legacy dataset (table 4-2) the entire list of 2071 differentially expressed genes with adjusted p-values <0.05 were also uploaded and analyzed via the Panther application. Pathways resulting from this analysis are presented in figure 4-1 B.

Finally, the same analysis was performed on the 814 differentially expressed genes (defined by adjusted p-value of <0.05) from the isogenic $BRAF^{V600}$ and wildtype model and the output is presented in figure 4-1 C. The 11 genes within this dataset contained with the angiogenesis signally pathway were compared to the AVAST-M data set (table 4-1) and presented in table 4-3.

Genes differentially expressed in all three datasets were merged into a venn diagram to discern differentially expressed genes in common across the datasets as well as to assess concordance (figure 4-2). The analysis identified 4 genes in common, ROR2, IGFBP2, LEF1 and ETV1 (table 4-5).

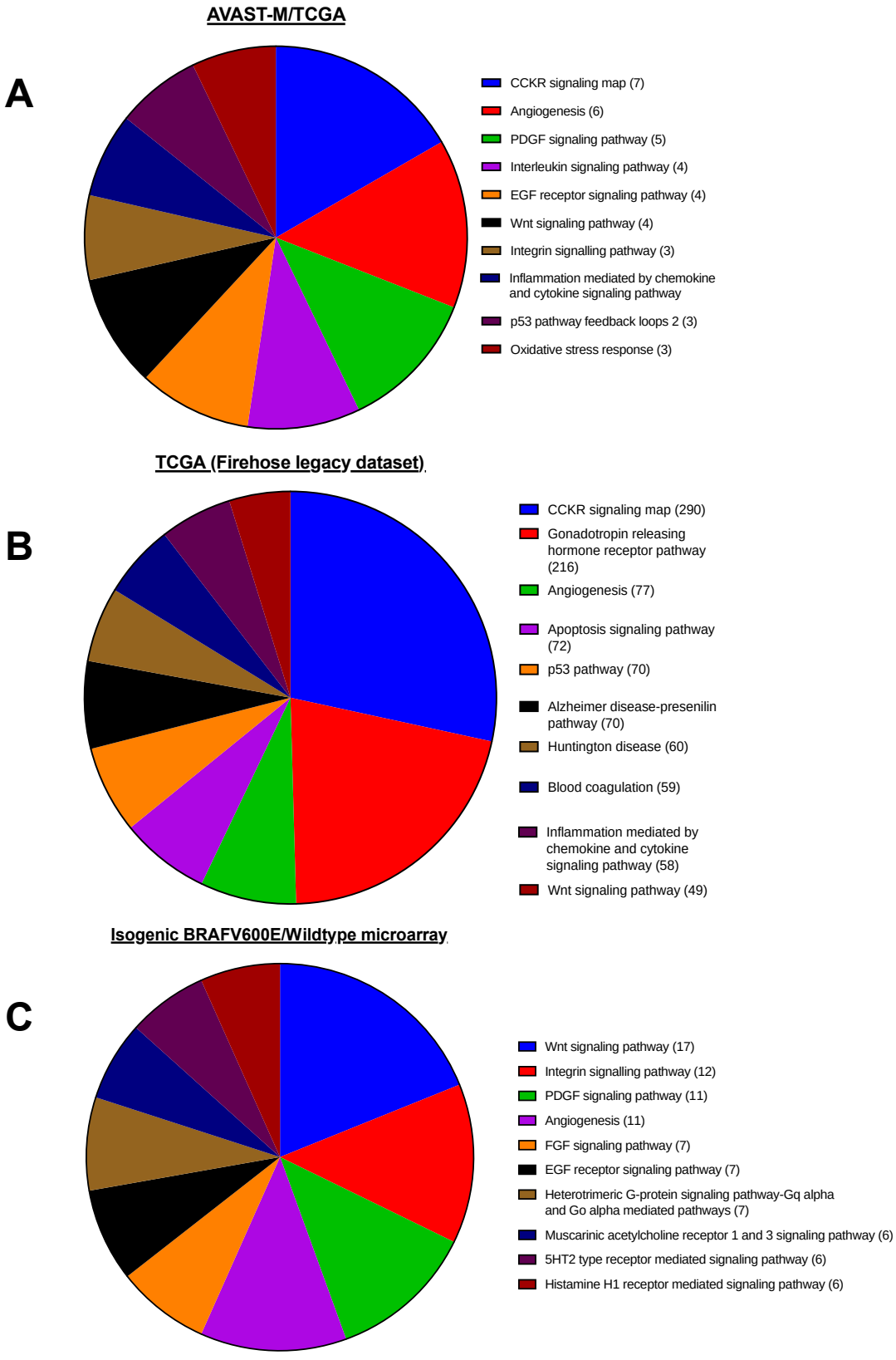

Figure 4-1: Classification of genes differentially expressed genes between BRAF^{V600E} and wildtype isogenic clones into signalling pathways. defined by the Panther classification system for A. The AVAST-M/TCGA dataset, B. TCGA (firehose legacy datset) and C. BRAF ^{V600E}/wildtype isogenic cell model array Top 10 represented pathways included. Numbers in brackets refer to the numbers of genes associating with that particular pathway

Gene symbol	Full name	Angiogenesis relevant associations	Expression in $BRAF^{V600}$ (isogenic model)	Expression in $BRAF^{V600}$ (AVAST-M)
PRKCH	Protein Kinase C	Activated downstream as a consequence of VEGF signalling (Aiello et al., 1997)	Up	NDE
NCK2	NCK adaptor protein 2	Component of PDGRFβ signalling promoting pathological retinal neovascularisation (Dubrac et al., 2018)	Up	NDE
GSK3B	Glycogen synthase kinase-3β	Negative regulator of angiogenesis (Kim et al., 2002)	Down	NDE
SFRP1	Secreted frizzled-related protein 1	Inhibits angiogenesis in HCC (Dubrac et al., 2018)	Down	Up
FZD3	Frizzled 3	Wnt receptor implicated in pathological retinopathy (Chen et al., 2011)	Up	NDE
PRKCB	Protein Kinase-Cβ	Expression induced in response to VEGF (Al-Sanabra et al., 2017)	Down	NDE
CRYAB	αB-crystallin	CRYAB expression enhances VEGF Secretion via resistance to proteolysis (Ruan et al., 2011)	Down	NDE
PRKCA	Protein Kinase-Cα	siRNA reduces VEGF mRNA in endothelial cells (Xu et al., 2008)	Up	NDE
RHOC	Ras homolog family member C	Activated by VEGFA/VEGFR2 signalling to promote endothelial cell proliferation via nuclear β catenin stabilisation (Hoeppner et al., 2015)	Down	NDE
ARAF		Kinase and important component of MAP-K pathway with effects on tumour proliferation and growth	Down	NDE
ETS1	V-Ets Avian Erythroblastosis Virus E26 Oncogene Homolog 1	Transcription factor with binding motifs present on many angiogenic mediators (including VEGF) (Chen et al., 2017)	Down	NDE

Table 4-4: Description of the 11 genes differentially expressed in the $BRAF^{V600E}$/Wildtype model associated with the angiogenesis signalling pathway as defined by Genecodis. Comparison made to differentially expressed genes in the AVAST-M data set. NDE = Not differentially expressed

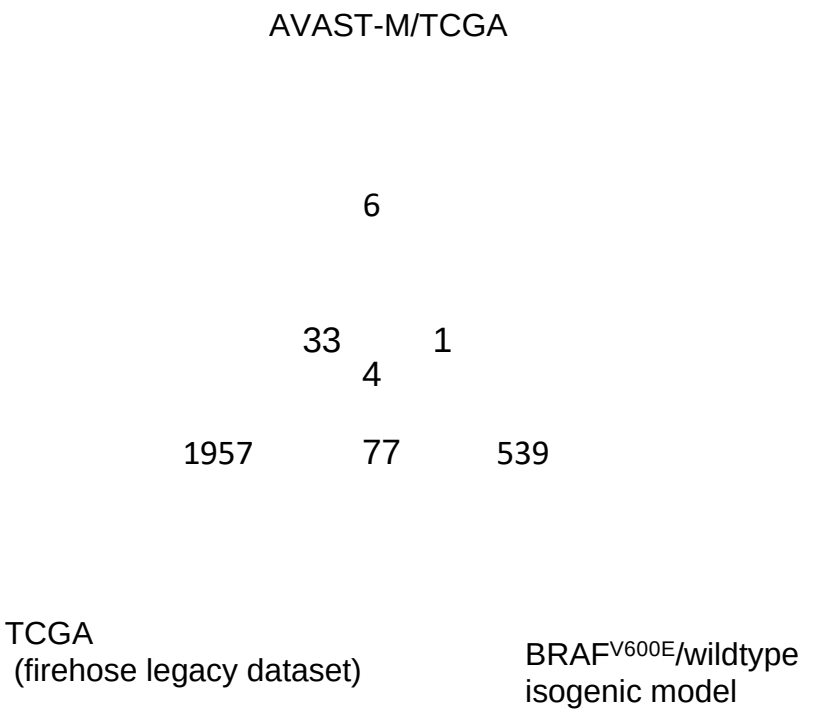

Figure 4-2: Venn diagram depicting total numbers of genes differentially expressed between BRAF mutant and wildtype in data sets described previously.

	AVAST-M/TCGA		TCGA (firehose legacy dataset)		Isogenic cell line model	
Gene	**Magnitude of change (t-value)**	**Adjusted p-value**	**Magnitude of change vs WT (log^2 ratio)**	**Adjusted p-value**	**Magnitude of change (Log fold change)**	**Adjusted p-value**
ROR2	2.09	0.263216	0.83	0.0028	0.92	1.78E-10
ETV1	2.28	0.22613	0.57	0.0038	0.55	1.48E-06
IGFBP2	3.27	0.049427	1.18	0.0004	0.61	2.62E-05
LEF1	4.15	0.004559	0.60	0.0192	0.51	0.00051

Table 4-5: Genes commonly differentially expressed between all three data sets described above

4.3. Testing for differential expression of VEGF between $BRAF^{V600}$ mutant and wildtype melanoma in the datasets

Given the clinical result in the AVAST-M clinical trial that demonstrated increased sensitivity to bevacizumab in patients with resected $BRAF^{V600E}$ mutant melanomas, these melanomas were hypothesised to express more *VEGF* mRNA than wildtype and to be more dependent on VEGF for their survival. *VEGF* mRNA expression was thus assessed in the three data sets described above.

4.3.1. VEGF expression compared between $BRAF^{V600}$ and wildtype samples in the AVAST-M and TCGA data sets (datasets 1 and 2)

VEGF mRNA was differentially expressed between $BRAF^{V600E}$ and wildtype melanomas from the AVAST-M data set (p= 0.016), however when corrected for multiple analyses, the statistical significance was lost (adjusted p value 0.143888). This raised the possibility that there is no real difference between the two genotypes in this population, paralleling the lack of difference seen following quantification of VEGF at the protein level in the patient samples via IHC (chapter 3).

Within the TCGA (firehose legacy) dataset described earlier, VEGF mRNA was not upregulated in $BRAF^{V600E}$ mutant melanomas (p=0.00009455, q=0.002729). In this dataset, 72% of tumours were stage pT4b according the AJCC 7^{th} edition and median

overall survival was approximately 34 months. In contrast, in the AVAST-M trial, 33% of patients had pT4b melanomas and median overall survival was not reached at 8 years (Corrie *et al.*, 2018). The TCGA data were therefore representative of higher stage disease.

Given the discrepancy between the AVAST-M and TCGA data, I quantified VEGF mRNA expression in the isogenic cell model.

4.3.2. Expression of VEGF in the BRAF^{V600E}/wildtype isogenic cell model

4.3.2.1. VEGF mRNA expression

VEGF mRNA expression was quantified in the isogenic BRAF^{V600E}/wildtype melanoma cell line model. Of note, VEGF mRNA was not one of the 814 genes found to be differentially expressed in the microarray analysis (table 4-3).
Primer sequences specific to the $VEGF_{165}$ isoform were identified from the literature (Medford *et al.*, 2009). $VEGF_{165}$ was chosen as this isoform is considered to have the most biological relevance to angiogenesis (Ferrara *et al.*, 2003). The selected primer sequences amplified a dominant single product (figure 4-3 A).

Eight isogenic cell clones (4 $BRAF^{V600E}$ mutant and 4 wildtype) were cultured for 48 hours and harvested. RNA was extracted using techniques described earlier. $VEGF_{165}$ mRNA expression was quantified using qRT-PCR.

In this model, $VEGF_{165}$ mRNA expression was not increased in the $BRAF^{V600E}$ clones compared to the wildtype clones (p=0.5801) (figure 4-3 B).

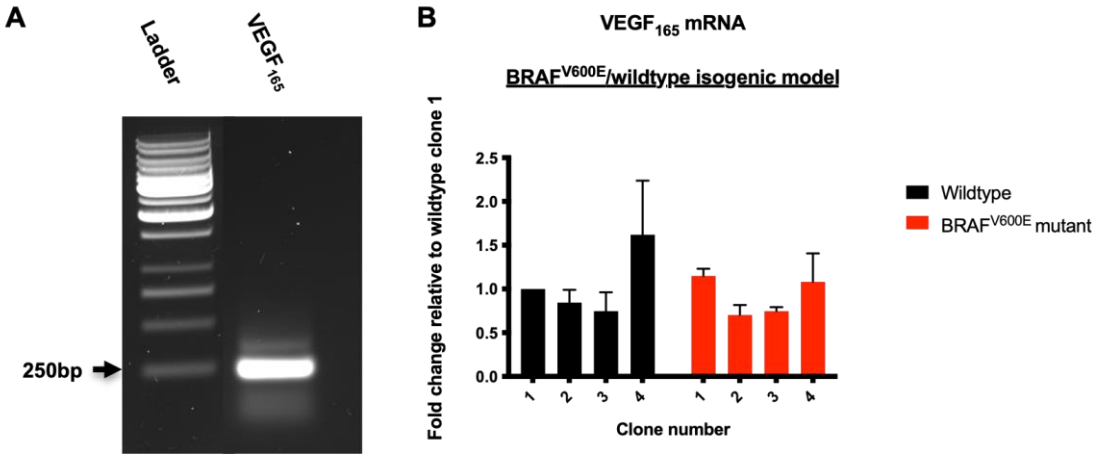

Figure 4-3: $VEGF_{165}$ in $BRAF^{V600E}$/wildtype isogenic cell line model. A. Amplified products from a RT-PCR reaction containing primers for $VEGF_{165}$ were analysed by agarose gel electrophoresis. The dominant product for the $VEGF_{165}$ primer was at the expected size (229bp). B. $VEGF_{165}$ mRNA expression the isogenic cell model was determined using qRT-PCR. TUBA6 was used as the housekeeping gene and data expressed as fold change relative to wildtype clone 1. No difference existed in expression between (grouped) $BRAF^{V600E}$ and wildtype clones. Statistics performed using unpaired students t-test. Experiment performed in biological duplicate each consisting of three technical repeats. Data expressed as mean value and error bars represent SEM.

4.3.2.2. VEGF protein expression

Given the absence of differential expression of VEGF at the mRNA level DPhil student Lina Guo proceeded to quantify intracellular and secreted VEGF in cell lysate and secreted medium, respectively. A VEGF ELISA kit (VEGF Quantikine kit, R &

D), specific for isoforms $VEGF_{165}$ and $VEGF_{121}$, was used for these experiments. Seven isogenic clones (3 wildtype, 4 $BRAF^{V600E}$ mutant) were cultured and VEGF content was quantified in both the cell lysate and separately in the conditioned medium.

In contrast to VEGF mRNA expression, $BRAF^{V600E}$ mutant clones appeared to express more VEGF both intracellularly (figure 4-4 B) and as a secreted form into the conditioned medium (figure 4-4 C). Although VEGF secretion varied considerably within $BRAF^{V600E}$ mutant clones it was undetectable in all the wildtype clones and a statistically significant difference was evident in a grouped comparison.

These data were consistent with the AVAST-M data set in that *VEGF* was not overexpressed in $BRAF^{V600E}$ mutant tumours at the mRNA level. Data from the protein level however (not available for the AVAST-M or TCGA data sets) demonstrated increased intracellular and secreted VEGF expression in $BRAF^{V600E}$ mutant clones, raising the possibility of a post-transcriptional mechanism of regulation.

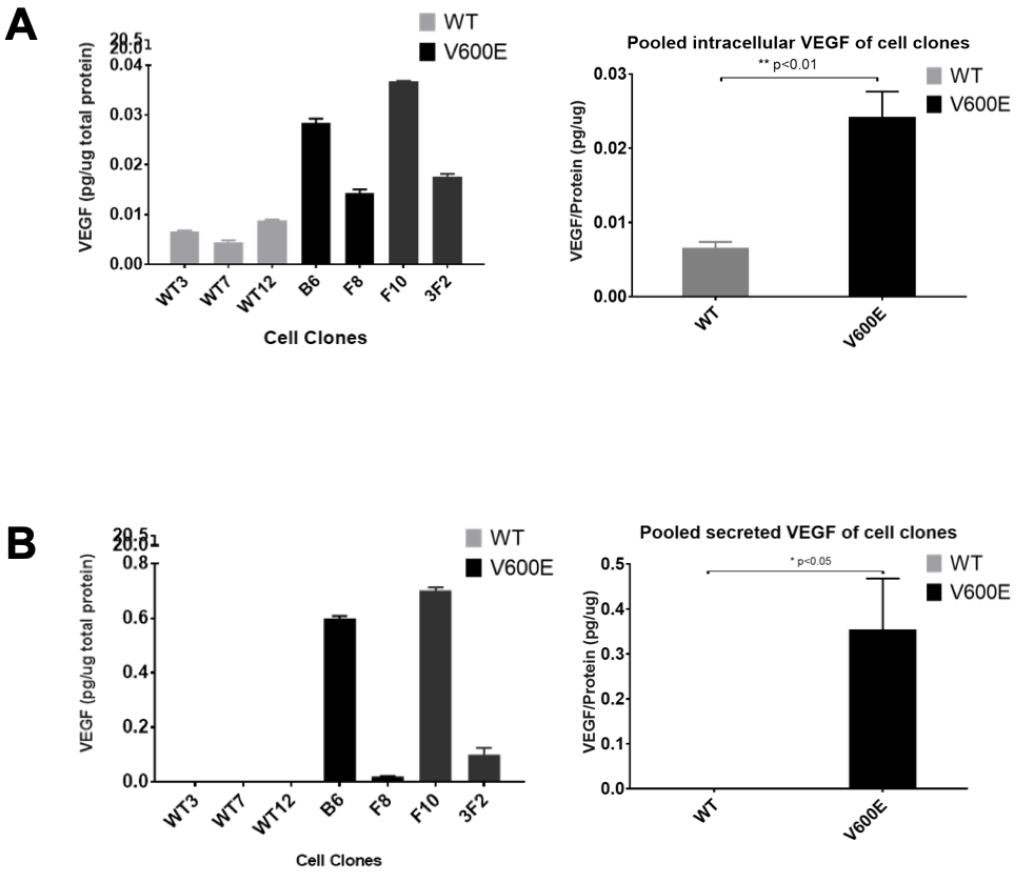

Figure 4-4: VEGF protein expression in BRAF^{V600E}/wildtype cell model. A. Intracellular VEGF levels as detected by VEGF ELISA. Data presented as mean +/- SEM pg/µg total protein of three independent replicates (total protein quantified using Pierce BCA protein assay). Pooled results for each genotype compared using unpaired students t-test. B. VEGF levels in conditioned medium after culture for 48 hours. Data presented as mean +/- SEM pg/µg total protein of three independent replicates. Pooled results for each genotype compared using unpaired students t-test. Experiments performed by Lina Guo

4.3.2.3. *Relationship between BRAF^{V600E} and HIF-1α and VEGFR2*

Given the data generated by Lina Guo, I next tested the effect of the BRAF^{V600E} mutation on other mediators of VEGF transcription and signalling, *HIF-1α* and *VEGFR2* mRNA expression in the isogenic cell model.

HIF-1α protein is well characterised as a transcription factor responsible for upregulating many genes, including VEGFA in response to hypoxia (Masoud *et al.*, 2015). Regulation of *HIF-1α* at the mRNA level, in contrast, is less well understood. Increased *HIF-1α* transcription has been associated with a poor prognosis in CLL and EGFR wildtype non small cell lung cancer (Park *et al.*, 2011; Kontos *et al.*, 2017). Furthermore, the kinetics of *HIF-1α* mRNA expression differ from HIF-1α protein, and can unexpectedly decrease in hypoxia (Chamboredon *et al.*, 2011). Given the potential discordance between HIF-1α protein and mRNA expression, a possible association between the BRAF^{V600E} mutation and *HIF-1 α* was explored in the isogenic cell line model.

VEGFR2 is the predominant receptor for VEGFA (Simons *et al.*, 2016). Data above have shown that isogenic cells harbouring a BRAF^{V600E} mutation express more VEGF protein, both intracellularly and in a secreted form. In melanoma, cell lines have been reported to express VEGFR2, supporting a potential role for VEGF/VEGFR2 autocrine and paracrine signalling pathways to augment angiogenic responses (Adamcic *et al.*, 2012). Increased VEGFR2 expression may therefore be an additional mechanism associating the BRAF^{V600E} mutation with angiogenic phenotypes. Therefore, VEGFR2 mRNA was quantified in the isogenic clones by qRT-PCR. *HIF-1α* mRNA expression was not altered between BRAF^{V600E} and wildtype clones

(p=0.3085) (figure 4-5 A). Subsequently, a possible association between the $BRAF^{V600E}$ mutation and HIF-1α protein levels was also explored and will be presented later in this thesis.

Expression of VEGFR2 mRNA was variable across the isogenic model and was highly expressed in two $BRAF^{V600E}$ clones (figure 4-5 B). This result was separately confirmed using flow cytometry to demonstrate expression of extracellular VEGFR2 in the same clones by Lina Guo. Due to the variability in expression, the difference in expression in a pooled comparison of $BRAF^{V600E}$ and wildtype clones did not reach statistical significance using a student t-test (p=0.1857). Nonetheless, the trend towards increased VEGFR2 expression within $BRAF^{V600E}$ mutant clones suggested increased VEGF signalling pathways associated with the $BRAF^{V600E}$ oncogene.

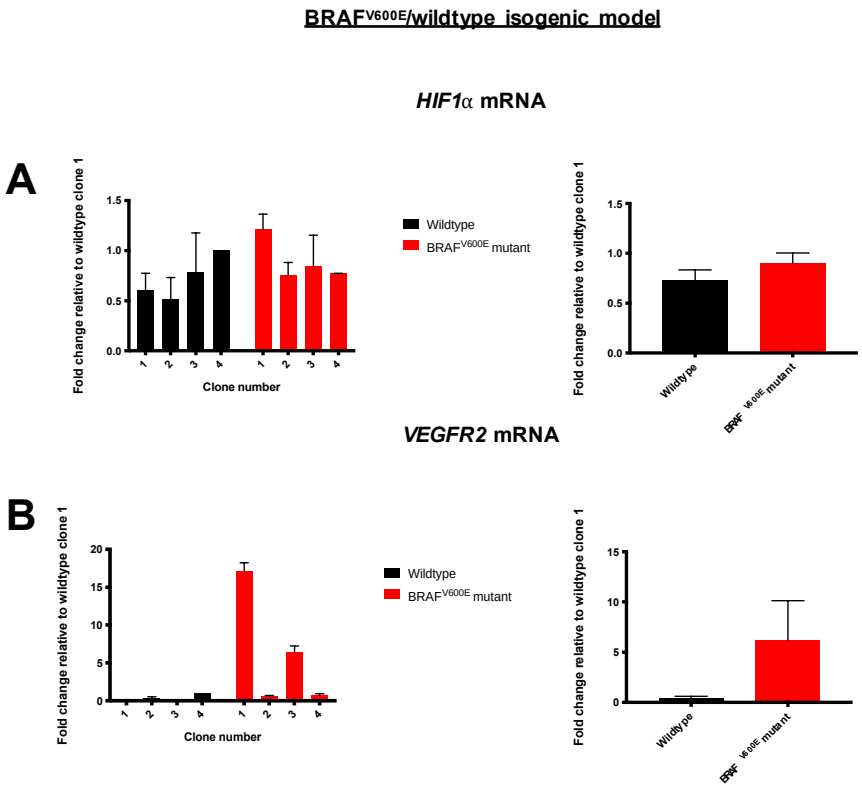

Figure 4-5: Expression of HIF-1 α and VEGFR2 in the BRAF^{V600E}/wildtype isogenic cell model. RNA was extracted as described earlier. qRT-PCR was used to determine mRNA expression of A. HIF-1 α and B. VEGFR2. TUBA6 was used as the housekeeping gene for both experiments. Statistics were performed using an unpaired student t-test comparing mean expression in BRAF^{V600E} clones with wildtype. Experiments performed in duplicate, each consisting of technical triplicates. Data expressed as mean value and error bars represent SEM.

4.4. Identification and validation of genes differentially expressed in BRAF^{V600} mutant melanomas that impact upon VEGF expression

The above analyses generated lists of genes differentially expressed between BRAF^{V600} mutant and wildtype melanomas from three data independent datasets. The next step in the project was to identify commonly differentially expressed genes in all three data sets. These would be candidates to pursue further for potential links to VEGF expression and angiogenic phenotypes.

The three data sets described above were not available simultaneously. Associate Professor Francesca Buffa's analysis (table 4-1) was available in the first year of my

project. Dataset 3 (table 4-4) was not available for another 12 months. In the interests of time, the validation strategy involved identifying genes differentially expressed in both the AVAST-M patient sample and TCGA data sets (table 4-1) with feasible relevance to angiogenesis, and then validating differential expression in the $BRAF^{V600E}$/wildtype isogenic melanoma cell line model (table 4-3).

The validation strategy was thus:

1) Filtering these genes differentially expressed in table 4-1 with feasible associations to VEGF expression, based upon a literature review.
2) Validating differential expression in the $BRAF^{V600E}$/wildtype isogenic cell model using qRT-PCR

Expression of target mRNA was calculated relative to housekeeping gene *TUBA6* using the $2^{-2\Delta CT}$ method reported by Livak and Schmittgen (Livak *et al.*, 2001). These housekeeping genes were selected as they exhibited minimal variability in expression between the $BRAF^{V600E}$ and wildtype clones.

Of the 44 genes differentially expressed in both the AVAST-M and TCGA data sets, 18 were selected for validation of differential expression in the isogenic cell line model.

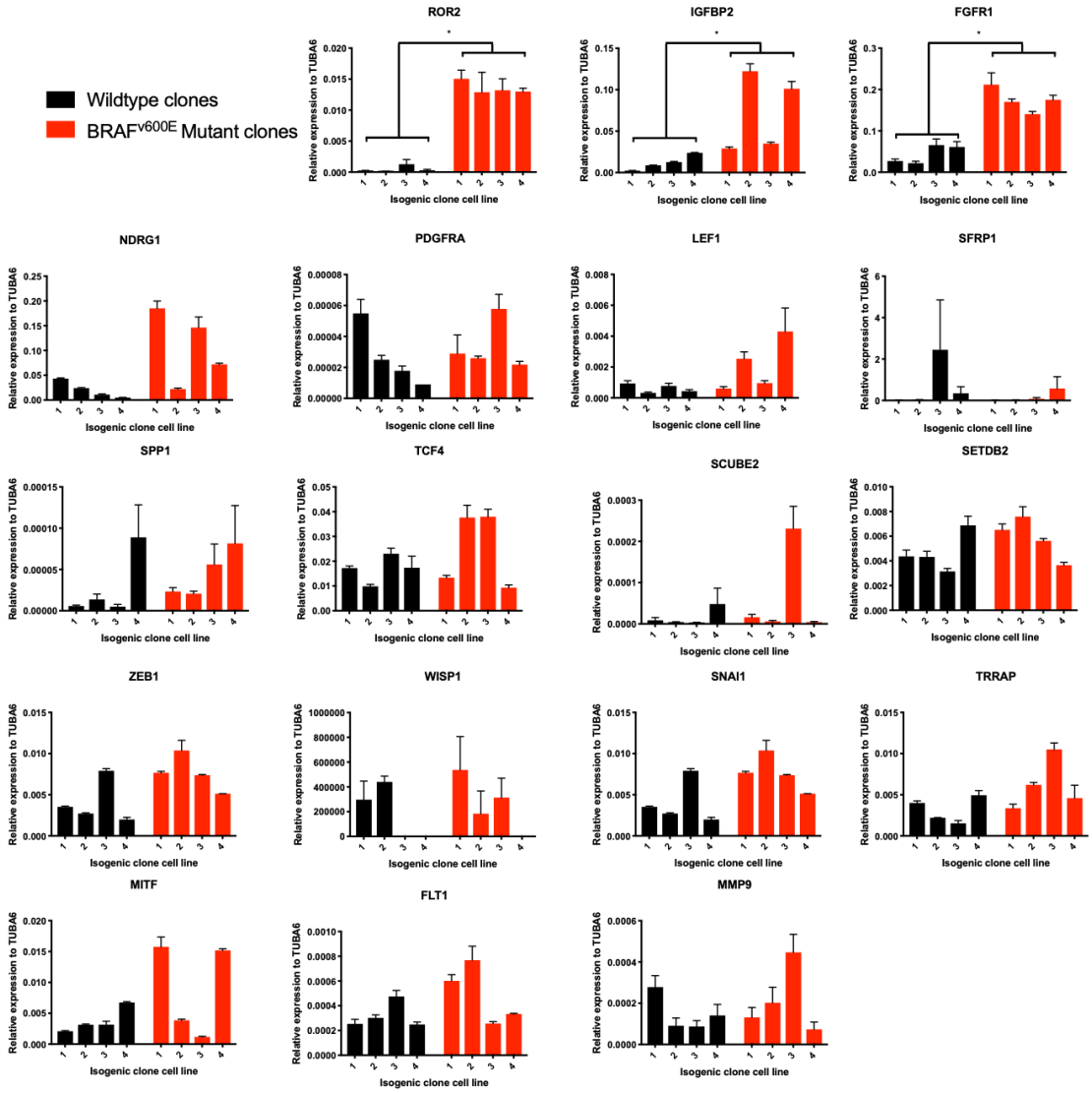

Figure 4-6: Genes commonly differentially expressed in the AVAST-M and TCGA datasets were tested for differential expression in the BRAF/wildtype isogenic model. Cell lines were cultured, harvested and underwent RNA extraction. Expression was determined by qRT-PCR and TUBA6 was used as a housekeeping gene. Values calculated by 2^-(CT_{gene} – $CT_{house\ keeping\ gene}$). Data presented as mean ± SEM. Statistics performed using unpaired students t-test comparing expression values pooled or $BRAF^{V600E}$ mutant vs wildtype clones for each gene. * = p<0.05. Experiments performed in biological duplicate with 3 technical replicates per experiment. Data expressed as mean value and error bars represent SEM.

4.5. Initial interrogation of Osteopontin as a candidate gene of interest

Osteopontin encoded by *SPP1,* was differentially upregulated in $BRAF^{V600E}$ mutant melanomas in both the AVAST-M and TCGA datasets (table 4-1). Before the availability of the isogenic cell model it was interrogated as a differentially expressed gene associated with VEGF expression.

The gene *SPP1* encodes for Osteopontin, a secreted glycoprotein that functions a cytokine and has a reported role in tumour cell migration and invasion (Rittling *et al.*, 2004). Osteopontin stabilises HIF-1α and augments VEGF mediated angiogenesis in hypoxic breast cancer cells (Raja *et al.*, 2014). Endothelial cells treated with recombinant osteopontin activate ERK and AKT signaling and subsequently increase VEGF expression that positively feeds back and promotes angiogenesis (Dai *et al.*, 2009).

Osteopontin was differentially upregulated in BRAF mutant melanomas in a panel of in-house cell lines (figure 4-7 A). Although Osteopontin expression was elevated in BRAF wildtype SKMEL23, this cell line has atypically high levels of BRAF activity due to BRAF gene amplification and has a phenotype of relative BRAF inhibitor sensitivity (Whittaker *et al.*, 2010).

Osteopontin expression influenced endothelial cell sprouting. HUVECs were grown as spheroids and plated in a fibrinogen/thrombin gel matrix. They were treated with VEGF depleted growth medium in a 1:1 ratio with conditioned medium from BRAF mutant A375P melanoma cells treated with either Osteopontin or control siRNA. Positive controls were supplemented with 100 pg of VEGF, replaced every other day. Negative controls were cultured in VEGF free EGM medium alone. Spheroids were observed daily and photographed under 4x magnification. The definition of an

endothelial sprout was arbitrarily determined as >20 pixels using image-J. Ten spheroids were randomly selected for each condition and cumulative sprout length calculated. Spheroids cultured in medium from Osteopontin knockdown A375P cells did not have a significant effect on sprouting compared to control (Figure 4-7 D).

When the isogenic cell model became available, Osteopontin was found not differentially expressed between the BRAF mutant and wildtype clones (figure 4-6 – marked as SPP1) nor did its expression decrease with pharmacological BRAF inhibition using PLX4720 (figure 4-7 B). The lack of a specific antibody also prevented assessment of osteopontin expression at the protein level. For these reasons, Osteopontin was not investigated further in this project.

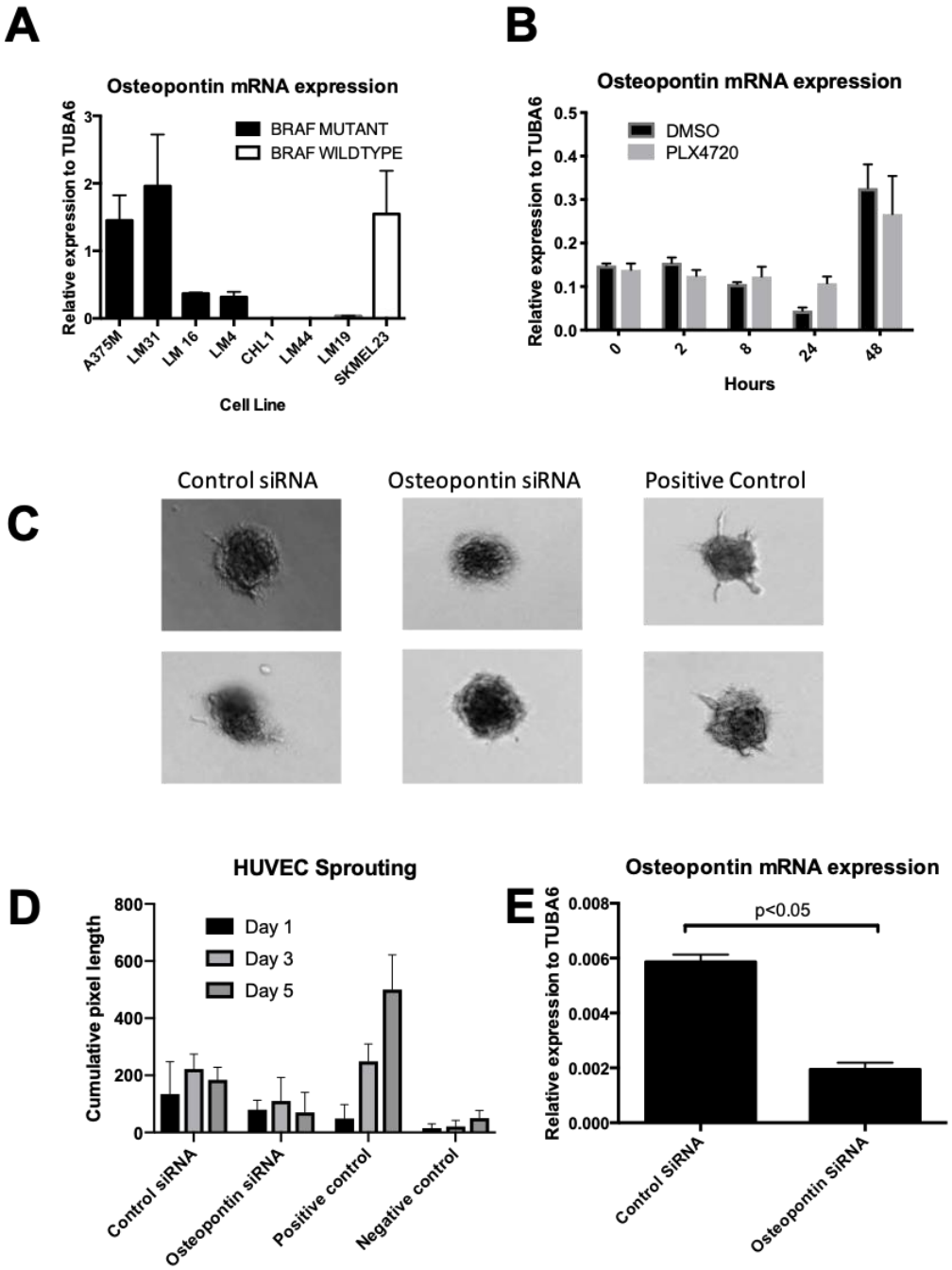

Figure 4-7: A. Osteopontin mRNA quantification from in house cell lines, normalised to house keeping gene TUBA6. Results represent mean ± SEM triplicate independent analyses each with 3 technical replicates. B. Osteopontin mRNA expression in A375P cells treated with 1uM of PLX4720 or DMSO (0.005%). Results compared between PLX4720 and DMSO at each time point using 1-way ANOVA. Results represent mean ± SEM triplicate independent analyses each with 3 technical replicates C. Impact of Osteopontin expression on HUVEC spheroid sprouting after exposure to conditioned medium from A375P cells were transfected with either osteopontin or control siRNA. Representative images after 3 days. D: Cumulative sprout length (sum of sprout length from n=20 spheroids, ie 10 spheroids measured from each of 2 independent experiments). Statistics performed using 1-way ANOVA comparing osteopontin siRNA vs Control at each time point. E. Confirmation of osteopontin knockdown

4.6. Selection of ROR2 as a gene expressed in association with the BRAFV600E mutation

4.6.1. Selection of ROR2 for further investigation

The above analysis identified two genes upregulated in BRAF mutant melanomas in all three data sets and validated in the isogenic model: ROR2, IGFBP2. FGFR1 was differentially expressed in the AVAST-M/TCGA dataset and TCGA (firehose legacy) dataset and validated in the isogenic cell line model. Of note, ROR2 was not significantly differentially expressed in the AVAST-M data set (table 4-1) when adjusted for multiple t-tests (adjusted p-value =0.26)

ROR2, the receptor tyrosine kinase is an orphan receptor implicated in non-canonical Wnt signaling (O'Connell *et al.*, 2010). Functioning as a receptor for its ligand, Wnt5a, ROR2 expression in melanoma cells has been associated with aggressive phenotypic features of increased invasion, motility and metastatic potential (O'Connell *et al.*, 2010). Associations with angiogenesis and VEGF expression had not been reported.

IGFBP2 is a circulating protein that traditionally modulates the function of the insulin-like growth factors IGF-1 and IGF-2 (Firth *et al.*, 2002). IGFBP2 is present in the extracellular environment in many cell types and is considered to play a role in growth and development through interactions with IGF as well as additional targets in the extracellular matrix or cell surface glycoproteins (Park *et al.*, 2015). IGFBP2 overexpression in neuroblastoma cells up-regulates many genes implicated in promoting aggressive phenotypes, including VEGF transcription through binding to the VEGF promoter (Azar *et al.*, 2011).

FGFR1 is a tyrosine kinase. Once bound by its ligand, Fibroblast Growth Factor 1

(FGF1), FGFR1 intracellular tyrosine domains are phosphorylated resulting in a signalling cascade involving the MAPK, Protein Kinase C and PI3K/AKT pathways (Raju *et al.*, 2014). FGF and FGFR1 have been shown to interact with VEGF/VEGFR2 signalling. In epithelial cells, FGF can upregulate VEGF and VEGFR2 and conversely, VEGF can increase the expression of FGF (Seghezzi *et al.*, 1998; Tsunoda *et al.*, 2007). At the clinical level, the expression intensity of FGFR1 has been shown to associate with the degree of microvessel density (MVD) in patients with non-small cell lung cancer, suggesting a role in pathological angiogenesis (Pu *et al.*, 2017).

ROR2 was selected for further interrogation because of its striking pattern of upregulation in $BRAF^{V600E}$ mutant isogenic clones (figure 4-8) and role in promoting aggressive phenotypes in melanoma, which were hypothesized to include increased VEGF expression.

4.6.2. Validation of differential expression of ROR2 at the protein level

The expression of ROR2 was next assessed at the protein level within the isogenic cell model. ROR2 depleted cells were used as controls for ROR2 antibody optimization. A BRAF mutant isogenic clone previously shown to express high levels of ROR2 mRNA (clone 3 from figure 4-7) was transfected with ROR2 or control siRNA. Knockdown was confirmed using qRT-PCR (figure 4-8 A). A western blot performed on lysates from parallel transfected cultures showed that the ROR2 antibody detected 3 products (marked X, Y and Z on figure 4-8 B). All three bands were reduced in the ROR2 depleted cells, supporting specificity for the chosen ROR2 antibody. Band X refers to 105 kDA predicted size of the ROR2 protein. ROR2 has been reported by others to appear as a doublet band on western blot analysis,

attributable to post-translational modification (Mikels *et al.*, 2009).

Lysates were prepared from 7 isogenic clones and parental CHL1 cells and analysed using western blot. As shown in figure 4-8 C, ROR2 protein was not detectable in the wildtype clones, was faintly detectable in the CHL1 parental bulk culture and clearly overexpressed in the BRAF mutant clones. ERK activation was also evident in the BRAF mutant clones which confirmed constitutive MAPK signaling, consistent with the findings of Lina Guo when validating the isogenic model. ROR2 appeared as a dominant band although a faint doublet was still visible. The differences between this result and figure 4-8 B were attributable to both higher protein loading volumes and longer exposure times during film development in the latter. This result was in parallel with expression at the mRNA level and suggested minimal post-transcriptional regulation.

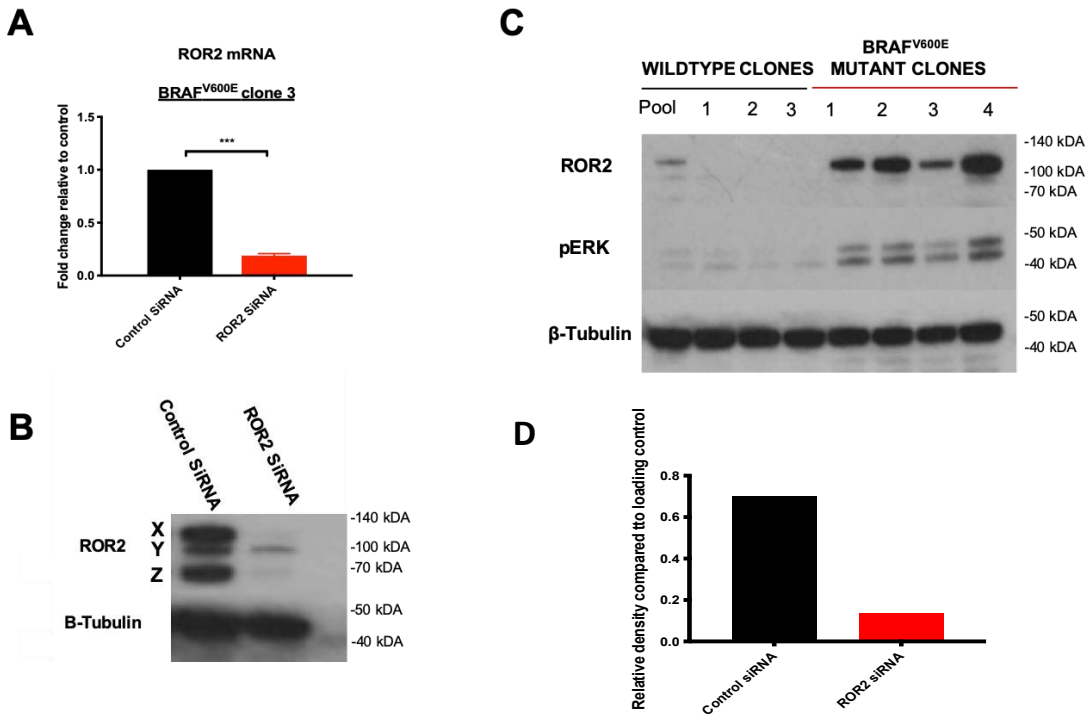

Figure 4-8: Detection of ROR2 protein by western blot. A BRAF^{V600E} mutant isogenic clone 3 was transfected with ROR2 or Control siRNA after 48 hours cells were harvested for RNA and protein extraction. A. Knockdown was confirmed by qRT-PCR using TUBA6 as a housekeeping gene B. Western blot identified three ROR2 bands (X, Y and Z) however all showed appropriate signal reduction in ROR2 siRNA transfected cells C. ROR2 protein expression in lysates from BRAF^{V600E}/wildtype isogenic cell model. D. Relative density of ROR2 expression (100 kDa band) in B compared to loading control). Density was calculated using image J. Experiments performed in triplicate. Statistics performed using students t-test *** p ≤ 0.001

4.6.3. ROR2 expression in a panel of non-isogenic BRAFV600E and wildtype melanoma cell lines

The expression of ROR2 using qRT-PCR was also explored in a panel of 8 non isogenic melanoma cell lines: $BRAF^{V600E}$ mutant: A375, SKMEL5, SKMEL28, LM31 and BRAF wildtype: SKMEL23, LM44, LM19, CHL1.

ROR2 mRNA was poorly expressed however was detectable in these cell lines. No significant difference existed between the BRAF mutant cell lines compared to wildtype. ROR2 protein expression in a selection of the below cell lines was quantified using western blot, however it was undetectable. This was consistent with previous experiments that had demonstrated concordance between mRNA and protein expression. For these reasons ROR2 protein expression was not presented

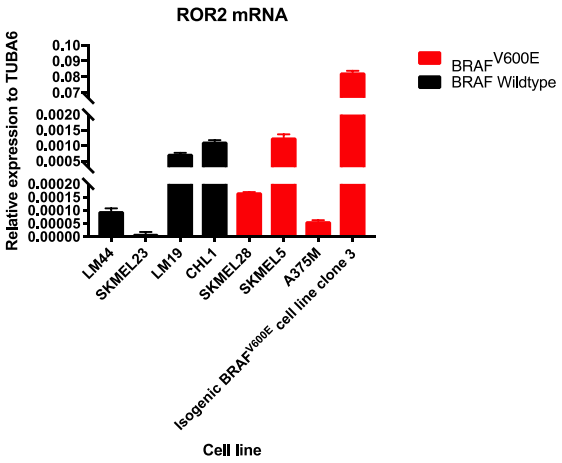

Figure 4-9: ROR2 expression across non-isogenic cell lines. Cell lines were cultured, harvested and underwent RNA extraction. Expression determined with RT-PCR. TUBA6 was used as a housekeeping gene. Values calculated by 2^-(CT_{gene} – $CT_{house\ keeping\ gene}$). Data presented as mean ± SEM. Statistics performed using unpaired students t-test comparing mean expression values pooled for BRAF mutant cell lines vs wildtype. Experiments performed in duplicate with 3 technical repeats per individual experiment.

4.7. The effect of pharmacological inhibition of BRAF signalling on ROR2 expression

To further test the association between ROR2 expression and mutant BRAF signalling, ROR2 expression was quantified in $BRAF^{V600E}$ mutant cell lines following pharmacological inhibition of BRAF, and its downstream target MEK. As the $BRAF^{V600E}$ mutation results in constitutive activation of the BRAF kinase, ROR2 expression was hypothesised to decrease with inhibition of BRAF and MEK.
The activity of PLX4270 is described in section 1.2.2.3. Trametinib is a potent, allosteric MEK 1/2 inhibitor, shown to inhibit downstream MAPK signalling at nanomolar concentrations (Gilmartin *et al.*, 2011). Trametinib also has clinical activity against $BRAF^{V600E}$ mutant melanoma (Flaherty *et al.*, 2012).

4.7.1. ROR2 mRNA expression in $BRAF^{V600E}$ mutant isogenic clone

The effect of $BRAF^{V600E}$ function on *ROR2* mRNA was initially explored in the isogenic cell line model. Two $BRAF^{V600E}$ mutant isogenic clones, previously shown to constitutively activate the MAPK kinase axis (clones 2 and 3 in figure 4-8) were treated with PLX4720 (1μM), trametinib (5nM) or solvent control (DMSO). Cells were harvested at baseline, and after 6, 24 and 48 hours of culture RNA was extracted, and *ROR2* mRNA expression determined using qRT-PCR with ROR2 primers used previously. *ROR2* mRNA expression in both cell lines was significantly decreased beyond 24 hours after treatment with trametinib in both cell lines. Treatment with PLX4720 did not significantly reduce ROR2 expression in either clone (figure 4-10 A and B).

4.7.2. ROR2 protein expression in BRAF^{V600E} mutant isogenic clone and in A375P cells

The effect of BRAF^{V600E} inhibition on ROR2 expression was next assessed at the protein level. A BRAF^{V600E} mutant isogenic cell clone (clone 3) and separately the BRAF^{V600E} mutant melanoma cell line, A375P were treated with PLX4720 and the BRAF^{V600E} mutant isogenic cell line was also treated with 5nM trametinib, as above. Cells were harvested at baseline, 6 and 24 hours. ROR2 protein expression was quantified on whole cell extracts by western blot. Blots were also probed for phospho-ERK and both PLX4720 and trametinib were confirmed to inhibit ERK activation. In both cell lines, ROR2 expression decreased with inhibition of the MAPK axis. In the isogenic clone, consistent to the pattern observed at the mRNA level, the decrease in ROR2 expression was more evident following treatment with trametinib compared to BRAF inhibition with PLX4720 (figure 4-10 C and E). In A375P cells, treatment with PLX4270 also resulted in a decrease in ROR2 expression after 24 hours (figure 4-10 D and F). This result suggested that ROR2 expression is regulated by BRAF-MEK activity in melanoma cell lines harbouring endogenous BRAF^{V600E} mutations, in addition to isogenic cells in which this mutation had been introduced.

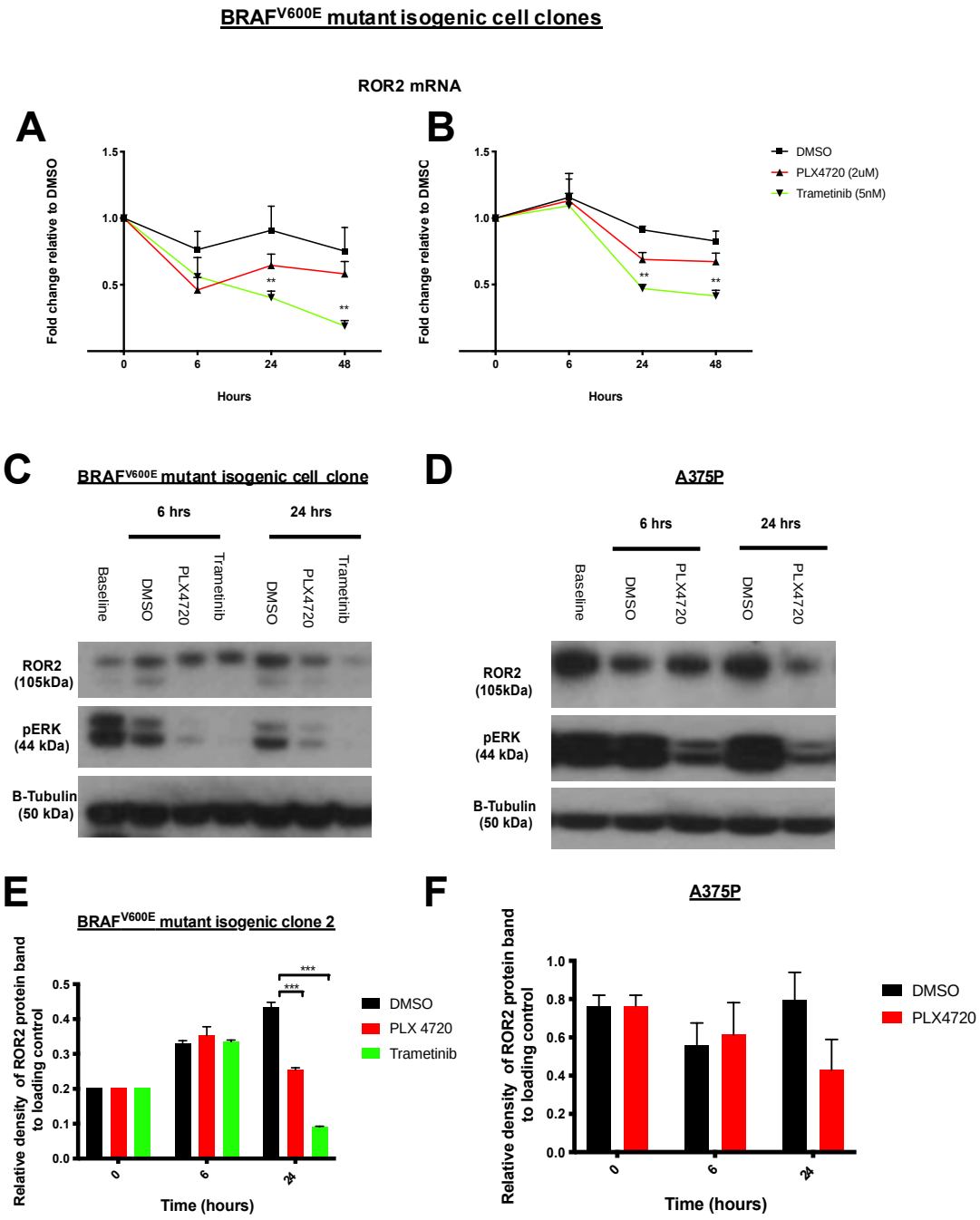

Figure 4-10: The effect of MAPK pathway inhibition on ROR2 expression A and B. Two BRAF^{V600E} mutant clones were cultured in DMSO, PLX4720 (2μM) or Trametinib (5nM) and harvested at time points shown. RNA was extracted and ROR2 mRNA expression quantified by RT-PCR and corrected using TUBA6 as a housekeeping gene. Graphs show mean ± SEM expressed as fold change relative to DMSO control at time point 0 (n=6 from two independent experiments each with 3 technical replicates). C BRAF^{V600E} mutant clone 3 was cultured and treated as above. ROR2 protein expression was determined via western blot. Experiment performed in triplicate with similar results across all repeats D. ROR2 protein expression in treated/control A375P cells. E. Relative density of ROR2 protein band from (C). F. Relative density of ROR2 protein band from (D). Experiment performed in duplicate with similar results across both repeats. Statistics performed using 2-way ANOVA, comparing each treatment to control at that timepoint. ** = p<0.005 * = <0.0001**

These results demonstrated that ROR2 is differentially expressed between BRAF mutant wildtype melanoma samples from three independent datasets and that BRAF-MEK inhibition suppresses ROR2 expression.

To place ROR2 in the context of other Wnt genes altered by the $BRAF^{V600E}$ in the above data sets, table 4-6 summarises Wnt genes differentially expressed in the TCGA (dataset 2) and isogenic model (dataset 3).

Gene	Expression direction in $BRAF^{V600}$ in TCGA	Expression direction in $BRAF^{V600E}$ in Isogenic cell line model	Concordant/discordant
ANKRD6	NDE	Up	
ARID1B	NDE	NDE	
ARRB1	Down	NDE	
AXIN1	Down	NDE	
BTRC	Down	NDE	Partially concordant
CCND1	NDE	NDE	
CDH13	Up	NDE	
CDH15	NDE	Down	
CDH2	NDE	Up	
CELSR2	Down	NDE	
CELSR3	Down	NDE	
CREBBP	Down	NDE	
CSNK1E	Down	NDE	
CTBP2	Down	NDE	
CTNNAL1	NDE	Up	Partially discordant
DKK1	NDE	Up	Partially discordant
DVL3	Down	NDE	
FZD1	Up	NDE	
FZD3	NDE	Up	
FZD6	Up	NDE	
FXD7	Up	NDE	
GNA14	NDE	NDE	
GNG4	NDE	Down	
GSK3B	NDE	Down	
ITPR2	NDE	NDE	
LEF1	Up	Up	Yes
MAP3K7CL	Up	NDE	
MYC	Down	NDE	Partially discordant
MYCN	NDE	NDE	
PCDH18	NDE	NDE	
PCDHGA3	NDE	NDE	
PLCB1	Up	NDE	
PPP2R5D	Down	NDE	
PRKCA	NDE	Up	
PRKCB	NDE	Down	
PRKCE	Down	NDE	
PRKCH	NDE	Up	
ROR2	Up	Up	Yes
SFRP1	Up	NDE	
SMAD4	NDE	NDE	
SMARCA1	NDE	Up	
SMARCA4	Down	NDE	
SMARCC1	Up	NDE	
SMARCD3	Up	NDE	
SRCAP	Down	NDE	
TBL1X	Down	Down	Partially concordant
TLE1	Down	NDE	
Wnt3A	NDE	NDE	
Wnt9B	NDE	NDE	

Table 4-6:Wnt genes differentially expressed in at least one of the three datasets described earlier. NDE = not differentially expressed

4.8. Discussion

Analysis of the AVAST-M, TCGA and $BRAF^{V600E}$/wildtype isogenic gene expression datasets showed that genes differentially expressed between $BRAF^{V600E}$ and wildtype melanomas were associated with angiogenesis pathways, in support of the hypothesis linking the oncogenic $BRAF^{V600E}$ mutation with this process.

The common functions shared by differentially expressed genes in all three datasets are in support of an angiogenic role for the $BRAF^{V600E}$ mutation despite contextual differences between the three datasets. The AVAST-M set was derived from primary and metastatic lymph node melanomas containing both tumour and stroma. The TCGA set was from patients with poor prognostic melanoma. The isogenic model was created from a BRAF wildtype melanoma cell line with an acquired BRAF mutation.

Some associations between the $BRAF^{V600E}$ mutation and angiogenesis have been reported. Kumar et al demonstrated that mutant $BRAF^{V600E}$ knockdown decreased HIF-1α protein expression and decreased viability in hypoxic conditions (Kumar *et al.*, 2007). Bottos et al reported that endothelial cells transfected with mutant BRAF expressed increased VEGF secretion and pharmacological BRAF inhibition of a melanoma cell line promoted vascular stabilisation via a presumed decrease in aberrant angiogenesis (Bottos *et al.*, 2012). In both studies however, phenotypes were not compared directly between BRAF mutant and wildtype, and experiments did not include human clinical samples.

Some of the genes differentially expressed in the datasets influenced VEGF expression via transcriptional mechanisms. As the BRAF mutation can stabilise the HIF-1α protein (Kumar *et al.*, 2007) in melanoma cells, the effect of the mutation

would be expected to increase transcription of *VEGF* mRNA by HIF-1α binding to the *VEGF* promoter. Within the AVAST-M dataset, *STAT3,* upregulated in BRAF mutant samples is reported to increase *VEGF* expression via increased transcription (Niu *et al.*, 2002). *ETS1*, differentially overexpressed in BRAF mutant isogenic clones, also promotes *VEGF* expression via increases in transcription (Chen *et al.*, 2017). *VEGF* (mRNA) was not, however differentially expressed in either the AVAST-M dataset (table 4-1) or isogenic cell model **(**table 4-3). The lack of differential expression of VEGF in the isogenic model was also confirmed with qRT-PCR (figure 4-3 B). In contrast, within the TCGA data set, VEGF mRNA was upregulated in BRAF mutant melanomas. However, this data set was representative of higher stage melanomas compared to the AVAST-M data set (stage T4b, 74% vs 33%, respectively) and thus, the BRAF mutation may influence VEGF transcription within the context of higher risk disease, however the results from a single data set does not prove this.

Inconsistent with the transcriptional data, $BRAF^{V600E}$ mutant isogenic clones expressed more VEGF protein, particularly in its secreted form (figure 4-4 B), These data provided support to the concept that the BRAF mutation may influence post transcriptional regulation of VEGF.

Additional genes found to be differentially expressed in the studied datasets are also capable of influencing VEGF secretion. CRYAB, differentially expressed in the isogenic melanoma model is upregulated during the unfolded protein response which maintains VEGF protein levels via inhibition of proteolysis (Ruan *et al.*, 2011). Other specific oncogenic $BRAF^{V600E}$ mediated mechanisms of post-transcriptional VEGF regulation have not been described in the literature. The VEGF phenotype evident in the isogenic cell model (figure 4-4) supports a post-transcriptional method of

regulation of VEGF in $BRAF^{V600E}$ mutant cells.

Genes associated with Wnt signalling pathways were also differentially expressed in all datasets. This pathway is relevant as the TCF/β-catenin complex, stabilised in canonical Wnt signalling, has 7 described binding sites on the *VEGF* promoter (Easwaran *et al.*, 2003). Consistent with this, *VEGF* mRNA is highly expressed in clinical cases of adenomatous polyposis coli, which is associated with aberrant Wnt-pathway activation. Wnt signalling is also important in the transcriptional regulation of the matrix metalloproteinases (MMPs) (Olsen *et al.*, 2017). MMPs can degrade extracellular matrix (ECM) bound to VEGF on the cell surface, thus releasing VEGF into the extracellular space and providing a post-transcriptional mechanism for VEGF regulation (Hawinkels *et al.*, 2008). MMPs are discussed later in this thesis.

SFRP-1, a Wnt inhibitor was also differentially expressed in all three datasets, albeit in different directions and was not validated in the isogenic cell model (figure 4-6). While historically classified as negative angiogenesis regulator, recent studies have identified strong pro-angiogenic function (Dufourcq *et al.*, 2008) that, requires the activity of the small RhoGTPase, Rac1. Rac1 plays a role in the re-organisation of F-actin necessary for the process of exocytosis (Dilyana *et al.*, 2017). Of note, Wnt5a, a ligand of the non-canonical Wnt pathway has been shown separately to induce VEGF secretion through exocytosis via a mechanism including Rac1 (Ekström *et al.*, 2014). SFRP-1 thus may also contribute to post-transcriptional regulation of VEGF expression.

VEGFR2 expression was upregulated in 2 BRAF mutant clones (figure 4-5 B). Although classically an endothelial cell receptor, VEGFR2 has also been identified on melanoma cells raising the possibility of autocrine or intracrine signalling networks (Adamcic *et al.*, 2012). The presence of VEGFR2 on these clones suggests such

networks may be influenced by the BRAF mutation which has not been reported previously. To further support his, evidence of increased VEGFR2 phosphorylation in the BRAF mutant clones would be required which was not performed.

Taken together, an analysis of independent data determining genes differentially expressed between $BRAF^{V600E}$ and wildtype melanoma has identified genes associated with known angiogenesis pathways. Some of these differentially expressed genes are reported to predominantly influence VEGF transcription, however others feasibly have post-transcriptional effects. *VEGF* mRNA itself was only significantly differentially expressed the TCGA data set. $BRAF^{V600E}$ mutant clones in the isogenic model were shown to secrete more VEGF without increases in *VEGF* mRNA or *HIF-1α* mRNA expression. The oncogenic $BRAF^{V600E}$ mutation may thus increase VEGF expression, independent of transcription.

ROR2 is associated with non-canonical Wnt signaling. In melanoma, non-canonical Wnt signaling has been implicated in the phenomenon of dynamic phenotype switching. Depending on context, melanomas possess an ability to change from a highly proliferative, non-invasive phenotype to a phenotype associated with invasion, increased motility and high metastatic potential (O'Connell *et al.*, 2010; O'Connell *et al.*, 2013). A shift from canonical to non-canonical Wnt signaling has been reported to drive the phenotype change from the former to the latter (O'Connell *et al.*, 2013) and the expression of ROR2 has been implicated in this transformation. ROR2 in melanoma therefore associates with a number of "hallmarks of malignancy" (Hanahan *et al.*, 2018) and a further association with angiogenesis was plausible. This concept is further supported by data showing that Wnt5a, the predominant ligand for ROR2 can induce VEGF secretion in melanoma cells, independent of changes in transcription (Ekström *et al.*, 2014). Based upon its striking pattern of differential

expression (figure 4-74), and reported associations with post-transcriptional VEGF expression, ROR2 was selected for further investigation.

There are no reports of an association between $BRAF^{V600}$ and ROR2 although mutant BRAF signalling has been linked to Wnt signalling. $BRAF^{V600E}$ melanomas with concurrent PTEN deficiency are reported to develop highly metastatic phenotypes through canonical Wnt, β-catenin signalling (Damsky *et al.*, 2011). In contrast other data in melanoma suggests that the $BRAF^{V600E}$ mutation negatively regulates β-catenin signalling, thereby promoting non-canonical signalling (Biechele *et al.*, 2012). The conflicting relationship between the $BRAF^{V600E}$ mutation and canonical/non conical Wnt signalling pathways was evident in the pattern of differentially expressed Wnt relevant genes in both the AVAST-M and isogenic cell line model datasets (table 4-6). LEF1, a well described component of canonical Wnt signalling, binds with TCF to stabilised (non phosphorylated) β-catenin to promote transcription of a number of Wnt target genes (Santiago *et al.*, 2017). LEF1 was upregulated in BRAF mutant melanomas in both the AVAST-M and isogenic cell model datasets, as was TCF in the AVAST-M dataset (table 4-1), therefore supporting canonical Wnt activation by the $BRAF^{V600E}$ mutation. However, ROR2 is an important facilitator of non-canonical Wnt signalling in melanoma (Da Forno *et al.*, 2008). Indeed the ligand for ROR2, Wnt5a has been shown to antagonise β-Catenin, and promote its destruction through a novel GSK-3 independent pathway involving activation of Siah and APC (Topol *et al.*, 2003).

Additional Wnt genes deregulated by the BRAF mutation included DKK1, a known inhibitor of canonical Wnt signalling (Chen *et al.*, 2012), which was upregulated in BRAF mutant cells in the isogenic cell line model, but downregulated in BRAF

mutant patient tumours from the AVAST-M clinical trial (tables 4-1 and 4-3). Other genes where expression varied in opposite directions in respect to BRAF genotype between the two data sets were CTNNAL1 and SFRP1, both reported to promote aggressive phenotypes in melanoma (Dufourcq *et al.*, 2008; Kreiseder *et al.*, 2013). Taken together, the data sets suggest the $BRAF^{V600E}$ mutation influenced both canonical and non canonical Wnt signalling pathways but the direction was inconsistent between data sets. One potential explanation for the heterogeneity is context. Wnt5a (non-canonical) expression associates with increasing melanoma stage (Da Forno *et al.*, 2008), the same researchers have also shown that as melanomas transition from a proliferative radial growth phase to the invasive vertical phases Wnt signalling switches from canonical to non-canonical. Such a concept may explain the differences between gene expression in the AVAST-M tumour samples, consisting of primary melanomas and the isogenic cell model, derived from a metastatic cell line. Another potential link between the oncogenic $BRAF^{V600E}$ mutation and ROR2 is Melanocyte Inducing Transcription Factor (MITF). MITF is a key regulator of melanoma gene expression that plays a central role in the transcription of genes that determine cell fate and phenotype (Dufourcq *et al.*, 2008; Hoek *et al.*, 2010; Kreiseder *et al.*, 2013). Melanoma cells with high levels of the MITF transcript increase expression of genes involved in melanoma differentiation such as PMEL and MART1 (Wellbrock *et al.*, 2005). Conversely, in melanomas that express low levels of MITF, cell fate is determined by Wnt5a, TGF-β and AXL, in which de-differentiated phenotypes dominate (Wellbrock *et al.*, 2015). In both the AVAST-M and TCGA datasets, MITF was downregulated in BRAF mutant melanomas. TGF-β was upregulated in the AVAST-M dataset (tables 4-1 and 4-2). Mutant BRAF signalling may therefore have increased non-canonical wnt signalling due to a reduction in

MITF expression. Consistent with this, ZEB1, the transcription factor associated with MITF suppression and the EMT phenotype was upregulated and ZEB2 was downregulated in $BRAF^{V600E}$ melanomas in both the AVAST-M and TCGA datasets (tables 4-1 and 4-2). The expression of PMEL was also decreased in the BRAF mutant melanomas from both datasets (table 4-1 and 4-2). Taken together, the AVAST-M and TCGA datasets support $BRAF^{V600E}$ as a potential driver of an EMT-like, poorly differentiated phenotype which would be consistent with ROR2 upregulation. Arguing against this however, in the isogenic clones, MITF was not differentially expressed (figure 4-6). One possible explanation for the discrepancy may be that BRAF mutation in the AVAST-M and TCGA melanomas was a driver mutation whereas the mutation in the isogenic clones was acquired and therefore the impact of MAPK signalling on MITF may have differed.

ROR2 was tested in a panel of in-house non-isogenic BRAF mutant and wildtype melanoma cell lines (figure 4-9) and no significant difference was detected ($p=0.3560$). This experiment was limited by testing only 8 cell lines and a broader panel would be required in order to confirm or refute differential expression.

ROR2 was notably not differentially expressed in the AVAST-M data set (table 4-1) after adjustment of the p-value for multiple tests ($p=0.263$). This result contrasts with the other datasets presented above. A potential reason for the discrepancy may be the fact that the AVAST-M dataset was derived from primary melanomas. The expression of ROR2 has been shown to increase with the vertical growth phase of melanoma and correlate with disease stage (Da Forno *et al.,* 2008) and thus assessment in a non-metastatic context may be one reason for the lack of differential expression. A subgroup analysis of the AVAST-M tumours stratified by tumour stage may have demonstrated differential expression in higher stage tumours. Due to time

constraints this analysis was not performed. The AVAST-M samples also contained stroma in addition to tumours and potentially the mixture of malignant and non-malignant tissue may have diluted the real result. Repeating the analysis, ideally after micro-dissection to enrich for tumour content alone may be informative to address this limitation.

5. Chapter V: Phenotypes associated with ROR2

5.1. The effect of ROR2 depletion on proliferation of melanoma cell lines

Having established an association between the $BRAF^{V600E}$ mutation and ROR2 expression in melanoma, phenotypes associated with ROR2 signalling were next explored, as well as the impact of the $BRAF^{V600E}$ mutation on these phenotypes. Although increased expression of ROR2 has been associated with aggressive melanoma phenotypes including increased invasion and metastatic potential (O'Connell *et al.*, 2010), the effect of the $BRAF^{V600E}$ mutation on this phenotype remains unknown. Furthermore, associations between ROR2 and VEGF expression remain uncharacterised.

Two $BRAF^{V600E}$ mutant melanoma cell lines (one $BRAF^{V600E}$ mutant isogenic clone and the cell line SKMEL5) and a BRAF wildtype isogenic clone were selected for this experiment. Cell lines were treated with ROR2 or control siRNA using methods described earlier. A fixed number of cells was added to a 96 well plate and daily cell count was performed for 72 hours. The total cell count was ascertained and the data expressed as the percentage change over baseline.

ROR2 siRNA decreased proliferation in both $BRAF^{V600E}$ mutant melanoma cell lines that were analysed (figure 5-1 A-B). Although the magnitude of difference was similar between SKMEL5 and the BRAF wildtype isogenic clone, a result in the latter was not statistically significant due the larger error bars (figure 5-1 C). ROR2 siRNA in the BRAF wildtype cell line was demonstrably less effective than in other cell lines (figure 5-1 D), presumably due to low baseline levels of ROR2 expression in the

BRAF wildtype isogenic clones.

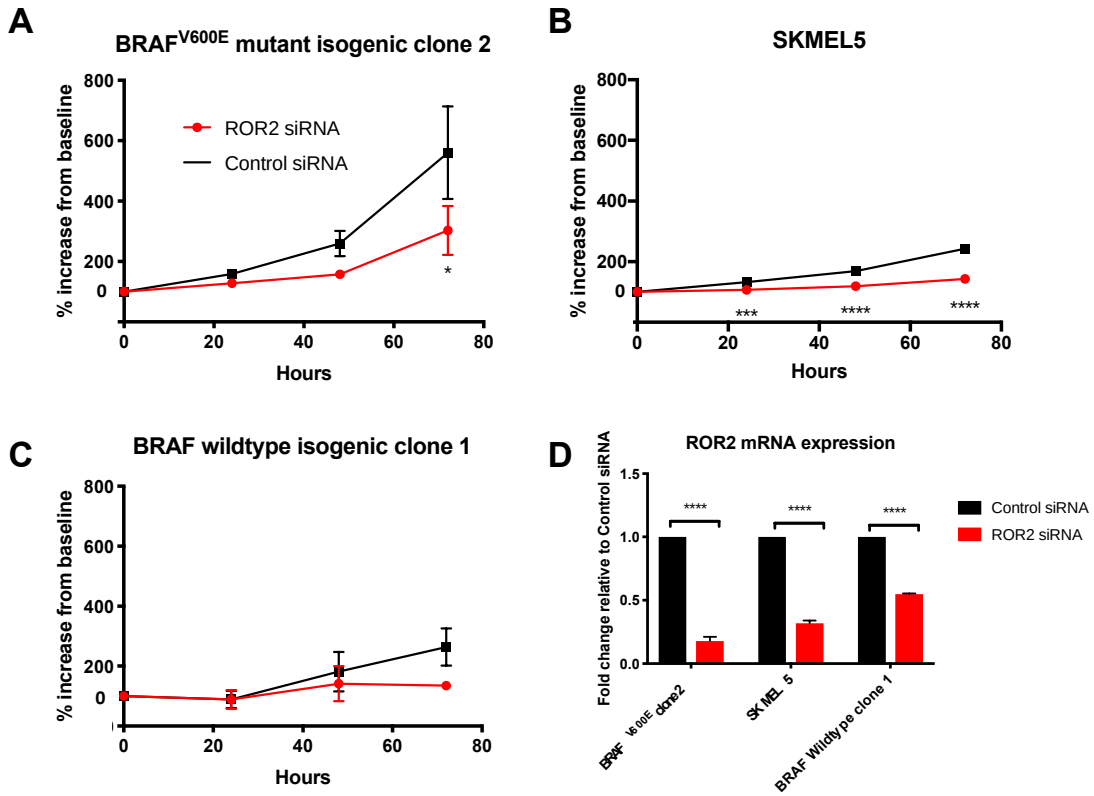

Figure 5-1: Effect of ROR2 depletion on melanoma cell proliferation. Cells were transfected with siRNA and the following day seeded in 96 well plates. Hoechst and Propidium Iodide were added at each time point and a total cell count determined. Data are presented as percentage count of reading taken at baseline. Data expressed as average three biological repeats, with experimental triplicates performed for each time point. Effect of ROR2 siRNA on proliferation of BRAF mutant melanoma cell lines (A and B) and BRAF wildtype isogenic clone (C). D. Assessment of ROR2 expression in cells transfected with siRNA with qRT-PCR. Statistical analysis performed with 1-way ANOVA. * p≤0.05 *** p ≤ 0.001 **** p ≤ 0.0001. Data expressed as mean value and error bars represent SEM.

5.2. The effect of ROR2 on invasion in melanoma

ROR2 has an established role in promoting cell migration and invasion. ROR2 depletion reduces migration, motility and invasion in ovarian cancer cells (Henry *et al.*, 2016). Similar phenotypes have been reported in melanoma. O'Connell et al have shown that Wnt5a/ROR2 signalling is mediated by clathrin mediated ROR2 internalisation. Treatment of the melanoma cell line UACC903 with clathrin siRNA significantly reduced motility, implicating ROR2 in this phenotype (Oconnell *et al.*, 2010). Although previously reported in other cell lines, the role of ROR2 on invasion was explored in $BRAF^{V600E}$ mutant cell clones from the isogenic model. The purpose of this experiment was to demonstrate a phenotype in these cells consistent with what has been published and therefore strengthen confidence to explore other novel phenotypes in this cell line.

A matrigel invasion assay based on the xCELLigence™ platform was chosen to quantify invasion using methodology described in chapter 2 (section 2.5.2). A $BRAF^{V600E}$ mutant isogenic clone was transfected with either ROR2 or control siRNA. In this experiment, ROR2 depletion inhibited migration of $BRAF^{V600E}$ mutant isogenic clones across 0%, 5% and 10% matrigel (figure 5-2 A-C). This result was consistent with phenotypes reported in other cell lines (O'Connell *et al.*, 2010; Rasmussen *et al.*, 2014; Henry *et al.*, 2016). This result demonstrated that ROR2 functioned as expected in the $BRAF^{V600E}$ mutant isogenic clone. This cell line was therefore a reasonable model to study further phenotypes associated with ROR2.

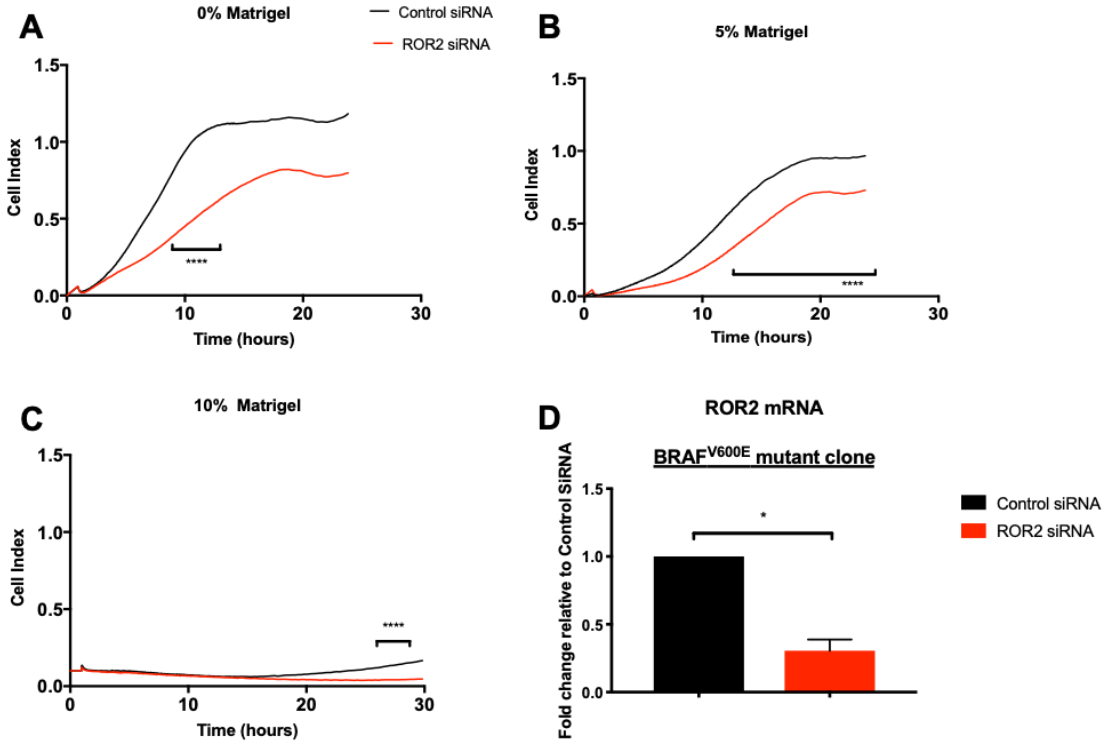

Figure 5-2: Effect of ROR2 depletion on invasion. BRAF^{V600E} mutant isogenic clone 2 was transfected with ROR2 or control siRNA and migration quantified using the xCELLigence™ platform. Analysis performed over 30 hours with readings every15 minutes. Readings taken as average of duplicate measures, averaged between two biological replicates, with technical duplicates for each individual experiment. Results for A, 0%; B, 5% and C. 10% matrigel. Error bars not included for presentation purposes. Statistical analysis determined by 2-way ANOVA and time points of greatest statistical difference presented **** $p \leq 0.0001$. G. ROR2 mRNA following treatment with siRNA. Pooled data from two independent replicates. Statistics performed using unpaired students t-test * $p \leq 0.05$. Data expressed as mean value and error bars represent SEM.

5.3. Relationship of ROR2 expression to VEGF expression

Earlier experiments have demonstrated that ROR2 was differentially overexpressed in BRAF^{V600E} mutant melanoma cells and was associated with a number of hallmarks of malignancy, namely proliferation and invasion. The association between ROR2 and the expression of VEGF, and by extension, angiogenesis, another malignant hallmark was next explored.

The effect of ROR2 expression on VEGF expression was investigated at three levels:

VEGF mRNA expression, VEGF intracellular protein production and VEGF secretion. These experiments were performed on a broader selection of cell lines: A375M ($BRAF^{V600E}$ mutant), SKMEL 28 ($BRAF^{V600E}$ mutant), a $BRAF^{V600E}$ mutant isogenic cell clone 2 and a BRAF wildtype isogenic cell clone 1 (also described above). These cells were selected to evaluate phenotypes across multiple $BRAF^{V600E}$ mutant cell lines and to investigate any differences relevant to BRAF mutational status.

5.4. The effect of ROR2 on VEGF mRNA expression

Cells were transfected with ROR2 or control siRNA and harvested after 48 hours. Following RNA extraction, ROR2 knockdown was confirmed with qRT-PCR using ROR2 specific primers in a one-step reaction. $VEGF_{165}$ mRNA expression was measured on the same RNAs again using qRT-PCR.

Silencing ROR2 expression decreased $VEGF_{165}$ mRNA in only $BRAF^{V600E}$ mutant clone 2 (figure 5-3 A). VEGF mRNA expression was increased in SKMEL28 (figure 5-3 C). ROR2 depletion did not influence VEGF mRNA expression in the BRAF wildtype clone 1(figure 5-3 D), although ROR2 silencing in this cell line was ineffective (figure 5-3 E). Overall, ROR2 silencing had no consistent effect on $VEGFA_{165}$ mRNA expression.

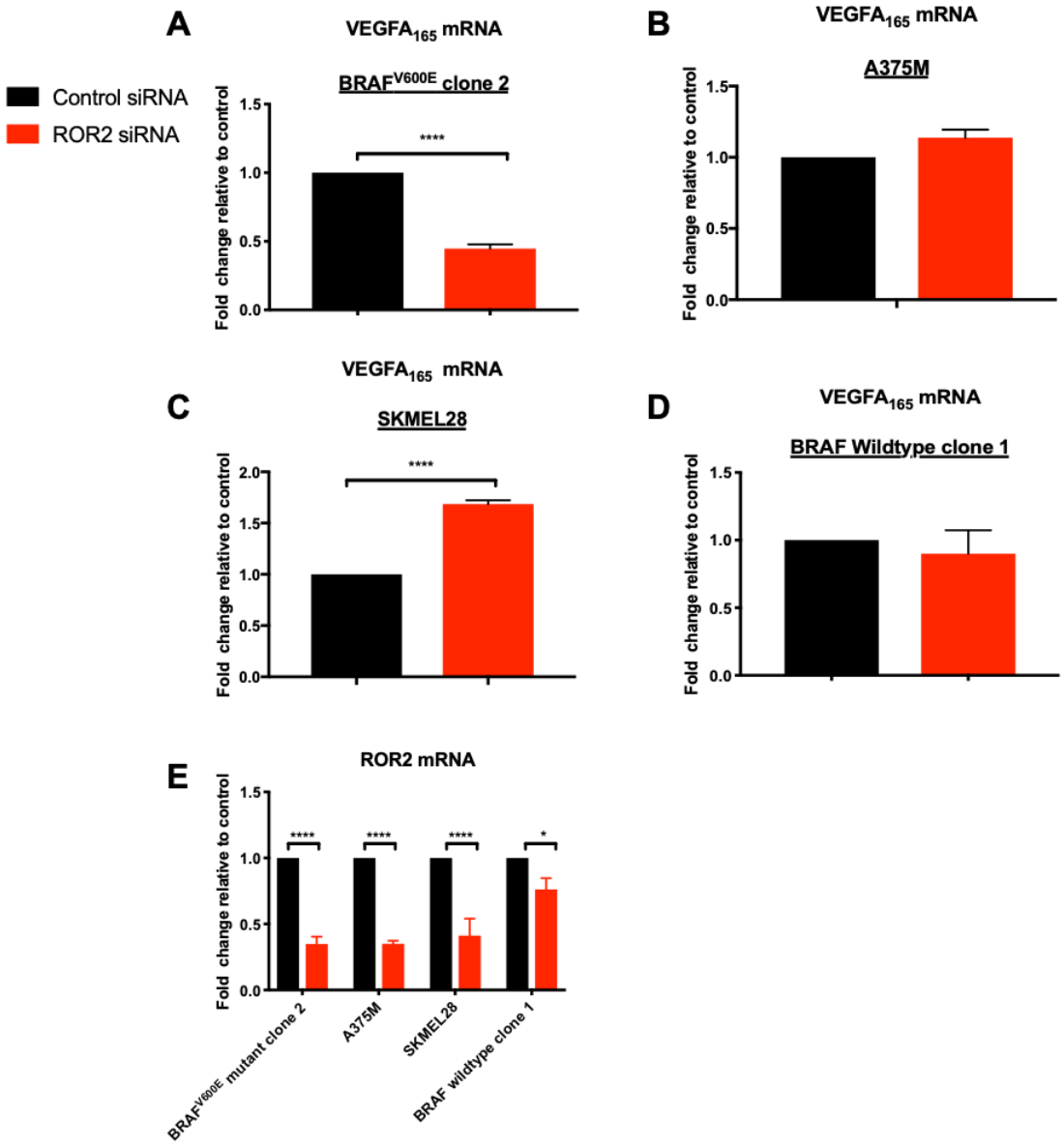

Figure 5-3: Effect of ROR2 siRNA on VEGFA$_{165}$. (A-D) Melanoma cell lines were transfected with ROR2 or control siRNA. Cells were harvested, RNA was extracted and qPCR performed using primers specific for VEGFA$_{165}$. TUBA6 was used as a housekeeping gene. Experiments performed in triplicate (with three technical replicates per experiment). Statistics determined using students t-test. **** = p<0.0001 E. Testing ROR2 knockdown (merged data from all three repeats) corrected for TUBA6 and expressed relative to control transfectants. Individual t-test used for each comparison * = p <0.05.

5.5. Effect of ROR2 silencing on VEGFA intracellular protein expression

The impact of ROR2 siRNA on the intracellular expression of VEGF was next investigated. VEGF protein was quantified using ELISA, due to difficulties identifying a specific VEGF antibody for immunoblot detection. As described earlier, the selected ELISA kit had sensitivity and specificity for biologically relevant VEGF isoforms, $VEGF_{165}$ and $VEGF_{121}$.

The same cell lines as used in 5.4 were transfected with ROR2 or control siRNA. After 48 hours, cells were harvested, counted and lysed in preparation for VEGF detection via ELISA. VEGF concentrations were determined from parallel assays of standards and expressed as concentration adjusted for cell count at harvest. Consistent with the effect of ROR2 siRNA on $VEGF_{165}$ mRNA, ROR2 depletion significantly reduced VEGF protein levels in the $BRAF^{V600E}$ mutant clone. Intracellular VEGFA was not altered in either A375M or SKMEL28, or the BRAF wildtype clone (figure 5-4 A-D). Taken together ROR2 silencing did not uniformly decrease intracellular VEGF concentrations.

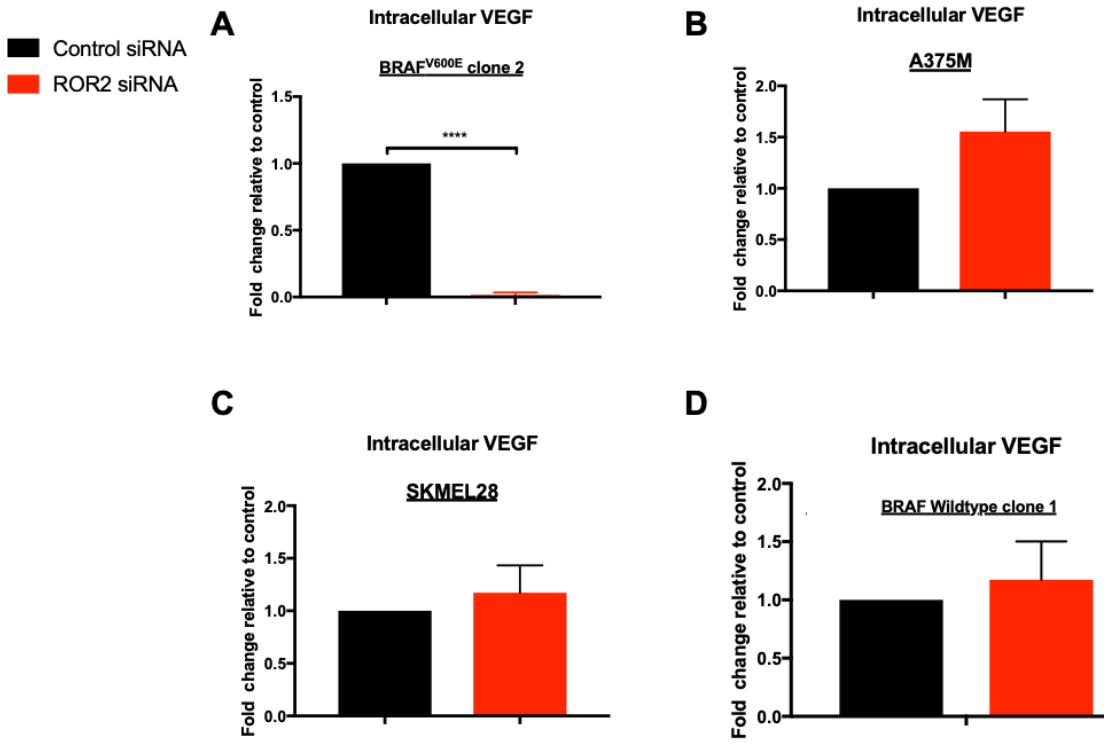

Figure 5-4: The effect of ROR2 depletion on intracellular VEGF expression. Cells were siRNA transfected, lysed and analysed after 48 hours. Experiments performed in triplicate (with three technical replicates per experiment). Statistics determined using students t-test. **** = p<0.0001

5.6. The effect of ROR2 depletion on secretion of VEGF

Malignant cells are capable of VEGF secretion (O'Connell *et al.*, 2010). Circulating VEGF in patients with melanoma is associated with a negative prognosis (Ferrara *et al.*, 2003), and has been considered to have an important pathological role. Therefore, the effect of ROR2 on VEGF secretion was explored in this next experiment using ELISA. Conditioned medium was collected from the same cell lines used in the above experiments, following transfection with either ROR2 or control siRNA. After 48

hours, cells were harvested and counted.

ROR2 depletion resulted in a significant decrease in VEGF secretion in the $BRAF^{V600E}$ mutant cell lines (figure 5-5 A-C), particularly evident in $BRAF^{V600E}$ mutant clone 2 and A375M (figure 5-5 A and B). The same phenotype was not seen in the BRAF wildtype clone 1 (figure 5-5 D). To compare directly the levels of VEGF secretion between the $BRAF^{V600E}$ mutant clone 2 and wildtype isogenic clone 1, these data were plotted together on the same scale (figure 5-5 E). ROR2 depletion in $BRAF^{V600E}$ mutant clone 2 reduced VEGF secretion to an amount comparable to the quantity expressed in the control transfected BRAF wildtype clone 1.

A second, independent ROR2 siRNA sequence (Qiagen) was tested to check the association specificity to ROR2 with secretion of VEGF. A375M cells were transfected with this second ROR2 siRNA or the non-silencing control. The second ROR2 siRNA similarly reduced VEGF secretion (figure 5-5 F) to a magnitude comparable with the original ROR2 siRNA.

This observation supported the specificity of the effect of ROR2 in influencing VEGF secretion in $BRAF^{V600E}$ mutant melanoma cells.

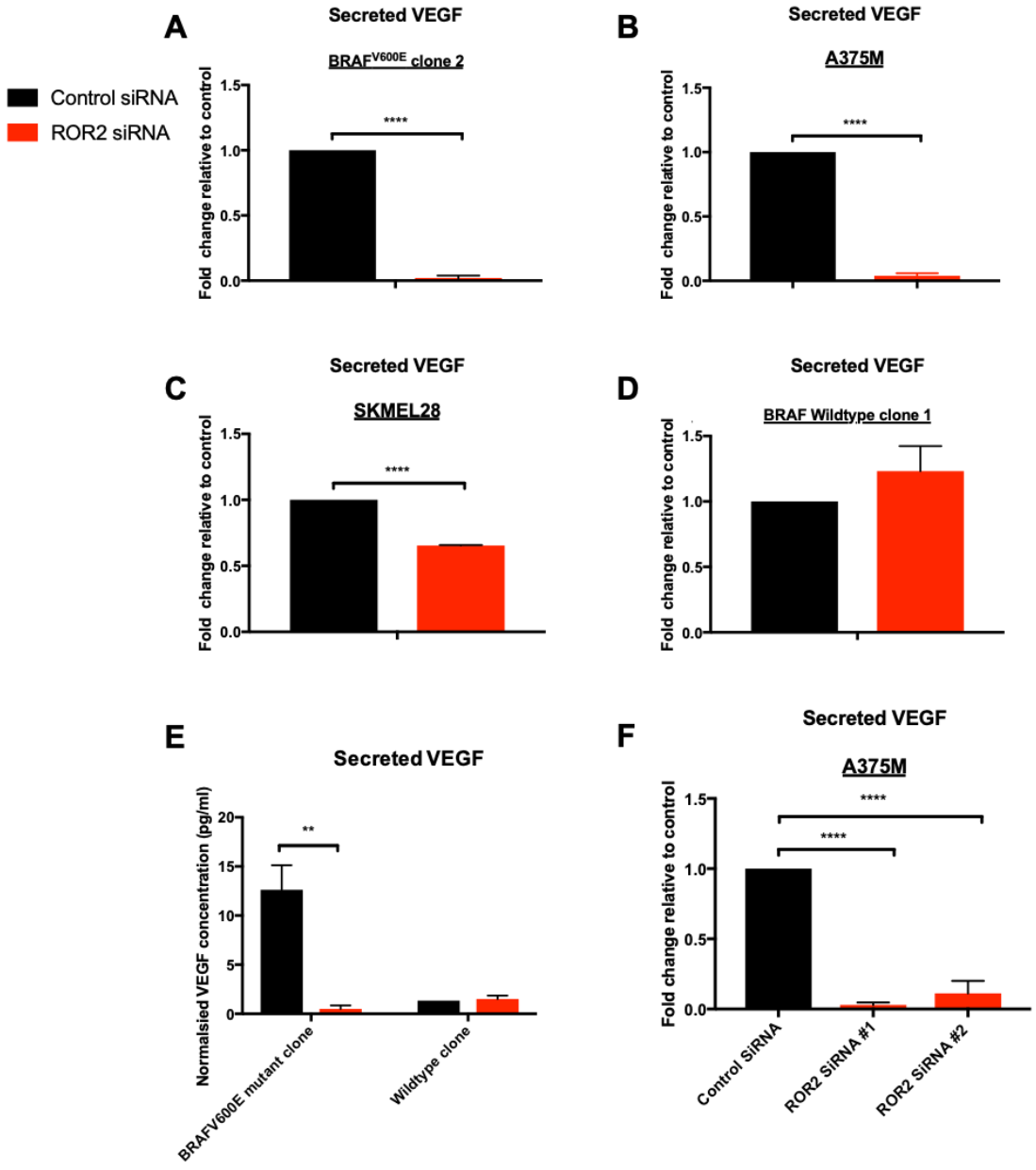

Figure 5-5 ROR2 depletion inhibits secretion of VEGF. (A-D) Cells were transfected with siRNA to ROR2 or control siRNA, and condition medium harvested after 48 hours. VEGF was quantified by ELISA adjusted for cell count and presented as fold change relative to control siRNA. E. Comparison of absolute adjusted VEGF concentrations in the conditioned medium between BRAF^{V600E} mutant and BRAF wildtype clone. F. Testing effect of VEGF secretion using two independent ROR2 siRNA's. Experiments performed in triplicate (with three technical replicates per experiment). Statistics determined using students t-test (A-E) or one way ANOVA (F) ** = p<0.01, **** = p<0.0001.

5.7. Testing the effect of siRNA transfection procedure on VEGF secretion

To check whether the stress of transfection could affect VEGF secretion, VEGF ELISA was performed in culture medium for transfected and untransfected cell lines. Transfection of the $BRAF^{V600E}$ mutant clone 2 with ROR2 siRNA resulted in a 50.3% decrease in VEGFA secretion relative to untransfected controls, although VEGF secretion was significantly increased those cells treated with control siRNA (figure 5-6 A). Given the decrease between ROR2 siRNA and untransfected cells, the effect on ROR2 depletion was not entirely explained by the confounding result of control siRNA treatment. Although there are no reports in the literature that VEGF is secreted in response to transfection a stress response to the transfection process was feasible. To address this confounding factor, VEGF secretion was also quantified in A375M and compared across ROR2, control, mock transfected and untransfected conditions (figure 5-6 B). The data in this cell line demonstrated a non-significant rise in VEGF associated with the transfection procedure, and for this reason A375M was identified as the cell line for further experiments testing the effects of ROR2 knockdown.

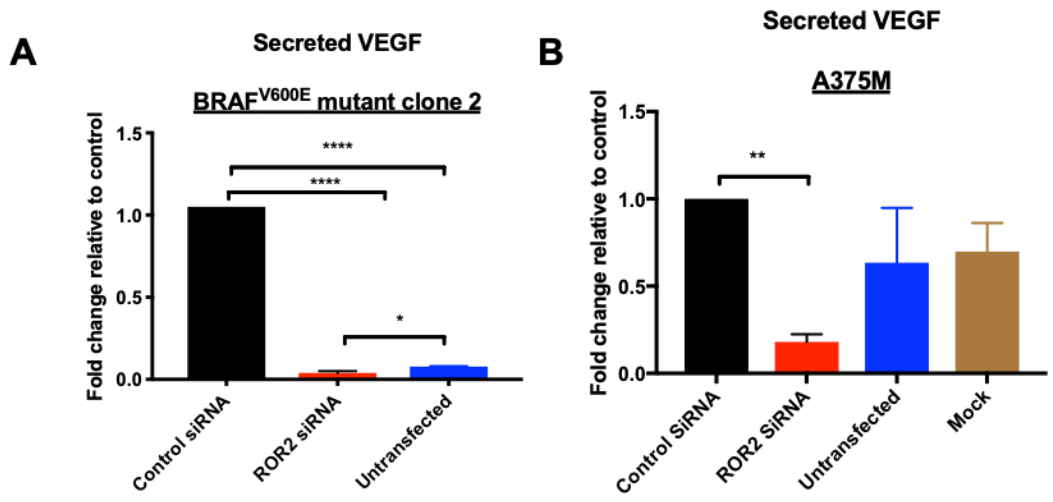

Figure 5-6: Effect of transfection procedure on (A) BRAF^{V600E} mutant clone 2 and (B) A375M cell line. Cells were transfected and VEGF in the conditioned medium determined following harvest 48 hours later. Cells were transfected with either Control siRNA, ROR2 siRNA, transfection reagent alone ("mock" in the case of A375M) or nil transfection reagents ("untransfected"). Experiments performed in duplicate. Statistics determined one-way ANOVA. *=p<0.05, ** = p<0.01, **** = p<0.0001

5.8. Effect of ROR2 siRNA on downstream targets

Having shown that ROR2 depletion significantly reduced VEGF secretion in BRAF^{V600E} mutant melanoma cell lines, the effect of ROR2 on putative downstream targets was next investigated.

Wnt5a is the ligand for ROR2. Wnt5a has been reported to upregulate SNAI1 (Snail) and MART1 (Dissanayake *et al.*, 2008), so the effect of ROR2 depletion on expression of these genes was next assessed.

The expression of MART1 and SNAI1 was quantified in a BRAF^{V600E} isogenic clone 2, A375M (BRAF^{V600E} mutant) and a BRAF wildtype clone 1.

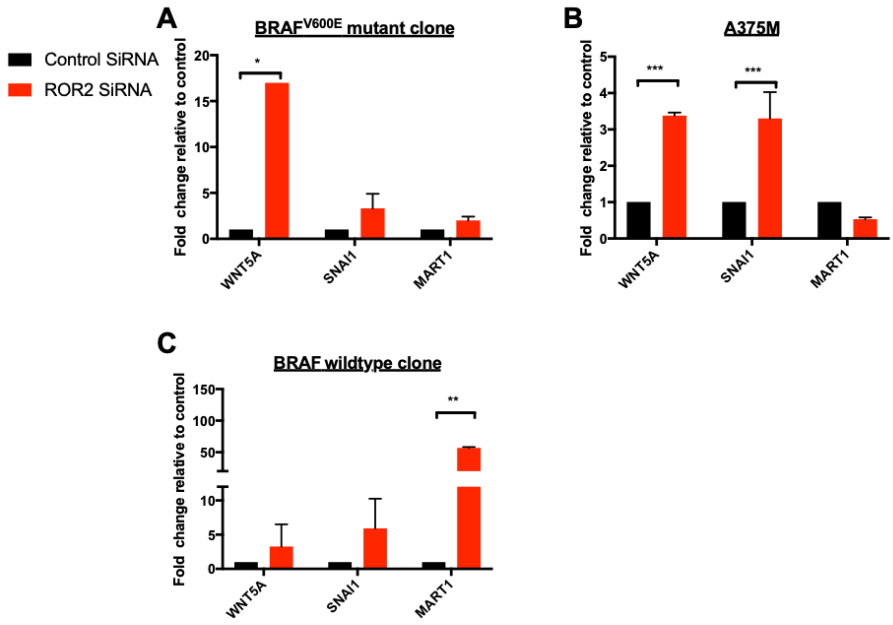

Figure 5-7: Effect of ROR2 depletion on potential downstream targets. A-C Cells were transfected with ROR2 or control siRNA and harvested after 48 hours. Expression was corrected for TUBA6 and expressed as field change relative to control transfectants. Statistics performed using 1-way ANOVA. * =p<0.05, ** = p<0.01, *** p<0.001. Data presented as average of duplicate experiments (each with technical triplicates).

In both BRAF^{V600E} mutant cell lines, Wnt5a expression increased in response to ROR2 siRNA (figure 5-7 A-B). The expression of SNAI1 did not significantly change in the BRAF^{V600E} mutant clone 2 (figure 5-7 A). MART1 expression in the BRAF^{V600E} mutant clones was unchanged in response to ROR2 depletion (figure 5-7 A).

The effect of ROR2 depletion in the BRAF wildtype isogenic clone contrasted to the results observed in the BRAF^{V600E} mutant melanoma cells. Wnt5a and SNAI1 expression were not affected however MART1 expression was significantly increased (figure 5-7 C).

5.9. Creation of ROR2 expressing stable cell lines

Having found evidence that ROR2 depletion decreased VEGF secretion in BRAF^{V600E} mutant melanoma cell lines, the effect of ROR2 overexpression was next explored.

5.9.1. ROR2 overexpression in CHL1

ROR2 overexpression was initially explored in the cell line CHL1, a BRAF wildtype melanoma cell line that served as the parental cell line to generate the isogenic model used in earlier experiments. CHL1 expresses low levels of ROR2 (figure 4-10 C) and secretes minimal VEGF (Guo, DPhil 2019) so was predicted to be a good model in which to asses any phenotypes associated with ROR2 overexpression. CHL1 cells were stably transfected with ROR2 cDNA or empty vector (figure 5-8) using the protocol described in chapter 2.

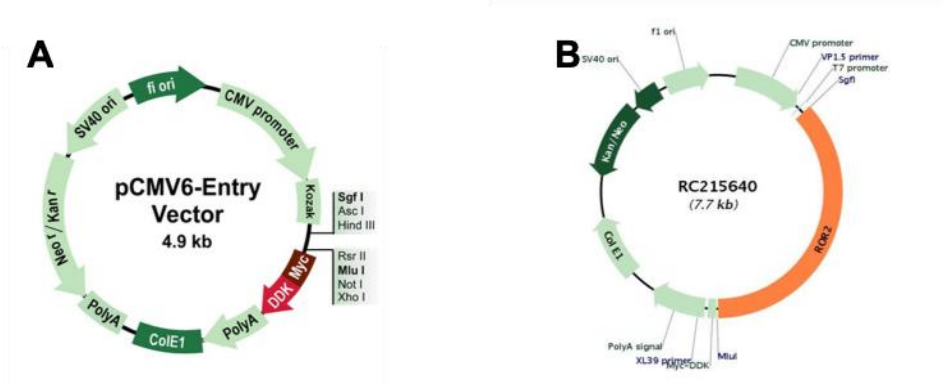

Figure 5-8: Plasmids used for the creation of ROR2 overexpressing cell lines A, Empty Vector B. ROR2 cDNA containing plasmid

Seventeen ROR2 cDNA transfected clones were screened using western blot and ROR2 overexpression was identified in 4 clones. Overexpression was confirmed in

these CHL1 clones (figure 5-9 A). Seven clones transfected with empty vector cDNA were screened, and 3 selected for the confirmatory western blot. ROR2 was not appreciably expressed in these controls (figure 5-9 B). For comparison, ROR2 expression in a $BRAF^{V600E}$ mutant isogenic clone was also quantified alongside both control and ROR2 overexpressing clones. ROR2 expression in the ROR2 transfected clones was considerably higher than in the $BRAF^{V600E}$ mutant clone (figure 5-9 A). Due to time restrictions, further clones could not be screened to identify ROR2 expression levels closer to that of the $BRAF^{V600E}$ isogenic clone 2.

ROR2 overexpressing clone 2 was selected for future experiments as the clone with a ROR2 expression level closest to the level identified in the $BRAF^{V600E}$ mutant clone 2.

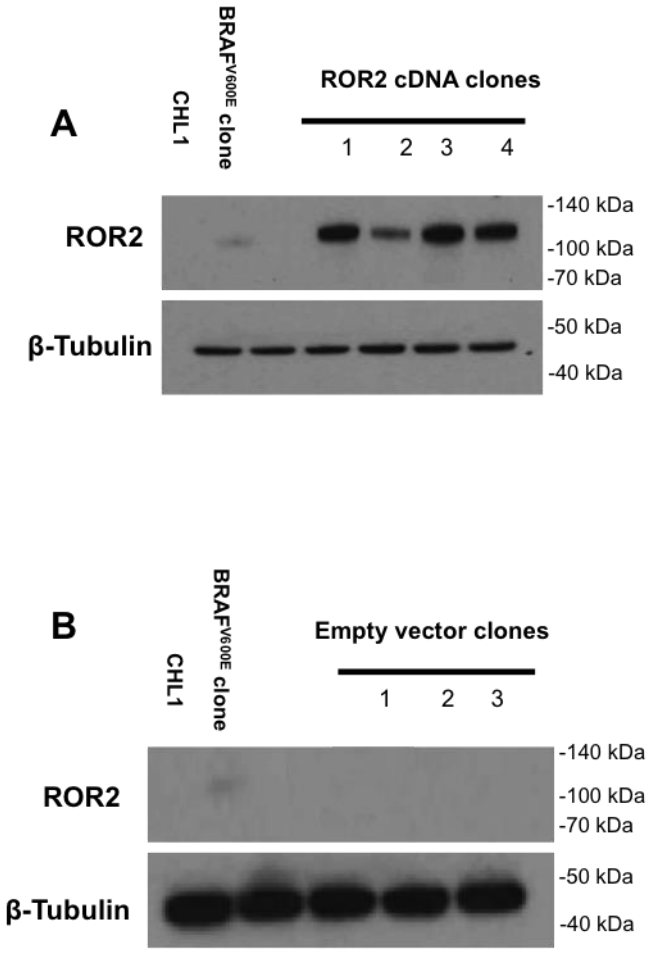

Figure 5-9: Assessment of stable ROR2 overexpression in CHL1 clones. CHL1 were cells transfected with A. ROR2 cDNA or B. empty vector. A $BRAF^{V600E}$ clone 2 used as positive control. CHL1 untransfected cell line used as negative control. The western blot film in B was exposed for longer than A to detect any low level ROR2 expression in the empty vector controls, but none was detected.

5.9.2. The effect of ROR2 overexpression on migration in the CHL1 cell line

Earlier experiments demonstrated that ROR2 depleted $BRAF^{V600E}$ mutant clone 2 was less motile and invasive compared to control (figure 5-2) Theoretically, if this phenotype was solely driven by ROR2 expression, overexpression of ROR2 in CHL1 was expected to promote these phenotypes. Motility and invasion were assessed using the xCELLigence™ system described earlier. Motility was assessed using the system without matrigel, and invasion with reduced growth factor matrigel at concentrations

of 5% and 10%. Overexpressing clone 2 (figure 5-9 A) was selected as the ROR2 overexpressing clone and empty vector clone 1 (figure 5-9 B) was selected as control. If time had permitted additional clones would have been tested to increase confidence that the lack of phenotype seen in this experiment was representative of the true result.

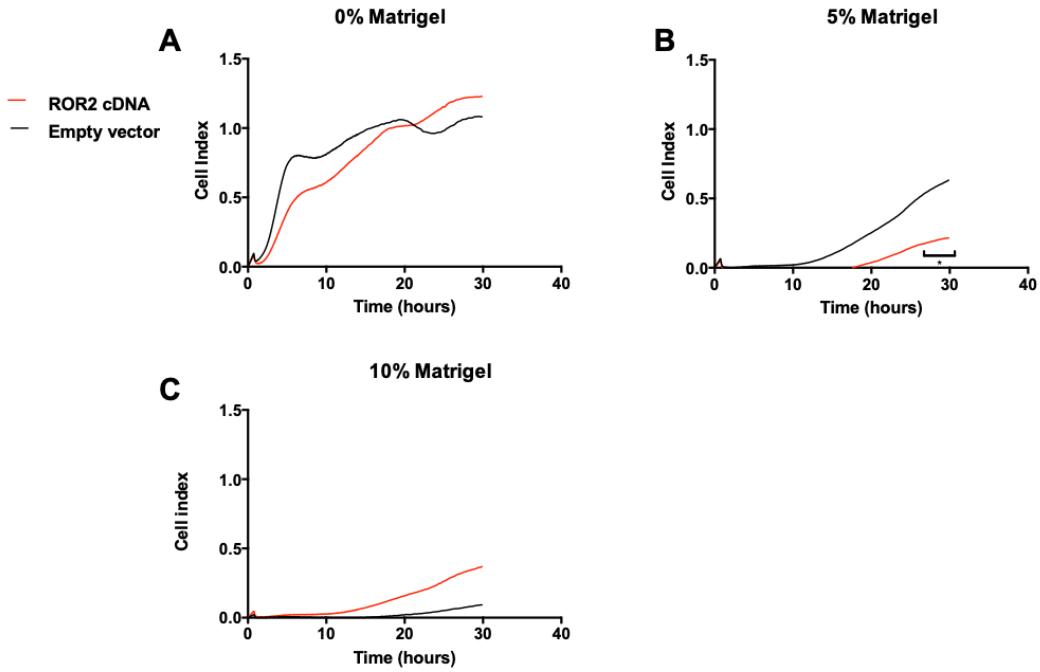

Figure 5-10: Effect of ROR2 overexpression on invasion of CHL1 cells. Cells were analysed in the xCELLigence system. Readings taken as average of duplicate measures, averaged between two biological replicates, with technical duplicates for each individual experiment. Results for A, 0%; B, 5% and C. 10% matrigel. Error bars not included for presentation purposes. Statistical analysis determined by 2 way ANOVA and time points of greatest statistical difference presented * $p \leq 0.05$.

ROR2 overexpression in the CHL1 cell line did not result in a uniform phenotype. ROR2 overexpression did not enhance motility (figure 5-10 A) or decreased invasion in 5% matrigel (figure 5-10 B).

Taken together, ROR2 overexpression in CHL1 cells did not reciprocate the phenotypes demonstrated with ROR2 siRNA in $BRAF^{V600E}$ mutant clones. The result suggested that either ROR2 overexpression was not solely responsible for this phenotype, or positive ROR2 phenotypes are only evident in the context of a $BRAF^{V600E}$ mutation.

5.9.3. The effect of ROR2 overexpression on VEGF secretion on the CHL1 cell line

Experiments above have shown that ROR2 depletion in $BRAF^{V600E}$ mutant cell lines resulted in reduced VEGF secretion. ROR2 overexpression in BRAF wildtype CHL1 cell lines was hypothesised to promote VEGF secretion.

ROR2 overexpressing clone 2 and empty vector clone 1 (figure 5-9 A-B) were cultured. After 48 hours the conditioned medium was harvested. A cell count was performed in parallel. Secreted VEGF was quantified using the ELISA method described earlier and normalised for cell count. VEGF secretion in the ROR2 overexpressing clone and control empty vector transfectant was negligible (figure 5-11 A) and did not differ between the two conditions. For this experiment the secreted VEGF data were not expressed as fold change, as such a method was considered misleading giving the minimal absolute quantities of VEGF secreted for both conditions. The concentration of VEGF in the ROR2 overexpressing and empty vector control (concentration normalised for cell count) was similar to the level in BRAF wildtype clone 1 (figure 5-5 E) further suggesting that ROR2 overexpression had no effect upon VEGF secretion in CHL1 cells.

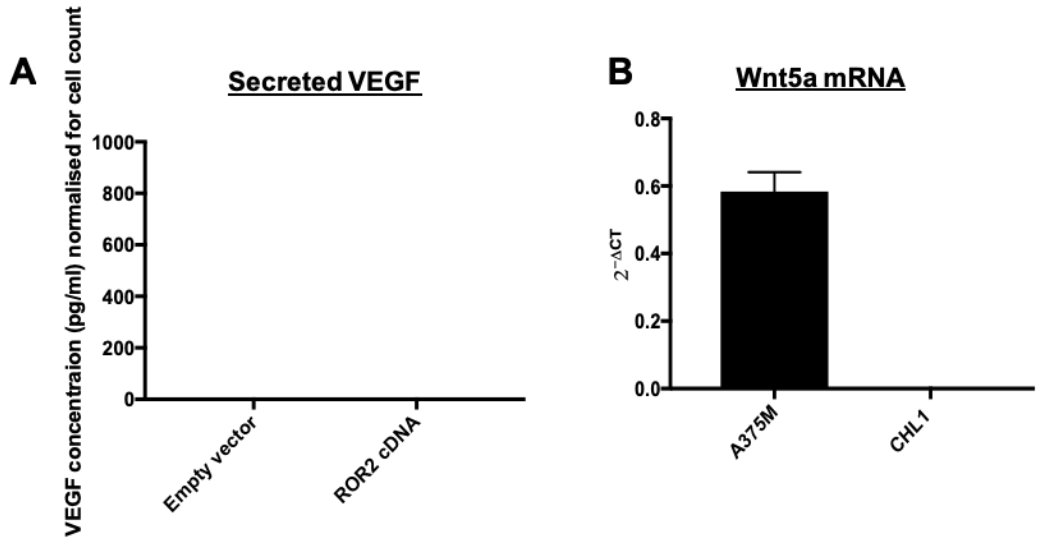

Figure 5-11: Effect of ROR2 overexpression on VEGF secretion in CHL1 cells. A: ROR2 cDNA clone 2 and Empty Vector clone 1 were cultured in 10cm plates for 48 hours. Conditioned medium was collected and analysed for VEGF content with ELISA. Data normalised against cell count, representing the average of three experiments, with two technical repeats per experiment. B. Wnt5a mRNA expression in CHL1, presented against A375M for comparison, obtained by qRT-PCR. Data average of duplicate experiments, each with triplet technical repeats.

Thus, overexpression of ROR2 in the CHL1 cell line was not associated with phenotypes expected following knockdown experiments. Importantly, overexpression in this cell line was not associated with any increase in VEGF compared to empty vector.

5.9.4. Testing ROR2 ligand expression in CHL1 and A375M cells

These two negative experiments suggested that either ROR2 does not play an important role in regulating VEGF secretion, invasion or motility in CHL1 cells, or the downstream targets of ROR2 may not be active, despite an abundance of the receptor.

This possibility prompted assessment of ROR2 ligand expression. These experiments demonstrated that the CHL1 cell line minimally expresses Wnt5a (figure 5-11 B), the

putative ligand for ROR2 that is necessary for receptor internalisation and presumably most of its reported phenotypes (O'Connell *et al.*, 2010).

Wnt5a was detected in A375M a $BRAF^{V600E}$ mutant melanoma cell (figure 5-11 B). Further experiments were therefore performed to test effects of ROR2 overexpression in this cell line.

5.10. Phenotypes associated with transient ROR2 overexpression in A375M

ROR2 was next overexpressed in the $BRAF^{V600E}$ mutant A375M cell line. Initially, transient transfection was performed to test phenotypes prior to creating stable cell lines.

ROR2 overexpression was confirmed using qRT-PCR on RNA extracted from the harvested cells (figure 5-12 A). Secreted VEGF was quantified in the conditioned medium by ELISA and normalised for cell count.

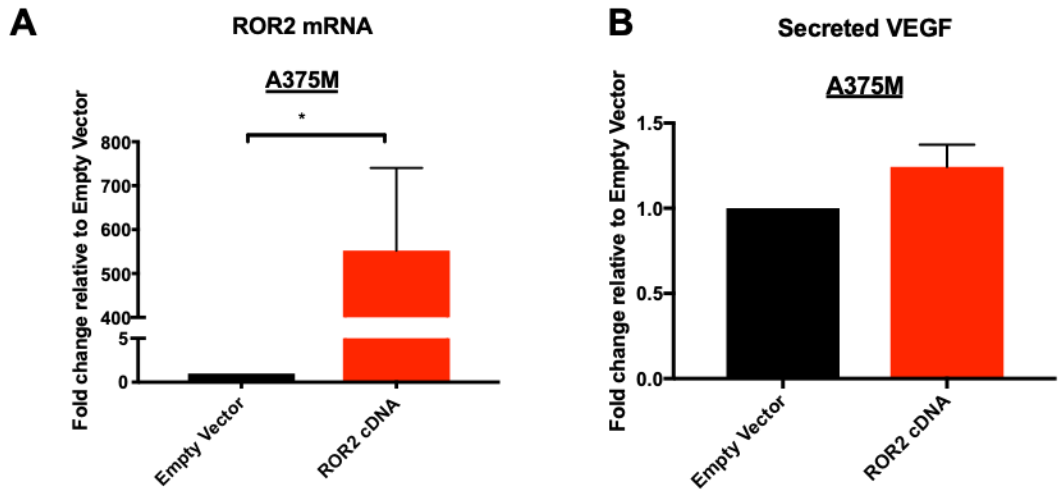

Figure 5-12: Effect of transient ROR2 overexpression on A375M cells. Cells were transiently transfected with ROR2 and Empty vector plasmids, and conditioned medium harvested after 48 hour. A. Overexpression of ROR2mRNA confirmed with qRT-PCR B. VEGF ELISA performed on conditioned medium. Results normalised against cell count and expressed as fold change relative to empty vector. Results the average of three experimental repeats, with two technical repeats per experiment. Statistics determined using students t-test * = p<0.05.

Transient transfection of ROR2 cDNA resulted in a very high level of ROR2 in the bulk culture (figure 5-12 A). VEGF secretion did not significantly change with ROR2 overexpression (p= 0.134) (figure 5-12 B).

The non-significant trend raised the possibility that ROR2 overexpression in A375M may have affected VEGF secretion but may have been diluted by the presence of untransfected cells. Stable ROR2 overexpressing A375M cell lines were therefore created for further experiments.

5.11. Stable ROR2 expression in A375M

Similarly to the methodology using in CHL1 cells above, a “kill curve” was established to determine the toxic dose of G418 for A375M cells, using a range of

G418 concentrations guided by the literature (Leaman *et al.*, 2002). A375M cells were transfected and with ROR2 plasmid or empty vector and selected with 700µg/ml G418.

ROR2 expression for each clone was quantified using western blot and RT-PCR.

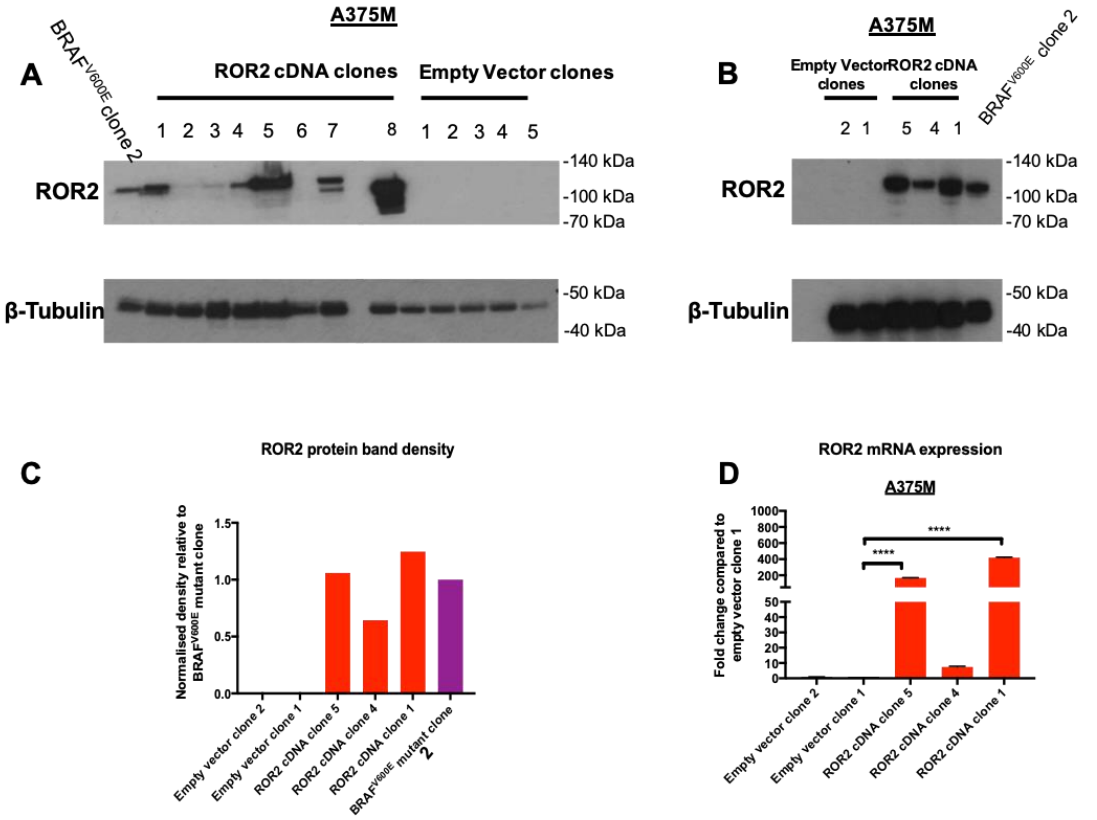

Figure 5-13: Stable ROR2 overexpression in A375M clones. A. 13 clones were harvested and screened for ROR2 expression. BRAF^{V600E} mutant clone 2 included for comparison. B. Three ROR2 cDNA and 2 empty vector clones were tested again for ROR2 expression in a confirmatory western blot expression. C. Protein band density of selected clones. The density of the protein band for clones in B were quantified and divided by the density (using image J) of the corresponding loading band. Results expressed relative to expression in BRAF^{V600E} clone 2. D. *ROR2* mRNA in the selected clones quantified using qRT-PCR. Statistics determined using one-way ANOVA **** p<0.0001. Experiments performed two independent repeats, each experiment compromising 3 technical replicates.

An initial screening blot was performed without protein level equalisation by lysing cells directly with Laemmli sample buffer and this identified five clones with ROR2 overexpression and undetectable expression in all empty vector controls (figure 5-13

A). Clone 8 was dismissed, as its level of ROR2 expression was extremely high compared to the level in $BRAF^{V600E}$ clone 2. Three ROR2 overexpressing clones were selected for further experiments: ROR2 cDNA clones 1, 4 and 5 and two empty vector controls (empty vector clones 1 and 2). ROR2 expression was confirmed in a second definitive western blot where unlike the screening experiment, protein concentrations were equalised (figure 5-13 B). Objectively quantifying the density of the protein band in the confirmatory western blot showed that ROR2 expression in the three selected overexpressing cell lines was similar to ROR2 expression in the $BRAF^{V600E}$ mutant clone (fig 5-13 C).

ROR2 expression at the level of mRNA was also quantified (figure 5-13 D) and confirmed *ROR2* mRNA overexpression in the appropriate clones. The mRNA data mirrored the results seen at the protein level, consistent with data already reported in this project demonstrating similar ROR2 expression between its mRNA and protein.

5.12. VEGF expression in stable ROR2 overexpressing A375M cell lines

5.12.1. The effect of ROR2 on VEGF secretion

Having confirmed stable ROR2 overexpression in A375M clones, the effect of this perturbation on VEGF expression and its secretion was next quantified. ROR2 overexpressing and control clones were seeded into 10cm plates and cultured for 48 hours in a fixed volume of G418 containing medium. After this time point, the conditioned medium from each dish was collected. Cells were harvested, counted and used for protein and mRNA quantification.

VEGF secretion in the ROR2 overexpressing clones was significantly increased

compared to empty vector controls (figure 5-14 A). This observation was evident in all ROR2 overexpressing clones. Furthermore, the relative magnitude of VEGF secretion approximated the differences in ROR2 protein expression between clones (figure 5-13 D).

This result, combined with the reciprocal phenotype observed in ROR2 depleted A375M cells (figure 5-5) further supported a significant role of ROR2 in VEGF secretion.

To check consistency with experiments performed with ROR2 siRNA, the effect of ROR2 overexpression on intracellular VEGF and VEGF mRNA was next quantified.

5.12.2. The effect of ROR2 overexpression on intracellular VEGF protein and VEGF mRNA

To further explore the pattern of VEGF expression following constitutive overexpression of ROR2, intracellular VEGF protein expression was also quantified. Overexpressing/control clones used above were cultured for 48 hours and RNA and protein were extracted. Intracellular VEGF protein was quantified using ELISA and normalised for cell count. ROR2 overexpression resulted in a statistically significant increase in intracellular VEGF concentration compared with control clones (figure 5-14 B), however the magnitude of increase was less than the increase in VEGF secretion under the same circumstances (figure 5-14 A).

VEGF mRNA expression was not affected by ROR2 overexpression (figure 5-14 C). This result paralleled earlier experiments using ROR2 siRNA (figure 5-5) and

supported a role of ROR2 in the post-transcriptional regulation of VEGF.

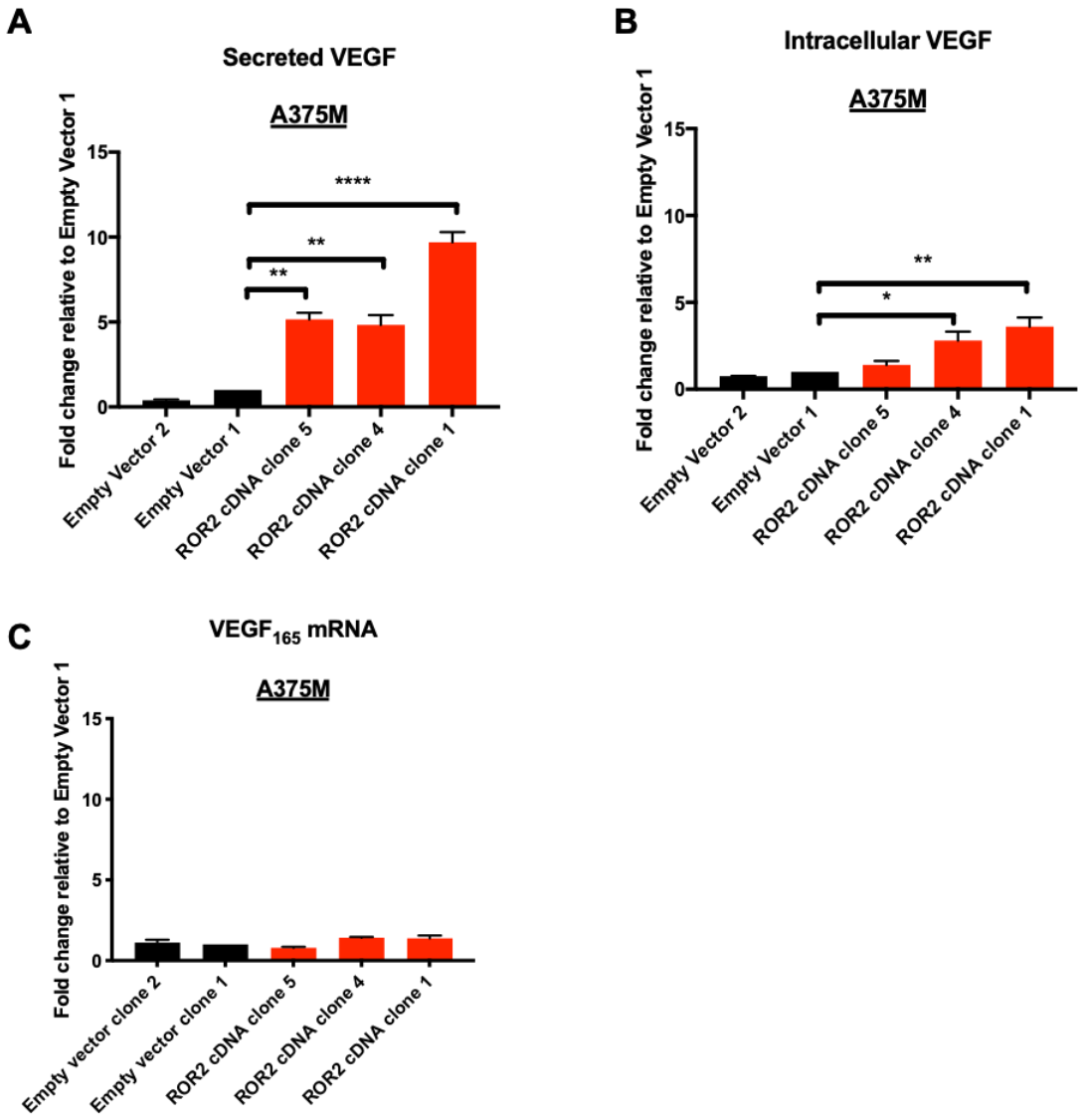

Figure 5-14: Effect of ROR2 overexpression on $VEGF_{165}$ expression. Selected A375M clones (as described) were cultured for 48 hours and then harvested as described previously. A. $VEGF_{165}$ secretion, determined using ELISA from conditioned medium with results normalised for cell count and expressed as fold change against empty vector clone 1. B. $VEGF_{165}$ in protein lysates. Cells harvested from the same experiments as A were lysed and analysed with an ELISA. For A and B, experiments were performed in triplicate with 2 technical replicates per experiments. Results were consistent between replicates. Due to variability in absolute values, data from a single experiment is presented C. $VEGF_{165}$ mRNA determined by qRT-PCR. Results combined average of duplicate experiments each with 3 technical replicates. Statistics performed using one-way ANOVA **** p=0.001, ** p=0.01 , * p=0.05

5.13. The effect of pharmacological BRAF^{V600E} inhibition on VEGF secretion in the context of ROR2 overexpression

The increase in VEGF secretion, and to a lesser extent, intracellular VEGF in response to ROR2 overexpression was hypothesised to occur by two broad mechanisms. First ROR2 itself perhaps, under the influence of mutant BRAF may have been responsible for the phenotype. Secondly, an interaction between the receptor and a possible BRAF^{V600E} driven ligand was another possibility. The latter hypothesis was considered particularly relevant given the absence of VEGF upregulation in ROR2 overexpressing BRAF wildtype CHL1 cells lines (figure 5-11 A).

To address the possibility that regulation of VEGF was driven by an interaction between the ROR2 receptor and BRAF^{V600E} influenced ligand, ROR2 overexpressing clones were treated with the MEK inhibitor Trametinib. ROR2 overexpressing clones were cultured for 24 hours in either Trametinib (5nM) or equivalent volume of DMSO. Conditioned medium was harvested after 24 hours and cells were harvested for cell count and protein lysate to confirm suppression of the MAPK signalling pathway. VEGF secretion was determined again via ELISA and data were normalised to cell count.

After 24 hours of Trametinib treatment minimal cell death was visible as evidence by non-viable cells floating in the medium. Trametinib treatment at 5nM effectively suppressed signalling downstream BRAF^{V600E} in the ROR2 overexpressing clones 1 and 4 but not 5 (figure 5-15 E).

Treatment with trametinib significantly decreased VEGF secretion in both ROR2 overexpressing and control clones (figure 5-15 A-B). No change was evident in empty vector 2, however this was most likely due inaccuracy of the ELISA to accurately quantify VEGF secretion in this cell line, as the absolute amount of VEGF produced was at the lower limit of sensitivity of the assay.

This effect of Trametinib on the clones gave weight to the possibility that VEGF secretion in A375M was also significantly influenced by an interaction between the ROR2 receptor and another factor. Given both control and overexpressing clones secreted less VEGF following pharmacological suppression of the MAPK axis, this other factor was hypothesised to be influenced by mutant BRAF activity. The putative ligand for ROR2, Wnt5A was proposed to be this other factor. The effect of MAPK silencing on its level of expression was assessed next.

5.14. Wnt5a is associated with constitutive BRAF activity and its interaction with ROR2 potentially influences VEGF secretion.

ROR2 overexpressing and control clones were cultured in either 5nM of Trametinib or control. After 24 hours, cells were harvested, RNA extracted and gene expression quantified using qRT-PCR.

Trametinib did not influence ROR2 expression in any clone (figure 5-15 C). As ROR2 expression in the overexpressing clones was under the control of a constitutively active CMV promoter this observation was not unexpected. There was a non-significant trend towards reduced ROR2 expression in empty vector clone 1 but not empty vector clone 2, which was contrary to earlier results in which 24 hour

Trametinib had downregulated ROR2 in $BRAF^{V600E}$ mutant A375M (figure 4-12). In A375M cells in this experiment, ROR2 mRNA expression was low and yielded CT values greater than 30 cycles, beyond the threshold for accurate interpretation of qRT-PCR data.

These results demonstrated that the decrease in VEGF secretion in the ROR2 overexpressing clones following treatment with Trametinib was unlikely due to changes in ROR2 expression.

Wnt5a mRNA expression was also quantified using qRT-PCR of RNA extracted from the same cells. Wnt5A expression decreased by over 95% in both empty vector and ROR2 overexpressing clones in cells treated with Trametinib (figure 5-15 E)

This result raised the possibility that both ROR2 and Wnt5a expression are under the influence of constitutive $BRAF^{V600E}$ activity. Both elements may be necessary to promote secretory VEGF phenotypes in $BRAF^{V600E}$ mutant melanomas.

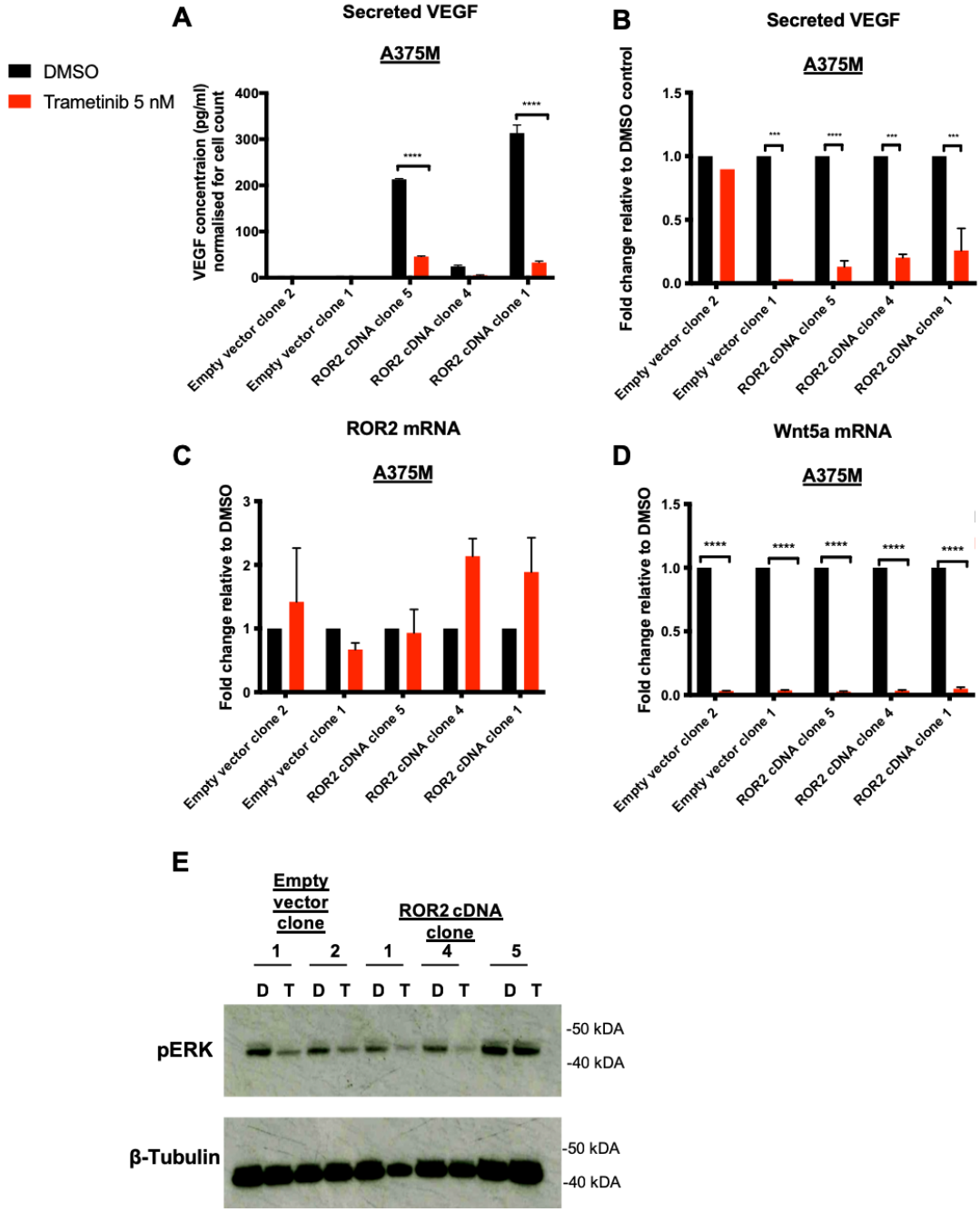

Figure 5-15: Effect of pharmacological MEK inhibition on ROR2 overexpressing A375M clones. Cells were treated with either Trametinib (5nM) or DMSO for 24 hours in equal volumes of medium (containing 10% FCS). $VEGF_{165}$ secretion was determined via ELISA on the conditioned medium. $VEGF_{165}$ levels for each treatment sample was normalised against cell count. ROR2 and Wnt5a mRNA expression was quantified using qRT-PCR and data normalised against TUBA6.
A. Secreted $VEGF_{165}$ expressed as absolute values B. Result of A expressed as fold change relative to paired control. Result representative of duplicate experiments, consisting of two technical replicates per experiment. C. ROR2 mRNA quantification D. Wnt5A mRNA quantification (C and D performed in triplicate). E. Phosphorylated ERK in both ROR2 overexpressing and empty vector clones using Western blot following 24 hour treatment with either 5nM Trametinib (T) or DMSO (D).
Statistics determined using 2-way ANOVA. **** p=0.0001 *** p=0.001

5.15. VEGF secreted in response to ROR2 overexpression is pro-angiogenic

Having shown that ROR2 overexpression increases the secretion of VEGF, and is associated with the $BRAF^{V600E}$ mutation the next experiment aimed to test whether this VEGF had angiogenic properties.

VEGF has many isoforms, including anti-angiogenic splice variants. Specifically, Woolard et al reported on the isoform $VEGFA_{165b}$, which has anti-angiogenic properties (Woolard *et al.*, 2004). Similarly to the putative angiogenic variant $VEGF_{165}$, $VEGF_{165b}$ also binds to VEGFR2, however does not initiate signalling of intracellular growth pathways within human umbilical endothelial cells (HUVECS). Application of exogenous $VEGF_{165}$ to endothelial cells drives proliferation (Keyt *et al.*, 1996), and therefore this readout was used as a surrogate marker for pro-angiogenic activity.

Endothelial tube formation was initially attempted as this assay is an effective quantitative method for this process (DeCicco-Skinner *et al.*, 2014). Although endothelial cells were successfully cultured into tube networks the data could not be reproducibly quantified and therefore endothelial cell proliferation was used for this experiment.

The VEGF ELISA used here has equal sensitivity to the anti-angiogenic isoform as it does for the angiogenic variant $VEGF_{165}$. Demonstrating that ROR2 influenced the angiogenic isoform was therefore essential before ROR2 could be implicated in the original hypothesis ie. as a gene differentially expressed in $BRAF^{V600E}$ mutant melanoma involved in promoting angiogenesis.

To determine if the $VEGF_{165}$ quantified in the assays above was angiogenic,

conditioned medium from ROR2 depleted or Control transfected A375M cells was cultured with Human Umbilical Endothelial Cells (HUVECs) and a proliferation assay was performed.

HUVECs cultured in the presence of conditioned medium taken from ROR2 depleted cells proliferated more slowly compared to control. Furthermore, the addition of recombinant $VEGF_{165}$ to endothelial cells cultured in this condition effectively reversed the phenotype (figure 5-16 B).

These results suggested that the VEGF isoform secreted under the influence of ROR2 in the A375M cell line promoted endothelial cell proliferation and therefore was likely to be pro-angiogenic.

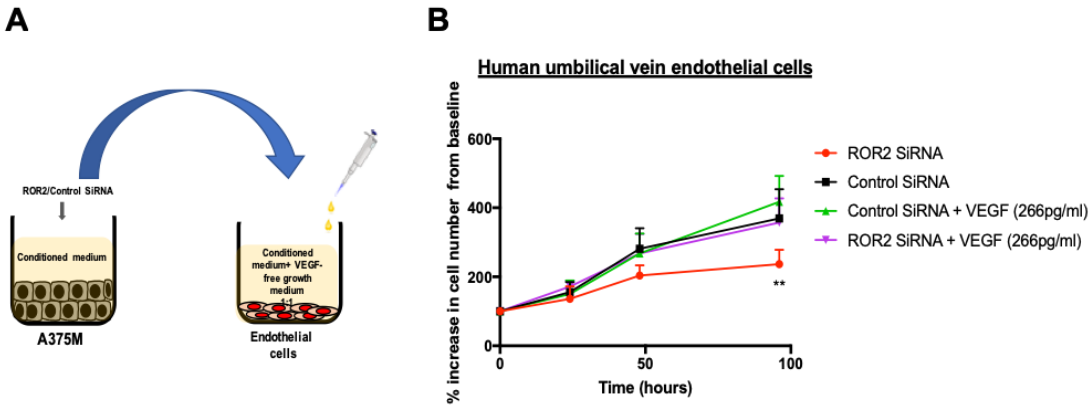

Figure 5-16: Effect of melanoma cell conditioned medium on endothelial cell proliferation. Conditioned medium from A375M cells treated with ROR2 or control siRNA was removed and added in a 1:1 ratio suspension of HUVEC cells cultured in VEGF depleted HUVEC specific culture medium. This suspension was cultured for 4 days. Recombinant $VEGF_{165}$ was added (total concentration 266pg/ml) as a positive control. A. Schematic. B. Cell counts were performed using Hoechst and propidium iodide staining with time points at baseline, 24, 48 and 96 hours. Data expressed as percentage change from baseline. Experiment performed in triplicate with three technical replicates per experiment. Statistics were performed to quantify the change from control siRNA at all time points using 2-way ANOVA. ** = p <0.01

5.16. Discussion

ROR2 depletion resulted in a decrease in proliferation and invasion in the melanoma cells tested above. The effect on proliferation is consistent with some but not all previously published data. Yang et al demonstrated ROR2 downregulation resulted in a decrease in proliferation in two renal cell cancer cell line lines (Yang *et al.,* 2017). The same study also reported that ROR2 silencing decreased invasion and migration in the same cell lines supporting the role of ROR2 as a mediator of aggressive phenotypes. Similar results have been reported in other studies on renal cell cancer (Rasmussen *et al.,* 2014) and ovarian cancer cell lines (Henry *et al.,* 2016). In the latter study, ROR2 expression was also implicated in platinum resistance potentially related to an association between ROR2 and co-expression of SNAI1 and SNAI2 to promote EMT transition. ROR2 expression in renal cell cancer has been associated with inferior clinical outcomes, further supporting its role in cancer progression (Rasmussen *et al.,* 2014).

Experiments in other cell lines however have yielded contrasting results. ROR2 downregulation secondary to promoter hypermethylation in colorectal cancer cell lines increased both invasion and proliferation (Ma *et al.,* 2016). Similarly, ROR2 overexpression in gastric cancer cells has been shown to decrease proliferation, which was associated with a reduction in β-catenin signalling (Yan *et al.,* 2016).
With such inconsistencies, the role of ROR2 appears to vary depending on context. The contextual elements that modulate phenotypes associated with ROR2 remain to be elucidated. One theory is that in tumours driven by β-catenin such as colorectal cancer, ROR2, by its antagonistic effect on canonical Wnt signalling functions as a

tumour suppressor. In contrast progression of tumours such as melanoma and renal cell carcinoma appear to β-catenin independent and ROR2 in these tumours may result in more malignant phenotypes (Ford *et al.*, 2013). Mutations in ROR2 are rare (Kubo *et al.*, 2009) and therefore the varying phenotypes associated with ROR2 are likely to be due to non-genomic regulation.

In melanoma, the phenotypes associated with ROR2 are implied from studies involving its ligand, Wnt5a. Wnt5a binds to ROR2, resulting in clathrin mediated internalisation of the receptor. Clathrin depletion decreased motility of the melanoma cell line UACC903 (O'Connell *et al.*, 2010). Melanoma cells treated with Wnt5a also demonstrated enhanced motility in a wound healing assay (Dissanayake *et al.*, 2008). *In vivo*, mice receiving tail vein injections of B16 melanoma cells transfected with ROR2 siRNA, were shown to have significantly fewer lung metastases (O'Connell *et al.*, 2010). Taken together, ROR2 in the context of melanoma appears to promote aggressive phenotypes, consistent with the results obtained here.

The effect of the $BRAF^{V600E}$ mutation on ROR2 phenotypes has not been described. In figure 5-1 C, ROR2 depletion in a BRAF wildtype melanoma clone did not statistically significantly impact upon proliferation. A possible caveat for this observation however may be the relatively minor degree of ROR2 knockdown (figure 5-1 D) possibly related to low endogenous ROR2 expression in this cell line. Poor target gene expression has been reported to decrease siRNA efficiency (Hong *et al.*, 2014). Phenotypes associated with ROR2 signalling in melanoma have been reported in both BRAF wildtype and BRAF mutant cells. The UACC-903 cell line, reported above by O'Connell et al to decrease mobility with Wnt5a-ROR2 inhibition harbours a $BRAF^{V600E}$ mutation, whereas the B16F10 murine melanoma cells, also reliant on ROR2 for an aggressive phenotype *in vivo*, are BRAF wildtype (O'Connell *et al.*,

2010). Overall however, there has been no direct comparison of phenotypes induced by ROR2 depletion in BRAF wildtype and mutant melanoma cells.

These data presented suggest that ROR2 influences post transcriptional control over VEGF secretion. This observation was demonstrated in separate experiments manipulating ROR2 with siRNA (figure 5-5 A-F) or overexpression (figure 5-14 A-C). Furthermore, the observed phenotype may require the concurrent expression of Wnt5a, which in itself may be a transcriptional target of $BRAF^{V600E}$, given that its expression decreased following pharmacological MAPK inhibition in the ROR2 overexpressing A375M cell line (figure 5-14 D).

In addition to affecting VEGF secretion, ROR2 depletion resulted in decreased $VEGF_{165}$ mRNA expression, but only the $BRAF^{V600E}$ mutant melanoma cell lines (figure 5-5). The decrease in the $BRAF^{V600E}$ mutant clone and not in A375M or SKMEL28 that harbour endogenous $BRAF^{V600E}$ mutations may be due to a number of factors. Firstly, the expression of ROR2 is much higher in the $BRAF^{V600E}$ mutant isogenic clone compared to the other BRAF mutant cell lines and as result, ROR2 manipulation may have resulted in an exaggerated phenotype. Secondly, the isogenic clone has an acquired $BRAF^{V600E}$ mutation and does not have "oncogenic addiction" (Sharma *et al.*, 2007) to the mutation, unlike A375M and SKMEL28. This difference in underlying biology may responsible for the difference in the phenotypes that were observed in this experiment.

ROR2 depletion in SKMEL28 resulted in an increase in VEGF mRNA expression (figure 5-3 C). Although both SKMEL28 and A375M harbour the $BRAF^{V600E}$ mutation, SKMEL28 also has a PTEN mutation (Haluska *et al.*, 2006). It is possible that the differences in VEGF mRNA expression between A375M and SKMEL28 in

response to ROR2 siRNA may be related to mutant PTEN influences over phenotype. This could be tested showing that PI3K/AKT signalling, the pathway negatively regulated by PTEN is increased in SKMEL28 cells. Subsequently, VEGF mRNA expression could be tested in ROR2 depleted SKMEL28 cells, with or without AKT inhibition (pharmacological or with siRNA). The absence of increased VEGF mRNA in AKT inhibited cells may suggest that PTEN status could have a role in the VEGF transcription following ROR2 depletion. As a reciprocal experiment, a silencing PTEN mutation (Stahl *et al.*, 2003) could also be introduced to the PTEN intact $BRAF^{V600E}$ mutant isogenic clone 2 to test if functional PTEN is a requirement for the decrease in VEGF mRNA shown in this cell line after ROR2 depletion.

A more consistent phenotype across the $BRAF^{V600E}$ mutant cell lines was evident when quantifying the impact of ROR2 depletion on VEGF secretion (figure 5-5 A-E). These data demonstrated a significant decrease in VEGF secretion in all BRAF mutant cell lines including SKMEL-28. In contrast ROR2 depletion did not affect VEGF secretion in the BRAF wildtype clone (figure 5-5 D). It was notable that ROR2 depletion of the $BRAF^{V600E}$ mutant isogenic clone decreased VEGF secretion to the concentration secreted by the wildtype clone (figure 5-5 E), suggesting the phenotypic differences between the two isogenic clones may be influenced by the expression of ROR2. ROR2 knockdown however was less effective in the wildtype clone (figure 5-3 E), which may have attributed to the final result and was attributed to the low level of basal ROR2 expression in this isogenic clone.

The effect of ROR2 depletion was most notable when assessing VEGF secretion. Possible post-transcriptional mechanisms of ROR2-influenced VEGF regulation are explored in chapter 6.

ROR2 depletion had variable effects upon reported downstream targets. As a driver of the Wnt5a-ROR2 axis of non-canonical Wnt signalling, ROR2 has been implicated in the promotion of melanoma de-differentiation and epithelial to mesenchymal transition (Dissanayake, *et al.*, 2008). Recombinant Wnt5a treatment of two $BRAF^{V600E}$ mutant cell lines, UACC903 and UACC1273 resulted in a decrease in the expression of the differentiation marker MART1 (Dissanayake, *et al.*, 2008). Therefore, as a mediator of Wnt5a driven phenotypes, ROR2 siRNA was expected to decrease MART1 expression, whereas no effect was observed in the two $BRAF^{V600E}$ mutant cell lines (figure 5-7 A-B). Paradoxically, SNA1, another EMT marker positively associated with Wnt5a (Dissanayake, *et al.*, 2008) unexpectedly increased in A375M following ROR2 depletion (figure 5-7 B).

These paradoxical effects may stem from the effect of ROR2 siRNA on Wnt5a. In both $BRAF^{V600E}$ mutant cell lines, ROR2 siRNA increased the expression of Wnt5a. This observation conflicts with published data as ROR2 siRNA has previously been reported to have no effect on the expression of Wnt5a in BRAF mutant UACC903 cells (O'Connell *et al.*, 2010). The increase in Wnt5a in the experiments presented here may explain the increase in expression of *SNA1*, however increased *Wnt5a* expression was expected to downregulate *MART1*, which was not observed (figure 5-7 A- B). Despite published evidence, the data presented here suggest that Wnt5a and ROR2 in the $BRAF^{V600E}$ mutant clones may exist in a feedback loop in which ROR2 downregulation leads to Wnt5a upregulation although further work is required to prove this. Increased *SNAI1* expression in A375M may suggest ongoing Wnt5a signalling, possibly through other known receptors such as LRP6 and Fzd4 (Webster *et al.*, 2013).

In contrast to the effect of ROR2 siRNA on $BRAF^{V600E}$ mutant cells, ROR2 depletion has no significant effect upon Wnt5a expression in the BRAF wildtype isogenic

clone, and the expected effect of *MART1* upregulation (figure 5-7 C). Although interpretation of results in this cell line need to be taken with caution given the modest ROR2 knockdown (figure 5-3 E), the result suggested ROR2 may have differential effects depending on BRAF mutational status.

The phenotypes tested upon ROR2 depletion were further explored using ROR2 overexpression which increased VEGF secretion in A375M (figure 5-14 A), reciprocating the results following ROR2 knockdown in the same cell line. This phenotype was independent of increases in VEGF mRNA level (figure 5-14 C). Although ROR2 overexpression did increase intracellular VEGF expression (figure 5-14 B), the magnitude of the difference was considerably lower than the effect on VEGF secretion

The effect of ROR2 overexpression was not uniform, with no effect upon VEGF secretion in BRAF wildtype CHL1 melanoma cells (figure 5-11 A). Differential expression of Wnt5a was hypothesised to account for this result as Wnt5a is the putative ligand for ROR2 and responsible for similar phenotypes associated with non-canonical Wnt signalling (O'Connell *et al.*, 2010). Wnt5a was not expressed in CHL1 cells, but was expressed in A375M, in support of this hypothesis (figure 5-11 B). As a secreted molecule (O'Connell *et al.*, 2009), expressed Wnt5a in A375M presumably bound overexpressed ROR2 that resulted in the secretory VEGF phenotype observed. The results also suggest that Wnt5a may be associated with the $BRAF^{V600E}$ mutation, which has not been reported previously. ROR2 overexpressing A375M clones treated with MEK inhibitor trametinib secreted significantly less VEGF compared to control treated cells (figure 5-15 A-B). This phenotype was not accompanied by changes in ROR2 expression (figure 5-15 C), which was expected as ROR2 expression in these

clones was under the control of a constitutively active promoter. Wnt5a, in contrast decreased significantly in all trametinib treated ROR2 overexpressing and empty vector clones (figure 5-15 D), implying an association between MAPK signalling its expression.

Further experiments are required to ascertain if Wnt5a specifically is sufficient to generate the phenotypes observed in ROR2 overexpressing cell lines. ROR2 overexpressing CHL1 cells treated with recombinant Wnt5a would secrete more VEGF if the ligand alone were required for the phenotype. Conversely, ROR2 overexpressing A375M cells treated with a commercially available Wnt5a inhibitory peptide, Box-5 (Jenei *et al.*, 2009) would be expected to secrete less VEGF. Due to time constraints these experiments were not performed.

The association of $BRAF^{V600E}$ with Wnt5a expression is novel. Wnt5a was not differentially expressed in any of the datasets described in chapter 4 although Wnt5a was not included in AVAST-M patient data set.

Wnt5a has not been described previously as a transcriptional target of $BRAF^{V600E}$ induced MAPK signalling. Multiple reports have however associated Wnt5a with $BRAF^{V600E}$ resistance (Tap *et al.*, 2010; O'Connell *et al.*, 2013; Anastas *et al.*, 2014). BRAF mutant melanoma cell lines resistant to $BRAF^{V600E}$ inhibitor PLX4720 have been shown to upregulate Wnt5a and sensitivity has been restored with Wnt5a depletion. Multiple mechanisms of BRAF inhibitor resistance have been described, however a fundamental mechanism remains re-activation of the MAPK signalling axis (Griffin *et al.*, 2017). The upregulation of Wnt5a in BRAF inhibitor resistant melanomas could feasibly result from MAPK pathway reactivation and supports an association between Wnt5a and $BRAF^{V600E}$ signalling activity.

Further experiments are required to test the association of Wnt5a with the $BRAF^{V600E}$ mutation. Differential expression could be tested in the $BRAF^{V600E}$/wildtype isogenic cell line model. The effect of the specific $BRAF^{V600E}$ inhibitor, PLX4720 on Wnt5a expression could ascertain if Wnt5a expression is specific to mutant BRAF activity as opposed to MAPK suppression globally. The experiments above should also be performed in a broader range of $BRAF^{V600E}$ and wildtype melanoma cell lines and testing Wnt5a expression in clinical samples of BRAF wildtype and mutant melanomas.

Taken together, these results suggest that both ROR2 and Wnt5a influence post-transcriptional regulation of VEGF, and the $BRAF^{V600E}$ mutation may regulate expression of both genes. $BRAF^{V600E}$ associations with the Wnt5a-ROR2 axis have not been previously been described. Given their association with pro-malignant phenotypes, both ROR2 and Wnt5a may be potential therapeutic targets for patients with $BRAF^{V600E}$ mutant melanoma. Possible mediators of the link between the $BRAF^{V600E}$ mutation, ROR2 expression and VEGF secretion are explored in the next chapter.

6. Chapter VI: Mechanisms linking ROR2 with increased VEGF secretion in $BRAF^{V600E}$ mutant melanoma

Work in the previous chapter demonstrated that ROR2 is differentially expressed in $BRAF^{V600E}$ mutant melanomas and influences the secretion of VEGF. Intermediaries linking $BRAF^{V600E}$ and ROR2 expression as well as mechanisms associating ROR2 with VEGF secretion were next explored.

6.1. Investigating HIF-1α as a candidate mediating the effect of the BRAFV600E mutation and ROR2 upregulation

HIF-1α, classically stabilised under hypoxic conditions, can also be stabilised under other conditions. Oncogenic $BRAF^{V600E}$ has been identified as one such factor with the capacity to stabilise HIF-1α (Masoud *et al.*, 2015). Experiments from O'Connell et al have shown that ROR2 expression is increased in hypoxic conditions, an effect largely dependent on the stabilisation of HIF-1α (O'Connell *et al.*, 2013). Based on this finding, $BRAF^{V600E}$ mediated HIF-1α stabilisation could plausibly promote ROR2 expression.

Two experiments were performed to test this association. Firstly, expression of the HIF-1α protein was quantified in the $BRAF^{V600E}$/wildtype isogenic cell model described earlier. As ROR2 was differentially expressed in this model, expression of HIF-1α was hypothesised to parallel ROR2 if HIF-1α was driving ROR2 upregulation in the $BRAF^{V600E}$ mutant melanoma clones.

$BRAF^{V600E}$ mutant and wildtype isogenic clones were cultured in normoxic conditions for 48 hours, then harvested and lysed. HIF-1α expression was quantified

using western blot with a validated HIF1α antibody(Masoud *et al.*, 2015). Lysate from MCF7 cells cultured in 1% oxygen for 6 hours was used as a positive control. HIF1α expression was not detected in either the $BRAF^{V600E}$ mutant or wildtype clones which suggested that the acquired $BRAF^{V600E}$ mutation in this cell line model did not promote HIF-1α stabilisation (figure 6-1 A).

The association between HIF-1α and ROR2 was explored in parallel to assess if ROR2 is upregulated in hypoxia. A375M cells were cultured in both normoxic and hypoxic conditions (1% oxygen) for 48 hours in order to induce HIF-1α stabilisation in the latter. After this point, cells were harvested and RNA was extracted.
As the *VEGF* promoter is well recognised as a HIF-1α target (Dobrynin *et al.*, 2017), *VEGF* mRNA was selected as a surrogate for HIF-1α expression. *VEGF* and *ROR2* mRNA expression were quantified in both normoxia and hypoxia using qRT-PCR. As expected *VEGF* mRNA was increased in A375M cells cultured in hypoxia (figure 6-1 B). ROR2 expression, in contrast was unaffected by the same conditions.
Taken together, the above data do not support the hypothesis that differential expression of ROR2 in $BRAF^{V600E}$ mutant clones is due to HIF-1α stabilisation nor provide evidence that ROR2 is a transcriptional target of HIF-1α in A375M cells.

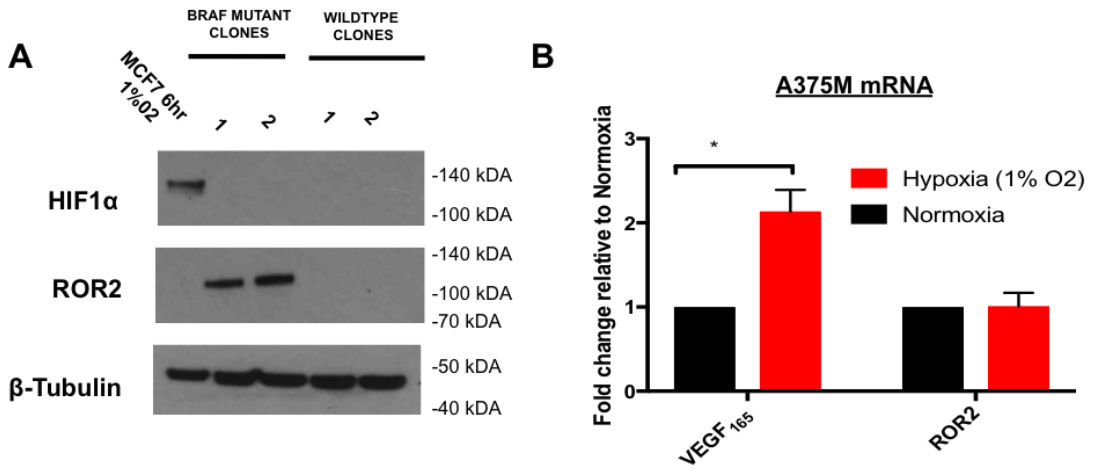

Figure 6-1: Testing the contribution of HIF-1α to ROR2 expression. A. Protein lysates from BRAF^{V600E} mutant and wildtype clones (two of each), all grown in normoxic conditions were probed for antibodies specific for HIF-1α and ROR2. MCF7 cells cultured in hypoxia (1% O_2) for 6 hours were used as a positive control. B. A375M cells were cultured in normoxia and 1% O_2. RNA was extracted and, $VEGF_{165}$ and ROR2 mRNA were quantified using RT-PCR. Results were corrected for expression of TUBA6 (housekeeping gene UBC) and expressed as fold change relative to normoxic control. Statistics determined using students t-test. *= p<0.005 . Experiments performed in biological triplicate.

6.2. Investigating MMP2 as an intermediary between ROR2 and VEGF secretion

As shown in chapter 5, ROR2 upregulation is associated with increased secretion of VEGF. A potential ROR2 induced intermediary responsible for this phenotype was next explored. The extracellular regulation of VEGF secretion and bioactivity is a complicated process. All isoforms of VEGF (with the exception of $VEGF_{121}$) contain a heparin binding site domain that allows secreted VEGF to bind to the extracellular matrix via heparan sulfate proteoglycans (Houck *et al.*, 1992). Binding of VEGF extracellularly provides an effective reservoir of VEGF for release in a secreted form when required. The matrix metalloproteases (MMPs) have been reported to cleave heparan sulfate proteoglycans and potentially play a role in the secretion of VEGF (Hawinkels *et al.*, 2008). Further studies have shown MMPs do not necessarily require the presence of extracellular matrix to induce VEGF secretion, as shown when MMP2 and MMP9 applied directly to ovarian cancer cells enhances VEGF secretion

(Belotti *et al.*, 2003).

ROR2 has already been linked to MMP2 expression and invasive phenotypes in renal cell carcinoma (RCC) cell lines. Rasmussen et al have demonstrated that ROR2 overexpressing RCC cells are more invasive and migratory relative to controls and show increased expression of MMP2. Inhibiting MMP2 in these cells abrogated these phenotypes, implicating it as an important mediator of the aggressive features associated with ROR2 expression (Rasmussen *et al.*, 2014).

In light of these reports, the relationship between ROR2 and MMP2 was explored in the A375M cell line.

6.2.1. The effect of ROR2 depletion on MMP2 expression in A375M cells

A375M cells were transfected with ROR2 or control siRNA and RNA was extracted after 48 hours. *MMP2* expression was quantified using qRT-PCR.

ROR2 depletion was confirmed in three independent experiments (figure 6-2 B). The same cDNAs were used to quantify *MMP2* mRNA which showed a statistically significant decrease in *MMP2* expression (figure 6-2 A), supporting the hypothesis that ROR2 influences the transcription of MMP2.

Primers for MMP9 were also created using the same process used for MMP2. However, *MMP9* mRNA expression was undetectable in A375M cells using RT-PCR and consequently it was not studied any further.

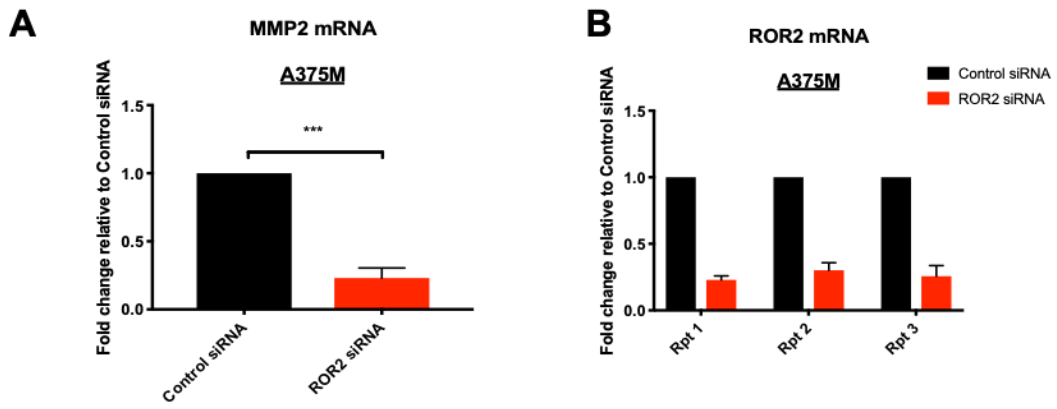

Figure 6-2: The effect of ROR2 depletion on MMP2 expression. A375M cells were transfected with ROR2 or control siRNA. After 48 hours RNA was extracted and expression of MMP2 quantified using qRT-PCR with data normalised to housekeeping gene TUBA6. A. MMP2 mRNA expression expressed as fold change relative to control. Pooled data from triplicate repeats. B. ROR2 mRNA expression from the individual experiments constituting A. Statistics performed using unpaired t-test *** = p<0.0005

6.2.2. Testing the effect of MMP2 inhibition on VEGF secretion in the A375M cell line

Having observed that the expression of MMP2 was downregulated with ROR2 depletion the next step was to determine if MMP2 expression influenced VEGF secretion. As a first approach A375M cells were treated with CT-1746, a pan-MMP inhibitor with activity against MMP2 (Kerkvliet *et al.*, 2003).

A concentration of 10µM of CT-1746 was selected as this concentration has been previously shown in the literature to effectively inhibit MMP2 activity (Kerkvliet *et al.*, 2003). Therefore, cells were treated with 10µM CT-1746 or solvent control (DMSO) and after 24 or 48 hours culture medium was collected and the cells harvested and counted.

VEGF secretion was assessed in culture medium using ELISA, and normalised to cell count. Treatment periods were 24 hours (1 repeat) and 48 hours (2 repeats). One repeat at 24 hours was performed in serum free conditions to facilitate subsequent zymography that was planned in the event of a positive result. None of the individual experiments demonstrated a difference between the two conditions and therefore the data were pooled. The merged data did not demonstrate a difference in the secretion of VEGF after treatment with CT-1746 (figure 6-3).

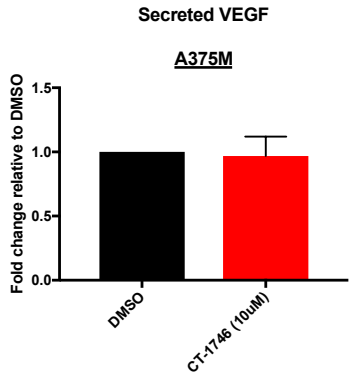

Figure 6-3: The effect of MMP2 inhibition on the secretion of VEGF from A375M cells. A375M cells were cultured in full medium (2 biological repeats) or serum free conditions (1 biological repeat) for 24 (1 biological repeat) or 48 hours (2 biological repeats) following treatment with CT-1746 (10μM) or solvent control. Data from all biological repeats were pooled and expressed as fold change relative to solvent control. Statistics performed using an unpaired students t-Test.

6.2.3. Testing effect of recombinant MMP2 on VEGF secretion

As a second approach A375M cells were treated with recombinant MMP2 to determine effects on VEGF secretion. MMP2 was hypothesised to abrogate the decrease in VEGF secretion mediated by ROR2 depletion. Therefore, A375M cells were transfected with control or ROR2 siRNA. After 24 hours, recombinant MMP2 (R&D) was activated with amino phenyl mercuric acetate (APMA) as described previously (Kerkvliet *et al.*, 2003). Solvent containing an equivalent volume of DMSO was also treated with APMA as a control. After activation, APMA was removed using a filter column and MMP2 (or equivalent volume of DMSO) added to fresh DMEM to a concentration of 6.6ng/µl, a concentration previously reported to increase VEGF secretion (Kerkvliet *et al.*, 2003). Activated MMP2 or solvent control was then added to siRNA transfected cells. After a further 24 hours, the conditioned medium was collected, the cells counted, and secreted VEGF quantified using ELISA on the conditioned medium., correcting the results according to cell count using the method described previously.

As shown below, results in two independent experiments confirmed effective ROR2 depletion (figure 6-4 A). VEGF ELISA showed a significant reduction in secreted VEGF in ROR2 depleted cells (figure 6-4 B) confirming the result seen earlier (figure 5-5 B). However, the decrease in secreted VEGF was not reversed following treatment with recombinant MMP2 (figure 6-4 A).

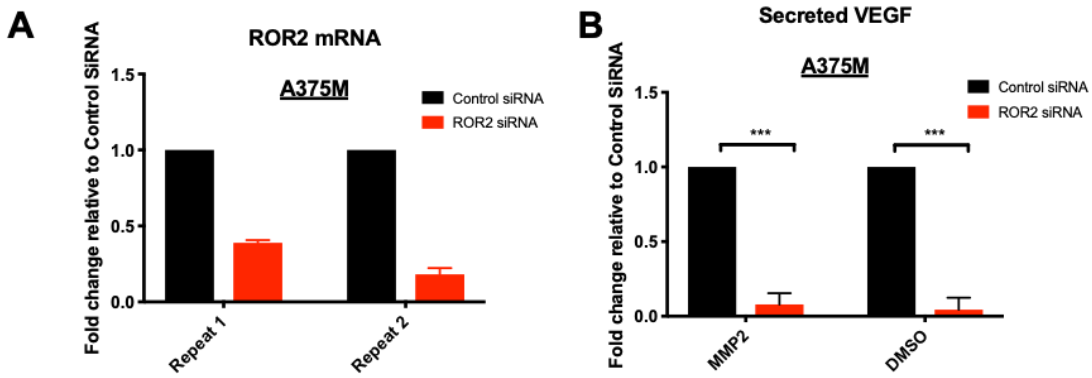

Figure 6-4: The effect of recombinant MMP2 on VEGF secretion in the context of ROR2 depletion. A375M cells transfected with ROR2 or control siRNA and after 24 hours were treated with either activated MMP2 (6.6ng/µl) or DMSO. The following day, VEGF in the conditioned medium was tested by ELISA. A. ROR2 mRNA in two biological repeats, as determined by RT-PCR. B. Results of VEGF ELISA adjusted for cell count. Statistics determined using two-way ANOVA (* p=0.001).**

6.2.4. Expression of MMP2 mRNA in ROR2 overexpressing A375M clones

MMP2 mRNA expression was quantified in A375M clones overexpressing ROR2. These cell lines have previously been shown (figure 5-14 A) to secrete increased VEGF relative to empty vector. *MMP2* mRNA expression was shown previously (figure 6-2) to downregulate in the same cell line following transfection with ROR2 siRNA, and this effect was also associated with decreased VEGF secretion (figure 6-4 B). *MMP2* mRNA expression was therefore predicted to increase in ROR2 overexpressing A375M clones. To test this, RNA was extracted from ROR2 overexpressing and empty vector clones and *MMP2* mRNA was quantified using qRT-PCR.

ROR2 overexpression was not associated with consistent change MMP2 expression (figure 6-5). This result was inconsistent with the results of transfecting the same cell line with ROR2 siRNA where ROR2 depletion downregulated MMP2 expression (figure 6-2).

In summary, although MMP2 was downregulated in ROR2 depleted A375M cells, recombinant MMP2 treatment in the same cell line had no significant effect on VEGF secretion. Furthermore, MMP2 expression was not upregulated in ROR2 overexpressing A375M clones.

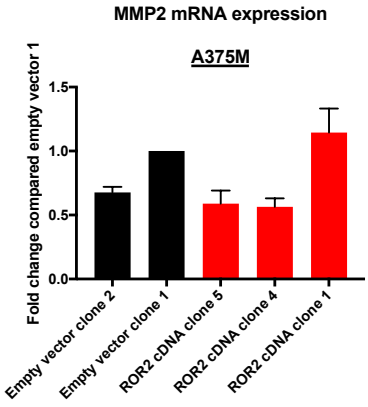

Figure 6-5: *MMP2* mRNA expression in A375M clones. RNA was extracted from empty vector and ROR2 overexpressing clones and MMP2 expression was determined using RT-PCR. Data expressed as fold change relative to empty vector 1. Statistics performed using 1 way ANOVA, comparing each clone to empty vector clone 1. Data represent two separate experiments, each with three technical repeats (ie 6 data points). Significance tested with one-way ANOVA, with Dunnetts correction to compare each clone to empty vector clone 1. No statistically significant differences were found.

6.3. The effect of ROR2 expression on exosome secretion

Exosomes contain various signalling proteins and growth factors that can be efficiently secreted and delivered to other cells, thus serving as a method of effective intercellular communication. The precise function of exosomes remains unknown however evidence exists that they play important tumour-relevant roles in immune suppression, microenvironmental modulation and drug resistance (Filipazzi *et al.*, 2012). In addition to these functions, exosomes have an important role in angiogenesis and of relevance to this this project can transport VEGF (Belotti *et al.*, 2003). Previous experiments have shown Wnt5a, the ligand for ROR2 increases

VEGF-containing exosome secretion in melanoma cells (Filipazzi *et al.*, 2012). Exosomes are therefore a possible mechanism through which ROR2 could influence VEGF secretion into the extracellular environment.

To test the hypothesis that ROR2 induced exosome secretion regulates VEGF secretion, ROR2 overexpressing and empty vector cells transfected A375M clones were cultured in medium containing exosome depleted foetal calf serum for 48 hours. For each biological repeat the exosome concentration was normalised for cell count against the cell count for the empty vector 1 control. The data demonstrated that ROR2 overexpression was not associated with an increase in overall exosome secretion (figure 6-6 A) into conditioned medium ($p=0.8332$). Exosome quantification for this experiment was performed using nanoparticle tracking analysis (NTA) by Dr Naveed Akbar (Division of Cardiovascular Medicine, Radcliffe Department of Medicine)/

In a parallel experiment, secreted VEGF was also quantified in the conditioned medium of A375M cells transfected with ROR2 or control siRNA following ultracentrifugation, to pellet extracellular material. ROR2 depletion of these cells had earlier decreased VEGF secretion (figure 5-14 A) and therefore this experiment tested the possibility that this observation was due to a reduction in VEGF contained in the extracellular material within exosomes.

From the pooled data from 3 independent biological repeats, a statistically significant decrease in VEGF secretion was not evident in conditioned medium from ROR2 depleted A375M cells when analysed after ultracentrifugation ($p=0.7617$) (figure 6-6 B). However, the three biological repeats were not consistent (figure 6-6 C). ROR2 depletion decreased VEGF secretion in two of the three repeats but increased VEGF secretion in one experiment. This was despite very similar ROR2 depletion in all

three experiments (figure 6-6 D).

Taken together, two of three experiments showed a reduction in VEGF secretion which could suggest that ROR2 depletion reduced the VEGF that was not contained within extracellular vesicles but the results are too variable to be conclusive and further repeats would be required.

An attempt was made to test VEGF in the pelleted material in the same samples after ultracentrifugation. Following resuspension however to a required volume, VEGF was undetectable in all samples with ELISA which possibly indicated that resuspension reduced the VEGF concentration below the threshold for detection in the assay.

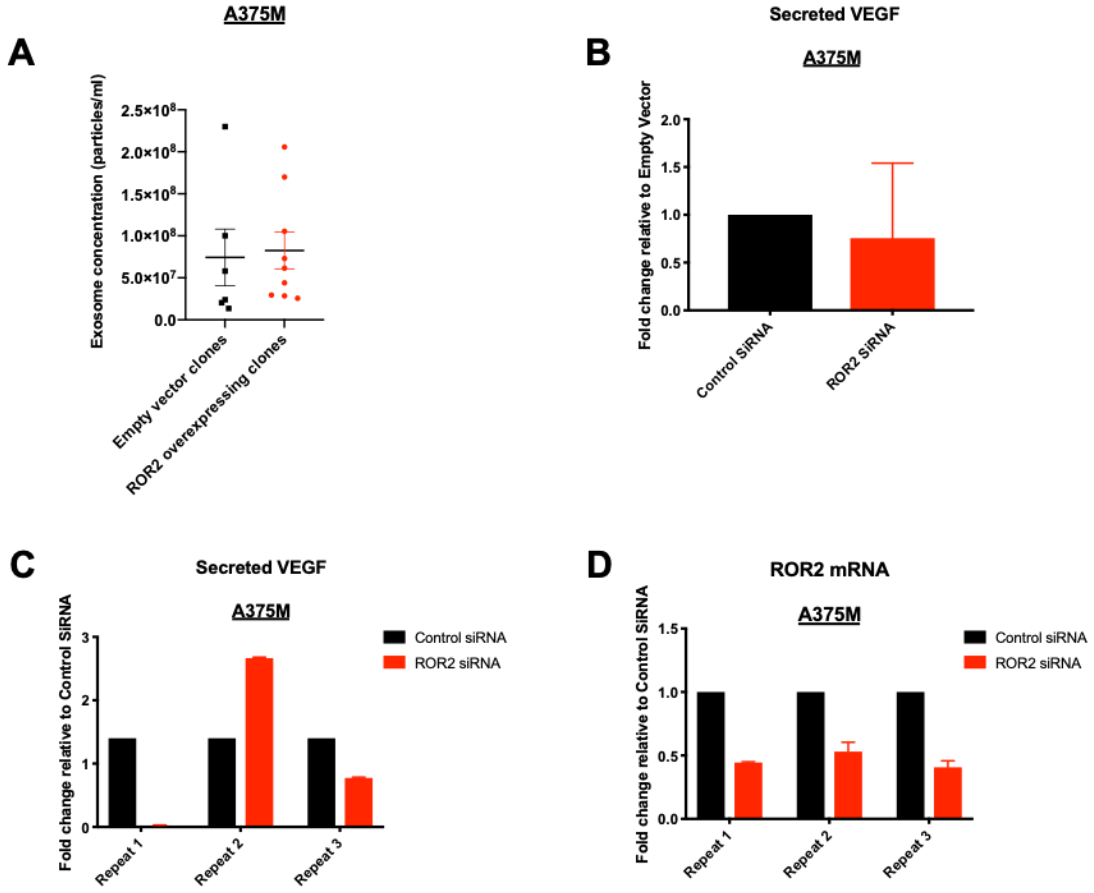

Figure 6-6: The effect of ROR2 overexpression on exosome production. A. Exosome concentrations from conditioned medium were determined using nanoparticle tracking analysis (NTA) from A375M cell lines overexpressing ROR2 (3 clones) or Empty vector (2 clones) performed in triplicate (3 biological repeats). Graph shows exosome concentration/ml corrected for cell count showing individual data points (three technical replicates from 3 biological repeats with mean ± SEM). Statistical significance tested using students t-test. NTA analysis performed by Dr Naveed Akbar B. VEGF concentrations in siRNA transfected A375M supernatants following ultracentrifugation (n=3 biological repeats). No statically significant difference determined with unpaired students t test. 3 biological repeats. C. Individual results of 3 separate experiments D. *ROR2* mRNA expression for cells used in B.

6.4. Discussion

Experiments described here aimed to explore intermediaries that could account for the observed association of the $BRAF^{V600E}$ mutation, ROR2 and the secretion of VEGF.

6.4.1. HIF-1α

HIF-1α can be stabilised as a consequence of signalling downstream of $BRAF^{V600E}$ (Sang *et al.*, 2003; Kumar *et al.*, 2007) and furthermore has been reported to increase the expression of ROR2 (O'Connell *et al.*, 2013). HIF-1α was therefore considered a plausible intermediary between the $BRAF^{V600E}$ mutation and ROR2 expression. However, there was no evidence that HIF-1α protein was detectable in normoxia in the isogenic CHL1 clones despite the upregulation of ROR2 in the $BRAF^{V600E}$ mutant clones (figure 6-1). As ROR2 was upregulated in the $BRAF^{V600E}$ clones in normoxic conditions, this experiment was not performed in hypoxia.

This result contrasts with a report from Kumar et al, where $BRAF^{V600E}$ mutant WM793 melanoma cells expressed less HIF1α mRNA and protein after depletion of mutant BRAF in a stable model using RNA interference constructs. The investigators also demonstrated that transient transfection of $BRAF^{V600E}$ into two BRAF wildtype melanoma cells (WM3211 and Sbcl2) led to HIF-1α upregulation at the protein and mRNA level (Kumar *et al.*, 2007).

One mechanism through which $BRAF^{V600E}$ upregulates HIF1α is via an increase in ERK phosphorylation (Masoud *et al.*, 2015), which promotes 4E-BP1 phosphorylation that consequently increases HIF1α translation. It is possible that the acquired BRAF mutation in the isogenic model induced less MAPK activity and subsequent 4E-BP1 phosphorylation, possibly explaining the negative result.

Although $BRAF^{V600E}$ mutant isogenic clones did demonstrate constitutive MAPK activity (figure 4-10 C) the magnitude of signalling may have been less in comparison to a melanoma cell line with a driver BRAF mutation. Although Kumar et al challenged this possibility by demonstrating an increase in HIF-1α in a BRAF wildtype cell line transfected to overexpress mutant BRAF (Kumar *et al.*, 2007), transient transfection was used which is associated with greater off target effects compared to stable transfection (Rao *et al.*, 2009). D.Phil student Lina Guo also demonstrated ERK phosphorylation was higher in CHL1 cells transiently transfected to express mutant BRAF compared to the stable BRAF mutant isogenic clones suggesting that the transfection method may influence phenotype (L Guo DPhil thesis, 2019).

The basal level of HIF-1α expression in CHL1 may have been less than in the cell lines used by Kumar et al (Kumar *et al.*, 2007) , another possible reason for the negative result. If time permitted, HIF1α together with 4EB-P1 expression could have been tested in the CHL1 clones alongside those used by Kumar et al.

Kumar et al also (Kumar *et al.*, 2007) demonstrated an association between the $BRAF^{V600E}$ mutation and *HIF-1α* mRNA. As shown earlier, *HIF-1α* mRNA did not differ between $BRAF^{V600E}$ and wildtype isogenic clones (figure 4-6 A). Taken together, it is possible that the discrepancies between this work and that of Kumar et al relate to cell line differences, and further experiments are required before refuting an association between HIF-1α and the $BRAF^{V600E}$ mutation. Future experiments could test the effects of either pharmacological BRAF inhibition or mutant BRAF depletion on HIF-1α expression in $BRAF^{V600E}$ driven A375M and in and a broader range of melanoma cell lines with the driver $BRAF^{V600E}$ mutation.

ROR2 overexpression did not increase in hypoxia, which contradicts another report (O'Connell *et al.*, 2013). In this study, two melanoma cell lines UACC1273 ($BRAF^{V600E}$ mutant) and M93-047 (NRAS mutant, BRAF wildtype) upregulated both *ROR2* and *Wnt5a* in hypoxia and downregulated both genes following transfection with HIF-1α siRNA. ROR2 has also been associated with HIF-1α in RCC where ROR2 expression was dependent on the presence of inactivating mutation in the von Hippel-Lindau (*VHL*) tumour suppressor gene (Wright *et al.*, 2010). As HIF stabilisation is a well known consequence of the VHL mutation (Maxwell *et al.*, 1999), the investigators explored the role of both HIF-1α and HIF-2α revealing that ROR2 expression in RCC cell lines was dependent on HIF-2α stabilisation, furthermore, a HIF-2α binding site was identified on the ROR2 promoter. However, ROR2 expression was not upregulated in hypoxia, nor after chemical inhibition of prolyl hydroxylation activity despite activation of other well known HIF targets serving as positive controls (Wright *et al.*, 2010).

The results obtained here are partially consistent, and partially inconsistent with these published data. It is possible that HIF-2α may be a more potent driver of ROR2 expression and thus it may be informative to quantify its expression in the $BRAF^{V600E}$/wildtype isogenic melanoma cell line model. The lack of ROR2 transcript expression changes in response to hypoxia is consistent with the results from Wright et al (Wright *et al.*, 2010), could suggest that other factors than hypoxia may drive ROR2 expression. The fact that ROR2 expression in RCC was dependent on VHL status but not hypoxia suggest the influence of other factors promoted by the VHL oncogenic mutation which could include VHL mutation dependent transcriptional co-factors necessary to facilitate HIF2α mediated ROR2 transcription. It is noted that A375, the parental form of A375M, the cell line studied here, expresses wildtype

VHL (https://portals.broadinstitute.org/ccle). It is plausible that in the A375M cell line a metastatic subline, which has a similar genotype to A375P, ROR2 expression is under the influence of other factors acting independent of hypoxia.

Another argument against an association between HIF-1α and the $BRAF^{V600E}$ mutation is the fact that *VEGF* mRNA was not differentially expressed in the isogenic cell model nor the AVAST-M patient data set studied in chapter 2. As possibly the best described transcriptional target of HIF-1α stabilisation (Masoud *et al.*, 2015), *VEGF* mRNA would be expected to have been differentially expressed in the isogenic model if the $BRAF^{V600E}$ mutation had a direct stabilising effect on HIF1α.

Additionally, other HIF-1α target genes, *GLUT1* and *EGLN3* were not differentially expressed in the isogenic model, further arguing against direct regulation by $BRAF^{V600E}$ of HIF-1α expression.

Hypoxia for these experiments was defined by an oxygen concentration of 1%. Precise definitions of hypoxia within tumour cells remains elusive however data pooled from 18 melanoma patients reported median tumour oxygen concentrations of 1.5%, considerably lower that the figure of 40.5% recorded from adjacent non-malignant tissue. Intra-tumoural oxygen concentrations varied considerably however with values of less than 0.2% reported in lymph node metastases (Lartigau et al., 1997). Notwithstanding this variability, the 1% concentration used in figure 6.1 to mimic hypoxia approximated intra tumoural hypoxic conditions were within the published range and was unlikely to explain the discrepant results with those in the literature.

6.4.2. MMP2

The association between ROR2 and MMP2 was also explored. Overexpression of ROR2 has been shown to upregulate MMP2 in RCC and contribute to tumour growth, invasion and migration (Rasmussen *et al.*, 2014). MMP2 is reputed to increase VEGF secretion by ovarian cancer cells (Belotti *et al.*, 2003) and has been hypothesised to degrade HSPGs, for which VEGF has a binding site (Hawinkels *et al.*, 2008), therefore releasing VEGF in its secreted form. The association between ROR2 and MMP2 was therefore explored as a potential mechanism explaining ROR2 mediated increase in VEGF secretion. In A375M cells, ROR2 depletion decreased MMP2 expression (figure 6-3). Similar MMP2 downregulation was reported in ROR2 depleted RCC 786-0 cells (Wright *et al.*, 2009) and MMP2 and ROR2 were shown to be highly associated in RCC tumours (Rasmussen *et al.*, 2014). However, ROR2 overexpression in A375M cells did not upregulate MMP2 (Figure 6-5). A number of possibilities may explain these discrepancies. Firstly, MMP2 expression in the parental A375P melanoma cell line is higher than that reported for the renal cancer cell line 786-0 investigated by Rasmussen et al (https://portals.broadinstitute.org/ccle**).** It is possible that MMP2 transcription was already maximal in A375M cells and therefore further increases were not possible, regardless of stimulus. Alternatively, the decrease in MMP2 expression induced with ROR2 siRNA may have been an off-target effect therefore it would be important to test expression of MMP2 following transfection at least one other ROR2 siRNA. The effect of ROR2 overexpression on MMP2 expression in additional melanoma cell lines with varying levels of basal MMP2 expression could also be assessed. Despite the inconsistencies described above, ROR2 overexpression in A375M cells was associated with a significant increase in VEGF secretion (figure 5-14 A) without

a change in MMP2 transcription (figure 6-5), suggesting that MMP2 upregulation was unlikely to explain the link between MMP2 and VEGF secretion. However, attempts were made to manipulate MMP2 activity and test the effect on VEGF secretion. Treatment of A375M with MMP2 inhibition (figure 6-3) or recombinant MMP2 inhibitor (figure 6-4) did not affect the secretion of VEGF. MMP2 is a secreted endopeptidase that requires activation by proteolytic removal of an NH_2-terminal propeptide (Wright *et al.*, 2009). CT-1746 (N1- [2-(S)-(3,3-dimethylbutanamidyl)]-N4-hydroxy-2-(R)- [3-(4-chlorophenyl)-propyl]succinamide) is a gelatinase inhibitor with a demonstrated inhibitory effect against the activation of MMP2 and MMP9 (Kerkvliet *et al.*, 2003). MMP activity has been associated with pathological angiogenesis in ovarian cancer (Belotti *et al.*, 2003) and treatment of two ovarian cancer cell lines with recombinant MMP2 led to an increase in VEGF secretion into the conditioned medium, suggesting direct or indirect stimulation of VEGF or mobilisation of extracellularly stored VEGF.

In the current study, treatment of A375M cells with CT-1746 did not demonstrate an increase in VEGF secretion (figure 6-3) and recombinant MMP2 did not rescue a reduction in VEGF secretion induced by ROR2 depletion (figure 6-4). Recombinant MMP2 is inactive and requires activation by AMPA. APMA activates MMP2 by reacting with cysteine containing zinc-binding residues and consequently exposing MMP's active site (Sayre, 2005). In order to interpret the negative results of treating A375M cells with recombinant MMP2 or CT-1746 it would be necessary to confirm MMP2 activation or inhibition with zymography. Zymography, a functional assay that confirms activity of an enzyme by digestion of a detectable substrate impregnated into polyacrylamide gel (Leber *et al.*, 1997). In this specific case, MMP2 activity could have been tested by assessing digestion of gelatin in an impregnated Coomassie blue-stained gel, at an electrophoretic mobility corresponding with the known

molecular weight of MMP2. Due to time constraints, and the fact that MMP2 transcription did not increase in ROR2 overexpressing A375M cells, despite an obvious VEGF secretory phenotype, this experiment was not performed. Also, the effect of MMP2 inhibition was assessed in A375M cells which express low endogenous levels of ROR2 mRNA. The contribution of MMP2 towards total VEGF secretion may have been relatively minor, explaining the minimal effect of MMP2 inhibition with CT-1746. ROR2 overexpressing A375M cells, with an exaggerated secretory VEGF phenotype may have been a more appropriate cell line to treat with the MMP inhibitor even though MMP2 mRNA itself was not upregulated by ROR2 overexpression.

Taken together, the above data support the concept that ROR2 partially upregulates MMP2 although there is no evidence that MMP2 influences VEGF secretory phenotypes in ROR2 overexpressing cells.

6.4.3. Exosome secretion

The effect of ROR2 on VEGF-containing exosome secretion was also explored, based on previous data showing that the Wnt5a/ROR2 axis increases intracellular Ca^{2+} and the Rab GTPase Cdc42 (Dejmek *et al.*, 2006; O'Connell *et al.*, 2009). In melanoma cells, recombinant Wnt5a induces Cdc42 mediated F-actin re-organisation that resulted in secretion of VEGF containing exosomes, independent of changes in VEGF mRNA (Ekström *et al.*, 2014). This increase in VEGF secretion, without changes in VEGF mRNA paralleled the changes identified here. Therefore, the impact of ROR2 on exosome containing VEGF was explored by assessing the effect of manipulating ROR2 expression on total exosome secretion and on VEGF secretion.

However, nano particle tracking analysis did not identify any significant change in exosome secretion from the conditioned medium of the ROR2 overexpressing

A375M clones compared to control (figure 6-6 A). This result suggested that ROR2 did not have an effect upon global exosome secretion. This negative results contradicts previous results by Ekstom et al, where Wnt5a induced morphological changes and altered F-actin localisation of Mewo melanoma cells that was interpreted as an increase in exosome secretion (Ekström *et al.*, 2014). The data shown in figure 6-6 were derived by quantifying exosomes using a nanoparticle tracker analyser which identified exosomes on the basis of size. Nanoparticle tracking analysis (NTA) is a recent technology highly sensitive for vesicle detection (Dragovic *et al.*, 2011; Akbar *et al.*, 2017), and was selected after discussion with Naveed Akbar (Division of Cardiovascular Medicine, Radcliffe Department of Medicine) who has published on this method (Akbar *et al.*, 2017), therefore it is plausible that this is a more direct and sensitive assay compared to the method used Ekstrom et al who inferred that changes in cell morphology were surrogates for exosome secretion (Ekström *et al.*, 2014). Nanoparticle tracking analysis however is not without limitations. The technology detects particles as small as 50nm with reduced sensitivity for particles over 300nm (Dragovic *et al.*, 2011). With such high sensitivity, NTA lacks specificity, as it has the potential to detect other non-exosome particles such as protein complexes and lipoproteins (Lötvall *et al.*, 2014). The experiments above were conducted using exosome free FCS and simple single *in vitro* cell line experiments, as opposed to animal or human plasma samples, that possibly minimised the detection of non exosome particles, but this confounding factor cannot be excluded. Increased confidence in the assay could have been achieved by testing the ultracentrifuged pelleted material for exosome specific markers, CD91, CD63, and absence of markers known to associate with non-exosome particles, CANX and GM130, via flow cytometry or western blot (Lötvall *et al.*, 2014). Transmission electron microscopy could also have been used to verify the size of the particles in the ultra centrifuged

pellet and reconcile this against the data generated by the NTA. Lastly it would have been helpful to include a negative control NTA analysis of non-conditioned medium to identify background extracellular particles. For time and cost reasons these experiments were not performed. Despite the limitations NTA is reported to be a quantitative method to assess exosome secretion (Akbar *et al.*, 2017) and was probably more sensitive and more specific than the indirect measure used by Ekstom et al (Ekström *et al.*, 2014).

Attempts were made to quantify VEGF in the supernatant after clearing of particulate matter, including exosomes by ultracentrifugation. The aim was to test whether the changes in VEGF induced by ROR2 depletion represent changes in exosome bound or in solution VEGF. Although results varied between biological repeats, two of three repeats demonstrated that ROR2 depletion caused a decrease in secreted VEGF that remained in solution after ultracentrifugation (figure 6-6 C).

Ultra-centrifugation differentiates particles on the basis of physical properties and is influenced by variables including rotor speed, time and temperature (Cvjetkovic *et al.*, 2014). The protocol and centrifuge settings used for these experiments has previously been published as a suitable method for exosome separation (Dragovic *et al.*, 2011; Akbar *et al.*, 2017). Others have shown however that prolonged centrifugation times increase exosome yield, albeit at a cost of specificity due to the pelleting of non-exosome protein matter (Cvjetkovic *et al.*, 2014). It is possible that ultra-centrifugation did not pellet the all exosomes secreted by A375M in the experiments conducted here which contributed to the variable result. The initial results shown here favour the concept that VEGF was not present in exosomes but rather free in solution, given that 2 of 3 experiments showed the same reduction in VEGF in medium of ROR2 depleted cells as had been observed when assaying unprocessed conditioned medium (figure 6-6 C)

It would have been informative to quantify VEGF using ELISA in the ultra-centrifuged pellet as a reduction in the ROR2 depleted conditions would have supported the hypothesis that ROR2 influences secretion of exosome encapsulated VEGF. Although attempted, this experiment was unsuccessful.

Taken together, despite previous evidence, results presented here do not support the involvement of ROR2 in total exosome secretion or in exosome secretion of VEGF

7. Chapter VII: The effect of the BRAFV600E mutation on tumour and stromal gene expression, identification of genes responsive to treatment with bevacizumab and exploration of ROR2 as a biomarker for bevacizumab sensitivity in the AVAST-M clinical trial

The experiments in this chapter were part of a broader remit and involved the work of collaborators. To place the ROR2 in broader context as a potential biomarker for bevacizumab sensitivity, data from these experiments will be presented, albeit with a focus on ROR2.

7.1. In vivo model of BRAF^{V600E} and wildtype isogenic melanomas treated with bevacizumab

As previously shown in (figure 4-5), in the isogenic BRAF^{V600E} and wildtype model, clones with an acquired BRAF^{V600E} mutation secreted more VEGF into conditioned medium compared to wildtype. To investigate this effect *in vivo,* D.Phil candidate Lina Guo and Dr Esther Bridges (post-doctoral researcher, Professor Harris laboratory group, Department of Oncology, Oxford University) xenografted BRAF^{V600E} and wildtype isogenic clones into immunodeficient CD31 nude mouse models and investigated the effect of the BRAF mutation on bevacizumab sensitivity.

The original experimental design involved inoculating 40 mice with tumours, 10 with each clone: BRAF^{V600E} clone 1, BRAF^{V600E} clone 2, BRAF wildtype clone 1 and BRAF wildtype clone 2. However, there was extremely rapid tumour growth in mice injected with BRAF^{V600E} clone 2, requiring culling before treatment could be started. Therefore, the BRAF wildtype clone 1 was also culled so that the tumours could be compared, and the effect of bevacizumab was tested in the 20 remaining mice, which consisted of 10 mice injected with BRAF^{V600E} clone 1 and 10 with BRAF wildtype

clone 2 cells (Lina Guo, DPhil thesis, 2019). Half (five) mice in each group (figure 7-1) were treated with bevacizumab and the remainder with PBS.

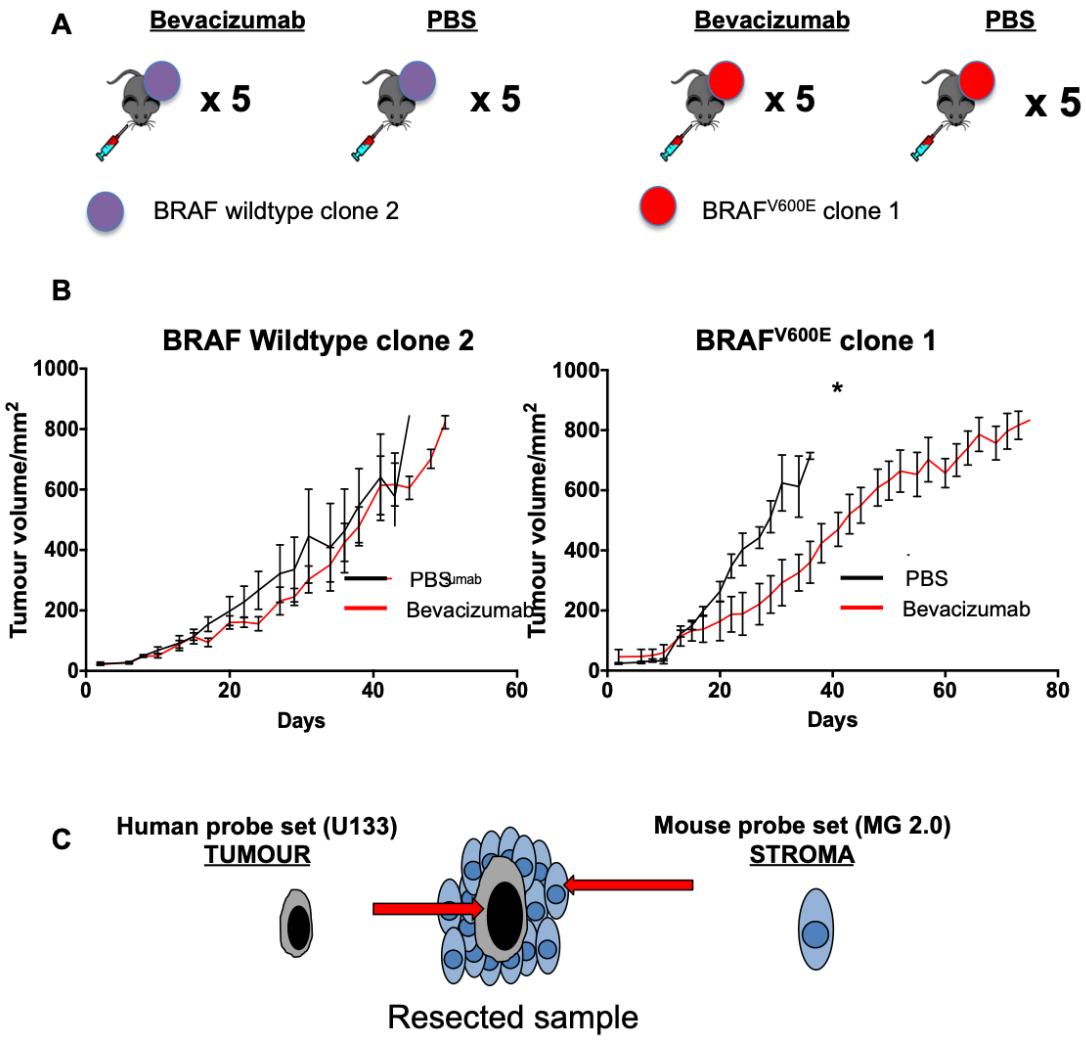

Figure 7-1: Investigating the effect of BRAF^{V600E} mutant/wildtype isogenic clones *in vivo*. A. BRAF wildtype clone 2 and BRAF^{V600E} clone 1 were xenografted in 10 mice each. Half of each group was treated with intra peritoneal bevacizumab (10mg/kg), the other half with equivalent volume of PBS for 3 times per week until tumour size had reached an endpoint of 1.44cm^2 surface area as permitted by the home office license (PPL30/3197). B. BRAF^{V600E} clone 2 was more sensitive to bevacizumab compared with BRAF wildtype clone 1. Data presented as mean tumour volume ± SEM. Statistics performed using two-way ANOVA. * = p<0.05. (Data generated by Lina Guo and Dr Esther Bridges) C. At sacrifice, tumour and surrounding stroma was resected. Gene expression was analysed using two separate platforms previously validated to differentiate tumour from stromal gene expression by exploiting species specificity

Results confirmed that the BRAF^{V600E} mutant xenograft was more sensitive to bevacizumab (figure 7-1 B) a finding that essentially recapitulated the findings of the

original AVAST-M clinical trial (figure 1-1). IHC analysis of the resected tumours after culling (performed by Dr Esther Bridges) showed increased CD31 positive blood vessels in the PBS treated $BRAF^{V600E}$ mutant clone 2 compared to BRAF wildtype 1. After treatment with bevacizumab, CD31 expression decreased in the $BRAF^{V600E}$ mutant clone and increased in the BRAF wildtype clone. Taken together this data supported the original hypothesis that the BRAF mutation was associated with increased angiogenesis and therefore more sensitive to the anti-VEGF effects of bevacizumab (Lina Guo, DPhil thesis, 2019).

7.2. Gene expression differences, in vivo, between $BRAF^{V600E}$ vs wildtype isogenic clones and surrounding stroma

To gain a greater understanding of transcriptional changes related to the phenotype observed above, gene expression was compared the xenografts treated with PBS and bevacizumab above. Gene expression was quantified in both tumour and stroma and used species specificity to differentiate between the two regions (figure 7-1 C). Lina Guo macroscopically resected tumours from the mice in the above experiment at the point of sacrifice and extracted and stored RNA.
I designed the gene expression analysis, sourced appropriate microarray platforms, co-ordinated logistics and analysed the data.

Human gene expression, representative of tumour cells, was assessed using the GeneChip® Human Genome U133 Plus 2.0 Arrays. The Affymetrix® mouse 4302 microarrays was used to quantify expression from stromal cells. Both platforms were selected based on data published by Professor Francesca Buffa's group (Dept of Oncology, Oxford University) that validated gene coverage and species specificity

(Masiero et al., 2013). Data analysis was performed by me using Transcriptome Analysis Console (TAC4.0).

Twenty RNA samples were available from this experiment of which 18 were suitable for analysis. These were 5 $BRAF^{V600E}$ mutant xenografts excised from mice treated with bevacizumab and 4 $BRAF^{V600E}$ mutant control xenografts (treated with PBS), 5 bevacizumab treated BRAF wildtype xenografts and 4 BRAF wildtype control treated xenografts. All RNAs underwent quality control and one control treated $BRAF^{V600E}$ and one control treated BRAF wildtype xenograft failed on account of unsatisfactory RNA integrity. One $BRAF^{V600E}$ mutant clone 2 and one BRAF wildtype clone 1 xenograft, both untreated, which were resected earlier due to rapid tumour growth, as explained earlier, were included in the control group to ensure even number between bevacizumab and control treated groups.

7.2.1. Differentially expressed genes between $BRAF^{V600E}$ vs wildtype melanomas

Differentially expressed human genes, representative of the $BRAF^{V600E}$ and wildtype melanomas are presented as a volcano plot in figure 7-2. There were 886 genes that were differentially expressed (defined by those genes with adjusted p-values of <0.05) and of these 210 genes were also differentially expressed in at least one of the data sets described in chapter 4 (tables 4-1, 4-3 and 4-4). ROR2 was significantly over expressed in the $BRAF^{V600E}$ mutant group as predicted from the earlier *in vitro* data. Pathway analysis (Genecodis) identified differentially expressed genes contained within VEGFA signalling pathways (figure 45 B). This identified 22 genes including 12 upregulated in the $BRAF^{V600E}$ tumours and 11 in the wildtype tumours that were

components of the VEGFA-VEGFR2 signalling pathway (table 7-1). Although ROR2 was differentially expressed in the $BRAF^{V600E}$ mutant tumours (log fold change 3.71, adjusted p-value p=0.0001), it is not a component of the Genecodis defined VEGF-VEGFR2 pathway, hence its omission from table 7-2. A list of the top 90 differentially expressed genes, in terms of ascending adjusted p-value, between the two tumour types is presented in table 7-1.

Gene Symbol	Fold Change	FDR P-val	Conc	Gene Symbol	Fold Change	FDR P-val	Conc	Gene Symbol	Fold Change	FDR P-val	Conc
XIST	169.81	6.63E-16		RAB31	5	2.7E-09	Yes	SEMA5A	-9.18	1.66E-08	
SALL3	16.23	1.41E-12		ZSCAN18	-8.8	2.9E-09	Yes	DCLK1	30.77	1.85E-08	Yes
PNMAL1	-17.27	5.21E-12		ABHD10	-3.32	3.86E-09	Yes	KBTBD7	11.75	2.13E-08	
FUCA2	-13.34	5.21E-12	Yes	TRIM6	7.39	3.91E-09		TNFSF8	-7.97	2.32E-08	Yes
ACOT9	-13.55	5.21E-12	Yes	MBNL3	-6.48	3.96E-09		SLN	-29.23	2.86E-08	Yes
STOM	-18.61	7.88E-12	Yes	MPPED2	22.04	4.24E-09		LYPD1	6.89	3.07E-08	Yes
SCML1	-28.74	7.88E-12	Yes	SORBS2	6.27	5.61E-09	Yes	IFI44	-9.51	3.13E-08	Yes
LOC283352	-21.32	1.98E-11		OPALIN	-8.66	5.7E-09		CAV1	-3.44	3.44E-08	
PBDC1	-20.46	3.57E-11		PEG10	-4.75	6.66E-09	Yes	FAM132B; HMGA1	3.46	3.47E-08	
TNS1	-9.35	8.63E-11		MAGEA10	18.12	6.75E-09		BMP8B	-2.89	3.65E-08	
OLFML2B	-9.81	8.63E-11	Yes	TSPAN13	5.66	6.87E-09	Yes	TTYH1	10.69	3.75E-08	Yes
C14orf169	-4.14	8.63E-11	Yes	MPC1	-2.56	6.87E-09		ZNF331	2.93	3.86E-08	
PCDHB6	31.56	1.01E-10		PLEKHB1	-3.42	7.16E-09	Yes	ADRB1	4.57	4.1E-08	
CRACR2A	-27.89	1.03E-10		C3orf70	-3.15	7.16E-09		EFNB3	2.52	4.2E-08	
DUSP23	-8.52	1.06E-10	Yes	MYO10	5.32	7.17E-09		AGMAT	4.62	4.26E-08	
VGF	6.27	1.81E-10	Yes	EDNRB	6.09	7.43E-09	Yes	POP1	-2.3	4.38E-08	
RAP1A	67.85	1.93E-10		CDH11	-5.62	7.7E-09		LOC441528	2.47	4.99E-08	
S100A4	-15.98	2.05E-10	Yes	MGAT4C	-26.96	8.47E-09	Yes	ELAVL3	-4.72	4.99E-08	
PLTP	4.51	2.92E-10		ARPP21	-8.8	8.47E-09		POPDC3	4.47	6.13E-08	
LOC101928100	-5.73	3.42E-10		AUTS2	5.39	8.63E-09	Yes	SDC1	2.62	8.03E-08	
KAZN	9.69	3.98E-10		PTPRK	3.71	8.94E-09		DYNC1I1	-2.93	0.0000001	
DOCK4	6.78	4.75E-10		TRIB2	3.63	9.96E-09		ITGA10	6.32	1.04E-07	
TMEM132D	11.83	5.97E-10	Yes	NELL1	18.59	1.03E-08		SIRT2	-3.34	1.17E-07	Yes
BMPR1B	-10.98	5.97E-10		ESRRG	-4.26	1.11E-08	Yes	HIST1H1C	3.56	1.18E-07	Yes
CXCR4	-13.54	1.04E-09		MATN3	4.58	1.16E-08		AREG	7.92	1.18E-07	
FEZ1	-5.59	1.49E-09	Yes	PRKCDBP	-3.71	1.22E-08	Yes	RAB7B	-3.21	1.38E-07	Yes
P2RX7	-7.16	2.01E-09		IL17RD	3.91	1.25E-08		ARSD	-3.02	1.38E-07	Yes
ODC1	4.06	2.01E-09	Yes	PSTPIP2	6.22	1.31E-08		PTGS2	16.39	1.41E-07	

Table 7-1: Top 90 differentially expressed genes between $BRAF^{V600E}$ and wildtype xenografted melanomas (ranked in order of ascending False Discovery Rate (FDR) adjusted p-value). Concordance (conc) also presented with genes differentially expressed in the $BRAF^{V600E}$/wildype isogenic cell line model (dataset 3)

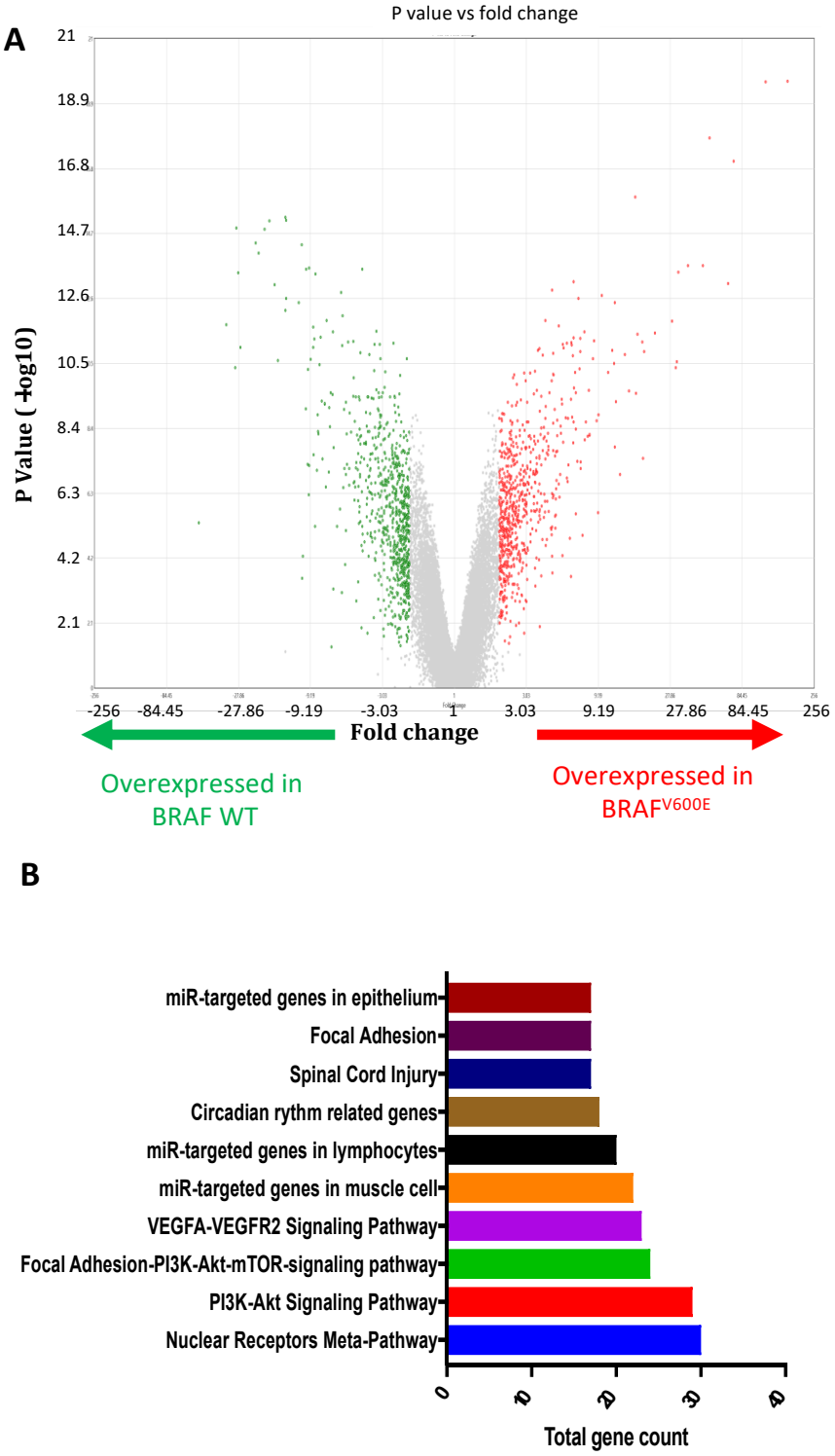

Figure 7-2: Human genes differentially expressed between BRAF^{V600E} vs wildtype melanomas A: volcano plot containing genes differentially expressed between BRAF^{V600E} and wildtype tumours (n=5 each group). B: Pathway analysis (Genecodis) on differentially expressed genes (defined by those with FDR adjusted p-values of <0.05).

Human genes upregulated in BRAF^{V600E} xenografts				
Gene symbol	**Name**	**Log fold change**	**Adjusted p value (FDR)**	**Angiogenic function**
ROCK2	Rho associated coiled-coil containing protein kinase 2	2	5.81E-07	Enhanced capillary network formation (Montalvo et al., 2013)
RAP1A	Ras-related protein Rap-1A	18.34	5.26E-06	Promotes VEGF-VEGFR2 kinase activation (Lakshmikanthan et al., 2011)
PTPRZ1	Receptor-type tyrosine-protein phosphatase zeta	3	2.27E-05	Ligand, PTN, promotes vascular abnormalisation in Glioma (Zhang et al., 2015)
ERN1	Endoplasmic reticulum–nuclei-1	2.18	2.12E-05	Promotes endoplasmic reticulum stress induced VEGF expression (Minchenko et al., 2012)
ANXA1	Annexin A1	2.95	4.13E-05	Vascular endothelial cell sprouting (Yi et al., 2009)
PTGS2	Prostaglandin-endoperoxide synthase 2 (COX-2)	16.39	1.41E-07	Induced in hypoxia and may enhance VEGF expression (Ben-Batalla et al., 2015)
EGR1	Early growth response-1	2.63	0.0117	Enhances VEGFA expression in lung cancer cells (Shimoyamada et al., 2010)
JAG1	Jagged 1	2.61	0.0002	Notch receptor ligand, implicated in endothelial stabilisation (Bellon et al., 2018)
PLAUR	Plasminogen Activator, Urokinase Receptor	6.89	3.07E-08	Mediator of VEGF induced endothelial cell migration (Alexander et al., 2012)
ACKR3	Atypical chemokine receptor 3	2.22	6.66E-05	Induces VEGF secretion and has an important role in endothelial tube formation (Qian et al., 2018)
GPC1	Heparan sulfate proteoglycan glypican-1	2.24	4.05E-05	GPC-1 silenced PANC-1 cells demonstrate decreased angiogenesis (Aikawa et al., 2008)
PGF	Placental growth factor	2.2	4.75E-05	Implicated in pathological retinal angiogenesis (Nguyen et al., 2018)

Human genes downregulated in BRAFV600E xenografts				
Gene symbol	**Name**	**Log fold change**	**Adjusted p value (FDR)**	**Angiogenic function**
SMARCA2	SWI/SNF related, matrix associated, actin dependent regulator of chromatin, subfamily a, member 2	-2.15	0.0026	Possible global transcription activator
PRKCB	Protein Kinase C Beta	-7.71	2.11E-07	Expression induced in response to VEGF (Al-Sanabra et al., 2017)
NRP1	Neuropillin 1	-3.24	0.0157	VEGFA Co-receptor (Kawamura et al., 2008)
TXNIP	Thioredoxin-interacting protein	-2.18	0.0016	Internalisation of VEGFR2 (Park et al., 2013)
RHOJ	Rho-related GTP-binding protein RhoJ	-2.12	0.0174	Modulates endothelial motility and tube formation in vitro (Shi et al., 2016)
TRPC1	Transient Receptor Potential Canonical 1	-2.03	0.0012	Required for VEGFA induced angiogenic phenotypes in zebrafish (Yu et al., 2010)
NFATC1	Nuclear factor of activated T-cells, cytoplasmic 1	-2.41	0.002	Transcription factor, mediates VEGF induced pulmonary endothelial cells (Johnson et al., 2003)
RCAN2	Regulator of calcineurin 2	-2.95	0.0004	Decreased in KRAS mutant colorectal cancer, supresses NFAT signalling (Yu et al., 2010)
ETS1	V-Ets Avian Erythroblastosis Virus E26 Oncogene Homolog 1	-2.14	0.0009	Master regulator of endothelial cell gene transcription. Binding motif present on the majority of transcriptional enhancers (Chen et al., 2017)
FLT1	Vascular endothelial cell receptor-1	-2.29	0.0073	Binds VEGFA with high affinity but reduced kinase activity aka VEGFA "trap" (Shibuya, 2011)

Table 7-2: Tumour derived human genes differentially expressed between BRAF^{V600E} and wildtype xenografts associating with the VEGF/VEGFR2 signalling pathway

ok

7.2.2. Comparison of stromal gene expression between BRAF^{V600E} and wildtype xenografts

In parallel with the above analysis, RNA from the resected tumours was further analysed using a mouse specific probe set (Mouse Genome 2.0), to investigate differences in the stromal gene expression between the BRAF^{V600E} mutant and wildtype xenografts. A volcano plot depicting differentially expressed genes is presented in figure 7-3 A. There were 111 genes that were differentially expressed within the stromal cells and of these 68 genes were overexpressed in the stroma of the BRAF^{V600E} melanomas and 43 genes were overexpressed in the stroma from the wildtype tumours. None of these genes were contained in the data sets described in chapter 4. Wnt5a, the ligand for the ROR2 receptor (O'connell *et al.*, 2010) was overexpressed in the BRAF^{V600E} mutant stroma and was the fifth most significantly differently expressed gene overall. No other Wnt related genes were differentially expressed. MMP9, referenced earlier as a potential mediator of VEGF secretion via HPSG cleavage (Belotti *et al.*, 2003) was upregulated in the stromal cells from the BRAF^{V600E} mutant melanomas and was the most significantly differentially expressed gene. MMPs 10 and 13 were also upregulated in the stroma of the BRAF^{V600E} mutant xenografts. None of the differentially expressed stromal genes were contained within the VEGF signalling pathways (figure 7-3 B).

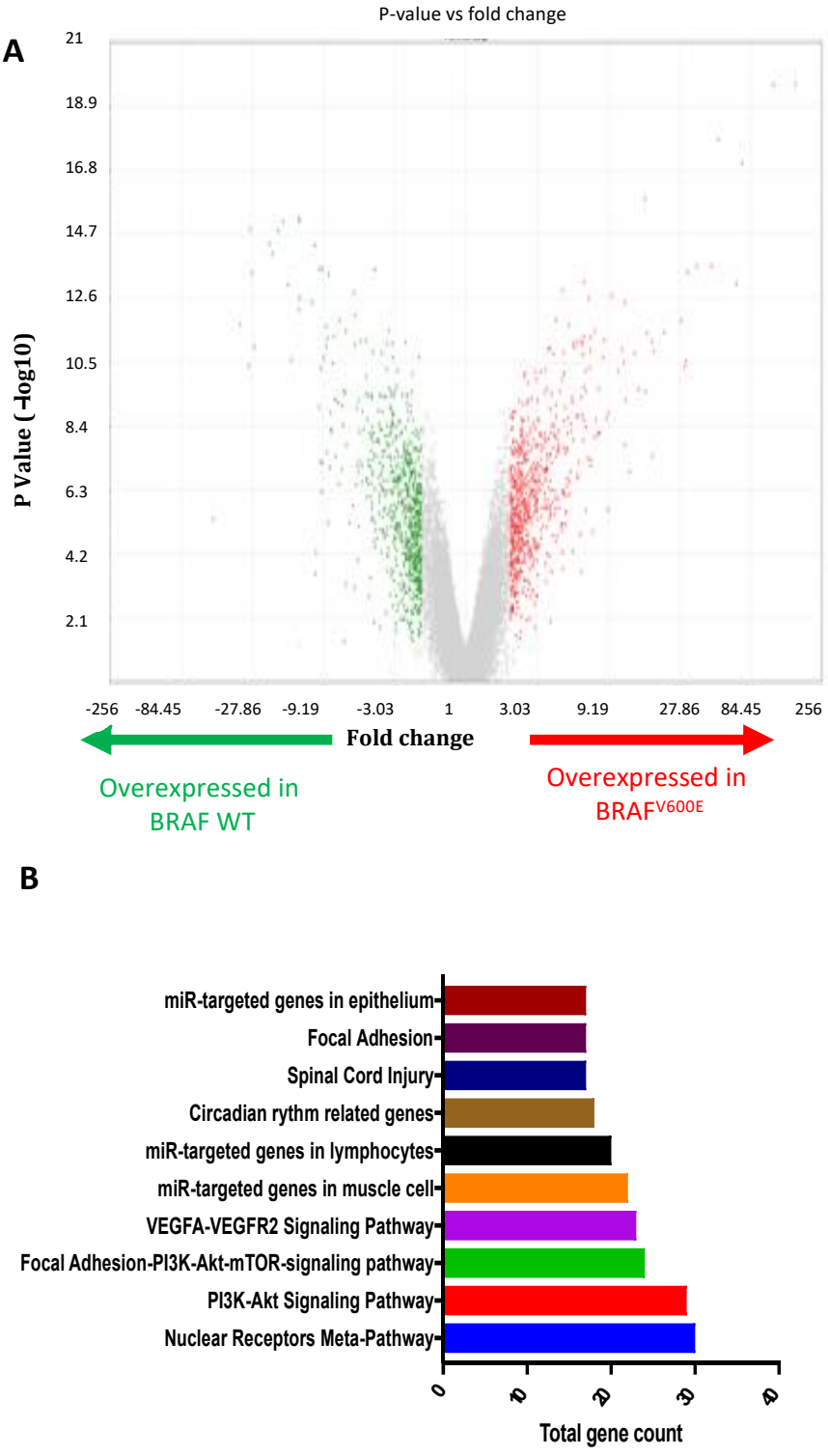

Figure 7-3: Genes differentially expressed within the stroma of BRAF^{V600E} vs wildtype xenografts (n=5 in each group). RNAs from the resected xenografts were analysed on a mouse specific microarray (mouse genome 2.0). Red dots refer to genes significantly upregulated in BRAF^{V600E} xenograft stroma and green dots refer to those genes upregulated in wildtype xenograft stoma B. Top 10 functional pathways represented by the differentially expressed genes (defined by those with FDR adjusted p-values of <0.05)

7.2.3. A comparison of bevacizumab regulated genes between BRAF^{V600E} mutant and wildtype human melanoma xenografts

The next analysis aimed to investigate the effects of bevacizumab in BRAF^{V600E} and wildtype xenografts. This was done to identify human genes upregulated or downregulated in the xenografts by comparing gene expression between bevacizumab and control conditions. BRAF^{V600E} and wildtype xenografts were analysed separately. Following treatment with bevacizumab, 26 genes in total that were altered in the BRAF^{V600E} mutant xenografts, 25 were upregulated and 1 was downregulated (figure 7-4 A). NRP1 and IGFBP7, both components of the VEGFA-VEGFR2 signalling pathway were upregulated by bevacizumab. Of the 26 total bevacizumab altered genes, 6 were contained within one of the data sets in chapter 4 (tables 4-1, 4-3 and 4-4). These were TFPI2, SLN, SEMA3a, CDH11,VCAN, LUM and were all upregulated by bevacizumab.

Within the wildtype xenografts, the expression of 7 genes was influenced by bevacizumab and 6 of these were upregulated. There were 2 genes present in one of the data sets from chapter 4: HTRA1 and CXCL2, both upregulated by bevacizumab. Immunoglobulin kappa chain complex (IgK) was downregulated over 13 fold in the bevacizumab treated cells relative to control. Pathway analysis of the differentially expressed genes implicated pathways as presented in figure 7-4. A single gene, RUNX2 (Runt related transcription factor 2) was present in 9 of the 10 pathways. Presenting the two groups of bevacizumab altered genes in BRAF^{V600E} and wildtype xenografts as a Venn diagram clarified that there were two distinct sets of bevacizumab influenced genes with no common genes deregulated by bevacizumab in

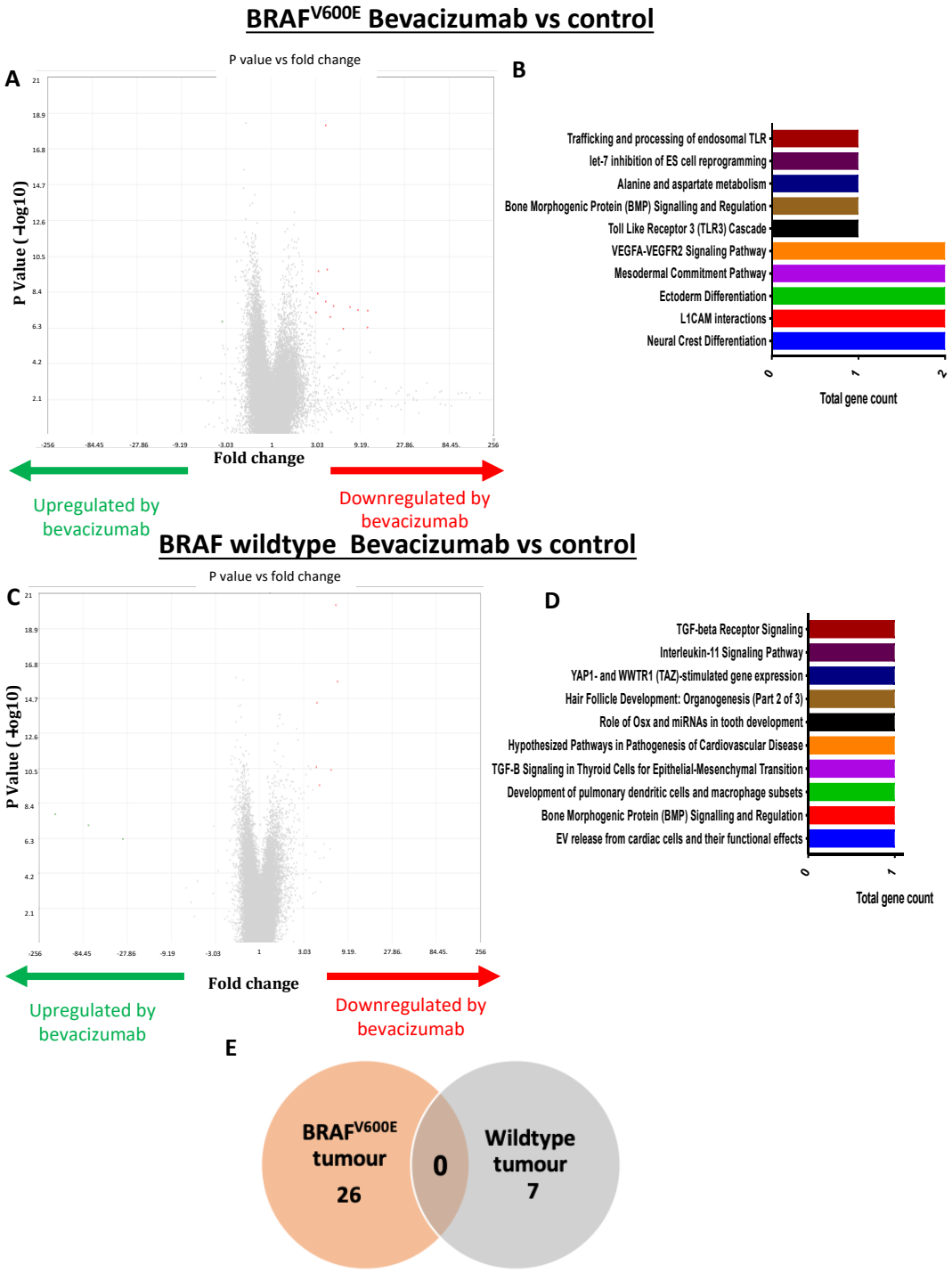

Figure 7-4: Tumour (human) derived genes differentially expressed in bevacizumab vs PBS control treated mice A. Volcano plot depicting genes differentially expressed in BRAF^{V600E} mutant xenografts (n=10) B. Pathway analysis of genes significantly differentially expressed C. Volcano plot depicting genes differentially expressed (p<0.05) in BRAF wildtype xenografts (n=10) D. Pathway analysis of significantly differentially expressed genes (defined by those with FDR adjusted p-values of <0.05) E. Venn diagram showing mutually exclusive bevacizumab deregulated genes between BRAF^{V600E} and wildtype xenografts

7.2.4. A comparison of stromal derived genes influenced by treatment with bevacizumab between BRAFV600E mutant and wildtype melanoma xenografts

The impact of bevacizumab on gene expression on murine stroma was next tested in the resected $BRAF^{V600E}$ mutant and wildtype xenografts. Within the stroma of the $BRAF^{V600E}$ xenograft stroma, 12 genes were altered in response to treatment with bevacizumab and 11 of these were upregulated. Pathway analysis indicated an absence of genes associated with VEGF signalling or angiogenesis relevant pathways (figure 7-5 A-B).

Within the stroma of the wild type xenografts, 19 genes were altered by bevacizumab and in contrast to the effect in the stroma from the $BRAF^{V600E}$ mutant xenograft, all but one of these genes were downregulated. Of the 19 bevacizumab influenced genes, 11 encoded for proteins involved in immunoglobulin synthesis. Pathway analysis again revealed an absence of known mediators of VEGF signalling or angiogenesis (figure 7-5 C-D). None of the stromal derived bevacizumab altered genes for either genotype were present in any datasets described in chapter 4 (tables 4-1, 4-4 and 4-5) A Venn diagram again indicated no overlap between genes differentially expressed in the stroma between $BRAF^{V600E}$ and wildtype samples (figure 7-5 E).

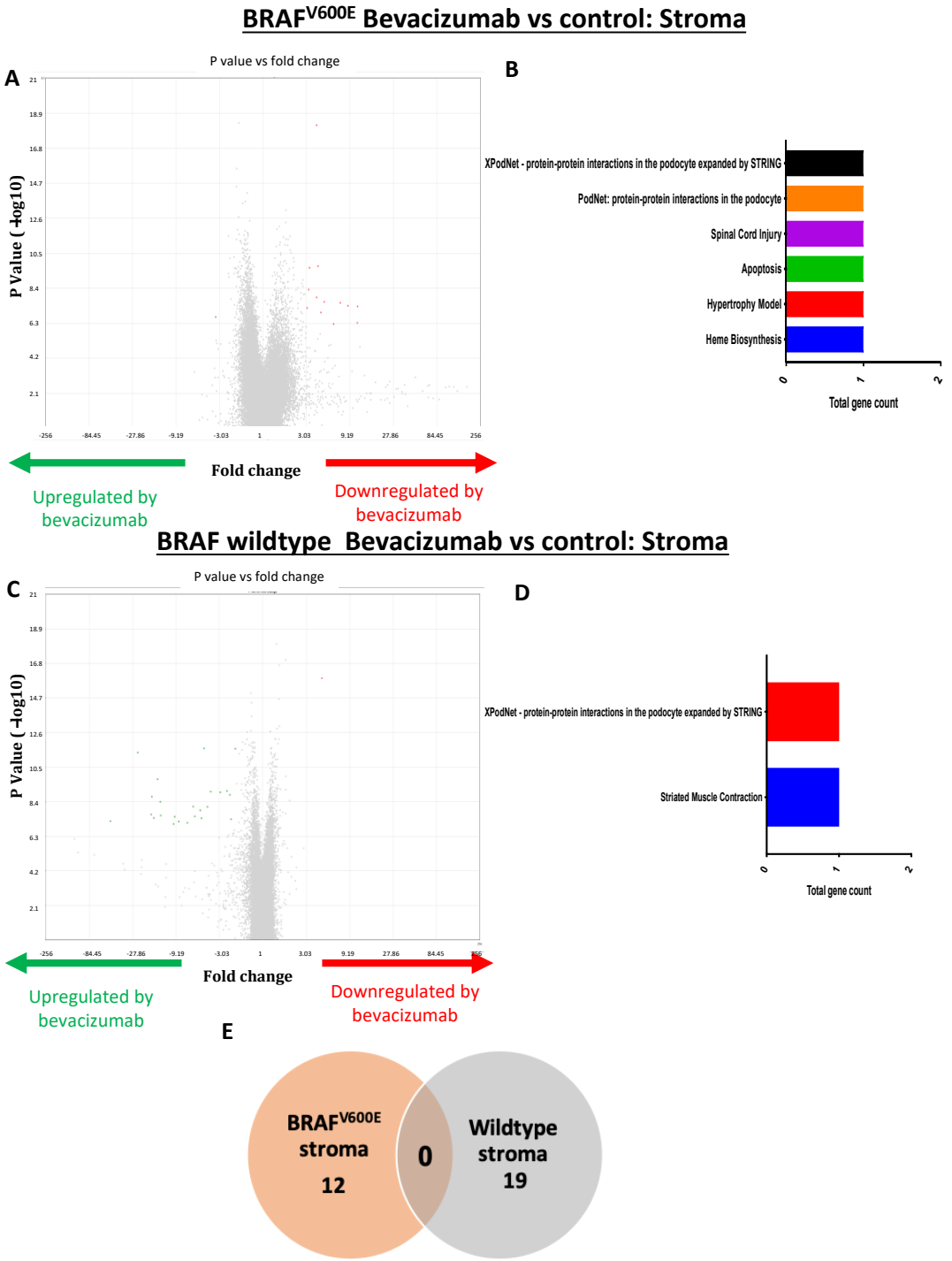

Figure 7-5: Stromal derived genes influenced by treatment with bevacizumab. RNA was analysed from the mouse derived stroma from resected xenografts. A. Representation of genes differentially expressed between bevacizumab vs control treated mice (n=10, 5 per group) in those mice xenografted with BRAF^{V600E} mutant melanomas. B. Pathway analysis of these differentially expressed genes (defined by those with FDR adjusted p-values of <0.05). C. Bevacizumab influenced genes in the stroma of mice xenografted with BRAF wildtype melanoma (defined by those with FDR adjusted p-values of <0.05) and pathway analysis of these genes (D.). E. Venn diagram depicting genes commonly and mutually exclusively differentially expressed between BRAF^{V600E} and wildtype stroma after treatment with bevacizumab vs control

7.3. Assessment of ROR2 as a predictive biomarker for bevacizumab sensitivity in patients recruited into the AVAST-M clinical trial

In vitro data presented earlier suggested that ROR2 influences the secretion of VEGF in $BRAF^{V600E}$ mutant melanoma cell lines. $BRAF^{V600E}$ mutant melanomas may therefore be increasingly dependent on VEGF expression for their survival and consequently more vulnerable to treatment with bevacizumab.

An exploration of ROR2 as a predictive biomarker for bevacizumab sensitivity in a clinical context was next performed by correlating ROR2 expression against clinical outcomes from the AVAST-M clinical trial (Corrie *et al.*, 2014). The statistics for this analysis were performed by Andrea Marshall, Principal Research Fellow in Medical Statistics, Warwick Clinical Trials Unit, Division of Health Sciences, University of Warwick. I initiated the concept for this experiment and defined the criteria for under and over expression or ROR2.

ROR2 expression data were available from 426 samples from 406 patients recruited to the AVAST-M clinical trial (19 patients provided 2 samples and 2 patients contributed 3 samples). For those patients supplying more than one sample, the ROR2 expression score was calculated as the average from all that patient's samples.

Of the 406 patients, 187 patients received bevacizumab and 219 were observed.

ROR2 gene expression scores for the 406 patients ranged from -3.37 to 3.01 with a median of -0.84 (inter-quartile range (IQR) -1.37 to -0.32) and was similar across the trial arms with a median of -0.86 (IQR -1.43 to -0.42) for the 187 patients on the Bevacizumab arm and median -0.78 (IQR -1.34 to -0.20) for the 219 patients on the observation arm.

ROR2 overexpression was defined as an expression score above the median value of -0.84. Using this value as a cut-off, 83 of the 187 (44%) on the bevacizumab arm overexpressed ROR2 and 110 of the 219 (50%) overexpressed ROR2 on the observation arm**.** There was no interaction between trial arm and degree of ROR2 expression (p=0.59).

For the entire population of 406 patients who had measurable ROR2 expression data, patients with bevacizumab had a superior disease-free survival compared to control HR 0.77 (0.59-0.99) p=0.04. This result was expected, given the AVAST-M interim result in all patients demonstrated a superior disease free survival for patients treated with bevacizumab (Corrie *et al.*, 2014).

For patients whose melanomas overexpressed ROR2 there was no difference in terms of disease-free survival in patients treated with bevacizumab compared to observation (HR 0.70 (0.48-1.03), p=0.07) (figure 7-6 C). Similarly, for those patients whose melanomas under-expressed ROR2 there was no significant impact from treatment with bevacizumab in terms of disease free survival (HR 0.82 (0.58-1.16), p=0.25) (figure 7-6 D). For patients in the observation arm, ROR2 overexpression did not influence disease free survival compared to under-expression (p=0.67).

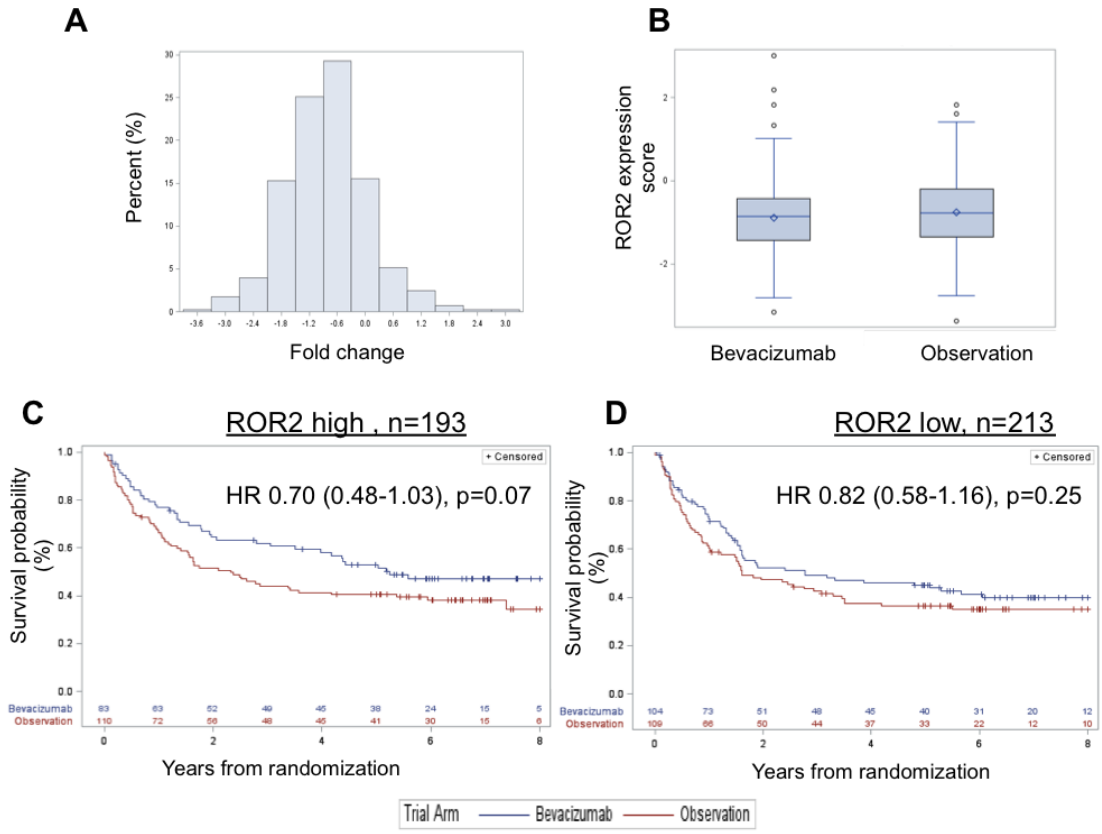

Figure 7-6: Exploration of ROR2 as a predictive biomarker for bevacizumab for patients recruited into the AVAST-M trial. ROR2 expression was available from 426 patient melanoma samples. A. Frequency histogram reflecting the distribution of ROR2 scores across the population where data was available B. ROR2 expression scores compared between the two treatment arms of the AVAST-M study. C. Kaplan Meier analysis comparing disease free survival in patients with ROR2"high" melanomas between those patients treated with bevacizumab vs observation. ROR2 "high" was defined as expression above the median value. D. Kaplan Meier analysis comparing disease free survival between the two treatment arms for those patients with ROR2 "low" melanomas. Figures and statistical analysis generated by Andrea Marshall.

7.4. Discussion

These above experiments assessed the impact of BRAF mutation status on gene expression within melanoma xenografts and stroma. The analysis also compared bevacizumab sensitive genes between the two genotypes, again within both the tumour and stroma. These experiments compared RNAs extracted from xenografts that previously demonstrated differences in bevacizumab sensitivity according to BRAF mutational status (figure 7-1 B). Therefore, differentially expressed genes were considered to mediate this response.

Over 800 genes were differentially expressed between the $BRAF^{V600E}$ mutant and wildtype tumours however only 210 were also differentially expressed between $BRAF^{V600E}$ mutant and wildtype melanomas cell lines. This, 676 genes were potentially altered in the isogenic cell model when grown *in vivo.* The reasons for this discrepancy suggest an interaction between the host and tumour. The tumour microenviroment plays an import role in the progression of malignancy. Signalling, via secretion of growth factors, proteases and cytokines from adjacent inflammatory cells, pericytes, fibroblasts and endothelial cells all impact on tumour progression (Hanahan *et al.*, 2018) and it is plausible that such interactions *in vivo* altered gene expression, potentially explaining the lack of concordance between this model and genes differentially expressed in the *in vitro* model of the same cell lines. Of the 810 differentially expressed genes within the tumours, 23 were involved in VEGF signalling (figure 7-2). This observation was expected given that the xenografts were the same isogenic $BRAF^{V600E}$/wildtype melanoma clones shown earlier to differentially express a number of genes relevant to the same signalling pathway

(figure 4-3). Of the 23 genes associated with VEGF/VEGFR2 signalling, 12 were upregulated and 11 were downregulated (table 7-1), suggesting that while the $BRAF^{V600E}$ mutation increased expression of some pro-angiogenic genes, it also downregulated others, possibly in compensation. Of the $BRAF^{V600E}$ upregulated genes, JAG1, FLT1 and PGF have well characterised angiogenic functions (table 7-1). JAG1 (fold change 3.28, adjusted p=9.86E-05) is a ligand for the Notch 1 receptor that antagonises Notch signalling via competitive inhibition of the canonical Notch 1 ligand, Dll4 Notch 1/Dll4 signalling in response to VEGFR2 activation promotes the formation of endothelial "stalk" cells, that support adjacent "tip" cells by providing structural integrity to sprouting blood vessels. Tip cells are endothelial cell phenotypes, negatively regulated by canonical notch signalling that are responsible for vascular sprouting during angiogenesis. JAG1 overexpressing endothelial cells develop excessive tip cell phenotypes and consequently highly prolific vascular sprouting (Benedito *et al.*, 2009). JAG1 upregulation in the $BRAF^{V600E}$ mutant xenografts may therefore have contributed to the relative abundant vascularity observed with IHC analysis of these tumours. Associations between the BRAF mutation and canonical Notch signalling have been reported. Maddodi et al showed that mutant BRAF overexpression in the 451Lu melanoma cell line decreased intracellular Notch cleavage and subsequent Notch activity (Maddodi *et al.*, 2010). JAG1 was not investigated as a possible mediator of this effect and remains an avenue for further investigation. Arguing against an association between JAG1 and the BRAF mutation, JAG1 was not differentially expressed any of the data sets described in chapter 4 (tables 4-1, 4-3 and 4-4). VEGFR1 (FLT1) (fold change 2.45, adjusted p=29E-07), upregulated in the $BRAF^{V600E}$ mutant xenografts is expressed in endothelial cells secondary to Notch1/Dll4 activity and supports "stalk" cell formation by inhibiting "tip" cell phenotypes (Blanco *et al.*, 2013). VEGFR1

upregulation in the $BRAF^{V600E}$ mutant xenografts may have reflected compensation due to excessive sprouting angiogenesis.

Placental growth factor (PGF) (fold change 2.17, adjusted p=3.00E-04), was also upregulated in the $BRAF^{V600E}$ tumours (table 7-1). PGF is a VEGF homologue and a potent inducer of angiogenesis (Pipp *et al.*, 2003). To date an association between oncogenic BRAF and PGF expression has not been described. Despite its angiogenic associations, PGF has been reported as a negative predictive biomarker for anti-VEGF directed therapy, possibly due to compensatory PGF-VEGFR1 pro angiogenic signalling (Natsume *et al.*, 2019) as an adaptive compensatory mechanism (Lebellec *et al.*, 2018). These reports however refer to secreted PGF, and the impact of increased PGF mRNA expression remains unknown.

Neuropillin 1 (NRP1) (-3.24 fold change, adjusted p=0.0157), a co-receptor for VEGFA (Kawamura *et al.*, 2008) was downregulated in the $BRAF^{V600E}$ mutant xenografts. It was also downregulated in the isogenic $BRAF^{V600E}$/Wildtype melanoma model described in chapter 4 (table 4-4) however not differentially expressed in the AVAST-M data set (table 4-1) and was upregulated in the TCGA data set (table 4-3). NRP1 expression typically increases with VEGF expression, to enhance angiogenesis. The unexpected downregulation in NRP1 seen in these experiments may reflect physiological attempts to achieve equilibrium in the face of an oncogenic driven angiogenesis process. Although implicated in BRAF inhibitor resistance in melanoma (Graziani *et al.*, 2015), NRP1 expression has not been previously associated with the oncogenic $BRAF^{V600E}$ mutation. Appreciating the inconsistent expression of NRP1 in the data sets studied earlier, further experiments are required to validate differential expression.

The analysis of stromal derived genes from the resected xenografts revealed 107

differentially expressed genes between $BRAF^{V600E}$ and wildtype samples (figure 7-3). Whilst the total number of stroma-derived differentially expressed genes was fewer than those differentially expressed by tumour cells, these data demonstrated that BRAF mutational status has an impact on the adjacent microenvironment. Unlike the differentially expressed genes originating from the tumours, VEGFA/VEGFR2 signalling pathway related genes were not represented in this compartment (figure 7-3 B). Wnt5a, the ligand for ROR2 and referred to earlier in chapter 5, was one of the most upregulated genes in the $BRAF^{V600E}$ stroma. As ROR2 was also a $BRAF^{V600E}$ upregulated gene within the tumour, $BRAF^{V600E}$ mediated ROR2-Wnt5a axis activity due to tumour and stromal co-operation could plausibly have contributed to the angiogenic phenotypes seen the $BRAF^{V600E}$ mutant xenografts. This novel observation warrants further exploration. For example, xenotransplantation of the same isogenic $BRAF^{V600E}$/wildtype melanoma clones into commercially available inducible Wnt5a knockout mice (as $Wnt5a^{-/-}$ mice uniformly incur perinatal mortality (Sato *et al.*, 2015)) would help ascertain the necessity of stroma derived Wnt5a in the angiogenic phenotype associated with $BRAF^{V600E}$ xenografts.

Matrix Metalloproteinases (MMPs) were also upregulated in the $BRAF^{V600E}$ mutant stroma. MMP's, discussed in chapter 4, cleave HSPG bound VEGF as a means to readily increase VEGF secretion, raising the possibility of another stromal-tumour interaction potentially promoting angiogenesis in the $BRAF^{V600E}$ mutant isogenic clones.

Within both the tumour and stroma there were no genes affected by bevacizumab in common between $BRAF^{V600E}$ mutant and wildtype xenografts (figures 7-4 and 7-5). This observation has not been reported previously and supports the hypothesis the impact of bevacizumab on melanoma may be influenced by BRAF genotype.

Of the bevacizumab sensitive genes from both stroma and tumour compartments, only NRP2 and IGFBP7 were relevant to angiogenesis/VEGF signalling. Both these genes were upregulated in BRAF mutant tumours in response to bevacizumab (figure 7-4). Increased NRP2 mRNA expression in response to bevacizumab has previously been reported in colorectal cancer cells and may represent an alternative escape pathway in response to VEGF neutralisation (Xu *et al.,* 2009). The Neuropilins, NRP1 and NRP2 are receptors for a broad range of ligands in addition to VEGF binding, including transforming growth factor β1 (TGFβ1), Hepatocyte growth factor 1 (HGF), PDGF and fibroblast growth factor (FGF) (Prud'homme *et al.*, 2012). Therefore it is plausible that the effect of bevacizumab in $BRAF^{V600E}$ mutant melanomas may impact upon a wider range of biological functions distinct from those observed in wildtype melanomas.

Semaphorin 3A (SEMA3A) was also uniquely upregulated in the $BRAF^{V600E}$ mutant tumours in response to bevacizumab. SEMA3A, a secreted protein is described as a potent inducer of vascular permeability and also has a possible role in bevacizumab resistance (Acevedo *et al.*, 2008). The upregulation of both NRP2 and SEMA3A in $BRAF^{V600E}$ mutant isogenic clones in response to bevacizumab may suggest two novel adaptive mechanisms unique to this genotype.

Runt related transcription factor 2 (RUNX2), upregulated in response to bevacizumab in the wildtype isogenic xenografts. RUNX2 is a transcription factor shown to increase proliferation and migration in melanoma cell lines (Boregowda *et al.*, 2014). RUNX2 also influences HIF-1α mediated VEGF vascularisation in bone (Kwon *et al.*, 2011). RUNX2 upregulation in the BRAF wildtype cells may be another compensatory mechanism to VEGF neutralisation determined by BRAF mutation status.

Analysis of stroma derived genes influenced by bevacizumab again revealed a distinct set of mutually exclusive genes between $BRAF^{V600E}$ and wildtype samples (figure 7-5). The absolute number of genes was small, and none of the affected genes for either genotype were associated with putative VEGF signalling or angiogenesis pathways. Notably, genes involved in immunoglobin synthesis were downregulated in the bevacizumab treated BRAF wildtype stroma raising the possibility of an immunomodulatory role for the drug in this genotype. VEGF suppresses T-Cell infiltration *in vivo* (Huang *et al.*, 2015) and stromal derived VEGF upregulates inhibitory immune checkpoints in tumours that promotes T-cell exhaustion (Voron *et al.*, 2015) . The clinical relevance of bevacizumab and immune checkpoint inhibition is under investigation and numerous clinical trials are currently recruiting (www.clinicaltrials.gov) for patients with gliomas, ovarian, urothelial, melanoma and lung cancer. None of these clinical trials are investigating the BRAF mutation as a predictive biomarker.

Taken together, the effects of bevacizumab on the tumour associated stroma in these experiments were influenced by BRAF status. Further analysis is required to determine any therapeutic value of these observations. In the first instance, repeating the experiment described in section 5.3 in knockout murine models unable to express candidate genes may implicate these stroma-expressed genes as mediators of bevacizumab sensitivity. Additionally, the differential expression of stroma genes identified above could be tested in mice engrafted with a broader range of BRAF mutant and wildtype cell lines to clarify if results are not specific to the isogenic cell line xenografts.

ROR2 was also assessed as a predictive biomarker for bevacizumab response for AVAST-M trial patients. Using an arbitrarily defined cut-off point based on the

median expression value, patients whose melanomas had high ROR2 expression and were randomised to treatment with bevacizumab trended, but did not have a significantly different disease-free survival interval compared to those within the observation arm (HR 0.70 (0.48-1.03), p=0.07) (figure 7-6 C). Similarly, patients with low ROR2 expressing melanomas derived no benefit from bevacizumab (HR 0.82 (0.58-1.16), p=0.25) (figure 7-6 D). Greater patient numbers are required to establish if ROR2 expression is a clinically useful predictor of increased sensitivity to bevacizumab.

Although ROR2 has not previously been assessed as a predictive biomarker for bevacizumab sensitivity a number of studies however have defined ROR2 as an adverse prognostic biomarker in range of tumour types including renal cell cancer (Rasmussen *et al.*, 2014), sarcoma (Edris *et al.*, 2012) and colorectal cancer (Mei *et al.*, 2014). Such clinical observations are unsurprising appreciating the aggressive phenotypes associated with ROR2 *in vitro* (O'Connell *et al.*, 2010; Rasmussen *et al.*, 2014). Such negative outcomes, as mentioned already in this thesis, imply that ROR2 expression contributes to the "hallmarks of malignancy" (Hanahan *et al.*, 2018), of which angiogenesis is a well described component. In the data presented here, ROR2 expression above and below the median value cut-off in patients in the observation arm was not associated with changes in disease free survival (p=0.67) This result contrasted with those described above in other tumour types and may reflect that ROR2 is not prognostic in melanoma.

Although not reported as a specific predictive biomarker for bevacizumab monotherapy, ROR2 expression was one of a collection of differentially expressed genes shown to predict tumour shrinkage at 12 weeks in patients with metastatic non small cell lung cancer treated with bevacizumab plus EGFR inhibitor, erlotinib (Baty *et al.*, 2017). Despite the effects on tumour shrinkage, ROR2 expression was not

associated with overall survival.

There is also *in vitro* evidence linking Wnt signalling with sensitivity to bevacizumab. Huang et al reported that decreased canonical Wnt signalling, via the transcriptional repressor BATF2 induced an EMT phenotype in bevacizumab treated U87MG glioblastoma cell line, which predicted for resistance (Huang *et al.*, 2017). As an inhibitor of canonical Wnt signalling in melanoma (Webster *et al.*, 2015), ROR2 expression could theoretically enhance bevacizumab sensitivity through a related mechanism, although this effect has not been demonstrated in any clinical data nor any melanoma specific context.

It is plausible that other genes differentially expressed between the $BRAF^{V600E}$ and wildtype xenografts may be predictive biomarkers for response to bevacizumab. PLAUR, (urokinase type plasminogen activator) upregulated in the $BRAF^{V600E}$ mutant xenograft melanoma cells (table 7-1), was quantified in tumour samples from a 35 patient phase II clinical trial of patients with metastatic melanoma treated with bevacizumab monotherapy. Elevated PLAUR expression in metastatic deposits was significantly associated with an objective response (p=0.003). Furthermore, PLAUR expression was positively associated with markers of activated angiogenesis, including proliferating vessels and glomeruleroid microvascular proliferations (Schuster *et al.*, 2018). A similar phenotype, CD31 positivity was identified in the $BRAF^{V600E}$ mutant xenografts above and PLAUR upregulation remains another plausible possibility for this effect. Secondly, single nucleotide polymorphisms of FLT-1 (VEGFR-1) , the VEGF "trap", which was downregulated in $BRAF^{V600E}$ mutant xenografts (table 7-1) has been associated an increased overall survival in patients with advanced colorectal cancer treated with bevacizumab plus chemotherapy (Rodriguez-Pascual *et al.*, 2017). Finally, placental growth factor (PGF) was

upregulated in $BRAF^{V600E}$ mutant xenografts and is a ligand of VEGFR-1 (Simons *et al.*, 2016). Although VEGFR-1 is classically anti-angiogenic, PGF binds VEGFR1 with high affinity and displaces VEGFA, which increases the VEGF-A available to bind to VEGFR2 (Kut *et al.*, 2007). PGF has been evaluated as a predictive biomarker for bevacizumab sensitivity. Increases in PGF following bevacizumab treatment have been associated with improved clinical outcome for patient with advanced rectal cancer (Rodriguez-Pascual *et al.*, 2017) however in contrast, PGF predicted a reduced progression free survival in patients with angiosarcoma treated with chemotherapy and bevacizumab, possibly functioning as an angiogenic escape mechanism following VEGF inhibition (Lebellec *et al.*, 2018). PGF secretion has been shown to increase in melanoma patients treated with bevacizumab, although its predictive value was not assessed (Pagani *et al.*, 2016).

In the current study there was no definitive evidence supporting a ROR2 as a predictive biomarker for adjuvant bevacizumab for patients with high risk melanoma (HR 0.70 (0.48-1.03), p=0.07, figure 7-6**)**. The findings reported here suggest that although ROR2 may have a role in the secretion of VEGF, as its interrogation at the *in vitro* level demonstrated, as single gene, ROR2 is very unlikely to completely control the clinically relevant angiogenic process, which is influenced by a complex set of additional variables including VEGF polymorphisms, co-factor expression and compensatory escape mechanisms (Ferrara and Adamis, 2016). The complex regulation of angiogenesis has been highlighted by the fact that despite much investment in the search for a predictive biomarker for bevacizumab across multiple tumour types, a definitively clinically relevant marker thus far remains elusive (Ferrara, 2017). Although of limited value as a stand-alone biomarker, ROR2 may also have a role as part of predictive signature for bevacizumab sensitivity in

combination with the multitude of other markers that have shown partial predictive ability including, for example and not limited to: hypertension, changes in Dynamic Contrast enhanced Magnetic Resonance Imaging, Epidermal Growth Factor (EGF) and interleukin 8 expression (Rodriguez-Pascual *et al.*, 2017).

For the work presented in this study, ROR2 expression was tested largely on primary melanomas. As ROR2 expression is higher in a metastatic melanoma versus a primary melanoma (O'Connell *et al.*, 2010), the assessment of ROR2 as predictive biomarker in the metastatic context may yield results with increased clinical significance.

Independent of any role as a predictive biomarker ROR2 clearly mediates aggressive phenotypes in melanoma and therefore pharmacological inhibition of ROR2 as a treatment strategy has clinically relevant potential. CAB-ROR2-ABC (referred to as BA3021) is an antibody-drug conjugate recently developed that has shown anti-tumour activity *in vitro,* in a cell line panel including the melanoma cell line SKMEL-5 (Sharp *et al.*, 2018). BA3021 is currently under evaluation in a Phase 1 clinical trial for patients with advanced solid tumours (clinicaltrials.gov identifier: NCT03504488). The data presented in this study suggest that stratifying by BRAF status or refining the patient population to those with $BRAF^{V600E}$ mutant melanoma may identify a population more likely to benefit.

8. Conclusions, summary and future directions

The AVAST-M clinical trial compared adjuvant bevacizumab to observation, the standard of care at the time, for patients with high risk melanoma. The interim results, published in 2014, reported increased benefit from bevacizumab in patients whose melanomas harboured a $BRAF^{V600}$ mutation (Corrie *et al.*, 2014). This result highlighted a previously unreported association between the BRAF mutation and sensitivity to bevacizumab. Although in the updated analysis, however, the improvement in disease free survival associated with bevacizumab treatment in the BRAF mutant patient group was no longer statistically significant (Corrie *et al.*, 2018) suggesting that over the longer term, additional, potentially compensatory mechanisms may mitigate the benefit demonstrated in the earlier interim analysis.
The work presented in this thesis has been aimed at understanding the molecular basis behind the differential sensitivity of $BRAF^{V600E}$ mutant melanomas to VEGF inhibition.
The project hypothesised that $BRAF^{V600E}$ mutant melanomas express more VEGF compared to wildtype and are therefore more vulnerable to anti-VEGF treatments. In the first results chapter (Chapter 3), this question was addressed by evaluating VEGF expression via IHC in patient samples from the AVAST-M trial. Contrary to the hypothesis, BRAF mutant samples did not express more VEGF using a semi-quantitative score. Conclusions regarding the assessment of the whole mount sections were limited due to the small number of samples that were available for assessment. Similarly, the assessment VEGF expression in the TMA's was also potentially limited due to sampling error and sample quality. Undertaking VEGF quantification in a larger number of whole mounts may be informative. CD31, a marker specific for

blood vessels (and by extension, angiogenesis) was also assessed in AVAST-M patients samples using automated quantification. In parallel with the VEGF results, no significant differences in CD31 expression existed between BRAF mutant and wildtype tumours. Again, based on the limitations described above when assessing VEGF, testing more whole mounts will be required for a definitive assessment.

In chapter 4, three independent data sets (2 from patient samples, 1 from cell lines) were interrogated for genes differentially expressed between $BRAF^{V600E}$ and wildtype melanomas that confer angiogenic phenotypes or influence VEGF expression. Pathway analysis of differentially expressed genes in all data sets identified substantial representation of genes involved in angiogenesis signalling pathways. Many differentially expressed genes were also elements of Wnt signalling, although both canonical and non-canonical pathways were represented. In the AVAST-M and TCGA data sets, the $BRAF^{V600E}$ mutation induced expression profiles associated with invasive, poorly differentiated and EMT-like phenotypes: *ZEB1* and *SNAI1* were upregulated, *MITF*, *ZEB2* and *PMEL* were downregulated. Although the BRAF mutation is known to drive such phenotypes (Caramel *et al.*, 2013), this association has not been previously reported in clinical samples. Of note, none of these genes were significantly altered in the $BRAF^{V600E}$/wildtype model, created by D Phil student Lina Guo and used in this project. Of particular importance, the $BRAF^{V600E}$ mutant clones in this model secreted more VEGF in the absence of changes at the mRNA level, the first indication that oncogenic BRAF may impact upon VEGF expression post-transcription.

Only 8 genes were differentially expressed in all three data sets. ROR2 was chosen for further interrogation based on known associations with a number of hallmarks of malignancy (Hanahan *et al.*, 2018) and the striking pattern of differential expression in the isogenic clones. Differential expression of ROR2 was validated in the isogenic

model and further experiments demonstrated reduced expression in two $BRAF^{V600E}$ cell lines with $BRAF^{V600E}$ and MEK inhibition, supporting a strong link between ROR2 expression and constitutive activation of the MAPK axis. ROR2 expression in a panel of in-house $BRAF^{V600E}$ and wildtype melanoma cell lines was highly variable and differential expression was not reproduced. Further experiments with a larger panel may provide further clarification.

Phenotypes associated with the expression of ROR2 were explored in chapter 5. ROR2 depletion in $BRAF^{V600E}$ mutant melanoma cell lines was associated with reduced proliferative and invasive phenotypes, consistent with reports on other tumour types in the literature. A lesser phenotype was present in the BRAF wildtype clone tested in parallel, this was possibly attributable to less effective gene silencing. ROR2 depletion in a panel of 4 melanoma cell lines significantly reduced VEGF secretion in the 3 $BRAF^{V600E}$ mutant cell lines tested without any comparable effect in a BRAF wildtype clone tested in parallel. VEGF secretion after ROR2 depletion in an $BRAF^{V600E}$ mutant isogenic clone was similar to that of a control siRNA transfected wildtype clone, suggesting that differences in VEGF secretion between $BRAF^{V600E}$ mutant and wildtype clones may be attributable to ROR2. ROR2 depletion in the same cell lines did not have a consistent effect upon *VEGF* mRNA. Complementing the result observed with ROR2 siRNA, ROR2 overexpression in A375M cells increased VEGF secretion, in the absence of changes at the mRNA level. ROR2 overexpression had no effect on VEGF secretion in CHL1, a BRAF wildtype melanoma cell line. This was hypothesised to relate to the very low level of *Wnt5a* expression in CHL1. Pharmacological MEK inhibition in ROR2 overexpressing A375M clones unexpectedly reduced VEGF secretion, in the absence of changes of constitutively expressed ROR2. A reduction in *Wnt5a* expression was hypothesised drive this phenotype and indeed, this was demonstrated. This result raised the

possibility that not only ROR2, but its ligand, Wnt5a are regulated by the MAPK pathway and both are required for a VEGF secretory phenotype.

In chapter 6, intermediaries between $BRAF^{V600E}$, ROR2 and VEGF were investigated. HIF-1α was considered very relevant, as the $BRAF^{V600E}$ mutation is known to increase its stability (Kumar *et al.*, 2007), and it has been shown to drive ROR2 expression in hypoxia (O'Connell *et al.*, 2013). Contradicting these data, HIF-1α was not stabilised in the $BRAF^{V600E}$ mutant isogenic clones, nor was ROR2 expression increased in A375M cells cultured in hypoxia. This result was consistent with the lack of HIF-1α target genes (*VEGF, GLUT1* and *EGLN)* upregulated in $BRAF^{V600E}$ mutant isogenic clones in the data set presented in chapter 4 and supports an argument that $BRAF^{V600E}$ driven VEGF secretory phenotypes may be HIF-1α independent. MMPs were hypothesised to promote VEGF release into the conditioned medium in the context of ROR2 expression. In parallel with results in RCC (Rasmussen *et al.*, 2014), ROR2 depletion reduced MMP2 expression in A375M however in further experiments, pharmacological MMP2 inhibition or recombinant MMP2 did not alter VEGF expression in the conditioned medium. As an exploratory investigation, secreted VEGF associated with ROR2 overexpression was not contained with exosomes.

In chapter 7, the effect of $BRAF^{V600E}$ on gene expression in both the tumour and microenvironment was investigated. Separate work by Lina Guo and Dr Esther Bridges confirmed that the $BRAF^{V600E}$ mutant isogenic clone xenografts, *in vivo*, were more sensitive to bevacizumab, essentially reproducing the effect described in the interim analysis of the AVAST-M clinical trial (Corrie *et al.*, 2014). As expected, the $BRAF^{V600E}$ impacted on the expression of 1329 genes, 22 of which were involved in VEGF/VEGFR2 signalling. Within the stroma, Wnt5a and MMPs 9, 10 and 13 were

upregulated in the mutant clones. This result, coupled with ROR2 overexpression in the melanoma raised the possibility of a tumour-stromal interaction driving VEGF expression. Bevacizumab treatment resulted in mutually exclusive gene expression changes between $BRAF^{V600E}$ mutant and wildtype melanomas in both tumour and stroma. These data may reflect genotype specific targets for bevacizumab or compensatory mechanisms. This analysis was largely exploratory and provides an insight to the broader gene expression changes associated with oncogenic $BRAF^{V600E}$. The data provides a source for innumerable further projects to investigate further associations between $BRAF^{V600E}$ and bevacizumab sensitivity.

ROR2 was finally evaluated as a predictive biomarker for bevacizumab sensitivity in the AVAST-M trial (Corrie *et al.*, 2014). Patients expressing ROR2 above the median value trended towards a superior disease-free survival in contrast to those with values below the median. Although far from definitive, and based on data at the interim analysis cut-off, this result supports the *in vitro* work presented earlier and suggests ROR2 tumours have also have an increased sensitivity to anti-VEGF treatments. Repeating the analysis on additional samples and using the updated clinical trial data (Corrie *et al.*, 2018) may add further clarity.

In summary, this project identified ROR2 as a gene upregulated in $BRAF^{V600E}$ melanoma that promotes expression of VEGF. This addresses the goals set out for this project, and suggests a number of further investigations that may be informative. Given the downregulation of Wnt5a with MEK inhibition in the ROR2 overexpressing A375M clones, its differential expression in $BRAF^{V600E}$ melanoma should be confirmed. This could simply tested by investigating its expression in the isogenic cell model and across a range of $BRAF^{V600E}$ and wildtype melanoma cell lines. Differential expression could also be assessed by IHC on AVAST-M patient

samples. Treating ROR2 overexpressing A375M cells with a commercially available Wnt5a inhibitor (Jenei *et al.*, 2009) could test the necessity of the ligand for VEGF secretory phenotypes associated with ROR2.

Despite its effect on VEGF expression, the effect of ROR2 on modulating bevacizumab sensitivity was not assessed. This could be investigated, *in vivo,* by comparing responses to bevacizumab in ROR2 overexpressing vs empty vector A375M xenografts, particularly as this cell line is known to grow satisfactorily in immunodeficient mice (Craft *et al.*, 2005).

In vivo experiments, preferably with an ROR2 inhibitor are required to evaluate ROR2 as a clinically relevant target. BA3021 is a conjugated anti-ROR2 antibody that is selectively released in the tumour microenvironment designed to minimise toxicity (Sharp *et al.*, 2018). If feasible, quantifying changes in VEGF secretion in $BRAF^{V600E}$ and wildtype isogenic xenografts treated with BA3021 would further clarify the role of ROR2 and VEGF secretion and resolve if BRAF mutant melanomas were more sensitive to this therapeutic approach.

BA3021 is currently being tested clinically in a phase 1/2 dose escalation and expansion study (ClinicalTrials.gov Identifier: NCT03504488). Melanoma patients are not eligible for the dose expansion component, and thus the clinical utility of ROR2 inhibition in melanoma will likely remain undefined for the foreseeable future.

In the broader context, melanoma treatments have progressed considerably since the AVAST-M study commenced. Median survival for metastatic disease presently approaches 3 years and the risk of recurrence following resection of high risk melanoma has approximately halved (Long *et al.*, 2016; Long *et al.*, 2017; Wolchok *et al.*, 2017; Eggermont *et al.*, 2018). Not all patients benefit, however. Recurrence after resection of stage IIIC melanoma (AJCC 7^{th} edition) still approaches 40% and

metastatic melanoma remains an incurable disease. Newer therapies and new strategies are still relevant. Work presented here has implicated ROR2 in VEGF secretion, and work from others has associated ROR2 with aggressive phenotypes (O'Connell *et al.*, 2009). ROR2 is thus a feasible target of relevance in melanoma. It may also be worthwhile targeting in combination with existing treatments for patients with melanoma.

LIST OF FIGURES

Figure 1-1: MAP-K/ERK signalling pathway. 22

Figure 1-2: Disease free survival in the AVAST-M clinical trial..... 45

Figure 2-1: Schematic of the xCELLigence® Real-Time Cell Analysis system 59

Figure 2-2: Plasmids used for the creation of ROR2 overexpressing cell lines 63

Figure 3-1: Serum VEGF concentrations from the AVAST-M patients according to genotype and treatment 74

Figure 3-2: Representative VEGF IHC images 81

Figure 3-3: Examples of semi-quantitative method used to score VEGF.. 82

Figure 3-4: VEGF IHC on AVAST-M TMAs..... 83

Figure 3-5: VEGF IHC on AVAST-M whole mount slides. 84

Figure 3-6: Representative CD31 IHC images 89

Figure 3-7: CD31 expression in AVAST-M patient samples. 90

Figure 4-1: Pathway analysis of genes differentially expressed in available datasets..... 108

Figure 4-2: Venn diagram of differentially expressed genes in available datasets... 109

Figure 4-3: $VEGF_{165}$ in $BRAF^{V600E}$/wildtype isogenic cell line model 112

Figure 4-4: VEGF protein expression in $BRAF^{V600E}$/wildtype cell model. 114

Figure 4-5: Expression of HIF-1 α and VEGFR2 in the $BRAF^{V600E/}$wildtype isogenic cell model.. 117

Figure 4-6: Validation of differentially expressed genes with qRT-PCR. 119

Figure 4-7: Initial interrogation of Osteopontin as a gene of interest 122

Figure 4-8: ROR2 protein expression 126

Figure 4-9: ROR2 expression across non-isogenic cell lines. 127

Figure 4-10: The effect of MAPK pathway inhibition on ROR2 expression..... 130

Figure 5-1: The effect of ROR2 depletion on melanoma cell proliferation. 142

Figure 5-2: The effect of ROR2 depletion on invasion. 144

Figure 5-3: The effect of ROR2 siRNA on $VEGFA_{165}$. 146

Figure 5-4: The effect of ROR2 depletion on intracellular VEGF expression 148

Figure 5-5 ROR2 depletion inhibits secretion of VEGF.. 150

Figure 5-6: The effect of transfection procedure on VEGF secretion..... 152

Figure 5-7: The effect of ROR2 depletion on potential downstream targets. 153

Figure 5-8: Plasmids used for the creation of ROR2 overexpressing cell lines 154

Figure 5-9: Testing stable ROR2 overexpression in CHL1 clones.. 156

Figure 5-10: The effect of ROR2 overexpression on invasion in CHL1 cells..... 158

Figure 5-11: The effect of ROR2 overexpression on VEGF secretion in CHL1 cells. 160

Figure 5-12: The effect of transient ROR2 overexpression on A375M cells 162

Figure 5-13: Testing stable ROR2 overexpression in A375M clones. 163

Figure 5-14: The effect of ROR2 overexpression on $VEGF_{165}$ expression in A375M cells 166

Figure 5-15: The effect of pharmacological MEK inhibition on ROR2 overexpressing A375M cells 170

Figure 5-16: The effect of melanoma cell conditioned medium on endothelial cell proliferation. 174

Figure 6-1: Testing the contribution of HIF-1α to ROR2 expression..... 185

Figure 6-2: The effect of ROR2 depletion on MMP2 expression. 187

Figure 6-3: The effect of MMP2 inhibition on the secretion of VEGF 188

Figure 6-4: The effect of recombinant MMP2 on VEGF secretion in the context of ROR2 depletion..... 190

Figure 6-5: *MMP2* mRNA expression in A375M clones.. 191

Figure 6-6: The effect of ROR2 overexpression on exosome production.. 194

Figure 7-1: Investigating the effect of $BRAF^{V600E}$ mutant/wildtype isogenic clones *in vivo*. 206

Figure 7-2: Human genes differentially expressed between $BRAF^{V600E}$ vs wildtype melanomas 211

Figure 7-3: Genes differentially expressed within the stroma of $BRAF^{V600E}$ vs wildtype xenografts 214

Figure 7-4: The effect of bevacizumab on tumour gene expression 216

Figure 7-5: Stromal derived genes influenced by treatment with bevacizumab..... 218

Figure 7-6: Exploration of ROR2 as a predictive biomarker for bevacizumab for patients recruited into the AVAST-M trial..... 221

LIST OF TABLES

Table 1-1: Tumour, Node and Metastases (TNM) descriptions based upon the AJCC 7th edition for melanoma 13

Table 1-2: Pathological stage groupings and prognosis according to the AJCC 7th staging edition for melanoma. 14

Table 1-3: Chemotherapy in combination in the treatment of stage IV cutaneous melanoma..... 17

Table 1-4: Outcomes from phase II and III trials evaluating bevacizumab in the treatment of metastatic melanoma 43

Table 2-1: Melanoma cell lines used in this project..... 49

Table 2-2: Antibodies used for western blotting in this project 52

Table 2-3: Sequences of all primers uses in this project 55

Table 3-1: Serum VEGF concentrations from patients recruited to the AVAST-M study, stratified by BRAF mutational status..... 73

Table 4-1: Genes differentially expressed between $BRAF^{V600E}$ and wildtype melanoma samples from the AVAST-M clinical trial 99

Table 4-2: Genes differentially expressed in $BRAF^{V600}$/wildtype patient melanomas in data extracted from the TCGA firehouse legacy dataset 102

Table 4-3: Top 100 differentially expressed genes between $BRAF^{V600E}$ mutant and wildtype clones, in the isogenic cell line model 106

Table 4-4: Differentially expressed genes in the isogenic cell associated with angiogenesis..... 109

Table 4-5: Genes commonly differentially expressed between all three data sets ... 110

Table 4-6:Wnt genes differentially expressed in at least one of the three datasets .. 132

Table 7-1: Differentially expressed genes between $BRAF^{V600E}$ and wildtype xenografted melanomas..... 210

Table 7-2: Differentially expressed tumour genes in $BRAF^{V600E}$ and wildtype melanoma xenografts associating with the VEGF/VEGFR2 signalling pathway..... 212

LIST OF COMMON ABBREVIATIONS

AJCC	American Joint Committee on Cancer
APC	Adenomatous Polyposis Coli
APMA	P-Aminophenylmercuric Acetate
ATP	Adenosine Triphosphate
CMV	Cytomegalovirus
CRISPR	Clustered Regularly Interspaced Short Palindromic Repeats
DMSO	Dimethyl Sulfoxide
DTIC	Dacarbazine
ECM	Extracellular Matrix
EGFR	Epidermal Growth Factor Receptor
ELISA	Enzyme-Linked Immunosorbent Assay
EMT	Epithelial–Mesenchymal Transition
FFPE	Formalin-Fixed, Paraffin-Embedded
GAP	GTPase-Activating Protein
GDP	Guanosine Diphosphate
GTP	Guanosine Triphosphate
HCC	Hepatocellular Carcinoma
HIF	Hypoxia-Inducible Factor
HKG	Housekeeping Gene
HPSG	Heparan Sulfate Proteoglycan
HUVEC	Human Umbilical Vein Endothelial Cells
IHC	Immunohistochemistry

IQR	Inter Quartile Range
MAPK	Mitogen-Activated Protein Kinase
MITF	Microphthalmia-Associated Transcription Factor
MMP	Matrix Metalloproteinase
MVD	Microvessel Density
NTA	Nanoparticle Tracking Analysis
PCR	Polymerase Chain Reaction
PDGFR	Platelet-Derived Growth Factor Receptor
PGF	Placental Growth Factor
PMEL	Premelanosome Protein
PTEN	Phosphatase and Tensin Homolog
RB	Retinoblastoma Protein
RCC	Renal Cell Carcinoma
RTK	Receptor Tyrosine Kinase
SEM	Standard Error of Mean
SOS	Son of Sevenless
TCF	Transcription Factor
TCGA	The Cancer Genome Atlas
TMA	Tissue Micro Array
UV	Ultraviolet
VEGF	Vascular Endothelial Growth Factor
VEGFR	Vascular Endothelial Growth Factor Receptor
VHL	Von Hippel–Lindau
WT	Wildtype

Bibliography

Abdel-Malek, Z. A., Kadekaro, A. L. and Swope, V. B. (2010) 'Stepping up melanocytes to the challenge of UV exposure.', *Pigment Cell Melanoma Res.* England, 23(2), pp. 171–186.

Acevedo, L. M., Barillas, S., Weis, S. M., Göthert, J. R., *et al.* (2008) 'Semaphorin 3A suppresses VEGF-mediated angiogenesis yet acts as a vascular permeability factor', *Blood.* American Society of Hematology, 111(5), pp. 2674–2680.

Adamcic, U., Skowronski, K., Peters, C., Morrison, J., *et al.* (2012) *The Effect of Bevacizumab on Human Malignant Melanoma Cells with Functional VEGF/VEGFR2 Autocrine and Intracrine Signaling Loops 1 2*, *Neoplasia*.

Agger, K., Cloos, P. A. C., Rudkjaer, L., Williams, K., *et al.* (2009) 'The H3K27me3 demethylase JMJD3 contributes to the activation of the INK4A-ARF locus in response to oncogene- and stress-induced senescence.', *Genes Dev.* Cold Spring Harbor Laboratory Press, 23(10), pp. 1171–6.

Aiello, L. P., Bursell, S. E., Clermont, A., Duh, E., *et al.* (1997) 'Vascular endothelial growth factor-induced retinal permeability is mediated by protein kinase C in vivo and suppressed by an orally effective beta-isoform-selective inhibitor.', *Diabetes*. United States, 46(9), pp. 1473–1480.

Aigner, K., Dampier, B., Descovich, L., Mikula, M., *et al.* (2007) 'The transcription factor ZEB1 (deltaEF1) promotes tumour cell dedifferentiation by repressing master regulators of epithelial polarity.', *Oncogene*. England, 26(49), pp. 6979–6988.

Aikawa, T., Whipple, C. A., Lopez, M. E., Gunn, J., *et al.* (2008) 'Glypican-1 modulates the angiogenic and metastatic potential of human and mouse cancer cells.', *J. Clin. Invest.* United States, 118(1), pp. 89–99.

Akbani, R., Akdemir, K. C., Aksoy, B. A., Albert, M., *et al.* (2015) 'Genomic Classification of Cutaneous Melanoma', *Cell*, 161(7), pp. 1681–1696.

Akbar, N., Digby, J. E., Cahill, T. J., Tavare, A. N., *et al.* (2017) 'Endothelium-derived extracellular vesicles promote splenic monocyte mobilization in myocardial infarction', *JCI Insight*. The American Society for Clinical Investigation, 2(17).

Al-Sanabra, O., Duckworth, A. D., Glenn, M. A., Brown, B. R. B., *et al.* (2017) 'Transcriptional mechanism of vascular endothelial growth factor-induced expression of protein kinase CβII in chronic lymphocytic leukaemia cells', *Sci. Rep.* Nature Publishing Group, 7, p. 43228.

Alexander, R. A., Prager, G. W., Mihaly-Bison, J., Uhrin, P., *et al.* (2012) 'VEGF-induced endothelial cell migration requires urokinase receptor (uPAR)-dependent integrin redistribution.', *Cardiovasc. Res.* England, 94(1), pp. 125–135.

Alitalo, K. (2011) 'The lymphatic vasculature in disease.', *Nat. Med.* United States, 17(11), pp. 1371–1380.

Amaral, T., Sinnberg, T., Meier, F., Krepler, C., *et al.* (2017) 'The mitogen-activated protein kinase pathway in melanoma part I – Activation and primary resistance mechanisms to BRAF inhibition', *Eur. J. Cancer*, 73, pp. 85–92.

Anastas, J., Zhang, W., Suto, M., Li, Y., *et al.* (2014) 'WNT5A enhances resistance of melanoma cells to targeted BRAF inhibitors', *Oncogene.* American Society for Clinical Investigation, 31(32), pp. 3696–3708.

Apte, R. S., Chen, D. S. and Ferrara, N. (2019) 'VEGF in Signaling and Disease: Beyond Discovery and Development.', *Cell*. United States, 176(6), pp. 1248–1264.

Ascha, M., Ascha, M. S., Tanenbaum, J. and Bordeaux, J. S. (2017) 'Risk Factors for Melanoma in Renal Transplant Recipients.', *JAMA dermatology*. United States, 153(11), pp. 1130–1136.

Avril, M. F., Aamdal, S., Grob, J. J., Hauschild, A., *et al.* (no date) 'Fotemustine Compared With Dacarbazine in Patients With Disseminated Malignant Melanoma: A Phase III Study', *J Clin Oncol*, 22, pp. 1118–1125.

Azar, W. J., Azar, S. H. X., Higgins, S., Hu, J.-F., *et al.* (2011) 'IGFBP-2 Enhances VEGF Gene Promoter Activity and Consequent Promotion of Angiogenesis by Neuroblastoma Cells', *Endocrinology*. Oxford University Press, 152(9), pp. 3332–3342.

Badalian-Very, G., Vergilio, J.-A., Degar, B. A., MacConaill, L. E., *et al.* (2010) 'Recurrent BRAF mutations in Langerhans cell histiocytosis.', *Blood*. United States, 116(11), pp. 1919–1923.

Balch, C. M., Gershenwald, J. E., Soong, S.-J., Thompson, J. F., *et al.* (2009) 'Final version of 2009 AJCC melanoma staging and classification', *J. Clin. Oncol.* 2009/11/16. American Society of Clinical Oncology, 27(36), pp. 6199–6206.

Bates, D. O., Catalano, P. J., Symonds, K. E., Varey, A. H. R., *et al.* (2012) 'Association between VEGF Splice Isoforms and Progression-Free Survival in Metastatic Colorectal Cancer Patients Treated with Bevacizumab', *Clin. Cancer Res.*, 18(22), pp. 6384 LP – 6391.

Baty, F., Joerger, M., Früh, M., Klingbiel, D., *et al.* (2017) '24h-gene variation effect of combined bevacizumab/erlotinib in advanced non-squamous non-small cell lung cancer using exon array blood profiling', *J. Transl. Med.* BioMed Central, 15(1), p. 66.

Bedikian, A. Y., Weiss, G. R., Legha, S. S., Burris, H. A. 3rd, *et al.* (1995) 'Phase II

trial of docetaxel in patients with advanced cutaneous malignant melanoma previously untreated with chemotherapy.', *J. Clin. Oncol.* United States, 13(12), pp. 2895–2899.

Behren, A., Anaka, M., Lo, P.-H., Vella, L. J., *et al.* (2013) 'The Ludwig institute for cancer research Melbourne melanoma cell line panel.', *Pigment Cell Melanoma Res.* England, 26(4), pp. 597–600.

Bellon, M., Moles, R., Chaib-Mezrag, H., Pancewicz, J., *et al.* (2018) 'JAG1 overexpression contributes to Notch1 signaling and the migration of HTLV-1-transformed ATL cells', *J. Hematol. Oncol.* BioMed Central, 11(1), p. 119.

Belotti, D., Paganoni, P., Manenti, L., Garofalo, A., *et al.* (2003) 'Matrix metalloproteinases (MMP9 and MMP2) induce the release of vascular endothelial growth factor (VEGF) by ovarian carcinoma cells: implications for ascites formation.', *Cancer Res.* American Association for Cancer Research, 63(17), pp. 5224–9.

Ben-Batalla, I., Cubas-Cordova, M., Udonta, F., Wroblewski, M., *et al.* (2015) 'Cyclooxygenase-2 blockade can improve efficacy of VEGF-targeting drugs', *Oncotarget*. Impact Journals LLC, 6(8), pp. 6341–6358.

Benedito, R., Roca, C., Sorensen, I., Adams, S., *et al.* (2009) 'The notch ligands Dll4 and Jagged1 have opposing effects on angiogenesis.', *Cell.* United States, 137(6), pp. 1124–1135.

Benedito, R., Rocha, S. F., Woeste, M., Zamykal, M., *et al.* (2012) 'Notch-dependent VEGFR3 upregulation allows angiogenesis without VEGF-VEGFR2 signalling.', *Nature*. England, 484(7392), pp. 110–114.

Bennett, D. C. (2008) 'How to make a melanoma: what do we know of the primary clonal events?', *Pigment Cell Melanoma Res.* England, 21(1), pp. 27–38.

Bergers, G., Brekken, R., McMahon, G., Vu, T. H., *et al.* (2000) 'Matrix metalloproteinase-9 triggers the angiogenic switch during carcinogenesis.', *Nat. Cell Biol.* England, 2(10), pp. 737–744.

Biechele, T. L., Kulikauskas, R. M., Toroni, R. A., Lucero, O. M., *et al.* (2012) 'Wnt/ -Catenin Signaling and AXIN1 Regulate Apoptosis Triggered by Inhibition of the Mutant Kinase BRAFV600E in Human Melanoma', *Sci. Signal.*, 5(206), pp. ra3–ra3.

Blanco, R. and Gerhardt, H. (2013) 'VEGF and Notch in tip and stalk cell selection', *Cold Spring Harb. Perspect. Med.* Cold Spring Harbor Laboratory Press, 3(1), pp. a006569–a006569.

Blomgren, B., Falconer, C. and Palmblad, J. (2002) 'Expression of the vascular endothelial growth factor (VEGF) family in human endometrial blood vessels AU - Mints, M.', *Scand. J. Clin. Lab. Invest.* Taylor & Francis, 62(3), pp. 167–175.

Bolos, V., Peinado, H., Perez-Moreno, M. A., Fraga, M. F., *et al.* (2003) 'The transcription factor Slug represses E-cadherin expression and induces epithelial to mesenchymal transitions: a comparison with Snail and E47 repressors.', *J. Cell Sci.* England, 116(Pt 3), pp. 499–511.

Boniol, M., Autier, P., Boyle, P. and Gandini, S. (2012) 'Cutaneous melanoma attributable to sunbed use: systematic review and meta-analysis.', *BMJ*, 345, p. e4757.

Boregowda, R. K., Olabisi, O. O., Abushahba, W., Jeong, B.-S., *et al.* (2014) 'RUNX2 is overexpressed in melanoma cells and mediates their migration and invasion', *Cancer Lett.* 2014/03/18, 348(1–2), pp. 61–70.

Bottos, A., Martini, M., Di Nicolantonio, F., Comunanza, V., *et al.* (2012) 'Targeting oncogenic serine/threonine-protein kinase BRAF in cancer cells inhibits angiogenesis and abrogates hypoxia', *Proc. Natl. Acad. Sci.*, 109(6), p. E353 LP-E359.

Brash, D. E. (2015) 'UV signature mutations.', *Photochem. Photobiol.* United States, 91(1), pp. 15–26.

Bucheit, A. D., Syklawer, E., Jakob, J. A., Bassett, R. L., *et al.* (2013) 'Clinical characteristics and outcomes with specific *BRAF* and *NRAS* mutations in patients with metastatic melanoma', *Cancer*, 119(21), pp. 3821–3829.

Budden, T. and Bowden, N. A. (2013) 'The role of altered nucleotide excision repair and UVB-induced DNA damage in melanomagenesis.', *Int. J. Mol. Sci.* Switzerland, 14(1), pp. 1132–1151.

Bulliard, J. L., Cox, B. and Elwood, J. M. (1994) 'Latitude gradients in melanoma incidence and mortality in the non-Maori population of New Zealand.', *Cancer Causes Control*. Netherlands, 5(3), pp. 234–240.

Burd, C. E., Liu, W., Huynh, M. V, Waqas, M. A., *et al.* (2014) 'Mutation-specific RAS oncogenicity explains NRAS codon 61 selection in melanoma.', *Cancer Discov.* United States, 4(12), pp. 1418–1429.

Camp, R. L., Charette, L. A. and Rimm, D. L. (2000) 'Validation of tissue microarray technology in breast carcinoma.', *Lab. Invest.* United States, 80(12), pp. 1943–1949.

Candido, S., Rapisarda, V., Marconi, A., Malaponte, G., *et al.* (2014) 'Analysis of the B-RafV600E mutation in cutaneous melanoma patients with occupational sun exposure.', *Oncol. Rep.* Greece, 31(3), pp. 1079–1082.

Caramel, J., Papadogeorgakis, E., Hill, L., Browne, G. J., *et al.* (2013) 'A Switch in the Expression of Embryonic EMT-Inducers Drives the Development of Malignant Melanoma', *Cancer Cell*, 24(4), pp. 466–480.

Carmeliet, P. (2005) 'VEGF as a key mediator of angiogenesis in cancer.', *Oncology*. Karger Publishers, 69 Suppl 3(Suppl. 3), pp. 4–10.

Chamboredon, S., Ciais, D., Desroches-Castan, A., Savi, P., *et al.* (2011) 'Hypoxia-

inducible factor-1α mRNA: a new target for destabilization by tristetraprolin in endothelial cells.', *Mol. Biol. Cell*, 22(18), pp. 3366–78.

Chantrain, C. F., DeClerck, Y. A., Groshen, S. and McNamara, G. (2003) 'Computerized Quantification of Tissue Vascularization Using High-resolution Slide Scanning of Whole Tumor Sections', *J. Histochem. Cytochem.*, 51(2), pp. 151–158.

Chapman, P. B., Einhorn, L. H., Meyers, M. L., Saxman, S., *et al.* (1999) 'Phase III multicenter randomized trial of the Dartmouth regimen versus dacarbazine in patients with metastatic melanoma.', *J. Clin. Oncol.*, 17(9), pp. 2745–51.

Chapman, P. B., Hauschild, A., Robert, C., Haanen, J. B., *et al.* (2011) 'Improved Survival with Vemurafenib in Melanoma with BRAF V600E Mutation', *N. Engl. J. Med.* Massachusetts Medical Society , 364(26), pp. 2507–2516.

Chen, J., Stahl, A., Krah, N. M., Seaward, M. R., *et al.* (2011) 'Wnt signaling mediates pathological vascular growth in proliferative retinopathy', *Circulation*. 2011/10/03, 124(17), pp. 1871–1881.

Chen, J., Li, H., Chen, H., Hu, D., *et al.* (2012) 'Dickkopf-1 inhibits the invasive activity of melanoma cells', *Clin. Exp. Dermatol.*, 37(4), pp. 404–410.

Chen, J., Fu, Y., Day, D. S., Sun, Y., *et al.* (2017) 'VEGF amplifies transcription through ETS1 acetylation to enable angiogenesis', *Nat. Commun.*, 8(1), p. 383.

Chen, T., Fallah, M., Forsti, A., Kharazmi, E., *et al.* (2015) 'Risk of Next Melanoma in Patients With Familial and Sporadic Melanoma by Number of Previous Melanomas.', *JAMA dermatology*. United States, 151(6), pp. 607–615.

Cicenas, J., Tamosaitis, L., Kvederaviciute, K., Tarvydas, R., *et al.* (2017) 'KRAS, NRAS and BRAF mutations in colorectal cancer and melanoma.', *Med. Oncol.* United States, 34(2), p. 26.

Cisowski, J., Sayin, V. I., Liu, M., Karlsson, C., *et al.* (2016) 'Oncogene-induced senescence underlies the mutual exclusive nature of oncogenic KRAS and BRAF.', *Oncogene*. England, 35(10), pp. 1328–1333.

Cocconi, G., Bella, M., Calabresi, F., Tonato, M., *et al.* (1992) 'Treatment of metastatic malignant melanoma with dacarbazine plus tamoxifen.', *N. Engl. J. Med.* United States, 327(8), pp. 516–523.

Comijn, J., Berx, G., Vermassen, P., Verschueren, K., *et al.* (2001) 'The two-handed E box binding zinc finger protein SIP1 downregulates E-cadherin and induces invasion.', *Mol. Cell*. United States, 7(6), pp. 1267–1278.

Connolly, D. T., Olander, J. V, Heuvelman, D., Nelson, R., *et al.* (1989) 'Human vascular permeability factor. Isolation from U937 cells.', *J. Biol. Chem.* , 264(33), pp. 20017–20024.

Corrie, P., Marshall, A., Lorigan, P., Gore, M. E., *et al.* (2017) 'Adjuvant

bevacizumab as treatment for melanoma patients at high risk of recurrence: Final results for the AVAST-M trial.', *J. Clin. Oncol.* American Society of Clinical Oncology, 35(15_suppl), p. 9501.

Corrie, P. G., Marshall, A., Dunn, J. A., Middleton, M. R., *et al.* (2014) 'Adjuvant bevacizumab in patients with melanoma at high risk of recurrence (AVAST-M): preplanned interim results from a multicentre, open-label, randomised controlled phase 3 study.', *Lancet. Oncol.* Elsevier, 15(6), pp. 620–30.

Corrie, P. G., Marshall, A., Nathan, P. D., Lorigan, P., *et al.* (2018) 'Adjuvant bevacizumab for melanoma patients at high risk of recurrence: survival analysis of the AVAST-M trial', *Ann. Oncol.*, 29(8), pp. 1843–1852.

Corrie, P. G., Basu, B. and Zaki, K. A. (2010) 'Targeting angiogenesis in melanoma: prospects for the future', *Ther. Adv. Med. Oncol.* SAGE Publications, 2(6), pp. 367–380.

Craft, N., Bruhn, K. W., Nguyen, B. D., Prins, R., *et al.* (2005) 'Bioluminescent imaging of melanoma in live mice', *J. Invest. Dermatol.*, 125(1), pp. 159–165.

Craig, S., Earnshaw, C. H. and Virós, A. (2018) 'Ultraviolet light and melanoma', *J. Pathol.* John Wiley & Sons, Ltd, 244(5), pp. 578–585.

CRUK (no date) *www.cancerresearchuk.org*.

Curtin, J. A., Busam, K., Pinkel, D. and Bastian, B. C. (2006) 'Somatic activation of KIT in distinct subtypes of melanoma.', *J. Clin. Oncol.* United States, 24(26), pp. 4340–4346.

Cvjetkovic, A., Lötvall, J. and Lässer, C. (2014) 'The influence of rotor type and centrifugation time on the yield and purity of extracellular vesicles', *J. Extracell. Vesicles.* Taylor & Francis, 3(1), p. 23111.

Dai, J., Peng, L., Fan, K., Wang, H., *et al.* (2009) 'Osteopontin induces angiogenesis through activation of PI3K/AKT and ERK1/2 in endothelial cells.', *Oncogene*. England, 28(38), pp. 3412–3422.

Damsky, W. E., Curley, D. P., Santhanakrishnan, M., Rosenbaum, L. E., *et al.* (2011) 'β-catenin signaling controls metastasis in Braf-activated Pten-deficient melanomas.', *Cancer Cell*. NIH Public Access, 20(6), pp. 741–54.

Davar, D., Ding, F., Saul, M., Sander, C., *et al.* (2017) 'High-dose interleukin-2 (HD IL-2) for advanced melanoma: a single center experience from the University of Pittsburgh Cancer Institute', *J. Immunother. cancer*. BioMed Central, 5(1), p. 74.

Davar, D., Tarhini, A. A. and Kirkwood, J. M. (2012) 'Adjuvant therapy for melanoma', *Cancer J.*, 18(2), pp. 192–202.

Davies, H., Bignell, G. R., Cox, C., Stephens, P., *et al.* (2002) 'Mutations of the BRAF gene in human cancer', *Nature*. Nature Publishing Group, 417(6892), pp. 949–

954.

Debebe, Z. and Rathmell, W. K. (2015) 'Ror2 as a Therapeutic Target in Cancer', *Pharmacol. Ther.* Pergamon, 150, pp. 143–148.

DeCicco-Skinner, K. L., Henry, G. H., Cataisson, C., Tabib, T., *et al.* (2014) 'Endothelial cell tube formation assay for the in vitro study of angiogenesis', *J. Vis. Exp.*, (91), pp. e51312–e51312.

Dejmek, J., Safholm, A., Kamp Nielsen, C., Andersson, T., *et al.* (2006) 'Wnt-5a/Ca2+-induced NFAT activity is counteracted by Wnt-5a/Yes-Cdc42-casein kinase 1alpha signaling in human mammary epithelial cells.', *Mol. Cell. Biol.* United States, 26(16), pp. 6024–6036.

Denecker, G., Vandamme, N., Akay, O., Koludrovic, D., *et al.* (2014) 'Identification of a ZEB2-MITF-ZEB1 transcriptional network that controls melanogenesis and melanoma progression.', *Cell Death Differ.* England, 21(8), pp. 1250–1261.

Dewing, D., Emmett, M. and Pritchard Jones, R. (2012) 'The Roles of Angiogenesis in Malignant Melanoma: Trends in Basic Science Research over the Last 100 Years.', *ISRN Oncol.* Egypt, 2012, p. 546927.

Dilyana, T., Stéphanie, S., Romaric, L., Florence, S., *et al.* (2017) 'Extracellular Vesicles in Angiogenesis', *Circ. Res.* American Heart Association, 120(10), pp. 1658–1673.

Dissanayake, S. K., Olkhanud, P. B., O'Connell, M. P., Carter, A., French, A. D., Camilli, T. C., Emeche, C. D., Hewitt, Kyle J, *et al.* (2008) 'Wnt5A regulates expression of tumor-associated antigens in melanoma via changes in signal transducers and activators of transcription 3 phosphorylation.', *Cancer Res.* NIH Public Access, 68(24), pp. 10205–14.

Dissanayake, S. K., Olkhanud, P. B., O'Connell, M. P., Carter, A., French, A. D., Camilli, T. C., Emeche, C. D., Hewitt, Kyle J., *et al.* (2008) 'Wnt5A regulates expression of tumor-associated antigens in melanoma via changes in signal transducers and activators of transcription 3 phosphorylation', *Cancer Res.* American Association for Cancer Research, 68(24), pp. 10205–10214.

Dragovic, R. A., Gardiner, C., Brooks, A. S., Tannetta, D. S., *et al.* (2011) 'Sizing and phenotyping of cellular vesicles using Nanoparticle Tracking Analysis', *Nanomedicine*. Elsevier, 7(6), pp. 780–788.

Dubrac, A., Künzel, S. E., Künzel, S. H., Li, J., *et al.* (2018) 'NCK-dependent pericyte migration promotes pathological neovascularization in ischemic retinopathy.', *Nat. Commun.* Nature Publishing Group, 9(1), p. 3463.

Dufourcq, P., Leroux, L., Ezan, J., Descamps, B., *et al.* (2008) 'Regulation of Endothelial Cell Cytoskeletal Reorganization by a Secreted Frizzled-Related Protein-1 and Frizzled 4- and Frizzled 7-Dependent Pathway: Role in Neovessel Formation', *Am. J. Pathol.*, 172(1), pp. 37–49.

Easwaran, V., Lee, S. H., Inge, L., Guo, L., *et al.* (2003) 'beta-Catenin regulates vascular endothelial growth factor expression in colon cancer.', *Cancer Res.*, 63(12), pp. 3145–53.

Edris, B., Espinosa, I., Mühlenberg, T., Mikels, A., *et al.* (2012) 'ROR2 is a novel prognostic biomarker and a potential therapeutic target in leiomyosarcoma and gastrointestinal stromal tumour', *J. Pathol.* 2012/02/17, 227(2), pp. 223–233.

Eggermont, A. M. M., Blank, C. U., Mandala, M., Long, G. V, *et al.* (2018) 'Adjuvant Pembrolizumab versus Placebo in Resected Stage III Melanoma.', *N. Engl. J. Med.* United States, 378(19), pp. 1789–1801.

Ekström, E. J., Bergenfelz, C., von Bülow, V., Serifler, F., *et al.* (2014) 'WNT5A induces release of exosomes containing pro-angiogenic and immunosuppressive factors from malignant melanoma cells', *Mol. Cancer*, 13(1), p. 88.

Ellis, L. M. (2006) 'The role of neuropilins in cancer.', *Mol. Cancer Ther.* United States, 5(5), pp. 1099–1107.

Elwood, J. M. and Jopson, J. (1997) 'Melanoma and sun exposure: an overview of published studies.', *Int. J. cancer.* United States, 73(2), pp. 198–203.

Emens, L. A., Ascierto, P. A., Darcy, P. K., Demaria, S., *et al.* (2017) 'Cancer immunotherapy: Opportunities and challenges in the rapidly evolving clinical landscape', *Eur. J. Cancer*, 81, pp. 116–129.

Erhard, H., Rietveld, F. J., van Altena, M. C., Bröcker, E. B., *et al.* (1997) 'Transition of horizontal to vertical growth phase melanoma is accompanied by induction of vascular endothelial growth factor expression and angiogenesis', *Melanoma Res.*, 7 Suppl 2, p. S19—26.

Fallowfield, M. E. and Cook, M. G. (1991) 'The vascularity of primary cutaneous melanoma.', *J. Pathol.* England, 164(3), pp. 241–244.

Faries, M. B., Thompson, J. F., Cochran, A. J., Andtbacka, R. H., *et al.* (2017) 'Completion Dissection or Observation for Sentinel-Node Metastasis in Melanoma.', *N. Engl. J. Med.* United States, 376(23), pp. 2211–2222.

Ferrara, N. (2017) 'Microvascular Density as a Predictive Biomarker for Bevacizumab Survival Benefit in Ovarian Cancer: Back to First Principles?', *JNCI J. Natl. Cancer Inst.*, 109(11).

Ferrara, N. and Adamis, Anthony P. (2016) 'Ten years of anti-vascular endothelial growth factor therapy', *Nat. Rev. Drug Discov.* Nature Publishing Group, 15(6), pp. 385–403.

Ferrara, N. and Adamis, Anthony P (2016) 'Ten years of anti-vascular endothelial growth factor therapy', *Nat. Rev. Drug Discov.* Nature Publishing Group, a division of Macmillan Publishers Limited. All Rights Reserved., 15, p. 385.

Ferrara, N., Gerber, H.-P. and LeCouter, J. (2003) 'The biology of VEGF and its receptors', *Nat. Med.* Nature Publishing Group, 9(6), pp. 669–676.

Ferrara, N., Hillan, K. J. and Novotny, W. (2005) 'Bevacizumab (Avastin), a humanized anti-VEGF monoclonal antibody for cancer therapy.', *Biochem. Biophys. Res. Commun.* United States, 333(2), pp. 328–335.

Ferrucci, P. F., Minchella, I., Mosconi, M., Gandini, S., *et al.* (2015) 'Dacarbazine in combination with bevacizumab for the treatment of unresectable/metastatic melanoma: a phase II study.', *Melanoma Res.* England, 25(3), pp. 239–245.

Filipazzi, P., Bürdek, M., Villa, A., Rivoltini, L., *et al.* (2012) 'Recent advances on the role of tumor exosomes in immunosuppression and disease progression', *Semin. Cancer Biol.* Academic Press, 22(4), pp. 342–349.

Firth, S. M. and Baxter, R. C. (2002) 'Cellular actions of the insulin-like growth factor binding proteins.', *Endocr. Rev.* United States, 23(6), pp. 824–854.

Fisher, R. I., Terry, W. D., Hodes, R. J., Rosenberg, S. A., *et al.* (1981) 'Adjuvant Immunotherapy or Chemotherapy for Malignant Melanoma: Preliminary Report of the National Cancer Institute Randomized Clinical Trial', *Surg. Clin. North Am.*, 61(6), pp. 1267–1277.

Flaherty, K., Robert, C., Hersey, P., Nathan, P., *et al.* (2012) 'Improved Survival with MEK Inhibition in BRAF-Mutated Melanoma', *N. Engl. J. Med.*, 367(2), pp. 107–114.

Folkman, J. (1971) 'Tumor Angiogenesis: Therapeutic Implications', *N. Engl. J. Med.* Massachusetts Medical Society, 285(21), pp. 1182–1186.

Forbes, S. A., Beare, D., Boutselakis, H., Bamford, S., *et al.* (2017) 'COSMIC: somatic cancer genetics at high-resolution.', *Nucleic Acids Res.* England, 45(D1), pp. D777–D783.

Ford, C. E., Qian Ma, S. S., Quadir, A. and Ward, R. L. (2013) 'The dual role of the novel Wnt receptor tyrosine kinase, ROR2, in human carcinogenesis', *Int. J. Cancer*, 133(4), pp. 779–787.

Da Forno, P. D., Pringle, J. H., Hutchinson, P., Osborn, J., *et al.* (2008) 'WNT5A expression increases during melanoma progression and correlates with outcome.', *Clin. Cancer Res.* American Association for Cancer Research, 14(18), pp. 5825–32.

Da Forno, P., Howard Pringle, J., Hutchinson, P., Osborn, J., *et al.* (2008) 'WNT5A expression increases during melanoma progression and correlates with outcome', *Clin. Cancer Res.*, 14(18), pp. 5825–5832.

Fukumura, D., Xavier, R., Sugiura, T., Chen, Y., *et al.* (1998) 'Tumor induction of VEGF promoter activity in stromal cells.', *Cell*. Elsevier, 94(6), pp. 715–25.

Mac Gabhann, F. and Popel, A. S. (2007) 'Dimerization of VEGF receptors and

implications for signal transduction: a computational study.', *Biophys. Chem.* Netherlands, 128(2–3), pp. 125–139.

Gaillard, I., Keramidas, M., Liakos, P., Vilgrain, I., *et al.* (2000) 'ACTH-regulated expression of vascular endothelial growth factor in the adult bovine adrenal cortex: a possible role in the maintenance of the microvasculature.', *J. Cell. Physiol.* United States, 185(2), pp. 226–234.

Gandini, S., Sera, F., Cattaruzza, M. S., Pasquini, P., *et al.* (2005) 'Meta-analysis of risk factors for cutaneous melanoma: III. Family history, actinic damage and phenotypic factors.', *Eur. J. Cancer*. England, 41(14), pp. 2040–2059.

Garcia-Foncillas, J., Domine, M., Rojo, F., Hernandez, T., *et al.* (2013) 'VEGF-A 165 family of isoforms as predictive biomarkers in patients with nonsquamous non-small cell lung cancer (NSCLC) treated with bevacizumab.', *J. Clin. Oncol.* American Society of Clinical Oncology, 31(15_suppl), pp. e19109–e19109.

Geiss, G. K., Bumgarner, R. E., Birditt, B., Dahl, T., *et al.* (2008) 'Direct multiplexed measurement of gene expression with color-coded probe pairs', *Nat. Biotechnol.* Nature Publishing Group, 26(3), pp. 317–325.

Gershenwald, J. E., Scolyer, R. A., Hess, K. R., Sondak, V. K., *et al.* (2017) 'Melanoma staging: Evidence-based changes in the American Joint Committee on Cancer eighth edition cancer staging manual.', *CA. Cancer J. Clin.* United States, 67(6), pp. 472–492.

Gilchrest, B. A., Eller, M. S., Geller, A. C. and Yaar, M. (1999) 'The pathogenesis of melanoma induced by ultraviolet radiation.', *N. Engl. J. Med.* United States, 340(17), pp. 1341–1348.

Gilmartin, A. G., Bleam, M. R., Groy, A., Moss, K. G., *et al.* (2011) 'GSK1120212 (JTP-74057) is an inhibitor of MEK activity and activation with favorable pharmacokinetic properties for sustained in vivo pathway inhibition.', *Clin. Cancer Res.* American Association for Cancer Research, 17(5), pp. 989–1000.

Gitay-Goren, H., Halaban, R. and Neufeld, G. (1993) 'Human melanoma cells but not normal melanocytes express vascular endothelial growth factor receptors.', *Biochem. Biophys. Res. Commun.*, 190(3), pp. 702–8.

Goggins, W. B. and Tsao, H. (2003) 'A population-based analysis of risk factors for a second primary cutaneous melanoma among melanoma survivors.', *Cancer*. United States, 97(3), pp. 639–643.

Goldstein, A. M., Chan, M., Harland, M., Hayward, N. K., *et al.* (2007) 'Features associated with germline CDKN2A mutations: a GenoMEL study of melanoma-prone families from three continents.', *J. Med. Genet.* England, 44(2), pp. 99–106.

Goodnight, J. E. J., Moseley, H. S., Eilber, F. R., Sarna, G., *et al.* (1979) 'Cis-dichlorodiammineplatinum(II) alone and combined with DTIC for treatment of disseminated malignant melanoma.', *Cancer Treat. Rep.* United States, 63(11–12),

pp. 2005–2007.

Graziani, G. and Lacal, P. M. (2015) ‘Neuropilin-1 as Therapeutic Target for Malignant Melanoma’, *Front. Oncol.* Frontiers Media S.A., 5, p. 125.

Griffin, M., Scotto, D., Josephs, D. H., Mele, S., *et al.* (2017) ‘BRAF inhibitors: resistance and the promise of combination treatments for melanoma’, *Oncotarget*. Impact Journals LLC, 8(44), pp. 78174–78192.

Grignol, V. P., Olencki, T., Relekar, K., Taylor, C., *et al.* (2011) ‘A phase 2 trial of bevacizumab and high-dose interferon alpha 2B in metastatic melanoma.’, *J. Immunother.* United States, 34(6), pp. 509–515.

Grotegut, S., von Schweinitz, D., Christofori, G. and Lehembre, F. (2006) ‘Hepatocyte growth factor induces cell scattering through MAPK/Egr-1-mediated upregulation of Snail.’, *EMBO J.* England, 25(15), pp. 3534–3545.

Grugel, S., Finkenzeller, G., Weindel, K., Barleon, B., *et al.* (1995) ‘Both v-Ha-Ras and v-Raf stimulate expression of the vascular endothelial growth factor in NIH 3T3 cells.’, *J. Biol. Chem.*, 270(43), pp. 25915–9.

Guy, G. P. J., Berkowitz, Z., Watson, M., Holman, D. M., *et al.* (2013) ‘Indoor tanning among young non-Hispanic white females.’, *JAMA Intern. Med.* United States, 173(20), pp. 1920–1922.

Hafez, N. H. and Tahoun, N. S. (2016) ‘Expression of cyclooxygenase 2 and vascular endothelial growth factor in gastric carcinoma: Relationship with clinicopathological parameters’, *J. Egypt. Natl. Canc. Inst.*, 28(3), pp. 149–156.

Haluska, F. G., Tsao, H., Wu, H., Haluska, F. S., *et al.* (2006) ‘Genetic Alterations in Signaling Pathways in Melanoma’, *Clin. Cancer Res.*, 12(7), pp. 2301s LP-2307s.

Hanahan, D. and Weinberg, R. A. (2018) ‘Hallmarks of Cancer: The Next Generation’, *Cell*. Elsevier, 144(5), pp. 646–674.

Hauschild, A., Grob, J.-J., Demidov, L. V, Jouary, T., *et al.* (2012) ‘Dabrafenib in BRAF-mutated metastatic melanoma: a multicentre, open-label, phase 3 randomised controlled trial.’, *Lancet (London, England)*. England, 380(9839), pp. 358–365.

Hauschild, A., Dummer, R., Schadendorf, D., Santinami, M., *et al.* (2018) ‘Longer Follow-Up Confirms Relapse-Free Survival Benefit With Adjuvant Dabrafenib Plus Trametinib in Patients With Resected BRAF V600-Mutant Stage III Melanoma.’, *J. Clin. Oncol.* United States, p. JCO1801219.

Hawinkels, L. J. A. C., Zuidwijk, K., Verspaget, H. W., de Jonge-Muller, E. S. M., *et al.* (2008) ‘VEGF release by MMP-9 mediated heparan sulphate cleavage induces colorectal cancer angiogenesis.’, *Eur. J. Cancer*, 44(13), pp. 1904–13.

Hayward, N. K., Wilmott, J. S., Waddell, Nicola, Johansson, P. A., *et al.* (2017) ‘Whole-genome landscapes of major melanoma subtypes.’, *Nature*. England,

545(7653), pp. 175–180.

Hellstrom, M., Phng, L.-K., Hofmann, J. J., Wallgard, E., *et al.* (2007) 'Dll4 signalling through Notch1 regulates formation of tip cells during angiogenesis.', *Nature*. England, 445(7129), pp. 776–780.

Henry, C. E., Llamosas, E., Djordjevic, A., Hacker, N. F., *et al.* (2016) 'Migration and invasion is inhibited by silencing ROR1 and ROR2 in chemoresistant ovarian cancer', *Oncogenesis*. Nature Publishing Group, 5(5), pp. e226–e226.

Hirobe, T. (2011) 'How are proliferation and differentiation of melanocytes regulated?', *Pigment Cell Melanoma Res.* England, 24(3), pp. 462–478.

Hodi, F. S., Soiffer, R. J., Clark, J., Finkelstein, D. M., *et al.* (2002) 'Phase II study of paclitaxel and carboplatin for malignant melanoma.', *Am. J. Clin. Oncol.* United States, 25(3), pp. 283–286.

Hodi, F. S., O'Day, S. J., McDermott, D. F., Weber, R. W., *et al.* (2010) 'Improved Survival with Ipilimumab in Patients with Metastatic Melanoma', *N. Engl. J. Med.*, 363(8), pp. 711–723.

Hoek, K. S., Schlegel, N. C., Brafford, P., Sucker, A., *et al.* (2006) 'Metastatic potential of melanomas defined by specific gene expression profiles with no BRAF signature', *Pigment Cell Res.* Blackwell Publishing Ltd, 19(4), pp. 290–302.

Hoek, K. S., Eichhoff, O. M., Schlegel, N. C., Dobbeling, U., *et al.* (2008) 'In vivo switching of human melanoma cells between proliferative and invasive states.', *Cancer Res.* United States, 68(3), pp. 650–656.

Hoek, K. S. and Goding, C. R. (2010) 'Cancer stem cells versus phenotype-switching in melanoma.', *Pigment Cell Melanoma Res.* England, 23(6), pp. 746–759.

Hoeppner, L. H., Sinha, S., Wang, Y., Bhattacharya, R., *et al.* (2015) 'RhoC maintains vascular homeostasis by regulating VEGF-induced signaling in endothelial cells', *J. Cell Sci.* The Company of Biologists, 128(19), pp. 3556–3568.

Hong, S. W., Jiang, Y., Kim, S., Li, C. J., *et al.* (2014) 'Target gene abundance contributes to the efficiency of siRNA-mediated gene silencing', *Nucleic Acid Ther.* 2014/02/14. Mary Ann Liebert, Inc., 24(3), pp. 192–198.

Houck, Keith A, Leung, D. W., Rowland11, A. M., Wirier, J., *et al.* (1992) 'Dual Regulation of Vascular Endothelial Growth Factor Bioavailability by Genetic and Proteolytic Mechanisms*', *J. Biol. Chem.*, 267(36), pp. 26031–26037.

Houck, K. A., Leung, D. W., Rowland, A. M., Winer, J., *et al.* (1992) 'Dual regulation of vascular endothelial growth factor bioavailability by genetic and proteolytic mechanisms', 267(36), pp. 26031–26037.

Huang, H., Langenkamp, E., Georganaki, M., Loskog, A., *et al.* (2015) 'VEGF suppresses T-lymphocyte infiltration in the tumor microenvironment through

inhibition of NF-kappaB-induced endothelial activation.', *FASEB J. Off. Publ. Fed. Am. Soc. Exp. Biol.* United States, 29(1), pp. 227–238.

Huang, W., Zhang, C., Cui, M., Niu, J., *et al.* (2017) 'Inhibition of Bevacizumab-induced Epithelial-Mesenchymal Transition by BATF2 Overexpression Involves the Suppression of Wnt/beta-Catenin Signaling in Glioblastoma Cells.', *Anticancer Res.* Greece, 37(8), pp. 4285–4294.

Ilan, N. and Madri, J. A. (2003) 'PECAM-1: old friend, new partners.', *Curr. Opin. Cell Biol.*, 15(5), pp. 515–24.

Ito, N., Wernstedt, C., Engstrom, U. and Claesson-Welsh, L. (1998) 'Identification of vascular endothelial growth factor receptor-1 tyrosine phosphorylation sites and binding of SH2 domain-containing molecules.', *J. Biol. Chem.* United States, 273(36), pp. 23410–23418.

Jain, R. K. (2005) 'Normalization of Tumor Vasculature: An Emerging Concept in Antiangiogenic Therapy', *Science (80-.).*, 307(5706), pp. 58–62.

Jenei, V., Sherwood, V., Howlin, J., Linnskog, R., *et al.* (2009) 'A t-butyloxycarbonyl-modified Wnt5a-derived hexapeptide functions as a potent antagonist of Wnt5a-dependent melanoma cell invasion.', *Proc. Natl. Acad. Sci. U. S. A.* United States, 106(46), pp. 19473–19478.

Johnson, E. N., Lee, Y. M., Sander, T. L., Rabkin, E., *et al.* (2003) 'NFATc1 mediates vascular endothelial growth factor-induced proliferation of human pulmonary valve endothelial cells', *J. Biol. Chem.* 2002/11/09, 278(3), pp. 1686–1692.

Kandel, J., Bossy-Wetzel, E., Radvanyi, F., Klagsbrun, M., *et al.* (1991) 'Neovascularization is associated with a switch to the export of bFGF in the multistep development of fibrosarcoma.', *Cell*. United States, 66(6), pp. 1095–1104.

Kanthou, C., Dachs, G. U., Lefley, D. V, Steele, A. J., *et al.* (2014) 'Tumour cells expressing single VEGF isoforms display distinct growth, survival and migration characteristics', *PLoS One*. Public Library of Science, 9(8), pp. e104015–e104015.

Karkkainen, M. J., Haiko, P., Sainio, K., Partanen, J., *et al.* (2004) 'Vascular endothelial growth factor C is required for sprouting of the first lymphatic vessels from embryonic veins.', *Nat. Immunol.* United States, 5(1), pp. 74–80.

Karlsson, M., Mathers, J., Dickinson, R. J., Mandl, M., *et al.* (2004) 'Both nuclear-cytoplasmic shuttling of the dual specificity phosphatase MKP-3 and its ability to anchor MAP kinase in the cytoplasm are mediated by a conserved nuclear export signal.', *J. Biol. Chem.* United States, 279(40), pp. 41882–41891.

Katoh, Masuko and Katoh, Masaru (2007) 'WNT signaling pathway and stem cell signaling network.', *Clin. Cancer Res.* American Association for Cancer Research, 13(14), pp. 4042–5.

Kawamura, H., Li, X., Goishi, K., van Meeteren, L. A., *et al.* (2008) 'Neuropilin-1 in

regulation of VEGF-induced activation of p38MAPK and endothelial cell organization.', *Blood*. United States, 112(9), pp. 3638–3649.

Kerkvliet, E. H. M., Jansen, I. D. C., Schoenmaker, T. A. M., Docherty, A. J. P., *et al.* (2003) 'Low molecular weight inhibitors of matrix metalloproteinases can enhance the expression of matrix metalloproteinase-2 (gelatinase A) without inhibiting its activation', *Cancer*. Wiley-Blackwell, 97(6), pp. 1582–1588.

Kevil, C. G., Payne, D. K., Mire, E. and Alexander, J. S. (1998) 'Vascular permeability factor/vascular endothelial cell growth factor-mediated permeability occurs through disorganization of endothelial junctional proteins.', *J. Biol. Chem.* United States, 273(24), pp. 15099–15103.

Keyt, B. A., Berleau, L. T., Nguyen, H. V, Chen, H., *et al.* (1996) *The Carboxyl-terminal Domain (111-165) of Vascular Endothelial Growth Factor Is Critical for Its Mitogenic Potency*.*

Khouja, M. H., Baekelandt, M., Sarab, A., Nesland, J. M., *et al.* (2010) 'Limitations of tissue microarrays compared with whole tissue sections in survival analysis', *Oncol. Lett.* 2010/09/01. D.A. Spandidos, 1(5), pp. 827–831.

Kidger, A. M., Rushworth, L. K., Stellzig, J., Davidson, J., *et al.* (2017) 'Dual-specificity phosphatase 5 controls the localized inhibition, propagation, and transforming potential of ERK signaling.', *Proc. Natl. Acad. Sci. U. S. A.* United States, 114(3), pp. E317–E326.

Kim, H.-S., Skurk, C., Thomas, S. R., Bialik, A., *et al.* (2002) 'Regulation of Angiogenesis by Glycogen Synthase Kinase-3β', *J. Biol. Chem.* , 277(44), pp. 41888–41896.

Kim, K. B., Sosman, J. A., Fruehauf, J. P., Linette, G. P., *et al.* (2012) 'BEAM: a randomized phase II study evaluating the activity of bevacizumab in combination with carboplatin plus paclitaxel in patients with previously untreated advanced melanoma.', *J. Clin. Oncol.* United States, 30(1), pp. 34–41.

Kirkwood, J. M., Strawderman, M. H., Ernstoff, M. S., Smith, T. J., *et al.* (1996) 'Interferon alfa-2b adjuvant therapy of high-risk resected cutaneous melanoma: the Eastern Cooperative Oncology Group Trial EST 1684.', *J. Clin. Oncol.* United States, 14(1), pp. 7–17.

Kiuru, M. and Busam, K. J. (2017) 'The NF1 gene in tumor syndromes and melanoma', *Lab. Invest.* 2017/01/09, 97(2), pp. 146–157.

Koch, S., Tugues, S., Li, X., Gualandi, L., *et al.* (2011) 'Signal transduction by vascular endothelial growth factor receptors', *Biochem. J.*, 437(2), pp. 169 LP – 183.

Kontos, C. K., Papageorgiou, S. G., Diamantopoulos, M. A., Scorilas, A., *et al.* (2017) 'mRNA overexpression of the hypoxia inducible factor 1 alpha subunit gene (HIF1A): An independent predictor of poor overall survival in chronic lymphocytic leukemia', *Leuk. Res.* Pergamon, 53, pp. 65–73.

Kottschade, L. A., Suman, V. J., Perez, D. G., McWilliams, R. R., *et al.* (2013) 'A randomized phase 2 study of temozolomide and bevacizumab or nab-paclitaxel, carboplatin, and bevacizumab in patients with unresectable stage IV melanoma : a North Central Cancer Treatment Group study, N0775.', *Cancer*. United States, 119(3), pp. 586–592.

Koutras, A., Kotoula, V. and Fountzilas, G. (2015) 'Prognostic and predictive role of vascular endothelial growth factor polymorphisms in breast cancer', *Pharmacogenomics*, 16(1), pp. 79–94.

Krauthammer, M., Kong, Y., Bacchiocchi, A., Evans, P., *et al.* (2015) 'Exome sequencing identifies recurrent mutations in NF1 and RASopathy genes in sun-exposed melanomas.', *Nat. Genet.* United States, 47(9), pp. 996–1002.

Kreiseder, B., Orel, L., Bujnow, C., Buschek, S., *et al.* (2013) 'α-Catulin downregulates E-cadherin and promotes melanoma progression and invasion', *Int. J. Cancer*, 132(3), pp. 521–530.

Kubo, T., Kuroda, Y., Shimizu, H., Kokubu, A., *et al.* (2009) 'Resequencing and copy number analysis of the human tyrosine kinase gene family in poorly differentiated gastric cancer.', *Carcinogenesis*. England, 30(11), pp. 1857–1864.

Kumar, S. M., Yu, H., Edwards, R., Chen, L., *et al.* (2007) 'Mutant V600E BRAF Increases Hypoxia Inducible Factor-1α Expression in Melanoma', *Cancer Res.*, 67(7), pp. 3177 LP – 3184.

Kusumanto, Y. H., Meijer, C., Dam, W., Mulder, N. H., *et al.* (2007) 'Circulating vascular endothelial growth factor (VEGF) levels in advanced stage cancer patients compared to normal controls and diabetes mellitus patients with critical ischemia.', *Drug Target Insights*. SAGE Publications, 2, pp. 105–9.

Kut, C., Mac Gabhann, F. and Popel, A. S. (2007) 'Where is VEGF in the body? A meta-analysis of VEGF distribution in cancer.', *Br. J. Cancer*. Nature Publishing Group, 97(7), pp. 978–85.

Kwon, T.-G., Zhao, X., Yang, Q., Li, Y., *et al.* (2011) 'Physical and functional interactions between Runx2 and HIF-1alpha induce vascular endothelial growth factor gene expression.', *J. Cell. Biochem.* United States, 112(12), pp. 3582–3593.

Lakshmikanthan, S., Sobczak, M., Chun, C., Henschel, A., *et al.* (2011) 'Rap1 promotes VEGFR2 activation and angiogenesis by a mechanism involving integrin alphavbeta(3).', *Blood*. United States, 118(7), pp. 2015–2026.

Lanahan, A., Zhang, X., Fantin, A., Zhuang, Z., *et al.* (2013) 'The neuropilin 1 cytoplasmic domain is required for VEGF-A-dependent arteriogenesis.', *Dev. Cell*. United States, 25(2), pp. 156–168.

Lawrence, M. S., Stojanov, P., Polak, P., Kryukov, G. V, *et al.* (2013) 'Mutational heterogeneity in cancer and the search for new cancer-associated genes', *Nature*. Nature Publishing Group, a division of Macmillan Publishers Limited. All Rights

Reserved., 499, p. 214.

Leaman, D. W., Chawla-Sarkar, M., Vyas, K., Reheman, M., *et al.* (2002) 'Identification of X-linked Inhibitor of Apoptosis-associated Factor-1 as an Interferon-stimulated Gene That Augments TRAIL Apo2L-induced Apoptosis*'.

Lebellec, L., Bertucci, F., Tresch-Bruneel, E., Ray-Coquard, I., *et al.* (2018) 'Prognostic and predictive factors for angiosarcoma patients receiving paclitaxel once weekly plus or minus bevacizumab: an ancillary study derived from a randomized clinical trial', *BMC Cancer*, 18(1), p. 963.

Leber, T. M. and Balkwill, F. R. (1997) 'Zymography: a single-step staining method for quantitation of proteolytic activity on substrate gels.', *Anal. Biochem.* United States, 249(1), pp. 24–28.

Legha, S. S., Ring, S., Papadopoulos, N., Plager, C., *et al.* (1989) 'A prospective evaluation of a triple-drug regimen containing cisplatin, vinblastine, and dacarbazine (CVD) for metastatic melanoma.', *Cancer*. United States, 64(10), pp. 2024–2029.

Leiter, U., Stadler, R., Mauch, C., Hohenberger, W., *et al.* (2016) 'Complete lymph node dissection versus no dissection in patients with sentinel lymph node biopsy positive melanoma (DeCOG-SLT): a multicentre, randomised, phase 3 trial.', *Lancet. Oncol.* England, 17(6), pp. 757–767.

Lertkiatmongkol, P., Liao, D., Mei, H., Hu, Y., *et al.* (2016) 'Endothelial functions of platelet/endothelial cell adhesion molecule-1 (CD31)', *Curr. Opin. Hematol.*, 23(3), pp. 253–259.

Li, F. Z., Dhillon, A. S., Anderson, R. L., McArthur, G., *et al.* (2015) 'Phenotype switching in melanoma: implications for progression and therapy', *Front. Oncol.* Frontiers Media S.A., 5, p. 31.

Li, R., Zhang, L., Jia, L., Duan, Y., *et al.* (2014) 'Long non-coding RNA BANCR promotes proliferation in malignant melanoma by regulating MAPK pathway activation.', *PLoS One*. Public Library of Science, 9(6), p. e100893.

Linos, E., Swetter, S. M., Cockburn, M. G., Colditz, G. A., *et al.* (2009) 'Increasing burden of melanoma in the United States.', *J. Invest. Dermatol.* United States, 129(7), pp. 1666–1674.

Livak, K. J. and Schmittgen, T. D. (2001) 'Analysis of Relative Gene Expression Data Using Real-Time Quantitative PCR and the 2−ΔΔCT Method', *Methods*, 25(4), pp. 402–408.

Loercher, A. E., Tank, E. M. H., Delston, R. B. and Harbour, J. W. (2005) 'MITF links differentiation with cell cycle arrest in melanocytes by transcriptional activation of INK4A', *J. Cell Biol.*, 168(1), pp. 35 LP – 40.

Long, G. V., Hauschild, A., Santinami, M., Atkinson, V., *et al.* (2017) 'Adjuvant Dabrafenib plus Trametinib in Stage III *BRAF* -Mutated Melanoma', *N. Engl. J. Med.*

Massachusetts Medical Society, 377(19), pp. 1813–1823.

Long, G. V., Flaherty, K., Stroyakovskiy, D., Gogas, H., *et al.* (2017) 'Dabrafenib plus trametinib versus dabrafenib monotherapy in patients with metastatic BRAF V600E/K-mutant melanoma: long-term survival and safety analysis of a phase 3 study.', *Ann. Oncol. Off. J. Eur. Soc. Med. Oncol.* England, 28(7), pp. 1631–1639.

Long, G V, Atkinson, V., Ascierto, P. A., Robert, C., *et al.* (2016) 'Effect of nivolumab on health-related quality of life in patients with treatment-naive advanced melanoma: results from the phase III CheckMate 066 study.', *Ann. Oncol. Off. J. Eur. Soc. Med. Oncol.* England, 27(10), pp. 1940–1946.

Long, Georgina V, Weber, J. S., Infante, J. R., Kim, K. B., *et al.* (2016) 'Overall Survival and Durable Responses in Patients With BRAF V600-Mutant Metastatic Melanoma Receiving Dabrafenib Combined With Trametinib.', *J. Clin. Oncol.* American Society of Clinical Oncology, 34(8), pp. 871–8.

Lötvall, J., Hill, A. F., Hochberg, F., Buzás, E. I., *et al.* (2014) 'Minimal experimental requirements for definition of extracellular vesicles and their functions: a position statement from the International Society for Extracellular Vesicles', *J. Extracell. Vesicles.* Taylor & Francis, 3(1), p. 26913.

Lovly, C. M., Dahlman, K. B., Fohn, L. E., Su, Z., *et al.* (2012) 'Routine multiplex mutational profiling of melanomas enables enrollment in genotype-driven therapeutic trials.', *PLoS One*. United States, 7(4), p. e35309.

Lynch, H. T., Frichot, B. C. 3rd and Lynch, J. F. (1978) 'Familial atypical multiple mole-melanoma syndrome.', *J. Med. Genet.* England, 15(5), pp. 352–356.

Ma, S. S. Q., Srivastava, S., Llamosas, E., Hawkins, N. J., *et al.* (2016) 'ROR2 is epigenetically inactivated in the early stages of colorectal neoplasia and is associated with proliferation and migration', *BMC Cancer*, 16(1), p. 508.

Maae, E., Nielsen, M., Steffensen, K. D., Jakobsen, E. H., *et al.* (2011) 'Estimation of Immunohistochemical Expression of VEGF in Ductal Carcinomas of the Breast', *J. Histochem. Cytochem.*, 59(8), pp. 750–760.

Maddodi, N., Bhat, K. M. R., Devi, S., Zhang, S.-C., *et al.* (2010) 'Oncogenic BRAFV600E Induces Expression of Neuronal Differentiation Marker MAP2 in Melanoma Cells by Promoter Demethylation and Down-regulation of Transcription Repressor HES1', *J. Biol. Chem.* , 285(1), pp. 242–254.

Marie-Louise Robertson, F. and Fitzgerald, L. (2017) 'Skin cancer in the youth population of the United Kingdom', *J. Cancer Policy*, 12, pp. 67–71.

Marien, K. M., Croons, V., Waumans, Y., Sluydts, E., *et al.* (2016) 'Development and Validation of a Histological Method to Measure Microvessel Density in Whole-Slide Images of Cancer Tissue'.

Marsden, J. R., Newton-Bishop, J. A., Burrows, L., Cook, M., *et al.* (2010) 'Revised

UK guidelines for the management of cutaneous melanoma 2010', *Br. J. Plast. Surg.*, 63, pp. 1401–1419.

Masiero, M., Simões, F. C., Han, H. D., Snell, C., *et al.* (2013) 'A Core Human Primary Tumor Angiogenesis Signature Identifies the Endothelial Orphan Receptor ELTD1 as a Key Regulator of Angiogenesis', *Cancer Cell*, 24(2), pp. 229–241.

Masoud, G. N. and Li, W. (2015) 'HIF-1α pathway: role, regulation and intervention for cancer therapy', *Acta Pharm. Sin. B*, 5(5), pp. 378–389.

Matsumura, T., Wolff, K. and Petzelbauer, P. (1997) 'Endothelial cell tube formation depends on cadherin 5 and CD31 interactions with filamentous actin.', *J. Immunol.* American Association of Immunologists, 158(7), pp. 3408–16.

Maxwell, P. H., Wiesener, M. S., Chang, G. W., Clifford, S. C., *et al.* (1999) 'The tumour suppressor protein VHL targets hypoxia-inducible factors for oxygen-dependent proteolysis.', *Nature*. England, 399(6733), pp. 271–275.

McWhirter, E., Quirt, I., Gajewski, T., Pond, G., *et al.* (2016) 'A phase II study of cediranib, an oral VEGF inhibitor, in previously untreated patients with metastatic or recurrent malignant melanoma.', *Invest. New Drugs*. United States, 34(2), pp. 231–235.

McWilliams, R. R., Allred, J. B., Slostad, J. A., Katipamula, R., *et al.* (2018) 'NCCTG N0879 (Alliance): A randomized phase 2 cooperative group trial of carboplatin, paclitaxel, and bevacizumab +/- everolimus for metastatic melanoma.', *Cancer*. United States, 124(3), pp. 537–545.

Medford, A. R., Douglas, S. K., Godinho, S. I., Uppington, K. M., *et al.* (2009) 'Vascular Endothelial Growth Factor (VEGF) isoform expression and activity in human and murine lung injury'.

Mehnert, J. M., McCarthy, M. M., Aziz, S. A., Sznol, M., *et al.* (2007) 'VEGF, VEGFR1, and VEGFR2 expression in melanoma', *J. Clin. Oncol.* American Society of Clinical Oncology, 25(18_suppl), p. 8520.

Mei, H., Lian, S., Zhang, S., Wang, W., *et al.* (2014) 'High expression of ROR2 in cancer cell correlates with unfavorable prognosis in colorectal cancer', *Biochem. Biophys. Res. Commun.*, 453(4), pp. 703–709.

Meisenberg, B. R., Ross, M., Vredenburgh, J. J., Jones, R., *et al.* (1993) 'Randomized trial of high-dose chemotherapy with autologous bone marrow support as adjuvant therapy for high-risk, multi-node-positive malignant melanoma.', *J. Natl. Cancer Inst.* United States, 85(13), pp. 1080–1085.

Menzies, A. M., Haydu, L. E., Visintin, L., Carlino, M. S., *et al.* (2012) 'Distinguishing Clinicopathologic Features of Patients with V600E and V600K BRAF-Mutant Metastatic Melanoma', *Clin Cancer Res*, 18(12), pp. 3242–9.

Middleton, M. R., Grob, J. J., Aaronson, N., Fierlbeck, G., *et al.* (2000) 'Randomized

phase III study of temozolomide versus dacarbazine in the treatment of patients with advanced metastatic malignant melanoma.', *J. Clin. Oncol.* American Society of Clinical Oncology, 18(1), pp. 158–66.

Mikels, A., Minami, Y. and Nusse, R. (2009) 'Ror2 receptor requires tyrosine kinase activity to mediate Wnt5A signaling', *J. Biol. Chem.* 2009/08/31. American Society for Biochemistry and Molecular Biology, 284(44), pp. 30167–30176.

Minchenko, D. O., Kubaichuk, K. I., Ratushna, O. O., Komisarenko, S. V., *et al.* (2012) 'The vascular endothelial growth factor genes expression in glioma U87 cells is dependent from ERN1 signaling enzyme function', *Adv. Biol. Chem.* Scientific Research Publishing, 02(02), pp. 198–206.

Mocellin, S., Pasquali, S., Rossi, C. R. and Nitti, D. (2010) 'Interferon alpha adjuvant therapy in patients with high-risk melanoma: a systematic review and meta-analysis.', *J. Natl. Cancer Inst.* United States, 102(7), pp. 493–501.

Monje, P., Hernandez-Losa, J., Lyons, R. J., Castellone, M. D., *et al.* (2005) 'Regulation of the transcriptional activity of c-Fos by ERK. A novel role for the prolyl isomerase PIN1.', *J. Biol. Chem.* United States, 280(42), pp. 35081–35084.

Montalvo, J., Spencer, C., Hackathorn, A., Masterjohn, K., *et al.* (2013) 'ROCK1 & 2 perform overlapping and unique roles in angiogenesis and angiosarcoma tumor progression', *Curr. Mol. Med.* 2013/01/. Bentham Science Publishers, 13(1), pp. 205–219.

Moreno-Bueno, G., Cubillo, E., Sarrio, D., Peinado, H., *et al.* (2006) 'Genetic profiling of epithelial cells expressing E-cadherin repressors reveals a distinct role for Snail, Slug, and E47 factors in epithelial-mesenchymal transition.', *Cancer Res.* United States, 66(19), pp. 9543–9556.

Napolitano, S., Brancaccio, G., Argenziano, G., Martinelli, E., *et al.* (2018) 'It is finally time for adjuvant therapy in melanoma.', *Cancer Treat. Rev.* Netherlands, 69, pp. 101–111.

Natsume, M., Shimura, T., Iwasaki, H., Okuda, Y., *et al.* (2019) 'Placental growth factor is a predictive biomarker for ramucirumab treatment in advanced gastric cancer', *Cancer Chemother. Pharmacol.*, 83(6), pp. 1037–1046.

Ng, Y.-S. (2008) 'The Biology of Vascular Endothelial Cell Growth Factor Isoforms', in *VEGF Dev.* New York, NY: Springer New York, pp. 1–13.

Nguyen, Q. D., De Falco, S., Behar-Cohen, F., Lam, W.-C., *et al.* (2018) 'Placental growth factor and its potential role in diabetic retinopathy and other ocular neovascular diseases', *Acta Ophthalmol.* 2016/11/22. John Wiley and Sons Inc., 96(1), pp. e1–e9.

Niault, T. S. and Baccarini, M. (2010) 'Targets of Raf in tumorigenesis', *Carcinogenesis*. Oxford University Press, 31(7), pp. 1165–1174.

Niu, G., Wright, K. L., Huang, M., Song, L., *et al.* (2002) 'Constitutive Stat3 activity up-regulates VEGF expression and tumor angiogenesis', *Oncogene*, 21(13), pp. 2000–2008.

Noonan, F. P., Zaidi, M. R., Wolnicka-Glubisz, A., Anver, M. R., *et al.* (2012) 'Melanoma induction by ultraviolet A but not ultraviolet B radiation requires melanin pigment.', *Nat. Commun.* England, 3, p. 884.

O'Connell, M. P., Fiori, J. L., Xu, M., Carter, A. D., *et al.* (2010) 'The orphan tyrosine kinase receptor, ROR2, mediates Wnt5A signaling in metastatic melanoma', *Oncogene*, 29(1), pp. 34–44.

O'Connell, Michael P., Marchbank, K., Webster, M. R., Valiga, A. A., *et al.* (2013) 'Hypoxia induces phenotypic plasticity and therapy resistance in melanoma via the tyrosine kinase receptors ROR1 and ROR2', *Cancer Discov.*, 3(12), pp. 1378–1393.

O'Connell, M. P., Marchbank, K., Webster, M. R., Valiga, A. A., *et al.* (2013) 'Hypoxia Induces Phenotypic Plasticity and Therapy Resistance in Melanoma via the Tyrosine Kinase Receptors ROR1 and ROR2', *Cancer Discov.*, 3(12), pp. 1378–1393.

O'Connell, M. and Weeraratna, A. T. (2009) 'Hear the wnt ror: How melanoma cells adjust to changes in Wnt', *Pigment Cell Melanoma Res.*

Oconnell, M. P., Fiori, J. L., Xu, M., Carter, A. D., *et al.* (2010) 'The orphan tyrosine kinase receptor, ROR2, mediates Wnt5A signaling in metastatic melanoma', *Oncogene*, 29(1), pp. 34–44.

Okada, F., Rak, J. W., Croix, B. S., Lieubeau, B., *et al.* (1998) 'Impact of oncogenes in tumor angiogenesis: mutant K-ras up-regulation of vascular endothelial growth factor/vascular permeability factor is necessary, but not sufficient for tumorigenicity of human colorectal carcinoma cells.', *Proc. Natl. Acad. Sci. U. S. A.*, 95(7), pp. 3609–14.

Olofsson, B., Pajusola, K., Kaipainen, A., von Euler, G., *et al.* (1996) 'Vascular endothelial growth factor B, a novel growth factor for endothelial cells.', *Proc. Natl. Acad. Sci. U. S. A.* United States, 93(6), pp. 2576–2581.

Olsen, J. J., Pohl, S. Ö.-G., Deshmukh, A., Visweswaran, M., *et al.* (2017) 'The Role of Wnt Signalling in Angiogenesis.', *Clin. Biochem. Rev.* The Australian Association of Clinical Biochemists, 38(3), pp. 131–142.

Orlandini, M., Marconcini, L., Ferruzzi, R. and Oliviero, S. (1996) 'Identification of a c-fos-induced gene that is related to the platelet-derived growth factor/vascular endothelial growth factor family.', *Proc. Natl. Acad. Sci. U. S. A.* United States, 93(21), pp. 11675–11680.

Osman, W. M. and Youssef, N. S. (2015) 'Combined use of COX-1 and VEGF immunohistochemistry refines the histopathologic prognosis of renal cell carcinoma', *Int. J. Clin. Exp. Pathol.* e-Century Publishing Corporation, 8(7), pp. 8165–8177.

Pagani, E., Ruffini, F., Antonini Cappellini, G. C., Scoppola, A., *et al.* (2016) 'Placenta growth factor and neuropilin-1 collaborate in promoting melanoma aggressiveness.', *Int. J. Oncol.* Greece, 48(4), pp. 1581–1589.

Park, S.-Y., Shi, X., Pang, J., Yan, C., *et al.* (2013) 'Thioredoxin-interacting protein mediates sustained VEGFR2 signaling in endothelial cells required for angiogenesis', *Arterioscler. Thromb. Vasc. Biol.* 2013/02/07, 33(4), pp. 737–743.

Park, S., Ha, S. Y., Cho, H. Y., Chung, D. H., *et al.* (2011) 'Prognostic implications of hypoxia-inducible factor-1α in epidermal growth factor receptor-negative non-small cell lung cancer', *Lung Cancer*. Elsevier, 72(1), pp. 100–107.

Park, S. H., Kim, K. W. and Kim, J. C. (2015) 'The Role of Insulin-Like Growth Factor Binding Protein 2 (IGFBP2) in the Regulation of Corneal Fibroblast DifferentiationRegulatory Role of Fibroblast Lineage of IGFBP2', *Invest. Ophthalmol. Vis. Sci.*, 56(12), pp. 7293–7302.

Perl, A. K., Wilgenbus, P., Dahl, U., Semb, H., *et al.* (1998) 'A causal role for E-cadherin in the transition from adenoma to carcinoma.', *Nature*. England, 392(6672), pp. 190–193.

Pertovaara, L., Kaipainen, A., Mustonen, T., Orpana, A., *et al.* (1994) 'Vascular endothelial growth factor is induced in response to transforming growth factor-beta in fibroblastic and epithelial cells.', *J. Biol. Chem.* United States, 269(9), pp. 6271–6274.

Peyton, J. D., Spigel, D. R., Burris, H. A., Lane, C., *et al.* (2009) 'Phase II trial of bevacizumab and everolimus in the treatment of patients with metastatic melanoma: Preliminary results', *J. Clin. Oncol.* American Society of Clinical Oncology, 27(15_suppl), p. 9027.

Philpott, C., Tovell, H., Frayling, I. M., Cooper, D. N., *et al.* (2017) 'The NF1 somatic mutational landscape in sporadic human cancers', *Hum. Genomics*, 11(1), p. 13.

Pinto, M. P., Badtke, M. M., Dudevoir, M. L., Harrell, J. C., *et al.* (2010) 'Vascular Endothelial Growth Factor Secreted by Activated Stroma Enhances Angiogenesis and Hormone-Independent Growth of Estrogen Receptor–Positive Breast Cancer', *Cancer Res.*, 70(7), pp. 2655 LP – 2664.

Pipp, F., Heil, M., Issbrucker, K., Ziegelhoeffer, T., *et al.* (2003) 'VEGFR-1-selective VEGF homologue PlGF is arteriogenic: evidence for a monocyte-mediated mechanism.', *Circ. Res.* United States, 92(4), pp. 378–385.

Pisacane, A. M., Picciotto, F. and Risio, M. (2007) 'CD31 and CD34 expression as immunohistochemical markers of endothelial transdifferentiation in human cutaneous melanoma.', *Cell. Oncol.*, 29(1), pp. 59–66.

Pisacane, A. M. and Risio, M. (2005) 'VEGF and VEGFR-2 immunohistochemistry in human melanocytic naevi and cutaneous melanomas.', *Melanoma Res.*, 15(1), pp.

39–43.

Plotnikov, A., Zehorai, E., Procaccia, S. and Seger, R. (2011) ‘The MAPK cascades: signaling components, nuclear roles and mechanisms of nuclear translocation.’, *Biochim. Biophys. Acta*. Netherlands, 1813(9), pp. 1619–1633.

Premi, S., Wallisch, S., Mano, C. M., Weiner, A. B., *et al.* (2015) ‘Photochemistry. Chemiexcitation of melanin derivatives induces DNA photoproducts long after UV exposure.’, *Science*. United States, 347(6224), pp. 842–847.

Prud’homme, G. J. and Glinka, Y. (2012) ‘Neuropilins are multifunctional coreceptors involved in tumor initiation, growth, metastasis and immunity’, *Oncotarget*. Impact Journals LLC, 3(9), pp. 921–939.

Pu, D., Liu, J., Li, Z., Zhu, J., *et al.* (2017) ‘Fibroblast Growth Factor Receptor 1 (FGFR1), Partly Related to Vascular Endothelial Growth Factor Receptor 2 (VEGFR2) and Microvessel Density, is an Independent Prognostic Factor for Non-Small Cell Lung Cancer.’, *Med. Sci. Monit.* International Scientific Information, Inc., 23, pp. 247–257.

Pufe, T., Paulsen, F., Petersen, W., Mentlein, R., *et al.* (2003) ‘The angiogenic peptide vascular endothelial growth factor (VEGF) is expressed in chronic sacral pressure ulcers.’, *J. Pathol.* England, 200(1), pp. 130–136.

Pusztaszeri, M., Seelentag, W. and Bosman, F. (2006) *Immunohistochemical Expression of Endothelial Markers CD31, CD34, von Willebrand Factor, and Fli-1 in Normal Human Tissues, J. Histochem. Cytochem.*

Qian, T., Liu, Y., Dong, Yan, Zhang, L., *et al.* (2018) ‘CXCR7 regulates breast tumor metastasis and angiogenesis in vivo and in vitro’, *Mol. Med. Rep.* 2017/12/15. D.A. Spandidos, 17(3), pp. 3633–3639.

Van Raamsdonk, C. D., Bezrookove, V., Green, G., Bauer, J., *et al.* (2009) ‘Frequent somatic mutations of GNAQ in uveal melanoma and blue naevi’, *Nature*. 2008/12/10, 457(7229), pp. 599–602.

Raja, R., Kale, S., Thorat, D., Soundararajan, G., *et al.* (2014) ‘Hypoxia-driven osteopontin contributes to breast tumor growth through modulation of HIF1alpha-mediated VEGF-dependent angiogenesis.’, *Oncogene*. England, 33(16), pp. 2053–2064.

Rajabi, P., Neshat, A., Mokhtari, M., Rajabi, M. A., *et al.* (2012) ‘The role of VEGF in melanoma progression’, *J. Res. Med. Sci.* India: Medknow Publications & Media Pvt Ltd, 17(6), pp. 534–539.

Raju, R., Palapetta, S. M., Sandhya, V. K., Sahu, A., *et al.* (2014) ‘A Network Map of FGF-1/FGFR Signaling System.’, *J. Signal Transduct.* United States, 2014, p. 962962.

Rao, D. D., Vorhies, J. S., Senzer, N. and Nemunaitis, J. (2009) ‘siRNA vs. shRNA:

similarities and differences.', *Adv. Drug Deliv. Rev.* Netherlands, 61(9), pp. 746–759.

Rasmussen, N. R., Debebe, Z., Wright, T. M., Brooks, S. A., *et al.* (2014) 'Expression of Ror2 mediates invasive phenotypes in renal cell carcinoma.', *PLoS One*. Public Library of Science, 9(12), p. e116101.

Rittling, S. R. and Chambers, A. F. (2004) 'Role of osteopontin in tumour progression.', *Br. J. Cancer*. England, 90(10), pp. 1877–1881.

Robert, C., Ribas, A., Schachter, J., Arance, A., *et al.* (2019) 'Pembrolizumab versus ipilimumab in advanced melanoma (KEYNOTE-006): post-hoc 5-year results from an open-label, multicentre, randomised, controlled, phase 3 study.', *Lancet. Oncol.* England, 20(9), pp. 1239–1251.

Rodrigues, L. K., Leong, S. P., Ljung, B. M., Sagebiel, R. W., *et al.* (2000) 'Fine needle aspiration in the diagnosis of metastatic melanoma.', *J. Am. Acad. Dermatol.* United States, 42(5 Pt 1), pp. 735–740.

Rodriguez-Pascual, J. and Cubillo, A. (2017) 'Dynamic Biomarkers of Response to Antiangiogenic Therapies in Colorectal Cancer: A Review', *Curr. Pharmacogenomics Person. Med.* 2017/12/. Bentham Science Publishers, 15(2), pp. 81–85.

Ruan, Q., Han, S., Jiang, W. G., Boulton, M. E., *et al.* (2011) 'alphaB-crystallin, an effector of unfolded protein response, confers anti-VEGF resistance to breast cancer via maintenance of intracrine VEGF in endothelial cells.', *Mol. Cancer Res.* United States, 9(12), pp. 1632–1643.

Rydén, L., Jirström, K., Bendahl, P.-O., Fernö, M., *et al.* (2005) 'Tumor-specific expression of vascular endothelial growth factor receptor 2 but not vascular endothelial growth factor or human epidermal growth factor receptor 2 is associated with impaired response to adjuvant tamoxifen in premenopausal breast cancer.', *J. Clin. Oncol.* American Society of Clinical Oncology, 23(21), pp. 4695–704.

Sa-Nguanraksa, D., Kooptiwut, S., Chuangsuwanich, T., Pongpruttipan, T., *et al.* (2014) 'Vascular endothelial growth factor polymorphisms affect gene expression and tumor aggressiveness in patients with breast cancer.', *Mol. Med. Rep.* Greece, 9(3), pp. 1044–1048.

Sacchetto, L., Zanetti, R., Comber, H., Bouchardy, C., *et al.* (2018) 'Trends in incidence of thick, thin and in situ melanoma in Europe.', *Eur. J. Cancer*. England, 92, pp. 108–118.

Saha, M., Carriere, A., Cheerathodi, M., Zhang, X., *et al.* (2012) 'RSK phosphorylates SOS1 creating 14-3-3-docking sites and negatively regulating MAPK activation', *Biochem. J.*, 447(1), pp. 159–166.

Saito, T., Shibasaki, K., Kurachi, M., Puentes, S., *et al.* (2011) 'Cerebral capillary endothelial cells are covered by the VEGF-expressing foot processes of astrocytes.', *Neurosci. Lett.* Ireland, 497(2), pp. 116–121.

Salven, P., Heikkilä, P. and Joensuu, H. (1997) ‘Enhanced expression of vascular endothelial growth factor in metastatic melanoma’, *Br. J. Cancer*. Cancer Research Campaign, 76, p. 930.

Sang, N., Stiehl, D. P., Bohensky, J., Leshchinsky, I., *et al.* (2003) ‘MAPK Signaling Up-regulates the Activity of Hypoxia-inducible Factors by Its Effects on p300’, *J. Biol. Chem.* , 278(16), pp. 14013–14019.

Santiago, L., Daniels, G., Wang, D., Deng, F.-M., *et al.* (2017) ‘Wnt signaling pathway protein LEF1 in cancer, as a biomarker for prognosis and a target for treatment.’, *Am. J. Cancer Res.* e-Century Publishing Corporation, 7(6), pp. 1389–1406.

Sato, A., Kayama, H., Shojima, K., Matsumoto, S., *et al.* (2015) ‘The Wnt5a-Ror2 axis promotes the signaling circuit between interleukin-12 and interferon-γ in colitis’, *Sci. Rep.* The Author(s), 5, p. 10536.

Savoia, P., Fava, P., Casoni, F. and Cremona, O. (2019) ‘Targeting the ERK Signaling Pathway in Melanoma’, *Int. J. Mol. Sci.* MDPI, 20(6), p. 1483.

Sayre, L. M. (2005) ‘Chemical Reagents for Protein Modification, 3rd ed By Roger L. Lundblad (Consultant in biotechnology, Chapel Hill, NC). CRC Press: Boca Raton, FL. 2005. xii + 340 pp. $129.95. ISBN 0-8493-1983-8.’, *J. Am. Chem. Soc.* American Chemical Society, 127(26), pp. 9656–9657.

Schneider, B. P., Wang, M., Radovich, M., Sledge, G. W., *et al.* (2008) ‘Association of vascular endothelial growth factor and vascular endothelial growth factor receptor-2 genetic polymorphisms with outcome in a trial of paclitaxel compared with paclitaxel plus bevacizumab in advanced breast cancer: ECOG 2100.’, *J. Clin. Oncol.* American Society of Clinical Oncology, 26(28), pp. 4672–8.

Schumacker, P. T. and Samsel, R. W. (1989) ‘Analysis of oxygen delivery and uptake relationships in the Krogh tissue model.’, *J. Appl. Physiol.* United States, 67(3), pp. 1234–1244.

Schuster, C., Akslen, L. A., Stokowy, T. and Straume, O. (2018) ‘Predictive value of angiogenic proteins in patients with metastatic melanoma treated with bevacizumab monotherapy’, *J. Pathol. Clin. Res.* John Wiley & Sons, Inc., 5(1), pp. 53–62.

Seghezzi, G., Patel, S., Ren, C. J., Gualandris, A., *et al.* (1998) ‘Fibroblast growth factor-2 (FGF-2) induces vascular endothelial growth factor (VEGF) expression in the endothelial cells of forming capillaries: an autocrine mechanism contributing to angiogenesis.’, *J. Cell Biol.* United States, 141(7), pp. 1659–1673.

Senger, D. R., Galli, S. J., Dvorak, A. M., Perruzzi, C. A., *et al.* (1983) ‘Tumor cells secrete a vascular permeability factor that promotes accumulation of ascites fluid.’, *Science*. United States, 219(4587), pp. 983–985.

Shapiro, G. I. (2006) ‘Cyclin-Dependent Kinase Pathways As Targets for Cancer Treatment’, *J. Clin. Oncol.* American Society of Clinical Oncology, 24(11), pp.

1770–1783.

Sharma, S. V. and Settleman, J. (2007) ‘Oncogene addiction: Setting the stage for molecularly targeted cancer therapy’, *Genes Dev.* Cold Spring Harbor Laboratory Press, 21(24), pp. 3214–3231.

Sharp, L. L., Chang, C., Frey, G., Wang, J., *et al.* (2018) ‘Abstract 833: Anti-tumor efficacy of BA3021, a novel Conditionally Active Biologic (CAB) anti-ROR2 ADC’, *Cancer Res.*, 78(13 Supplement), pp. 833 LP – 833.

Shaughnessy, M., Klebanov, N. and Tsao, H. (2018) ‘Clinical and therapeutic implications of melanoma genomics’, *J. Transl. Genet. Genomics*.

Sheppard, K. E. and McArthur, G. A. (2013) ‘The Cell-Cycle Regulator CDK4: An Emerging Therapeutic Target in Melanoma’, *Clin. Cancer Res.*, 19(19), pp. 5320 LP – 5328.

Shi, T.-T., Li, G. and Xiao, H.-T. (2016) ‘The Role of RhoJ in Endothelial Cell Biology and Tumor Pathology’, *Biomed Res. Int.* Hindawi, 2016, pp. 1–9.

Shibuya, M. (2011) ‘Vascular Endothelial Growth Factor (VEGF) and Its Receptor (VEGFR) Signaling in Angiogenesis: A Crucial Target for Anti- and Pro-Angiogenic Therapies’, *Genes Cancer*. SAGE Publications, 2(12), pp. 1097–1105.

Shibuya, M. (2013) ‘VEGFR and type-V RTK activation and signaling.’, *Cold Spring Harb. Perspect. Biol.* United States, 5(10), p. a009092.

Shimoyamada, H., Yazawa, T., Sato, H., Okudela, K., *et al.* (2010) ‘Early growth response-1 induces and enhances vascular endothelial growth factor-A expression in lung cancer cells.’, *Am. J. Pathol.* United States, 177(1), pp. 70–83.

Simanshu, D. K., Nissley, D. V and McCormick, F. (2017) ‘RAS Proteins and Their Regulators in Human Disease.’, *Cell*. United States, 170(1), pp. 17–33.

Simonetti, O., Lucarini, G., Brancorsini, D., Nita, P., *et al.* (2002) ‘Immunohistochemical expression of vascular endothelial growth factor, matrix metalloproteinase 2, and matrix metalloproteinase 9 in cutaneous melanocytic lesions.’, *Cancer*. United States, 95(9), pp. 1963–1970.

Simons, M., Gordon, E. and Claesson-Welsh, L. (2016) ‘Mechanisms and regulation of endothelial VEGF receptor signalling’, *Nat. Publ. Gr.*, 17.

Simpson, J. F., Ahn, C., Battifora, H. and Esteban, J. M. (1996) ‘Endothelial area as a prognostic indicator for invasive breast carcinoma’, *Cancer*, 77(10), pp. 2077–2085.

Slingluff, C. L. J., Petroni, G. R., Molhoek, K. R., Brautigan, D. L., *et al.* (2013) ‘Clinical activity and safety of combination therapy with temsirolimus and bevacizumab for advanced melanoma: a phase II trial (CTEP 7190/Mel47).’, *Clin. Cancer Res.* United States, 19(13), pp. 3611–3620.

Snyder, A., Makarov, V., Merghoub, T., Yuan, J., *et al.* (2014) 'Genetic basis for clinical response to CTLA-4 blockade in melanoma.', *N. Engl. J. Med.* United States, 371(23), pp. 2189–2199.

Soh, E. Y., Sobhi, S. A., Wong, M. G., Meng, Y. G., *et al.* (1996) 'Thyroid-stimulating hormone promotes the secretion of vascular endothelial growth factor in thyroid cancer cell lines.', *Surgery*, 120(6), pp. 944–7.

Soker, S., Takashima, S., Miao, H. Q., Neufeld, G., *et al.* (1998) 'Neuropilin-1 is expressed by endothelial and tumor cells as an isoform-specific receptor for vascular endothelial growth factor.', *Cell*. United States, 92(6), pp. 735–745.

Song, K. S., Seong, J.-K., Chung, K. C., Lee, W.-J., *et al.* (2003) 'Induction of MUC8 gene expression by interleukin-1 beta is mediated by a sequential ERK MAPK/RSK1/CREB cascade pathway in human airway epithelial cells.', *J. Biol. Chem.* United States, 278(37), pp. 34890–34896.

Spitler, L. E., Boasberg, P., O'Day, S., Hamid, O., *et al.* (2015) 'Phase II study of nab-paclitaxel and bevacizumab as first-line therapy for patients with unresectable stage III and IV melanoma.', *Am. J. Clin. Oncol.* United States, 38(1), pp. 61–67.

Srivastava, A., Hughes, L. E., Woodcock, J. P. and Shedden, E. J. (1986) 'The significance of blood flow in cutaneous malignant melanoma demonstrated by Doppler flowmetry.', *Eur. J. Surg. Oncol.* England, 12(1), pp. 13–18.

Srivastava, A., Laidler, P., Davies, R. P., Horgan, K., *et al.* (1988) 'The prognostic significance of tumor vascularity in intermediate-thickness (0.76-4.0 mm thick) skin melanoma. A quantitative histologic study', *Am. J. Pathol.*, 133(2), pp. 419–423.

Stahl, J. M., Cheung, M., Sharma, A., Trivedi, N. R., *et al.* (2003) 'Loss of PTEN Promotes Tumor Development in Malignant Melanoma', *Cancer Res.*, 63(11), pp. 2881 LP – 2890.

Takahashi, T., Yamaguchi, S., Chida, K. and Shibuya, M. (2001) 'A single autophosphorylation site on KDR/Flk-1 is essential for VEGF-A-dependent activation of PLC-gamma and DNA synthesis in vascular endothelial cells.', *EMBO J.* England, 20(11), pp. 2768–2778.

Tap, W. D., Gong, K.-W., Dering, J., Tseng, Y., *et al.* (2010) 'Pharmacodynamic characterization of the efficacy signals due to selective BRAF inhibition with PLX4032 in malignant melanoma.', *Neoplasia*. United States, 12(8), pp. 637–649.

Tayama, M., Furuhata, T., Inafuku, Y., Okita, K., *et al.* (2011) 'Vascular endothelial growth factor 165b expression in stromal cells and colorectal cancer.', *World J. Gastroenterol.* Baishideng Publishing Group Inc, 17(44), pp. 4867–74.

Thiery, J. P. (2002) 'Epithelial-mesenchymal transitions in tumour progression.', *Nat. Rev. Cancer*. England, 2(6), pp. 442–454.

Tomlinson, J., Barsky, S. H., Nelson, S., Singer, S., *et al.* (1999) 'Different patterns of

angiogenesis in sarcomas and carcinomas.', *Clin. Cancer Res.*, 5(11), pp. 3516–22.

Topol, L., Jiang, X., Choi, H., Garrett-Beal, L., *et al.* (2003) 'Wnt-5a inhibits the canonical Wnt pathway by promoting GSK-3–independent β-catenin degradation', *J. Cell Biol.*, 162(5), pp. 899–908.

Tsai, J., Lee, J. T., Wang, W., Zhang, J., *et al.* (2008) 'Discovery of a selective inhibitor of oncogenic B-Raf kinase with potent antimelanoma activity', *Proc. Natl. Acad. Sci.*, 105(8), pp. 3041–3046.

Tsunoda, S., Nakamura, T., Sakurai, H. and Saiki, I. (2007) 'Fibroblast growth factor-2-induced host stroma reaction during initial tumor growth promotes progression of mouse melanoma via vascular endothelial growth factor A-dependent neovascularization.', *Cancer Sci.* England, 98(4), pp. 541–548.

Tzen, Chi-Yuan, Wu, Y.-H. and Tzen, Chin-Yuan (2014) 'Characterization of KIT mutation in melanoma', *Dermatologica Sin.*, 32(1), pp. 7–12.

Ugurel, S., Rappl, G., Tilgen, W. and Reinhold, U. (2001) 'Increased serum concentration of angiogenic factors in malignant melanoma patients correlates with tumor progression and survival.', *J. Clin. Oncol.* American Society of Clinical Oncology, 19(2), pp. 577–83.

Vandamme, N. and Berx, G. (2014) 'Melanoma cells revive an embryonic transcriptional network to dictate phenotypic heterogeneity.', *Front. Oncol.* Switzerland, 4, p. 352.

Varker, K. A., Biber, J. E., Kefauver, C., Jensen, R., *et al.* (2007) 'A randomized phase 2 trial of bevacizumab with or without daily low-dose interferon alfa-2b in metastatic malignant melanoma.', *Ann. Surg. Oncol.* United States, 14(8), pp. 2367–2376.

Veldman-Jones, M. H., Brant, R., Rooney, C., Geh, C., *et al.* (2015) 'Evaluating Robustness and Sensitivity of the NanoString Technologies nCounter Platform to Enable Multiplexed Gene Expression Analysis of Clinical Samples'.

Veronesi, U., Adamus, J., Aubert, C., Bajetta, E., *et al.* (1982) 'A Randomized Trial of Adjuvant Chemotherapy and Immunotherapy in Cutaneous Melanoma', *N. Engl. J. Med.* Massachusetts Medical Society , 307(15), pp. 913–916.

Viskochil, D., Buchberg, A. M., Xu, G., Cawthon, R. M., *et al.* (1990) 'Deletions and a translocation interrupt a cloned gene at the neurofibromatosis type 1 locus.', *Cell.* United States, 62(1), pp. 187–192.

Voron, T., Colussi, O., Marcheteau, E., Pernot, S., *et al.* (2015) 'VEGF-A modulates expression of inhibitory checkpoints on CD8+ T cells in tumors.', *J. Exp. Med.* United States, 212(2), pp. 139–148.

Wajapeyee, N., Serra, R. W., Zhu, X., Mahalingam, M., *et al.* (2008) 'Oncogenic BRAF induces senescence and apoptosis through pathways mediated by the secreted

protein IGFBP7.', *Cell*. Elsevier, 132(3), pp. 363–74.

Walker, L., Schalch, H., King, D. M., Dietrich, L., *et al.* (2005) 'Phase II trial of weekly paclitaxel in patients with advanced melanoma.', *Melanoma Res.* England, 15(5), pp. 453–459.

Wan, P. T. C., Garnett, M. J., Roe, S. M., Lee, S., *et al.* (2004) 'Mechanism of Activation of the RAF-ERK Signaling Pathway by Oncogenic Mutations of B-RAF', *Cell*, 116(6), pp. 855–867.

Warburg, O., Wind, F. and Negelein, E. (1927) 'THE METABOLISM OF TUMORS IN THE BODY.', *J. Gen. Physiol.* United States, 8(6), pp. 519–530.

Warren, R. S., Yuan, H., Matli, M. R., Ferrara, N., *et al.* (1996) 'Induction of Vascular Endothelial Growth Factor by Insulin-like Growth Factor 1 in Colorectal Carcinoma', *J. Biol. Chem.* . United States, 271(46), pp. 29483–29488.

Webster, M. R., Kugel, C. H., Weeraratna, A. T. and Weeraratna, A. T. (2015) 'The Wnts of change: How Wnts regulate phenotype switching in melanoma.', *Biochim. Biophys. Acta*. NIH Public Access, 1856(2), pp. 244–51.

Webster, M. R. and Weeraratna, A. T. (2013) 'A Wnt-er migration: the confusing role of beta-catenin in melanoma metastasis.', *Sci. Signal.* United States, 6(268), p. pe11.

Wehner, M. R., Chren, M.-M., Nameth, D., Choudhry, A., *et al.* (2014) 'International Prevalence of Indoor Tanning', *JAMA Dermatology*, 150(4), p. 390.

Weidemann, A. and Johnson, R. S. (2008) 'Biology of HIF-1α', *Cell Death Differ.*, 15(4), pp. 621–627.

Wellbrock, C. and Arozarena, I. (2015) 'Microphthalmia-associated transcription factor in melanoma development and MAP-kinase pathway targeted therapy.', *Pigment Cell Melanoma Res.* Wiley-Blackwell, 28(4), pp. 390–406.

Wellbrock, C. and Marais, R. (2005) 'Elevated expression of MITF counteracts B-RAF-stimulated melanocyte and melanoma cell proliferation.', *J. Cell Biol.* United States, 170(5), pp. 703–708.

West, C. C., Brown, N. J., Mangham, D. C., Grimer, R. J., *et al.* (2005) 'Microvessel density does not predict outcome in high grade soft tissue sarcoma', *Eur. J. Surg. Oncol.*, 31(10), pp. 1198–1205.

Whittaker, S., Menard, D., Kirk, R., Ogilvie, L., *et al.* (2010) 'A novel, selective, and efficacious nanomolar pyridopyrazinone inhibitor of V600EBRAF.', *Cancer Res.* United States, 70(20), pp. 8036–8044.

Wiesener, M. S., Jurgensen, J. S., Rosenberger, C., Scholze, C. K., *et al.* (2003) 'Widespread hypoxia-inducible expression of HIF-2alpha in distinct cell populations of different organs.', *FASEB J. Off. Publ. Fed. Am. Soc. Exp. Biol.* United States, 17(2), pp. 271–273.

Wiesner, T., Obenauf, A. C., Murali, R., Fried, I., *et al.* (2011) 'Germline mutations in BAP1 predispose to melanocytic tumors.', *Nat. Genet.* United States, 43(10), pp. 1018–1021.

Wiesner, T., Kiuru, M., Scott, S. N., Arcila, M., *et al.* (2015) 'NF1 Mutations Are Common in Desmoplastic Melanoma.', *Am. J. Surg. Pathol.* United States, 39(10), pp. 1357–1362.

Willmore-Payne, C., Holden, J. A., Tripp, S. and Layfield, L. J. (2005) 'Human malignant melanoma: detection of BRAF- and c-kit–activating mutations by high-resolution amplicon melting analysis', *Hum. Pathol.*, 36(5), pp. 486–493.

Wolchok, J. D., Chiarion-Sileni, V., Gonzalez, R., Rutkowski, P., *et al.* (2017) 'Overall Survival with Combined Nivolumab and Ipilimumab in Advanced Melanoma.', *N. Engl. J. Med.* United States, 377(14), pp. 1345–1356.

Woodfin, A., Voisin, M.-B. and Nourshargh, S. (2007) 'ATVB In Focus Vascular Adhesion Molecules PECAM-1: A Multi-Functional Molecule in Inflammation and Vascular Biology'.

Woods, D., Parry, D., Cherwinski, H., Bosch, E., *et al.* (1997) 'Raf-induced proliferation or cell cycle arrest is determined by the level of Raf activity with arrest mediated by p21Cip1.', *Mol. Cell. Biol.*, 17(9), pp. 5598–611.

Woolard, J., Wang, W.-Y., Bevan, H. S., Qiu, Y., *et al.* (2004) 'VEGF₁₆₅b, an Inhibitory Vascular Endothelial Growth Factor Splice Variant', *Cancer Res.*, 64(21), pp. 7822 LP – 7835.

Wright, T. M., Brannon, A. R., Gordan, J. D., Mikels, A. J., *et al.* (2009) 'Ror2, a developmentally regulated kinase, promotes tumor growth potential in renal cell carcinoma', *Oncogene*. Macmillan Publishers Limited, 28, p. 2513.

Wright, T. M. and Rathmell, W. K. (2010) 'Identification of Ror2 as a Hypoxia-inducible Factor Target in von Hippel-Lindau-associated Renal Cell Carcinoma', *J. Biol. Chem.*, 285(17), pp. 12916–12924.

Wu, S., Han, J., Laden, F. and Qureshi, A. A. (2014) 'Long-term ultraviolet flux, other potential risk factors, and skin cancer risk: a cohort study.', *Cancer Epidemiol. Biomarkers Prev.* United States, 23(6), pp. 1080–1089.

Xu, H., Czerwinski, P., Hortmann, M., Sohn, H.-Y., *et al.* (2008) 'Protein kinase C α promotes angiogenic activity of human endothelial cells via induction of vascular endothelial growth factor', *Cardiovasc. Res.*, 78(2), pp. 349–355.

Xu, L., Duda, D. G., di Tomaso, E., Ancukiewicz, M., *et al.* (2009) 'Direct evidence that bevacizumab, an anti-VEGF antibody, up-regulates SDF1alpha, CXCR4, CXCL6, and neuropilin 1 in tumors from patients with rectal cancer', *Cancer Res.* 2009/10/13, 69(20), pp. 7905–7910.

Yan, L., Du, Q., Yao, J. and Liu, R. (2016) 'ROR2 inhibits the proliferation of gastric

carcinoma cells via activation of non-canonical Wnt signaling', *Exp. Ther. Med.* Greece, 12(6), pp. 4128–4134.

Yang, A. S. and Chapman, P. B. (2009) 'The history and future of chemotherapy for melanoma', *Hematol. Oncol. Clin. North Am.*, 23(3), pp. 583–x.

Yang, C.-M., Ji, S., Li, Y., Fu, L.-Y., *et al.* (2017) 'Ror2, a Developmentally Regulated Kinase, Is Associated With Tumor Growth, Apoptosis, Migration, and Invasion in Renal Cell Carcinoma.', *Oncol. Res.* United States, 25(2), pp. 195–205.

Yang, J., Mani, S. A., Donaher, J. L., Ramaswamy, S., *et al.* (2004) 'Twist, a master regulator of morphogenesis, plays an essential role in tumor metastasis.', *Cell*. United States, 117(7), pp. 927–939.

Yang, J., Yan, J. and Liu, B. (2018) 'Targeting VEGF/VEGFR to Modulate Antitumor Immunity', *Front. Immunol.*, p. 978.

Yi, M. and Schnitzer, J. E. (2009) 'Impaired tumor growth, metastasis, angiogenesis and wound healing in annexin A1-null mice', *Proc. Natl. Acad. Sci.*, 106(42), pp. 17886 LP – 17891.

You, Y. H., Lee, D. H., Yoon, J. H., Nakajima, S., *et al.* (2001) 'Cyclobutane pyrimidine dimers are responsible for the vast majority of mutations induced by UVB irradiation in mammalian cells.', *J. Biol. Chem.* United States, 276(48), pp. 44688–44694.

Yu, H., McDaid, R., Lee, J., Possik, P., *et al.* (2009) 'The Role of BRAF Mutation and p53 Inactivation during Transformation of a Subpopulation of Primary Human Melanocytes', *Am. J. Pathol.*, 174(6), pp. 2367–2377.

Yu, P., Gu, S., Bu, J. and Du, J. (2010) 'TRPC1 is essential for in vivo angiogenesis in zebrafish.', *Circ. Res.* United States, 106(7), pp. 1221–1232.

Zhan, T., Rindtorff, N. and Boutros, M. (2016) 'Wnt signaling in cancer', *Oncogene*. The Author(s), 36, p. 1461.

Zhang, L., Kundu, S., Feenstra, T., Li, X., *et al.* (2015) 'Pleiotrophin promotes vascular abnormalization in gliomas and correlates with poor survival in patients with astrocytomas.', *Sci. Signal.* United States, 8(406), p. ra125.